UNIVERSITY OF CAMBRIDGE

GLYCOPROTEIN M AND ESCRT IN HERPES SIMPLEX VIRUS TYPE 1 ASSEMBLY

Yudan Ren

Robinson College

This dissertation is submitted for the degree of Doctor of Philosophy

Division of Virology

Department of Pathology

October, 2011

Dedication

This thesis is dedicated to my parents, 任吉林 (**Jilin Ren**) and 金桂凤 (**Guifeng Jin**).

Acknowledgements

This thesis would not have been possible without the help and support that I have received during my PhD study in the last three years.

First of all, I would like to thank my supervisor, Dr Colin Crump, who has supported me with his scientific knowledge and skills, his excellent problem-solving abilities and great patience.

I would also like to thank the members in the Crump laboratory. Thanks to Helen for always being helpful and encouraging as well as the extra fun in the lab. I thank Susie for her excellent technical support and help. Thanks to all of the past and present PhD students in the lab; Tobi, Stáňa and Kathy for their help and friendship.

I am grateful to have done my PhD in the Division of Virology, which is a unique research unit with great collaborations across the research groups. Thanks to everyone for creating such a friendly and enjoyable research environment. Especially, I'd like to thank my mentor Stacey for listening and his patience and for guiding me through the interview stages for the Career Development Fellow position at the LMB. Many thanks to Tony for solving my funding problems at the beginning of my PhD and the insightful discussions about my research work. Thanks to Mike for giving everlasting encouragement and humour towards everything. Thanks to Daniel for his scientific expertise and helpful discussion about my experiments. Many thanks also go to many other people in the division for their help, inspiration and entertaining spirits. I am also grateful to the pleasant residence at Robinson College during my PhD study. I'm sure these limited words cannot express all of my gratitude and there are many more people to be thanked.

It has been an honour to receive the joint funding support towards my PhD from Cambridge Overseas Trust, Robinson College, the Board of Graduate Studies, and the Department of Pathology.

Last but not least, I would like to thank my brother and my family in China, as well as my friends (especially Laurence, Danfeng and Xin) for their love and support.

Summary

Herpes simplex virus type 1 (HSV-1) has a large linear double-stranded DNA genome in an icosahedral capsid shell, a cell-derived lipid envelope and a proteinaceous tegument layer. There are over fifty viral proteins and many host proteins identified in HSV-1 virions. The final formation of mature virus particles requires the membrane wrapping of tegumented capsids in the cytoplasm, a process termed secondary envelopment. This process involves the coordination of numerous viral and cellular proteins and results in double-membrane structures with enveloped virions contained within cellular vesicles. Mature viruses are then released through the fusion of these virion-containing vesicles and plasma membranes. This thesis describes investigation into the functions of viral glycoprotein M (gM) and the cellular Endosomal Sorting Complexes Required for Transport (ESCRT) in secondary envelopment.

Firstly, it has been reported that gH/L can be efficiently internalised and targeted to the TGN by the co-expression of gM in transfection assays. In order to examine the role of gM in guiding the localisation of viral proteins in infected cells, a HSV-1 gM deletion virus (ΔgM), and its revertant virus were constructed. The major phenotype demonstrated was that the absence of gM caused the internalisation of cell surface gH/L to be inhibited and higher levels of gH/L to be observed on the cell surface. Further, lower levels of gH/L were detected in purified ΔgM virions, which was in agreement with the delayed entry kinetics, smaller plaque sizes and greater replication deficits at low multiplicity of infection observed in ΔgM infected cells. Over all the results presented in this thesis demonstrate that in infected cells the efficient incorporation of gH/L into virions relies on the function of gM in HSV-1.

Secondly, during HSV-1 secondary envelopment the budding and scission of the viral envelope from the host membrane share topological similarities with the formation of intraluminal vesicle in multivesicular bodies, retrovirus budding, and abscission at the end of cytokinesis, processes that require the cellular ESCRT machinery. There are four multiprotein ESCRT complexes and many associated proteins involved in their regulation. It has been previously shown that the ESCRT-III complex and a functional ATPase VPS4 are required for HSV-1 secondary envelopment, but different from the strategy utilised by HIV-1, the recruitment of ESCRT during HSV-1 infection is independent of TSG101 and/or ALIX. Data presented in this thesis demonstrate that CHMP4A/B/C proteins of the ESCRT-III complex are specifically crucial for HSV-1 secondary envelopment.

Simultaneous depletion of CHMP4A/B/C proteins significantly inhibited HSV-1 replication. Ultrastructure analysis revealed that there were virtually no extracellular virions in CHMP4A/B/C depleted samples while more free capsids were observed in the cytoplasm, although the nuclear capsids and primary envelopment events appeared to be normal. In order to identify interactions between HSV-1 and ESCRT proteins, 22 HSV-1 tegument proteins were cloned and tested against a panel of ESCRT and ESCRT-associated proteins in yeast two-hydrid assays. Analysis of positive hits from yeast two-hybrid interaction screens using GST pull-down, co-immunoprecipitation and protein co-localisation assays have validated interactions of pUL47 with CC2D1A/1B, CIN85, CHMP6 and ALIX, pUL46 and pUL49 with CC2D1A/1B and CIN85, and pUL16 with CC2D1A/1B. Furthermore, the newly identified ESCRT associated proteins CC2D1A and CC2D1B have been detected in purified virions. The role of the identified ESCRT proteins in HSV-1 replication has been investigated using siRNA depletion. Unfortunately siRNA depletions of the various ESCRT candidates individually or in combinations did not show any significant effect on HSV-1 replication. Overall these data suggest that unlike HIV and other retroviruses, HSV-1 has evolved multiple parallel pathways to hijack the ESCRT machinery to facilitate its replication, particularly, through the interactions that lead directly to the recruitment of CHMP4A/B/C proteins. Disruption of some of these pathways did not prevent HSV-1 replication in tissue culture, suggesting any one potential pathway is sufficient for ESCRT recruitment to sites of HSV-1 assembly.

Declaration

This thesis is the result of my own work and includes nothing which is the outcome of work done in collaboration, except where specifically indicated in the text. The work presented was undertaken at the Division of Virology, Department of Pathology, University of Cambridge, UK, between September 2008 and October 2011. No part of this thesis has been submitted for a degree to this or any other university. This thesis contains approximately 50000 words and 55 figures.

Some of the work in this thesis has been published:

Yudan Ren, Susanne Bell, Helen L Zenner, S-Y Kathy Lau and Colin M Crump, J Gen Virol (2011), Glycoprotein M is important for the efficient incorporation of glycoprotein H/L into HSV-1 particles.

Yudan Ren

October, 2011

Abbreviations

aa amino acid (Nomenclature follows JCBN recommendations)

ATPase adenosine triphosphatase

BAC bacterial artificial chromosome

bp base pair(s)

cDNA complementary DNA

CHMP charged multivesicular body protein

kDa kilo Dalton

DNA deoxyribonucleic acid

ER endoplasmic reticulum

ESCRT endosomal sorting complex required for transport

gB, gD, gH, gM, etc. glycoprotein B, D, H, M etc.

GST glutathione S-transferase

HIV human immunodeficiency virus

HSV herpes simplex virus

ILV intraluminal vesicle

L domain late domain

L particle light particle

MOI multiplicity of infection

mRNA messenger RNA

MVB multivesicular body

PEG polyethylene glycol

PBS phosphate-buffered saline

PCR polymerase chain reaction

PFU plaque forming unit

RNA ribonucleic acid

SDS-PAGE sodium dodecyl sulfate polyacrylamide gel electrophoresis

siRNA small interfering RNA

TEM transmission electron microscopy

TGN trans Golgi network

VPS vacuolar protein sorting

Y2H yeast two-hybrid

YFP/GFP yellow/green fluorescent protein

Contents

List of Figures

List of Tables

1 Introduction

1.1 The order *Herpesvirales*

1.1.1 Classification

Our earliest recorded knowledge of herpes simplex virus (HSV) can be traced back to the ancient Greeks who used the word 'herpes' to describe lesions that appeared to creep or crawl along the skin. However, it was not until 1981 that the definition, nomenclature and taxonomy of *Herpesviridae* had been established (Roizman & Whitley, 2001). The members of *Herpesviridae* family were initially classified based on the structures and biological properties of the virions by the Herpesvirus Study Group of the International Committee on the Taxonomy of Viruses (ICTV). Herpesviruses have a broad host range and up to 135 species have been identified in animals as varied as shellfish and mammals (Davison *et al.*, 2009). Recently, the taxonomy has been updated by ICTV. The former family *Herpesviridae* has been split into three families and incorporated into the new order *Herpesvirales*. In the new classification system, the family *Herpesviridae* retains the mammal, bird and reptile viruses. The two new families are *Alloherpesviridae* (*Allo* is from Greek meaning other or different), which incorporates the fish and frog viruses, and *Malacoherpesviridae* (*Malaco* is from Greek meaning soft), which currently contains only one bivalve virus (*Ostreid herpesvirus 1*). The family *Herpesviridae* consists of three sub-families: *Alphaherpesvirinae* (containing the *Simplexvirus*, *Varicellovirus*, *Mardivirus* and *Iltovirus* genera), *Betaherpesvirinae* (containing the *Cytomegalovirus*, *Muromegalovirus*, *Roseolovirus* and *Proboscivirus* genera) and *Gammaherpesvirinae* (containing the *Lymphocryptovirus*, *Rhadinovirus*, *Macavirus* and *Percavirus* genera). Three new genera, *Proboscivirus*, *Macavirus* and *Percavirus*, have been added to the new herpesvirus taxonomy. Members in the family *Herpesviridae* have mature virions that vary in size from 120 to 300 nm. The distinct morphologies of herpesviruses virions includes at least four structure features: 1) a linear double-stranded DNA genome that varies from approximately 125 to 290 kbp; 2) an icosahedral (T=16) capsid with a diameter of approximately 100 nm containing the viral genome; 3) a proteinaceous layer between the capsid and the envelope termed the tegument; 4) a lipid envelope derived from cell membrane structures carrying viral glycoprotein spikes. These four features of virion

morphology are the primary criterion for inclusion of an agent into this family (Davison *et al.*, 2009; Mettenleiter, 2002; Mettenleiter *et al.*, 2006; 2009; Pellett & Roizman, 2007).

Despite the common characteristics, members of the *Herpesviridae* family have a wide range of biological properties. The three sub-families under the family *Herpesviridae* were initially classified according to these biological properties of the viruses without the information on their genome sequences (Table 1.1) (Pellett & Roizman, 2007; Weir, 1998). Subsequently, the sequence information (gene organisation and arrangement according to DNA sequencing and protein homology from aa sequences) has become the primary basis for classification. This sequence analysis has proved that the previous classification system was very accurate in representing the relatedness of different species of herpesviruses. However, the classification of a few members has been changed according to the newly identified biological properties. For instance, the Marek's disease virus type 1 was classified as a gammaherpesvirus as the virus causes lymphloid tumors in chickens, but sequence data indicated that it is more related to alphaherpesviruses (Weir, 1998).

Table 1.1 Sub-families of *Herpesviridae*.

Sub-family	Biological properties
Alphaherpesvirinae	A variable host range, relatively short reproductive cycle, rapid spread in culture, efficient destruction of host cells and capability to establish latency primarily in sensory ganglia.
Betaherpesvirinae	A more restricted host range, relatively long reproductive cycle, slow infection progress in culture, infected cells frequently become enlarged and capable to establish latency in secretory glands, lymphoreticular cells, kidneys and other tissues.
Gammaherpesvirinae	A restricted host range limited to the natural hosts, replicate in lymphoblastoid cells in vitro, lytic infections could be caused in some epithelioid and fibroblastic cells, latency is usually in lymphoid tissue and viruses are specific for either T or B lymphocytes.

The human herpesviruses are among the best characterised viruses from the *Herpesviridae* family. There are eight members infecting humans as the natural host (Table 1.2). These viruses frequently infect human beings and are associated with various human diseases, including vesicular skin lesion, viral encephalitis, mononucleosis, and cancer (Schleiss, 2009). The formal names for the eight human herpesviruses are human herpesvirus (HHV) 1-8, but the common names for some of these viruses are more frequently used.

Table 1.2 List of human herpesviruses.

Virus	Common name	Genome	Sub-family	Related disease
HHV-1	HSV-1	152 kbp	α	Encephalitis (an acute inflammation of the brain) Aseptic meningitis (viral meningitis) Herpetic keratitis (infection of the corneal epithelium) Gingivostomatitis/pharyngitis (peri- and intraoral lesions involving the pharyngeal mucosa) Herpetic whitlow (primary lesion involves the fingers or hand)
HHV-2	HSV-2	152 kbp	α	Herpes gladiatorum (primary cutaneous infection associated with the close, skin-to-skin contact during athletic competitions) Eczema herpeticum (cutaneous infection in children with atopic dermatitis) Genital herpes, neonatal herpes, herpes labialis and erythema multiforme
HHV-3	VZV	125 kbp	α	Varicella (chickenpox) Herpes zoster (shingles) Encephalitis Fetal varicella syndrome
HHV-4	EBV	172 kbp	γ	Infectious mononucleosis (glandular fever) EBV-associated malignancies
HHV-5	HCMV	248 kbp	β	Mononucleosis Congenital CMV infection
HHV-6A/B	NA	159-170 kbp	β	Encephalitis Congenital transmission Febrile seizures (a convulsion associated with a significant rise in body temperature)
HHV-7	NA	145 kbp	β	Roseola infantum (exanthem subitum; rose rash of infants)
HHV-8	KSHV	170-210 kbp	γ	Kaposi sarcoma Castleman's disease

HSV-1/2: Herpes simplex virus-1/2. VZV: Varicella-zoster virus. EBV: Epstein-Barr virus. HCMV: Human cytomegalovirus. HHV-6A/B: Human herpesvirus-6A/B. HHV-7: Human herpesvirus-7. KSHV: Kaposi's sarcoma-associated herpesvirus.

Herpes Simplex Virus type 1 (HSV-1) belongs to the sub-family *Alphaherpesvirinae*. It has a high worldwide infection rate of between 40-80% (Diefenbach *et al.*, 2008) and is one of the common human pathogens causing most forms of non-genital herpes simplex infection (such as cold sores) in human beings. HSV-1 is relatively easy to work with in culture and serves as a good model for research into the conserved functions of viral proteins. Therefore HSV-1 is the virus model employed in this thesis and the subsequent part of the introduction related to virus genome, structure and life cycle will be mainly focussed on this virus.

1.1.2 HSV-1 genome organisation

The viral genome of HSV-1 (strain 17, Refseq: NC_001806) consists of approximately 152 kilo base pairs and has a G + C content of 68% (Weir, 1998). The genome is composed of two covalently linked segments called Long (L) and Short (S) according to their relative length. L and S segments contain unique long (UL) (108 kb) and unique short (US) (13 kb) sequence regions respectively, and these regions are flanked by inverted repeat sequences including two internal repeats (IR) and two terminal repeats (TR). Therefore the six regions in the viral genome are presented as: TRL – UL – IRL – IRS – US – TRS. There is only a single copy for each viral gene located in the unique regions. However, genes encoded in the repeat regions (*e.g.,* ICP0 and ICP4) have two copies (Weir, 1998). Viral genes are usually named based on their positions in the L or S region (*e.g.,* UL1 or US2), and the protein products of these genes are often named by adding the prefix 'p' to the gene (*e.g.,* pUL10). However, many viral proteins are also named according to other features including function (*e.g.,* origin binding protein), infected cell protein number (*e.g.,* ICP0), and virion polypeptide/protein number (*e.g.,* VP5) (Pellett & Roizman, 2007).

The HSV-1 genome contains three origins of replication: one copy of *ori*L, which is located in the UL region, and two copies of *ori*S, which are located in IRS and TRS. These origins of replication contain multiple binding sites for the viral origin binding protein (pUL9). It has been reported that either *ori*L or one of the *ori*S is sufficient for viral replication. During viral DNA synthesis, progeny genomes are generated in the form of long concatemers and need to be cleaved into monomers. Within the inverted repeat regions there are two DNA sequence elements, *pac*1 and *pac*2, to ensure proper cleavage and packaging of the viral genome (Igarashi *et al.*, 1993; Polvino-Bodnar *et al.*, 1987; Taylor *et al.*, 2002). For HSV-1, there are at least 74 open-reading frames (ORFs), which encode all the proteins required to form the virus capsid, tegument and envelope as a virus particle,

as well as to regulate the viral replication and infectivity (McGeoch *et al.*, 2006; Mettenleiter *et al.*, 2006). All of these characteristics of the genome form the foundation of the large, complex herpesviruses.

1.1.3 HSV-1 virion structure

With the emergence of highly sensitive techniques, such as mass spectrometry and electron microscopy, the HSV-1 virion structure has gradually been uncovered. HSV-1 is a large complex enveloped virus with a diameter of 170-200 nm. The viral genomic DNA is densely packed in an icosahedral (T = 16) shaped viral capsid, which is 115 to 130 nm in diameter and about 15 nm in thickness. The capsid has 162 surface capsomeres including 150 hexons and 12 pentons. The hexons have six-fold symmetry occupying the faces and edges of the icosahedral structure while the pentons have five-fold symmetry located at the vertices (Newcomb *et al.*, 1993). The three-dimensional structure of HSV virions determined using cryo-electron tomography was reported in 2003 by A. Steven's group. The virions are pleomorphic membrane-bound particles and generally have a spherical shape although some particles have genuine non-spherical shapes. The viral envelope bilayer membrane is about 5 nm thick and the envelope is 170 to 200 nm in diameter (mean, 186 nm). The array of glycoprotein spikes on the virions makes the full diameter around 225 nm on average. Within the envelope the viral capsid is located at an eccentric position occupying about one-third of the volume and the rest of the volume is occupied by the tegument. Linkers with about 4 nm length were observed and they connected the tegument cap to the envelope. There are 595 to 758 spikes on each virion with length ranging from 10 to 25 nm (Grunewald *et al.*, 2003).

HSV-1 virions are large and have complex structures. A unique structure is the tegument, a protein layer located between the capsid and envelope, which often has been described as amorphous. The tegument consists of many proteins which are non-essential in tissue culture and the exact roles of many individual proteins are unknown. Recently, the component profile of extracellular HSV-1 virions has been revealed from a mass spectrometry study and the reported work has shown 8 capsid proteins, 13 envelope proteins (including pUL20), 23 tegument proteins and up to 49 distinct host cellular proteins in purified HSV-1 virions (Loret *et al.*, 2008). In addition, three envelope proteins, gJ, gK and pUL49.5, were not detected in the reported mass spectrometry study. The virion incorporation of these glycoproteins is still an open question as other studies have reported that these membrane proteins are constituents of mature viruses (Adams *et al.*,

1998; Ghiasi *et al.*, 1998; Klupp *et al.*, 1998; Loret *et al.*, 2008). All of the HSV-1 tegument proteins detected by mass spectrometry are listed in Table 1.3. In addition, the asymmetric form of tegument around the capsid, especially the 'actin-like' substructure observed by cyto-electron tomograms, and functional roles of HSV-1 tegument proteins that have been discovered suggest that there is an order among the numerous tegument proteins (Grunewald *et al.*, 2003; Kelly *et al.*, 2009).

Table 1.3 HSV-1 tegument proteins.

Gene	Common protein name	Size (kDa)	Roles* *in vitro*	Conservation in *Herpesviridae* (+/-)	Functions
UL36	VP1/2	336	E	+	Important for capsid transport (Abaitua & O'Hare, 2008; Coller & Lee, 2007), viral DNA uncoating (Ojala *et al.*, 2000), secondary envelopment (Roberts *et al.*, 2009), transport of the virus along axons (Shanda & Wilson, 2008), addition of pUL37 and pUL48 (Ko *et al.*, 2010), has deubiquitinating activity (Schlieker *et al.*, 2005).
UL37	/	121	E	+	Tightly associated with pUL36, important for secondary envelopment (Roberts *et al.*, 2009), capsid transport (Krautwald *et al.*, 2009; Pasdeloup *et al.*).
UL48	VP16	54	E	-	Infectious virus particle assembly (Weinheimer *et al.*, 1992), regulates viral gene transcription (Stern *et al.*, 1989).

RS1	ICP4	133	E	-	Regulates viral gene transcription (Smith *et al.*, 1993).
UL7	/	33	NE	+	Interacts with mitochondrial protein (Tanaka *et al.*, 2008).
UL11	/	10	NE	+	Involved in secondary envelopment (Leege *et al.*, 2009).
UL13	/	57	NE	+	Has protein kinase activity to phosphorylate other viral proteins (Kato *et al.*, 2006), involved in nuclear lamins disruption during nuclear egress (Cano-Monreal *et al.*, 2009).
UL14	/	24	NE	+	Important for transporting of VP16 and capsid nuclear targeting (Yamauchi *et al.*, 2008).
UL16	/	40	NE	+	Forms complex with pUL11 (Loomis *et al.*, 2003) and pUL21 (Harper *et al.*, 2010), interacts with gE (Yeh *et al.*, 2011) and transiently with capsid (Meckes & Wills, 2007).
UL21	/	58	NE	-	Important for other viral protein incorporation (Michael *et al.*, 2007), forms a complex with UL11 and UL16 (Harper *et al.*, 2010).
UL23	TK	41	NE	-	Has thymidine kinase activity to phosphorylate deoxythymidine, related to viral DNA replication (Brown *et al.*, 1995).
UL41	VHS	55	NE	-	Host shutoff protein, has mRNA-specific RNase activity,

					induces shutoff of host protein synthesis, disruption of preexisting polysomes, and degradation of host mRNAs (Saffran *et al.*, 2010).
UL46	VP11/12	78	NE	-	Interacts with VP16, possibly involved in modulation of host cell signalling pathways (Wagner & Smiley, 2009; 2011).
UL47	VP13/14	74	NE	-	Contains nuclear localisation and exporting signals, shuttles between nucleus and cytoplasm, has RNA binding activity (Donnelly & Elliott, 2001; Donnelly *et al.*, 2007; Verhagen *et al.*, 2006b; Williams *et al.*, 2008).
UL49	VP22	32	NE	-	Recruits ICP0 for virion incorporation (Maringer & Elliott, 2010), interacts with VP16 (Mouzakitis *et al.*, 2005).
UL50	/	39	NE	-	Encodes a dUTPase (Jons & Mettenleiter, 1996).
UL51	/	26	NE	+	Plays role in nuclear egress (Nozawa *et al.*, 2005).
UL55	/	21	NE	-	Unknown.
US2	/	33	NE	-	Interacts with cytokeratin 18 (Goshima *et al.*, 2001).
US3	/	53	NE	-	Encodes a protein kinase (Kato *et al.*, 2005), inhibits host cell apoptosis (Leopardi *et al.*, 1997).

US10	/	34	NE	-	Encodes a capsid/tegument-associated phosphoprotein (Yamada *et al.*, 1997).
US11	/	18	NE	-	Encodes an RNA binding protein (Roller & Roizman, 1990).
RL1	ICP34.5	26	NE	-	Encodes a viral neurovirulence factor (Brown *et al.*, 1994).
RL2	ICP0	79	NE	-	Has E3 ubiquitin-protein ligase activity and involved in cellular protein down regulation (Boutell *et al.*, 2005; Everett, 2000a; b).

* E: essential; NE: nonessential.

The diverse functional roles of HSV-1 tegument proteins have been reviewed in detail by Kelly and colleagues. According to the data reported from a combination of research approaches, it has been gradually uncovered that the tegument is not a simple protein layer without an ordered structure. Yeast two-hybrid screens have identified several interactions between HSV-1 tegument proteins and subsequently they have revealed broader interactions between the viral structure proteins. Among those interactions, there are capsid-tegument interactions (such as pUL35 and pUL37), tegument-tegument interactions (such as pUL37-pUL46) and tegument-envelope interactions (such as pUL49-pUS9) (Fossum *et al.*, 2009). Together with electron microscopy imaging showing the physical position of the tegument as the bridge between the capsid and envelope, these interactions linking capsid, tegument and envelope have offered further hints for the functional roles of the tegument in forming HSV-1 virions (Kelly *et al.*, 2009; Lee *et al.*, 2008; Vittone *et al.*, 2005). However, the functional redundancy among these proteins has increased the difficulty and complexity of research into tegument assembly.

1.1.4 HSV-1 life cycle

HSV-1 is a very successful human pathogen, probably due to such a long history of co-evolution. Primary infection occurs mainly in infants and young children, after which the virus becomes latent in the dorsal root ganglion, and can be periodically reactivated

throughout life (Gilden *et al.*, 2007). The ability of HSV-1 to establish latency for the life time of the host is a highly successful strategy that this family of virus has evolved in order to survive and it is a very interesting area of research. However, this thesis is focussed on assembly mechanisms of HSV-1 lytic infection, so the rest of this section will be primarily concerned with the HSV-1 life cycle during lytic replication (Figure 1.1).

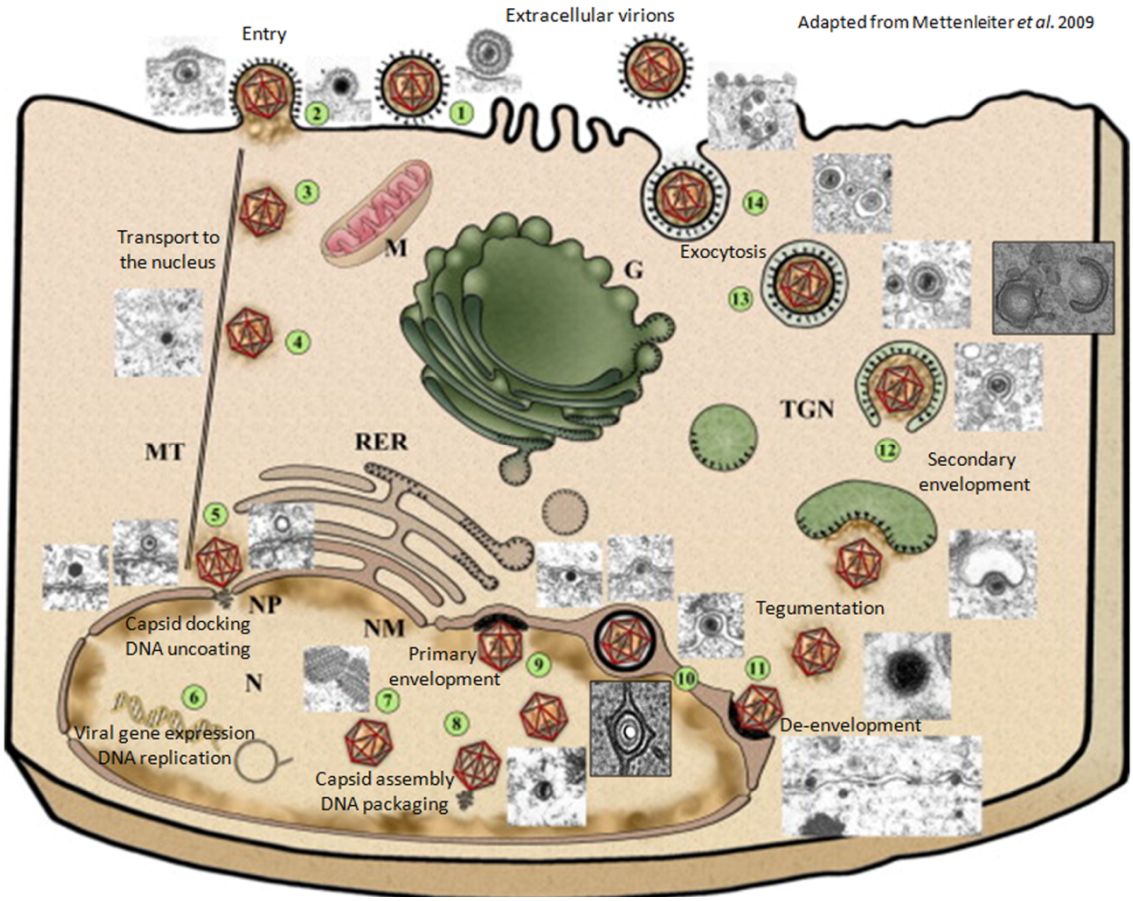

Figure 1.1: Diagram of HSV-1 life cycle.

1.1.4.1 Entry

An enveloped virus particle is composed of a lipid bilayer envelope, proteins and a nucleic acid genome. Viruses don't have full replication systems themselves and must rely on the machineries in host cells to support their life cycle. At the beginning of infection, the first hurdle the virus encounters is entering the host cell. The entry of herpesviruses is a complex process requiring the concerted interactions of multiple glycoproteins and multiple host receptors (Table 1-4). HSV-1 can enter cells by fusion at the plasma membrane at neutral pH or fusion with an endocytic membrane after endocytosis in either a pH-dependent or a pH-independent manner (Connolly *et al.*, 2011). For example, HSV-1

enters into Vero cells via fusion at the plasma membrane while in most cell types the virus appears to enter by endocytosis (Reske *et al.*, 2007). The viral glycoprotein involvement in the entry of HSV-1 into host cells can be roughly divided into three stages:

1) **The initial attachment of the virion to the cell surface.** Glycoprotein B (gB) and glycoprotein C (gC) are able to attach to the heparan sulfate on the surface. gC has the greater efficiency for the attachment although gC is not essential for either entry or replication. It has been reported that heparan sulfate is the cellular receptor of gC, although there are reported data suggesting a heparan sulfate independent receptor may mediate interaction with gB because a soluble form of gB interacts with the surface of cells independent of heparan sulfate (Reske *et al.*, 2007).

2) **The interaction of glycoprotein D (gD) with its cellular receptors.** After the initial attachment to the cell surface, the next stage requires the interaction of gD with one of the several potential entry receptors. These receptors are herpesvirus entry mediator (HVEM) (a member of the tumor necrosis factor (TNF) receptor family) (Montgomery *et al.*, 1996), nectin-1 (a member of the immunoglobulin superfamily) (Connolly *et al.*, 2005; Krummenacher *et al.*, 1998), and 3-O-sulfated heparan sulfate (Rey, 2006; Shukla *et al.*, 1999; Tiwari *et al.*, 2004). This diversity of potential receptors of gD may contribute to the ability of HSV-1 to infect a wide range of different cell types. Upon receptor binding, gD undergoes conformational changes to be the receptor-activated form, which is able to induce alteration in the gH/L complex as stated below.

3) **The fusion of viral envelope with the plasma or endosome membrane and release of the tegument and capsid into the cytoplasm.** gD is a type I membrane protein and does not have the characteristics of a fusion protein. It was assumed that the central fusion machinery involves gB and the heterodimer gH/L. Recently, the structures of gB (Heldwein *et al.*, 2006) and gH/L (Backovic *et al.*, 2010; Chowdary *et al.*, 2010a; Matsuura *et al.*, 2010) have been resolved. Multiple cellular receptors of gB have been reported and gH/L complex binds to integrins (Table 1.4). The structures reveal that gB is a class III viral fusion protein which is capable of inserting into target membranes and inducing fusion through conformational changes. However, the gH/gL heterodimer does not have viral fusion protein characteristics at the structural level. Thus gB is more likely to be the fusion protein and gH/L a regulator for the function of gB (Connolly *et al.*, 2011). The current data suggest that alterations in the gH/L complex induced by activated gD allows gH/L to interact with gB and up-

regulate the fusogenic potential of gB, which leads to the completion of membrane fusion between the host cell membrane and viral envelope (Atanasiu *et al.*, 2010).

Table 1.4 HSV-1 entry related glycoproteins.

Glycoprotein	Cell receptor	Function
gB	HS DC-SIGN PILRα MAG NMMHCIIA	Catalyses membrane fusion.
gC	HS	Facilitates entry by binding to host cells at initial stage, non-essential.
gD	HVEM Nectin 1/2 3-O-sulphated HS	Binds cells and triggers fusion.
gH/L	Integrins	Triggers/regulates fusion.

HS: heparan sulfate. DC-SIGN: dendritic cell-specific ICAM3-grabbing non-integrin (CD209). PILRα: paired immunoglobulin-like type 2 receptor-α. MAG: myelin-associated glycoprotein. NMMHCIIA: non-muscle myosin heavy chain IIA (myosin 9). HVEM: herpesvirus entry mediator.

Additional evidence to support this glycoprotein fusion machinery is that the simultaneous expression of these four glycoproteins by transfection is able to promote cell-cell fusion (Turner *et al.*, 1998). Overall, glycoprotein gB, gD and gH/L compose the membrane fusion machinery and they are essential for the entry of HSV-1.

1.1.4.2 Transport to the nucleus

HSV-1 is an enveloped virus that replicates and packages its viral DNA inside the cell nucleus. After the initial fusion event of the virus envelope and host plasma or endosome membrane, the viral capsid-tegument complex is released into the cytoplasm. This complex needs to move through the cytoplasm to the nucleus to release the viral genome. The cytoplasm is a crowded environment due to the presence of organelles, the cytoskeleton and high protein concentrations (up to 300 mg/ml) and it effectively restricts free diffusion of molecules larger than 500 kDa. Thus, for the capsid-tegument complex to rely on passive diffusion alone is virtually impossible. The cytoplasmic transport procedure must be an active process (Sodeik, 2000). Microtubules provide the 'high-way' system within the cells for long-distance transport of cargos (such as vesicles, organelles and chromosomes). Alpha-tubulin and beta-tubulin heterodimers are the building blocks of

microtubules, which have a structural polarity, with a highly dynamic "plus" end that can grow and shrink rapidly and a relatively stable "minus" end that is anchored at the microtubule-organizing centre (MTOC). There is plus-end-directed transport (also called anterograde direction), which involves the transport towards the periphery, and minus-end directed transport (also called retrograde direction), which involves transport from the periphery towards the MTOC respectively. Two types of molecular motors mediate these two types of transport: kinesins are plus-end-directed transport motors and dyneins are minus-end directed transport motors (Dodding & Way, 2011; Lyman & Enquist, 2009). The transport mediated by dynein shares the same direction with the transport of incoming viral capsids to the nucleus. Indeed, evidence has shown that upon penetration, HSV-1 hijacks the dynein for its movement towards the cell nucleus (Sodeik *et al.*, 1997).

It was initially observed in neuronal cells that HSV-1 capsids bind to microtubules through studies using electron microscopy (Lycke *et al.*, 1984). In Vero cells, Sodeik and colleagues demonstrated that the capsid transport in cytoplasm is mediated by microtubules and the presence of microtubule depolymerizing drugs (such as nocodazole) blocks the transport of capsids. Antibody labelling of dynein revealed the co-localisation of dynein and the viral capsids. Furthermore, the capsids had reached the nucleus and attached themselves to the nuclear pore complexes within 1 hpi during the transport procedure (Sodeik *et al.*, 1997). This suggests that after viral entry, the capsids bind to microtubules and employ dynein to delivery them from the cell periphery to the nucleus in a rapid and efficient manner. Subsequently, viral capsid transport was successfully reconstituted *in vitro*, which demonstrated that capsids moved along MT at up to 30 μm/s in the presence of ATP. Further, the blocking of the dynein co-factor, dynactin, inhibited capsid transport (Wolfstein *et al.*, 2006).

Viral components derived from the tegument are likely to be involved in capsid transport. For example, the large tegument protein VP1/2 (pUL36), a 336 kDa protein, is tightly associated with the capsids through the interaction with the capsids protein pUL25 (Coller & Lee, 2007). It has been shown that efficient movement of capsids along microtubules in vitro requires the HSV inner tegument proteins UL36 (VP1/2) and UL37, and removing outer tegument proteins from the capsids increased *in vitro* mobility. However, capsids harvested from cell nuclei without any tegument proteins had virtually no interactions with the motor molecules. This suggests the inner tegument is important for transport and these proteins may interact with dynein and/or dynactin (Lyman & Enquist, 2009; Wolfstein *et al.*, 2006). However, the microtubule mediated transport is not essential for

viral infection as it has been shown that the viral infection is only delayed in the absence of microtubules (Sodeik *et al.*, 1997), suggesting other pathways for the viral capsid transport after entry.

Unlike certain tegument proteins (such as VP1/2), the majority of the tegument dissociates from the capsid after fusion and does not travel together with the capsid to the nuclear pore complex. The distribution and/or transport of these tegument proteins are different due to their different functions. For instance, the structural component VP16 (pUL48, also called αTIF and Vmw65) needs to bind directly to a cellular protein called host cell factor (HCF) in the cytoplasm, which acts as a nuclear import factor and carries VP16 into the host cell nucleus (La Boissière *et al.*, 1999). Upon transport into the nucleus, the VP16-HCF complex binds to Oct-1 and forms the activator complex that drives IE gene expression (Stern & Herr, 1991). Another example is pUL41 (VHS) which plays an important role in preparing the cellular environment for efficient viral replication. pUL41 is an mRNA-specific RNase and causes non-specific degradation of mRNA, disruption of polyribosomes and shutoff of macro-molecular synthesis after infection (Smiley, 2004).

1.1.4.3 Capsid docking and DNA uncoating

After transport to the nucleus, the incoming capsids dock to nuclear pore complexes (NPCs). NPCs are large protein complexes consisting of key components including cytoplasmic filaments, spoke ring complex, transporter and nuclear basket (Allen *et al.*, 2000). The basic structure of NPCs is conserved from yeast to human. The proteins that make up the nuclear pore complex are known as nucleoporins and each NPC is composed of about 30 distinct nucleoporins, which were initially identified in yeast (Rout *et al.*, 2000). HSV-1 has evolved a strategy to utilise these NPCs as the channels to deliver its viral genome into the nucleus.

It has been observed that within 1 h after penetration the viral capsids associate with the NPCs, where they release the viral genomic DNA and empty capsid shells can be observed to remain at the cytoplasmic side of the nuclear pore complex (Sodeik *et al.*, 1997). Subsequently, the association between the capsid and NPC was reconstituted *in vitro* by Ojala and colleagues. During these assays, the viral capsids were isolated and incubated with cytosol and purified nuclei. It was found the capsids bind to NPCs and the binding could be inhibited by anti-NPC antibodies (Ojala *et al.*, 2000).

The ejection of viral DNA from the capsid to the nucleus is called DNA uncoating. It was reported that up to 60-70% of capsids docking on NPCs released their DNA genome,

implying the interactions between the capsid and NPC plays an important role during this stage (Ojala *et al.*, 2000). It has been reported that the capsid protein pUL25 interacts with nucleoporins, which is important for DNA release into the nucleus (Pasdeloup *et al.*, 2009). In addition, some tegument proteins that travel together with the capsids towards the nucleus are involved in the DNA uncoating. For instance, VP1/2 is important in the DNA uncoating stage as it has been reported that mutation in the UL36 gene causes the accumulation of DNA containing capsids at NPCs (Batterson *et al.*, 1983; Ojala *et al.*, 2000). Furthermore it has been demonstrated that the proteolytic cleavage of VP1/2 is important for DNA release (Jovasevic *et al.*, 2008).

1.1.4.4 Viral gene expression and DNA replication

Following the initial entry, the tegument protein VHS encoded by the UL41 gene is released in the cytoplasm to induce the shut-off of host cell protein expression. This procedure inhibits host cellular gene expression and reserves the gene expression machinery for the virus. After uncoating, the viral DNA genomes circularise by ligating head to tail in the cell nucleus and serve as the templates for gene transcription and replication (Duyk *et al.*, 1985; Garber *et al.*, 1993; Strang & Stow, 2005). HSV-1 genes can be divided into three groups according to the length of time for the viral gene to generate its product: immediate early (IE or α), early (E or β) and late (L or γ) genes. Despite the classification of HSV-1 genes into three groups, all three classes of genes are expressed in a continuous pattern rather than stages that have clear time boundaries. Furthermore, the expression of the products of the earlier gene groups affects the expression of the later groups. Thus the whole gene expression can be described in a temporal cascade fashion.

Host RNA polymerase II is responsible for synthesis of all viral mRNA and VP16 is a strong transactivator that stimulates immediate early gene transcription (Campbell *et al.*, 1984). The immediate early gene expression happens before any viral protein synthesis and this process activates the transcription of early genes, which leads to the viral DNA replication. As a final stage of viral gene expression, the late genes expression is induced by the DNA replication process. ICP4 and ICP27 are two IE genes which are important for gene regulation. ICP4 is essential for all early and late genes, while ICP27 is required for the late genes. However, this is not a completely strict rule. For example, the products of IE gene also initiate the transcription of certain late genes (named early/late, leaky late or γ_1 genes) although the expression levels of these genes are up-regulated by the DNA

replication. The rest of the late genes which only express after the viral DNA replication are called true late or γ_2 genes (Taylor *et al.*, 2002).

After the expression of IE genes and before the onset of late genes, viral DNA replication is initiated. There are seven viral genes coding four protein complexes which have essential roles during HSV-1 replication. 1) Origin binding protein is the product of gene UL9. It has DNA helicase activity and is able to bind both *ori*L and *ori*S origins in the HSV-1 genome. 2) Single-stranded DNA (ssDNA) binding protein (also called ICP8) encoded by UL29, which is able to bind ssDNA and stimulate DNA polymerase and helicase-primase activities. 3) The heterotrimer helicase-primase complex encoded by the UL5, UL8 and UL52 genes. 4) The heterodimer DNA polymerase (that also has exonuclease activities) encoded by the genes UL30 and UL42. Although the other early gene products (including thymidine kinase encoded by the gene UL23) are not essential for viral DNA replication in tissue culture, they are important *in vivo*, especially in non-dividing cells such as neurons.

The structures of DNA molecules and replication complexes observed within the cell nuclei were described as replication compartments (Quinlan *et al.*, 1984). At the beginning of DNA replication, the origin-binding protein pUL9 binds to either oriL or oriS to unwind the DNA by its helicase activity. ICP8 is recruited to bind to ssDNA and together with pUL9 the other five DNA replication proteins are recruited to the replication fork to initiate the theta type replication. The subsequent process has been described as a 'rolling-circle' mechanism and the newly synthesised DNA molecules accumulating in the cell nucleus are 'head-to-tail' concatemers containing four isomers (Jacob *et al.*, 1979). These concatemers have to be cleaved into monomers for packaging into capsids (see section 1.1.2).

1.1.4.5 Capsid assembly and DNA packaging

HSV-1 capsid assembly starts in the cell nucleus after late gene expression. Some proteins required for this assembly stage, including VP26 (pUL35), VP23 (pUL18) and the major capsid protein VP5 (pUL19), would remain in the cytoplasm if expressed alone. By forming complexes with other viral proteins that contain nuclear localisation signals (NLS), these proteins arrive at the nucleus for assembly. For example, VP5 can be transported into the nucleus by the capsid triplex protein VP19C (pUL38), or the scaffolding protein pre-VP22a (also called ICP35 encoded by gene UL26.5) (Taylor *et al.*, 2002).

Electron microscopy studies have shown four distinct stages of capsids in herpesvirus infected cells. The precursor of the other types of capsids, procapsid, contains a roughly

spherical porous outer shell surrounding an inner protein core. A capsids consist of an icosahedral protein shell while B capsids have the same protein shell as A capsids plus an inner spherical protein core. C capsids also have the indistinguishable outer protein shell but with the inner protein core replaced with the viral DNA genome (Baines *et al.*, 2007a; Mettenleiter *et al.*, 2006).

After protein expression and transport to the nucleus, capsid assembly itself is a host cell independent process. Newcomb and colleagues purified three capsid components from insect cells and described an *in vitro* cell free system to assemble HSV-1 procapsids (Newcomb *et al.*, 1996). These three components are: 1) the building blocks for hexons and pentons VP5; 2) the triplexes VP19C and VP23; 3) a scaffolding protein pre-VP22a. Interestingly, a hybrid scaffolding protein containing the N-terminal 364 amino acids of the HCMV scaffolding protein (UL80.5 gene product) and only the C-terminal 25 amino acids of HSV-1 pre-VP22a, is able to perform the role of pre-VP22a highlighting the conserved nature of herpesvirus capsid assembly (Newcomb *et al.*, 1999; Oien *et al.*, 1997).

Newly synthesised HSV-1 genomes are in the form of concatemers (refer to section 1.1.4.4), which need to be cleaved into unit-length monomers to be packaged into capsid in the nucleus. There are a group of conserved proteins involved during this stage. The HSV-1 capsid portal complex is a ring-like dodecameric complex of the portal protein (pUL6). The portal complex is located at one of the 12 vertices on the icosahedral capsid and forms the channel for viral DNA packaging and possibly for genome release through nuclear pores during the initial stage of infection (Chang *et al.*, 2007; Mettenleiter *et al.*, 2006; 2009). pUL15, pUL28 and pUL33 are the sub-units of the terminase, which is able to recognise the portal complex. Terminase is able to drive the DNA into the capsid and its nuclease activity performs the cleavages in the concatemers at specific sites to generate single genomes. Additionally, pUL17 and pUL25 form a complex named the C capsid-specific complex (CCSC), which is located on the capsid surface. pUL17 has been reported to be important for cleavage and packaging of HSV-1 DNA (Salmon *et al.*, 1998) and pUL25 is required for encapsidation (McNab *et al.*, 1998). CCSC is also likely to be involved in selecting DNA containing C capsid for nuclear egress (Johnson & Baines, 2011). Other viral proteins (such as pUL32) are also involved but their exact roles are still unclear (Mettenleiter *et al.*, 2006; 2009; Taylor *et al.*, 2002).

Interestingly the portal complex in the HSV-1 capsid, the process of capsid formation initiated by the scaffold protein and the viral genome cleavage/encapsidation all share similarities with DNA bacteriophage. This suggests that herpesvirus and bacteriophage

may have a common ancestor (Chang *et al.*, 2007; Mettenleiter *et al.*, 2006; 2009; Rixon, 2008).

1.1.4.6 Assembly and egress

Capsid assembly and viral genomic DNA packaging result in the formation of mature capsids in the cell nucleus. In order to acquire the numerous tegument proteins and the envelope required to form mature virus particles and subsequently be released from the infected cell, capsids encounter several physical obstacles within the highly structured host cell. For instance, translocation through the dense stable nuclear lamina structure lining the inner side of INM and the double membrane nuclear envelope, as well as the transport across the long distance of the host cytoplasm and being released through the plasma membrane as free virions. The virus assembly and egress process involves at least five stages: primary envelopment, de-envelopment, tegumentation, secondary envelopment and release through exocytosis.

Primary envelopment

The primary envelopment is the process where nucleocapsids bud into the INM and form primary virions in perinuclear space. The nuclear envelope is the same barrier that capsids face when they need to deliver the viral genome to the nucleus during entry (section 1.1.4.3), although in the opposite direction. Capsids, with a diameter approximately 125 nm, are too large to transport through the NPC. Herpesviruses have evolved the strategy where incoming capsids utilise NPCs to deliver the viral genomes into the nucleus, leaving the empty capsid shells in the cytoplasm. However, the progeny capsids assembled in the nucleus need to cross the nuclear envelope and enter the cytoplasm in an intact form and so different strategies are required to overcome the same barrier.

There are three lamin proteins (A, B and C) that make up the nuclear lamina structure. HSV-1 has evolved several mechanisms to disrupt the nuclear lamina at specific sites and this has been recently reviewed by Johnson and Baines: 1) the nuclear envelopment complex (NEC) formed by pUL31 and pUL34 is able to recruit cellular protein kinases to phosphorylate lamin B and cause disassembly of the lamina. 2) HSV-1 pUS3 and pUL13 both have kinase activities, and are able to catalyse the phosphorylation of lamin A and lamin C leading to solublisation of the lamins. 3) the nuclear lamina is formed by interactions between the lamins and lamin receptors, while HSV-1 pUL31 and pUL34 are able to bind to lamin A and lamin C. These interactions disrupt the normal lamin-lamin interactions to the benefit of the approaching capsids. 4) the viral/cellular kinases recruited

to those sites cause phosphorylation in lamin receptors and interfere with the lamin-receptor interactions (Johnson & Baines, 2011). After disruption of the nuclear lamina, the nucleocapsids may engage with certain tegument proteins (such as VP16) and bud through the INM resulting in primary enveloped virions in the space between the INM and ONM (also called perinuclear space) (Naldinho-Souto *et al.*, 2006). It has been found that gD and VP22 also can be detected in primary virions suggesting possible functions of these proteins during this stage (Padula *et al.*, 2009).

De-envelopment

There are two models for the subsequent pathway from the primary envelopment stage to the release of virus particles into the extracellular space: the lumenal pathway (also called "single envelopment" pathway) and the primary and secondary envelopment model (also called envelopment-deenvelopment-reenvelopment pathway, "two-step envelopment" pathway or reenvelopment model). The lumenal pathway model proposes that the primary virions travel through the lumen of endoplasmic reticulum (ER), which is continuous with the nuclear envelope, followed by vesicular transport through the Golgi apparatus and release to extracellular area through the normal secretory pathway (Enquist *et al.*, 1998; Taylor *et al.*, 2002). Some early evidence of the lumenal pathway is that enveloped particles within vesicles in cytoplasm were observed by electron microscopy (Roizman & Sears, 2001). However, a series of subsequent electron microscopy studies, data on the lipid content of the viral envelope compared to the nuclear membrane, and immunoelectron microscopy of ER-retrieved glycoproteins (Skepper *et al.*, 2001; van Genderen *et al.*, 1994) support the primary and secondary envelopment model and this has become the most widely accepted model of HSV-1 assembly and egress [reviewed in (Johnson & Baines, 2011; Mettenleiter, 2002; Mettenleiter *et al.*, 2006; 2009)]. The research in this thesis will be described and analysed based on this model.

In the secondary envelopment model, primary enveloped virions undergo a de-envelopment process. This de-envelopment is the process of membrane fusion involving the envelope of primary virions and the ONM. The first description of "de-envelopment" events in herpesvirus assembly and egress were made in the 1960s when Stackpole studied frog herpesvirus by electron microscopy and autoradiography using ^{3}H-thymidine. Viral particles were observed being enveloped by budding through the INM, and subsequently being de-enveloped in passing through the ONM and reaching the cytoplasm (Mettenleiter, 2004; Skepper *et al.*, 2001; Stackpole, 1969).

Recently, it has been shown that the tegument protein pUS3 is associated with primary enveloped virions in the perinuclear space (Padula *et al.*, 2009; Reynolds *et al.*, 2002). Deletion of US3 from the viral genome resulted in accumulation of primary virions in the perinuclear space (Farnsworth *et al.*, 2007). These reports imply pUS3 is likely to be involved in HSV-1 de-envelopment stage. In addition, gB and gH are also thought to be involved in the de-envelopment of HSV-1. Simultaneous mutations in both gB and gH led to the accumulation of primary virions in the perinuclear space, a phenotype similar to the observations with the US3 deletion virus. However, different from the membrane fusion during entry which requires both gB and gH/L, a single mutation in gB or gH/L did not significantly affect the de-envelopment stage (Farnsworth *et al.*, 2007). These data imply that the membrane fusion of primary virion envelope and ONM during de-envelopment is different from viral envelope fusion with host membranes during the initial entry and these two fusion processes require different viral proteins. Furthermore, pUS3 kinase activity has been shown to regulate gB mediated nuclear egress and down-regulates the cell surface expression of gB through phosphorylation in HSV-1 (Kato *et al.*, 2009; Wisner *et al.*, 2009). However, it is important to note that different from HSV-1, simultaneous double deletion combinations of gB, gD and gH/L did not show any effect on PRV nuclear egress (Klupp *et al.*, 2008), suggesting potential different mechanisms between these two alphaherpesviruses. The de-envelopment stage is one of the most poorly understood aspects of herpesvirus assembly and further research is needed to determine the mechanisms.

Tegumentation

Following the de-envelopment, the viral capsids are release into the cytoplasm, where they are coated with a layer of tegument proteins (a process called tegumentation). The tegument proteins which are closely associated with capsids are incorporated first to form the inner tegument layer and through interactions between the tegument proteins, the outer tegument layer is assembled. However, many tegument proteins have been shown to be nonessential in tissue culture (summarised in Table 1.3), and details of how the tegumentation occurs around the capsid are unclear. The assembly of outer tegument is thought to be closely related to the secondary envelopment stage and therefore is an important stage for the final formation of mature virus particles.

Three tegument proteins, pUL36, pUL37 and pUS3, constitute the inner tegument and they initially coat the nucleocapsid during tegumentation (Mettenleiter, 2006; Mettenleiter *et al.*, 2006). It has been shown that pUL37 directly interacts with pUL36 (Mijatov *et al.*,

2007; Vittone *et al.*, 2005). These two tegument proteins are both closely associated with capsids as the inner layer and remain attached to the capsids during the transport to the nucleus after entry. The interactions between pUL36 and the capsid protein pUL25 as well as the possible interaction of pUL37 and the capsid protein pUL35 are direct evidence for the early incorporation of pUL36 and pUL37 during tegumentation (Coller *et al.*, 2007; Lee *et al.*, 2008). pUS3 is a component of the primary virions in alphaherpesviruses and there is evidence for possible early involvement of pUS3 to regulate the function of pUL31 and pUL34 in the nucleus (Kato *et al.*, 2006; Reynolds *et al.*, 2002). Therefore, it is likely that pUS3 is incorporated as a tegument protein at an early stage. Furthermore, due to the essential role and multiple functions (listed in Table 1-3), pUL36 (and possibly pUL37) may function as a scaffold to recruit other tegument proteins to be assembled around capsids. The deletion of either UL36 or UL37 genes in the HSV-1 genome blocks tegumentation of the capsid in the cytoplasm and an accumulation of unenveloped capsids has been observed in infected cells (Roberts *et al.*, 2009). As the formation of C capsids was not affected in the absence of UL36 or UL37, it implies that the viral life cycle stages (including capsid assembly, DNA packaging and nuclear egress) before the capsids arrival in cytoplasm are not affected, but these proteins are important for the further addition of tegument. For example, direct interaction between HSV-1 pUL36 and pUL48 has been demonstrated and the expression of pUL36 is required for the association of pUL48 with capsids in infected cells (Ko *et al.*, 2010; Vittone *et al.*, 2005). However, whether the addition of pUL36 occurs in the nucleus or in the cytoplasm is still unclear.

Compared to the inner tegument layer, the incorporation of the outer tegument layer is much more complicated and it potentially involves 20 tegument proteins with significant redundancy (Loret *et al.*, 2008). It is conceivable that multiple ways are available for the virus to complete the outer tegument assembly. More evidence has been reported from recent studies but the details of this process are still not clear. Thus, the tegument proteins with high abundance and/or important functions will be focussed on in this introduction.

Firstly, HSV-1 pUL48 (VP16) is essential for replication in tissue culture, although it is not conserved among the three sub-families of *Herpesviridae*. It has been shown that VP16 is present in perinuclear virions in HSV-1 (Naldinho-Souto *et al.*, 2006), which implies an early involvement of VP16. However, it is not clear whether this is related to other VP16 functions in the nucleus or the incorporation of VP16 prior to the nuclear egress constitutes the population of VP16 in the tegument. Interestingly, studies on PRV showed the deletion of pUL48 did not have any effect on the association of pUL36 and pUL37

with the nascent capsids, which suggests that the incorporation of the inner tegument layer occurs earlier than pUL48. Furthermore, L particles (virus light particles without capsids) generated in cells infected by PRV with UL48 deletion were found to contain pUL46, pUL47 and pUL49 but not pUL36 or pUL37 (Fuchs *et al.*, 2002). These findings imply pUL48 might be the "linker" for the inner tegument layer to the outer layer of tegument. Indeed, pUL48 has been shown to interact with tegument proteins pUL46, pUL47, pUL49 as well as pUL41 (Elliott *et al.*, 1995; Smibert *et al.*, 1994; Vittone *et al.*, 2005). These interactions provide the possibility for pUL48 to recruit the outer tegument proteins.

Secondly, the complex formed by pUL11, pUL16 and pUL21 may be able to link the capsids and envelope during secondary assembly. pUL11 has been reported to be membrane associated and bind to the cytoplasmic side of cellular membranes (Baird *et al.*, 2008), while pUL21 was shown to associated with A, B and C capsids (Takakuwa *et al.*, 2001). In addition, pUL16 interacts with both pUL11 and pUL21 to form a complex (Table 1.3). These data suggest the possibility for this complex to directly link the capsids and envelope. However, all of these three tegument proteins are not essential for HSV-1 in cell culture. Therefore the link provided by this complex is dispensable, although it may offer an alternative route to pUL48 for capsids-outer tegument/envelope association and this might be of more importance *in vivo*.

Secondary envelopment

The secondary envelopment is also called re-envelopment, final envelopment or cytoplasmic assembly. It is the process where tegumented capsids bud into the lumen of membrane compartment in the cytoplasm and form mature virus particles. During the process the virus acquires the envelope embedded with various glycoproteins. Many different viral envelope proteins (gB, gC, gD, gE, gG, gH, gI, gJ, gK, gL, gM, gN/pUL49.5, pUL20, pUL45, pUL56, pUS9) have been identified in mature HSV-1 particles, and they need to be correctly localised to the appropriate cytoplasmic assembly sites to be incorporated into virions (Adams *et al.*, 1998; Foster *et al.*, 2001b; Ghiasi *et al.*, 1998; Loret *et al.*, 2008). Many herpesvirus envelope proteins contain targeting signals such as tyrosine-based motifs [YXXΦ, where X = any amino acid and Φ = a bulky hydrophobic residue such as phenylalanine (F) and tryptophan (W)] that are likely to play important roles in their efficient endocytosis and TGN localisation through mediating interactions with the clathrin adaptor proteins [reviewed in (Favoreel, 2006)]. Functional YXXΦ endocytosis motifs have been demonstrated to be present in the HSV envelope proteins gB and gE (Alconada *et al.*, 1999; Beitia Ortiz de Zarate *et al.*, 2007; Fan *et al.*, 2002). YXXΦ motifs

have also been identified in the cytoplasmic domains of the HSV-1 envelope proteins gM, gK and UL20, all of which are localised to the TGN (Crump *et al.*, 2004; Foster *et al.*, 2004). However, other HSV-1 envelope proteins do not contain any recognisable targeting motifs and when expressed in the absence of other viral proteins (gD and gH/L for example) they are localised to the plasma membrane. gD and gH/L together with gB constitute the entry machinery that is essential for fusion of the virus envelope with cellular membranes (Heldwein & Krummenacher, 2008). It is therefore critical for the production of infectious viruses that both gD and gH/L are correctly localised to the appropriate intracellular membrane compartments in order to be incorporated into the virion envelope. This is demonstrated by the reported experiment where gD or gH is artificially retained in the endoplasmic reticulum. Despite normal levels of enveloped particle release, the virions are significantly less infectious because they do not contain detectable gD or gH respectively (Browne *et al.*, 1996; Whiteley *et al.*, 1999).

Membrane protein trafficking in eukaryotic cells involves a series of dynamically interconnected membrane structures including the ER, Golgi apparatus, plasma membrane and vesicles generated through the membrane deformation and remodelling. Vesicles are cellular transporting vehicles for proteins cargos [reviewed in (Bonifacino & Rojas, 2006; Seaman, 2008)]. Many electron microscopy studies have shown capsids budding into membrane compartments and virion-containing vesicles and it is believed that HSV-1 hijacks this secretory pathway to obtain envelope and complete egress (Mettenleiter, 2004; Mettenleiter *et al.*, 2006; 2009). There are four possible sites for the capsids to acquire envelope proteins and form mature virus particles within a cellular vesicle: 1) TGN; 2) early endosome; 3) tubular endosomal network; 4) late endosome.

The exact assembly site in cytoplasm is still under debate [reviewed in (Johnson & Baines, 2011; Mettenleiter *et al.*, 2006; 2009)]. Multiple glycoproteins have been shown to co-localise with TGN markers in immunofluorescence microscopy studies and nascent viral capsids also appear to be localised at the TGN. This finding supports the hypothesis that the viral final assembly occurs at TGN where the glycoproteins are incorporated into the virions (the TGN assembly model) (Turcotte *et al.*, 2005). Recently, studies performed by Elliott and colleagues using horseradish peroxidise labelling and electron microscopy have challenged the TGN assembly model, where they have shown HSV-1 capsids are wrapped by tubules derived from the plasma membrane. Furthermore, the tubules have been characterised as newly endocytosed envelope protein containing plasma membrane, but

not derived from the exocytic pathway (Elliott *et al.*, IHW conference presentation 2010, 2011).

Physically located in between the capsid and virus envelope, the interactions between the outer tegument layer with envelope proteins are important for the secondary envelopment. It has been shown that pUL48 interacts with the cytoplasmic tails of HSV-1 gB, gD and gH (Gross *et al.*, 2003; Kamen *et al.*, 2005; Zhu & Courtney, 1994). In addition, pUL49 has been shown to interact with gE and gM (Stylianou *et al.*, 2009). These interactions may initiate the recognition of tegumented capsids and viral envelope protein embedded host membrane. In addition, viral proteins (most likely tegument and envelope proteins) also need to interact with host cellular proteins to facilitate secondary envelopment.

Exocytosis and release

Secondary assembly results in virion-containing vesicles and the mature virions are transported within these vesicles to the plasma membrane and released when the vesicle membrane fuses with the plasma membrane. Little information is known about the function of viral proteins involved in this stage. Presumably, the virus hijacks the cellular secretory pathway (exocytosis) for the release. Questions remain about the transport of the vesicles for subsequent release at the cell surface. The possible cytoplasmic assembly sites would all allow the virion-containing vesicles to be either transported "retrogradely" from endosomal membrane or "anteretrogradely" from the TGN directly to plasma membrane for release. In addition to the movement of cellular vesicles along microtubule tracks from the TGN to the plasma membrane, a transport network of actin filaments has recently been shown as a new dynamic and flexible way for intracellular vesicle movement (Schuh, 2011; Toomre *et al.*, 1999). Unfortunately for the host cells, these cellular transport networks could be hijacked by the virus.

Of the many viral and cellular factors involved in the viral assembly and egress, this thesis is concerned with the roles of glycoprotein M (gM) and the cellular Endosomal Sorting Complex Required for Transport (ESCRT).

1.2 Glycoprotein M and cytoplasmic assembly

1.2.1 Gene and protein predicted structure

Glycoprotein M (gM) is the product of gene UL10, which is located at nucleotide position 23204-24625 according to the online sequence of human herpesvirus 1 complete genome

(strain 17, Refseq: NC_001806). UL10 is a 1422 bp intronless gene encoding a protein of 473 aa and it has been described as a late (γ) gene (Baradaran *et al.*, 1994). However, the possible early function of gM at the nuclear membrane that has recently been suggested implies it might be an early gene (Zhang *et al.*, 2009a). In early research work, the UL10 gene product was predicted to be a membrane protein on the basis of the extent and size of the hydrophobic domains of the predicted protein (Baines & Roizman, 1991). Subsequent research revealed that the product of UL10 gave a sharp band (~50 kDa, immature form) and a broad band (~53-63 kDa, mature form) detectable by western blotting using a rabbit polyclonal antiserum. This protein was found to be N-glycosylated because both of these bands were labelled with [^{3}H] glucosamine and treatment with tunicamycin (which blocks the synthesis of all N-linked glycoproteins) resulted in a single precursor band (~47 kDa). Thereafter the UL10 protein has been designated glycoprotein M (Baines & Roizman, 1993).

UL10 is conserved throughout the *Herpesviridae*. Genomic comparison has suggested that the three sub-families (α, β and γ) were descended from a common ancestor up to 400 million years ago (McGeoch *et al.*, 2006), which implies that this gene has existed for a similar time. Despite the high conservation suggesting important functions of this gene, the exact functions of gM have not yet been clearly revealed. It has been predicted that gM is a type III membrane protein with eight transmembrane domains (Crump *et al.*, 2004).

1.2.2 Potential functions

As described in section 1.1.4.6, numerous glycoproteins need to be correctly localised to the assembly compartment membrane. HSV-1 gM contains four potential YXXΦ motifs within its predicted C-terminal cytoplasmic domain: $YDEV_{426}$, $YAKI_{438}$, $YDTV_{454}$ and $YSTV_{470}$. gM localises predominantly to the TGN when expressed in the absence of other viral proteins and by analogy to cellular TGN proteins with similar trafficking motifs, gM is likely to be actively transported between the TGN and the plasma membrane (Crump *et al.*, 2004). Previous work in the laboratory has demonstrated that gM may play a role in guiding other viral glycoproteins with no cellular targeting motifs to the assembly compartment. For example, both gD and gH/L can be efficiently internalised and targeted to the TGN by the co-expression of gM in transfection assays (Crump *et al.*, 2004). These data suggest that gM can directly or indirectly interact with gD or gH/L and drive their endocytosis and TGN localisation through the activity of targeting motifs present in the

cytoplasmic domain of gM. This may be one activity by which the essential envelope proteins gD and gH/L are correctly localised to sites of secondary envelopment.

Despite being one of the few conserved envelope proteins in the *Herpesviridae*, gM is not essential for growth in tissue culture of the alphaherpesviruses HSV-1 (Baines & Roizman, 1991; MacLean *et al.*, 1993), PRV (Dijkstra *et al.*, 1996), BHV-1 (Konig *et al.*, 2002), varicella-zoster virus (VZV) (Yamagishi *et al.*, 2008), infectious laryngotracheitis virus (ILTV) (Fuchs & Mettenleiter, 1999), EHV-1 (Osterrieder *et al.*, 1996) and equine herpesvirus type 4 (EHV-4) (Ziegler *et al.*, 2005). However, gM is essential for replication of the alphaherpesvirus Marek's disease virus (MDV) (Tischer *et al.*, 2002), the betaherpesvirus HCMV (Hobom *et al.*, 2000) and the gammaherpesvirus murine gammaherpesvirus 68 (MHV-68) (May *et al.*, 2005).

Despite the fact that gM is not essential, it has been reported that the mutant of HSV-1 strain 17 by insertion of *lacZ* into UL10 resulted in approximately 10-fold lower yields at low multiplicity (0.001 PFU/cell) and 2 to 10-fold at high multiplicity (MacLean *et al.*, 1991). A mutant virus with 972 bp deletion within the gene UL10 was created from wild type HSV-1 strain F and according to single-step growth analysis, this virus had approximately 10-fold lower yields than wild type strain F in both BHK and Vero cells (Baines & Roizman, 1991). However a mutation of UL10 in HSV-1 strain SC16 was reported to have normal plaque sizes and no reduction in growth compared to parental virus in both Vero and BHK cells at MOI of 10 PFU per cell (Browne *et al.*, 2004). One potential issue with this gM deletion mutant is that the *lacZ* insertion site is relatively close to the 3' end of the UL10 ORF and an altered polypeptide containing the first 380 amino acids of gM could potentially be expressed. Such a protein product would include all 8 of the predicted transmembrane domains of gM and thus could have some activity. More recently, a BAC cloned HSV-1 strain KOS with a deletion corresponding to codons 234-442 of UL10 has been constructed and this mutant virus had small plaques, an approximate 5-fold reduction in infectious virus production in Vero cells but a much greater effect of >100-fold decrease in RK13 cells infected at 5 PFU/cell (Leege *et al.*, 2009). Interestingly the authors also observed fewer extracellular virus particles and increased numbers of unenveloped capsids in the cytoplasm in HSV-1ΔgM infected cells suggesting a role of gM in secondary envelopment.

An *in vivo* study using a mouse model reported that HSV-1 with gM deletion was capable of establishing latency, although the virus growth at the periphery and spread to and/or growth within the nervous system were impaired (MacLean *et al.*, 1993). Therefore, HSV-1

gM is required for efficient infection both *in vitro* and *in vivo*, although gM is not essential in both cases.

1.3 ESCRT machinery

During the cytoplasmic assembly stage in the HSV-1 life cycle, the budding/wrapping of tegumented capsids to form mature virus particles requires membrane remodelling at the assembly sites. Previous data from the laboratory has demonstrated that the Endosomal Sorting Complex Required for Transport (ESCRT) machinery plays an important role during HSV-1 assembly (Crump *et al.*, 2007; Pawliczek & Crump, 2009).

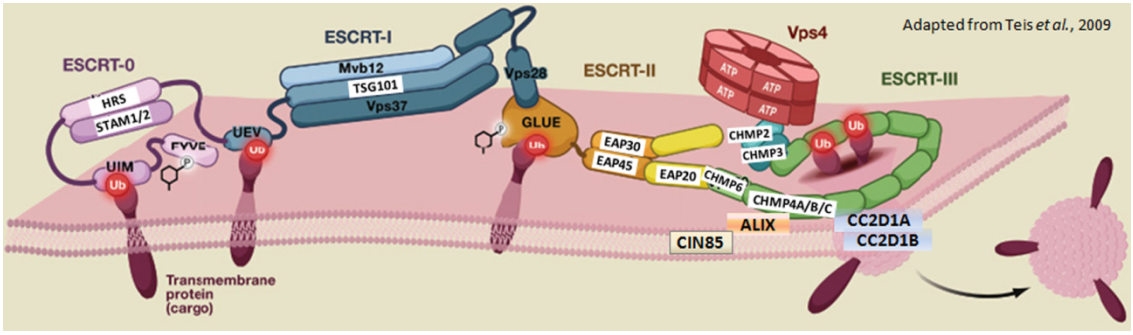

Figure 1.2: Diagram of ESCRT machinery and its associated proteins.

ESCRT is a cellular machinery consists of four multimeric protein complexes: ESCRT-0, -I, -II and -III (Figure 1.2). This machinery controls the sorting of endosomal cargo proteins into intraluminal vesicles (ILVs) of multivesicular bodies (MVBs). The ESCRT machinery is conserved from yeast to humans and the individual proteins forming the complexes were firstly identified in yeast cells.

During the studies of the vacuolar protein sorting pathway in yeast, the research groups of Stevens and Emr identified numerous genes in the model yeast system *Saccharomyces cerevisiae* [reviewed by (Coonrod & Stevens, 2010; Henne *et al.*, 2011)]. The yeast vacuole is regarded as the equivalent organelle of the mammalian lysosome. The loss of genes that displayed vacuolar protein sorting defects, termed 'vps' genes, resulted in certain vacuolar glycoproteins not being sorted to the vacuolar lumen but mis-localised to the cell surface. These genes were classed into three different groups (A, B and C), initially by Emr and colleagues. Subsequently, Stevens and colleagues identified in total 41 yeast vps mutants that were divided into six classes (A to F). The class E vps was named because disruption

of these gene products leads to formation of aberrant endosome-like compartments and it is the study of these genes that led to the discovery of the ESCRT complexes.

Subsequently, many homologous ESCRT proteins have been identified in a wide variety of organisms including humans, providing evidence for the extensive conservation of this machinery. Furthermore, ESCRT-like proteins have been identified in archaea, which function in the scission of the membrane neck between dividing cells suggesting an ancient origin for this machinery (Samson & Bell, 2009). The high conservation of ESCRTs implies the important functions of them in a wide range of living organisms.

In this section, the names and known functions of the four core ESCRT complexes will be introduced, followed by the relationship discovered for ESCRT and two cellular biological events as well as retrovirus budding (Field & Dacks, 2009). Finally, the crucial stage of membrane scission and the role of proteins of the ESCRT III complex will be described according to the current evidence in the literature. Research into ESCRT proteins is a rapidly growing research field and many review papers contain excellent and detailed information about ESCRT function in three major pathways: MVB formation, retrovirus budding and cytokinesis (Caballe & Martin-Serrano, 2011; Henne *et al.*, 2011; Martin-Serrano & Neil, 2011; Morita & Sundquist, 2004; Weiss & Gottlinger, 2011).

1.3.1 ESCRT complexes and their functions

Ubiquitin conjugation is one of the well characterised signals for membrane protein sorting during endocytosis and early endosomal protein trafficking. The ESCRT machinery can interact with ubiquitinated proteins via ubiquitin-binding domains and engage in the sorting of these protein cargos to MVBs for lysosome degradation. It has been shown that ubiquitination is necessary and sufficient to direct many proteins from the limiting membrane of the endosome into MVB vesicles. From the start of cargo recognition to the final degradation, it involves various interactions of the four ESCRT complexes, VPS4 ATPase and potentially many ESCRT associated proteins (Hicke & Dunn, 2003; Katzmann *et al.*, 2001; Morita & Sundquist, 2004).

ESCRT-0

This complex contains HRS (hepatocyte growth factor-regulated tyrosine kinase substrate) and STAM1/2 (signal transducing adaptor molecule 1/2) proteins (Vps27 and Hse1 in yeast) (Bilodeau *et al.*, 2002). It was proposed as an extension of the initially identified ESCRT-I, -II and –III complexes. ESCRT-0 complex binds to ubiquitin and is involved in the initial cargo recognition. It has been shown that this complex is a 1:1 heterodimer and

the hybrid structure of endogenous ESCRT-0 core complex in HeLa cells showed high similarity to yeast (Ren *et al.*, 2009). HRS contains two important domains: the UIM (ubiquitin-interacting motif) domain binds to ubiquitinated transmembrane protein cargo and the FYVE (Fab-1, YGL023, VPS27 and EEA1) domain binds to the lipid phosphatidylinositol 3-phosphate (PI3P) that is enriched on the late endosomal membrane. ESCRT-0 itself does not deform the membrane but it recruits late-acting ESCRT complexes and initiates the MVB pathway [reviewed in (Wollert & Hurley, 2010)].

ESCRT-I

The ESCRT-I complex is also involved in the cargo recruitment stage. It was initially characterised in yeast as a 350 kDa complex composed of Vps23, Vps28 and Vps37 proteins ten years ago (Katzmann *et al.*, 2001). Subsequently, Mvb12 (multivesicular body sorting factor of 12 kDa) was identified as another subunit of ESCRT-I (Audhya *et al.*, 2007; Oestreich *et al.*, 2007). Human ESCRT-I is a similar heterotetramer consisting of TSG101, VPS28, VPS37A/B/C/D and hMVB12A/B (VPS37 and hMVB12 have two or more isoforms) (Bishop & Woodman, 2001; Morita *et al.*, 2007a). The crystal structure of the yeast ESCRT-I complex shows an elongated shape with two end domains (Kostelansky *et al.*, 2007). ESCRT-I links ESCRT-0 and ESCRT-II complexes through the following interactions: the UEV domain of TSG101 binds to PTAP/PTAP-like motifs of HRS in ESCRT-0 and VPS28 interacts with the GLUE domain of EAP45 in the ESCRT-II complex. The structure of the TSG101 UEV domain in complex with the PTAP motif in HIV-1 Gag has been determined (Pornillos *et al.*, 2002), which revealed that HIV mimics the interaction between ESCRT-0 and TSG101 to recruit this machinery (Henne *et al.*, 2011; Hurley & Emr, 2006).

ESCRT-II

ESCRT-II is a ~155 kDa heterotetramer formed of EAP45, EAP30 and two EAP20 molecules (Vps36, Vps22 and two Vps25 in yeast) (Babst *et al.*, 2002). Together with ESCRT-I, these complexes are responsible during the cargo recruitment and initial membrane deformation. The structure of this complex is of a 'Y' shape (Im & Hurley, 2008; Teo *et al.*, 2004). EAP45 and EAP30 form the base and two copies of EAP20 form the arms. The GLUE domain of EAP45 binds PI3P, VPS28 and ubiquitinated membrane proteins, demonstrating the link of this complex to ESCRT-I and protein cargo recognition. EAP20 interacts with CHMP6 of the ESCRT-III complex, which suggests a

role of ESCRT-II in initiating ESCRT-III action (Teo *et al.*, 2004; Wollert & Hurley, 2010; Yorikawa *et al.*, 2005).

ESCRT-III

The ESCRT-III complex is required for the last steps of MVB sorting, cargo sequestration, and MVB vesicle formation. It is still unclear about the detailed mechanisms underlining the processes, including the shaping of the membrane into buds and solutions to the energy barrier during the scission event that separates the membranes. However, the ESCRT-III complex has been shown to be important for the membrane scission stage. The results observed from *in vitro* studies carried out using giant unilamellar vesicles (GUVs) by Wollert and colleagues have revealed that the ESCRT-III complex is crucial for the scission stage. The researchers observed that the purified yeast ESCRT-III component Snf-7 (sucrose non-fermenting, the homologue of CHMP4 proteins in human) plays a key role for membrane pinching, as ILVs detached within GUVs after the addition of purified Snf-7 protein (Wollert *et al.*, 2009).

ESCRT-III assembles into a highly ordered filament-like hetero-oligomer and, different from the other ESCRT complexes, it is not a stable complex. Therefore there is as yet no crystal structure of the entire complex. Studies of the yeast ESCRT-III component has revealed that a transient complex of 450 kDa formed on endosomes (Teis *et al.*, 2008). The mammalian subunits of ESCRT-III are named as CHarged Multivesicular body Proteins (CHMPs), although they were originally indentified as CHromatin-Modifying Proteins (Piper & Katzmann, 2007). There are four key subunits: CHMP6, CHMP4A/B/C, CHMP3 and CHMP2A/B (Vps20, Snf7, Vps24 and Vps2 in yeast). As ESCRT-III proteins have a positively charged N terminus and a negatively charged C-terminus, intramolecular interactions between these termini form an autoinhibited status (Bajorek *et al.*, 2009; Lata *et al.*, 2009). Studies of the yeast proteins have demonstrated ESCRT-III activation is initiated by the binding between EAP20 and CHMP6 (Vps20) (Teo *et al.*, 2004). CHMP6 nucleates the homo-oligomerisation of CHMP4A/B/C (Snf-7 in yeast) proteins into circular filaments which have been observed by electron microscopy and they are thought to constitute the neck of the membrane bud and to be sufficient to allow scission (Hanson *et al.*, 2008). During this process, it has been shown that the oligomerisation of CHMP4A/B/C requires both interactions with the cellular membrane and CHMP6. To terminate CHMP4A/B/C oligomerisation the filaments are capped by CHMP3 (Vps24 in yeast), which further recruits CHMP2A/B (Vps2 in yeast) and initiates VPS4-dependent ESCRT-III disassembly (Saksena *et al.*, 2009; Teis *et al.*, 2008).

VPS4 complex

VPS4 was firstly identified as a 48 kDa protein belonging to the protein family of AAA (ATPase associated with various cellular activities) ATPases from the studies in yeast cells. It has been shown that the loss of ATPase activity of VPS4 results defects in vacuolar protein transport (Babst *et al.*, 1997). It has two isoforms (A and B) in human cells (Scheuring *et al.*, 2001). VPS4 is the energy providing complex in the ESCRT machinery and disassembles ESCRT-III into monomeric subunits and catalyses the final step of the MVB pathway (Lata *et al.*, 2008; Saksena *et al.*, 2009). However, it is still unclear how the protein oligomerises into an active ATPase that is associated with the ESCRT-III complex. It has been reported that the N-terminal MIT (microtubule-interacting and trafficking) domain of VPS4 interacts directly with the C-terminal MIMs (MIT interacting motifs) of ESCRT-III subunit Vps2 (CHMP2A/B) (Stuchell-Brereton *et al.*, 2007; Vajjhala *et al.*, 2007). Furthermore, structural association has been shown between VPS4 and LIP5 (Vta1 in yeast), which contains two MIT domains, and this interaction may initiate the assembly of the active VPS4 and enhance the activity of VPS4 to facilitate the ESCRT-III disassembly (Yang & Hurley, 2010).

ESCRT associated proteins

In addition to the many proteins that form the core complexes of the ESCRT machinery, there are also many ESCRT associated cellular factors that have been identified (Agromayor *et al.*, 2009; Doyotte *et al.*, 2008; Tsang *et al.*, 2006). In this section, the reported links and functions of four ESCRT associated proteins (ALIX, CIN85, HD-PTP and CC2D1A/1B) will be presented, which will be closely related to the studies and analysis in Chapter 3 and Chapter 4.

ALIX (apoptosis-linked gene-2 interacting protein X) is also named as AIP1 and both of these names come from its interacting partner ALG-2 (apoptosis-linked gene-2), which was initially found to be involved in apoptotic signalling. ALIX has a Bro1 domain at its N-terminal region, a "V" shaped central domain composed of two extended helix bundles and a C-terminal proline-rich domain (Fisher *et al.*, 2007; Usami *et al.*, 2007). The yeast orthologous protein is Bro1. ALIX was also found to be engaged in the ESCRT mediated MVB pathway through direct interactions. ALIX interacts with ESCRT-I component TSG101 through its C-terminal prolin-rich domain, while the N-terminal Bro1 domain interacts with the C-terminus of ESCRT-III proteins CHMP4A/B/C (McCullough *et al.*, 2008). Therefore ALIX is able to act as a bridge between ESCRT-I and ESCRT-III

complexes. In addition, the interaction between CHMP4s and ALIX is thought to stabilise the CHMP4 oligomerisation (Peck *et al.*, 2004). Gag proteins encoded by retroviruses (such as HIV-1) contain YPXnL (Xn indicates 1-3 unspecified amino acid) motifs, which can directly bind to ALIX and facilitate virus budding (Strack *et al.*, 2003).

About ten years ago, CIN85 (Cbl-interacting protein of 85 kDa) was initially characterised as a novel adaptor protein that interacts with c-Cbl (Take *et al.*, 2000). It has been recently reported that CIN85 also binds to the C-terminal proline-rich domain of ALIX (Usami *et al.*, 2007). As this interaction may modulate the activity of ALIX, CIN85 has been included as an ESCRT-associated protein.

HD-PTP was identified as a novel protein tyrosine phosphatase (PTP) from human cDNA, and is also called type N23 protein tyrosine phosphatase (PTPN23). According to the amino acid sequence, it has a similar N-terminal domain to yeast Bro1 and human ALIX. Similarly as ALIX, the Bro1 domain of HD-PTP also been shown to interact with the ESCRT-III component CHMP4B. Furthermore, depletion of HD-PTP by siRNA was reported to impair endosomal cargo sorting and disrupt the morphogenesis of MVBs (Doyotte *et al.*, 2008; Toyooka *et al.*, 2000).

CC2D1A (coiled-coil and C2 domain containing 1A) is also called Freud-1 (5' repressor element under dual repression binding protein-1), and has been reported to be involved in regulating expression of the 5-hydroxytryptamine (serotonin) receptor 1A (5-HT1A) gene in neuronal cells (Ou *et al.*, 2003). CC2D1B (coiled-coil and C2 domain containing 1B, also called Freud-2), which shares 50% amino acid identity with CC2D1A, was also identified to be involved in 5-HT1A regulation as a repressor (Hadjighassem *et al.*, 2009). It has been shown that the regulation in both cases were at the gene expression stage. Furthermore, studies performed on Drosophila have shown that C2 domain binds to membrane of endosomes and homologues of CC2D1A/1B play roles in the regulation of endosomal trafficking (Gallagher & Knoblich, 2006; Jaekel & Klein, 2006). Additionally, CC2D1A has been reported to interact with all three CHMP4 isoforms according to a yeast two-hybrid study (Tsang *et al.*, 2006). Hence, it is plausible that CC2D1A, and potentially its homologous protein CC2D1B, may be involved in regulating cellular receptor(s) through the interaction with ESCRT machinery at a protein level.

Many other ESCRT-associated proteins also have been reported. In addition to ALIX and HD-PTP mentioned above, there are other Bro1 domain-containing proteins, Brox and Rhophilin (Popov *et al.*, 2009). Human increased sodium tolerance (hIST) has been shown

to interact with VPS4, CHMP1A/B, LIP5, SPG20 and the MIT domain-containing proteins (MITD1, AMSH, UBPY and Spastin) (Agromayor *et al.*, 2009; Renvoise *et al.*, 2010). Interactions between ESCRT and centrosome protein 55 (CEP55) have been demonstrated during cytokinesis (Carlton & Martin-Serrano, 2007) while various interactions have been reported between ESCRT and the arrestin-related trafficking proteins [arrestin domain-containing protein (ARRDC1-4) and thioredoxin-interacting protein (TXNIP)] (Rauch & Martin-Serrano, 2011). In addition, ESCRT associated ubiquitin ligases (WWP1, WWP2, Itch and Nedd4) (Rauch & Martin-Serrano, 2011; Sette *et al.*, 2010) also have been shown to have function in the MVB pathway.

1.3.2 ESCRT in membrane deformation events

Biological membranes consist of phospholipid bilayers with numerous membrane proteins embedded. The plasma membrane is a selectively permeable membrane barrier between the inside of the cell and outside environment. The membrane wrapped organelles [such as the endoplasmic reticulum (ER) and the Golgi apparatus] are involved in various membrane trafficking pathways. They are all highly dynamic and organised biological structures involved in many processes to support living organisms from yeast to primates. There are a variety of biological events (*e.g.,* forming two separate daughter cells during cell division and vesicle biogenesis) involving membrane deformation and reorganisation. Although there is some evidence for the ESCRT machinery involvement in other events (*e.g.,* autophagy) (Lee *et al.*, 2007), the following sections of this introduction will be focused on the reported functional involvement of this machinery during three biological events: the MVB pathway, cell division and retrovirus budding at the plasma membrane.

1.3.2.1 ESCRT and MVB formation

During the down regulation of membrane proteins from the plasma membrane, these proteins usually acquire ubiquitin as the sorting signal and are internalised by endocytosis, and subsequently delivered to the complex endosomal system by fusion of endocytic vesicles with early endosomes. The endosomes further undergo a maturation process leading to the incorporated membrane proteins being internalised into vesicles that form within the lumen of the endosome. These so called intra-luminal vesicles (ILVs) are completely segregated from the cytoplasm. The vesicle containing endosomes ultimately fuse with lysosomes and their contents are degraded by the lysosomal enzymes. This cellular journey for membrane protein degradation is called MVB pathway (Barelli & Antonny, 2009; Nickerson *et al.*, 2007).

The first observation of MVBs goes back over fifty years when large vesicles containing small internal vesicles were observed by electron microscopy [reviewed in (Henne *et al.*, 2011; Piper & Katzmann, 2007)]. The name MVBs was given to those large cellular vesicles at the time before any knowledge about their functions. Pioneering work on the regulation of epidermal growth factor receptor (EGFR) in human cancer cells led to the observation that EGFR is sorted into ILVs of endosomes (Haigler *et al.*, 1979). Subsequent work indentified a crucial role for ubiquitination in the targeting of EGFR into ILVs, a process we now know is directly associated with the ESCRT machinery. Lysosomes (equivalent to the vacuole in yeast) are the major cellular sites for the degradation of ubiquitin labelled membrane proteins, and the formation of ILVs within the MVB pathway via ESCRT function is crucial for delivering cargos for degradation in the yeast vacuole and the mammalian lysosome.

1.3.2.2 ESCRT and retroviruses

All viruses are intracellular parasites and they require host cell factors and machineries to complete their life cycle. This section explains the discovered relationship between human immunodeficiency virus (HIV) and the ESCRT machinery.

After initial viral infection and viral gene expression, it is the Gag protein of HIV that drives the virus assembly and subsequent release. Gag associates closely with the inner side of the plasma membrane and the oligomerisation of the Gag protein is able to deform the lipid bilayer to form spherical protein shells. It was reported twenty years ago that the disruption of the p6 region of Gag in HIV-1 resulted in defects in virus budding. Further investigations revealed a PTAP amino acid motif within p6 and mutation of this motif also caused defects in HIV-1 budding (Gottlinger *et al.*, 1991; Martin-Serrano *et al.*, 2001; 2003b). This early research offered a hint to initiate the idea that viruses might hijack a common cellular machinery to assist their budding. Subsequently, the YPX_nL motif was also found in HIV Gag, which has a similar function to the PTAP motif (Morita & Sundquist, 2004; Strack *et al.*, 2003). As disruption of these motifs results in defects during the late stage of virus assembly/budding, they were named late (L) domain motifs. Consequently it has been discovered that Gag protein interacts with the ESCRT-I component TSG101 and the ESCRT associate protein ALIX through the L domain motifs PTAP and YPX_nL respectively. The late-acting components of this machinery, ESCRT-III proteins, are recruited through these interactions to the sites of HIV budding. The release of HIV-1 particles from the plasma membrane through pinching off from the cell surface

relies on the oligomerisation of ESCRT-III proteins (CHMPs) at the cytoplasmic side of the membrane (Weiss & Gottlinger, 2011).

1.3.2.3 ESCRT and cell division

More recently, research work reported from different laboratories have provided evidence for a crucial role of the ESCRT machinery in the final stages of cytokinesis.

The first evidence came from experiments performed in *Arabidopsis*, as cells containing multiple nuclei were observed among various cell types when the TSG101 homologue gene *elch* was mutated. The reported results implied that cell division was impaired by this mutation (Spitzer *et al.*, 2006). Soon after, it was reported that the human ESCRT component TSG101 is involved in the abscission stage of cytokinesis during HeLa cell division when Carlton and colleagues demonstrated interactions between TSG101 and CEP55, a centrosome and midbody protein essential for abscission. In addition, not only the ESCRT-I component TSG101 but also the ESCRT associated protein ALIX interacts with CEP55 (Carlton & Martin-Serrano, 2007). Furthermore, studies from the same research group reported that the human increased sodium tolerance (hIST) binds to VPS4 and ESCRT-III components and it is required for cytokinesis in mammalian cells (Agromayor *et al.*, 2009). Subsequently, through high-resolution structured illumination microscopy and time-lapse imaging, Elia and colleagues found TSG101, the ESCRT-III component CHMP4B and VPS4 proteins are sequentially localised to the narrow constriction sites during abscission between two daughter cells (Elia *et al.*, 2011). Furthermore several other ESCRT-III subunits have been found to be involved in the abscission stage during cytokinesis [reviewed in (Caballe & Martin-Serrano, 2011)].

For all the processes involving the ESCRT machinery described above, the late stage is the recruitment of the ESCRT-III complex to complete physical separation of membranes. The recruitment of ESCRT-III can be accomplished through different routes, either via ubiquitination and ESCRT-0 and/or ESCRT-I interactions or direct interaction with ESCRT-I and/or ALIX with retroviral Gag or cellular CEP55. It is conceivable that other processes that require ESCRT mediated membrane scission could achieve this by any mechanism that allows the appropriate recruitment and activation of ESCRT-III.

1.3.2.4 ESCRT and HSV-1

The secondary envelopment of HSV-1 shares topological similarities with MVB formation and it also requires membrane deformation and scission to form mature HSV-1 virus

particles. It has been reported that transient expression of dominant-negative VPS4 inhibits HSV-1 replication during secondary assembly stage and the expression of dominant-negative ESCRT-III proteins also reduces HSV-1 infectious virus production. Interestingly, different from HIV, the recruitment of ESCRT by HSV-1 is independent of TSG101 and/or ALIX (Crump *et al.*, 2007; Pawliczek & Crump, 2009). However, very little is known about how HSV-1 interacts with the ESCRT machinery.

1.4 Hypotheses

For large complex viruses, such as HSV-1, the assembly of virus particles involves the functions of many viral and host cellular proteins. The complex networks between viral and cellular proteins are still far from understood. As a large complex virus which assembles in the cytoplasm, HSV-1 assembly requires many viral proteins to be present at intracellular assembly sites. Especially, the cellular localisation of essential proteins is important for virus survival. Glycoproteins that arrive at the cell surface through the secretory pathway need to be internalised in order to be incorporated into the virions. It has been previously reported that gM causes the relocalisation of gD and gH/L from the plasma membrane to TGN in transfection assays (Crump *et al.*, 2004), suggesting a role of gM in targeting viral glycoproteins to the viral assembly sites for incorporation. It was therefore hypothesized that gM is able to relocalise certain HSV-1 glycoproteins to the viral assembly sites in infected cells for efficient virion incorporation.

In addition, many host proteins are also required for the viral assembly. The secondary envelopment shares topological similarities with the MVB formation, which involves the function of the ESCRT machinery. It has been previously shown that the ESCRT machinery is important for HSV-1 replication (Crump *et al.*, 2007). However, no direct interactions between HSV-1 viral proteins and ESCRT have been reported. It was therefore hypothesized that the tegument proteins, which are located between the capsid and envelope, could mediate direct interactions with ESCRT/ESCRT associated proteins leading to the recruitment of the ESCRT machinery.

1.5 Aims of this thesis

As one of the few glycoproteins found throughout the *Herpesviridae* family, gM has been conserved for millions of years. Although such conservation of a gene usually indicates important function(s) for the organism, gM has previously been shown to be non-essential

for HSV-1 in tissue culture. Hitherto, many research studies have been carried out and phenotypic results have been reported where the gM gene in several herpesviruses has been disrupted. However, it is still unclear what role(s) gM plays during HSV-1 infection. According to the previous published data from the laboratory (Crump *et al.*, 2004), it has been demonstrated in transfection assays that gM has the ability to cause relocalisation of other viral proteins, particularly gD and gH/L, in host cells. The first part of this thesis is therefore aimed at investigating the role(s) of gM in the cytoplasmic assembly stage during HSV-1 life cycle, particularly to examine the function of gM in relocalisation of other viral glycoproteins during infection.

In addition to gM, there are many other viral and cellular factors involved in the cytoplasmic assembly of HSV-1 to form such large and complex infectious virus particles. In a parallel project to that investigating gM, the roles of certain cellular proteins were also studied. In 2007, the laboratory published the first evidence that HSV- 1 cytoplasmic assembly requires the function of VPS4 (Crump *et al.*, 2007), suggesting a crucial role of the ESCRT machinery in the HSV-1 life cycle. Subsequently, further data from the laboratory were published demonstrating that the ESCRT-III components are important for HSV-1 replication, while different from HIV-1, TSG101 and/or ALIX are dispensable. Aiming at understand further details about the role ESCRT-III components in HSV-1 replication, the direct role of CHMP4A/B/C proteins of ESCRT-III was investigated in this thesis. In addition, as there were no reported interactions between HSV-1 and ESCRT proteins, Y2H screening was performed for HSV-1 tegument proteins with a panel of human ESCRT and ESCRT associated proteins in order to identify interactions between the virus and cellular ESCRT machinery. These studies were aimed at understanding the complex interplay between HSV-1 and the human ESCRT machinery.

The studies carried out for this thesis have been aimed at exploring the functions of both viral and host cellular proteins in HSV-1 secondary assembly. On one hand, the role of viral glycoproteins during cytoplasmic assembly was examined with a primary focus on gM. On the other hand, the function of the cellular ESCRT machinery during this stage and virus-host interactions that could recruit this machinery were investigated.

2 The role of glycoprotein M in HSV-1 cytoplasmic assembly

2.1 Introduction

Being structurally complex viruses, a large number of different proteins need to be coordinated to successfully assemble new infectious herpesvirus particles. At least fifteen different viral transmembrane proteins have been identified in HSV-1 particles, all of which must be correctly localised to the appropriate cellular membrane sites to be incorporated into virions (Adams *et al.*, 1998; Foster *et al.*, 2001a; Foster *et al.*, 2001b; Ghiasi *et al.*, 1998; Loret *et al.*, 2008).

The envelope proteins, gB, gH, gL, gM and gN/pUL49.5, are conserved in all herpesviruses, which implies important functions of these proteins. The essential function of gB and the gH/L complex in herpesvirus entry is now well established and crystal structures of HSV-1 gB and HSV-2 gH/L have been recently solved (Chowdary *et al.*, 2010b; Heldwein *et al.*, 2006). However, the role of gM and gN/pUL49.5 in the herpesvirus life cycle remains unclear. HSV-1 gM is a type III viral membrane protein encoded by gene UL10. It is predicted to have eight transmembrane domains and has been demonstrated to form a disulphate linked complex with gN/pUL49.5 in many herpes viruses (Crump *et al.*, 2004). In several herpes viruses, gM has been shown to inhibit membrane fusion assays. For example, PRV gM has been reported to inhibit glycoprotein-mediated fusion (Klupp *et al.*, 2000). HSV-1 gM has also been shown to inhibit the fusion induced by HSV-1 gB, gD, gH and gL in a similar manner although with higher efficiency when co-expressed with HSV-1 pUL49.5 (Crump *et al.*, 2004). Previous studies in the laboratories have shown that gM may have functional roles in localising other viral envelope proteins to sub-cellular compartments. Both PRV gM and HSV-1 gM are localised to the TGN when expressed in cells by transfection. In addition, these proteins can cause both gD and gH/L to be relocalised from the plasma membrane to a juxtanuclear compartment. These data suggest the mechanism of fusion inhibition is likely to be the removal of fusion proteins from the cell surface by gM. Furthermore, it also suggests a possible role of gM in targeting gD and/or gH/L to viral assembly sites (Crump *et al.*, 2004).

Similar as gM, pUL43 is also a type III membrane protein and it is among the least characterised herpesvirus membrane proteins. It has been reported that the PRV pUL43 was able to inhibit fusion induced by PRV glycoproteins in a transient expression-fusion assay to a similar extent as gM. pUL43 has been predicted to contain 9 transmembrane domains with a hydrophilic loop in the middle region and an N-terminal hydrophilic extension (Klupp *et al.*, 2005). Due to the structure similarity and a similar ability to inhibit cell fusion, pUL43 and gM may have redundant function(s).

The previous investigations of gM and pUL43 were carried out in cell models where the proteins were transiently expressed by transfection. The behaviours of these proteins could be different with the context of viral infection. In addition, the possible role of pUL43 in HSV-1 replication has not been reported. In this study, a gM deletion virus (ΔgM) and its revertant (gMR), as well as a gM and pUL43 double deletion virus (ΔgM/ΔUL43) and gM revertant were created (gMR/ΔUL43). These recombinant viruses were used to investigate the function of HSV-1 type III membrane proteins, with a primary focus on gM.

2.2 Result

2.2.1 Virus construction

2.2.1.1 Glycoprotein M deletion virus

HSV-1 strain SC16 isolated from a human recurrent lesion (Hill *et al.*, 1975) was used in this study. The design and construction of ΔgM and gMR were carried out by Dr C. Crump and S. Bell. Briefly, ΔgM was constructed by replacing codons 134 to 466 of UL10 with a β-galactosidase (β-gal) reporter gene using homologous recombination. The revertant virus was generated as a control by replacing the *lacZ* reporter gene with the wild type UL10 fragment (Figure 2.1).

2.2.1.2 Glycoprotein M and pUL43 double deletion virus

The design and construction of ΔgM/ΔUL43 and gMR/ΔUL43 were carried out by Dr C. Crump and S. Bell. Briefly, HSV-1 ΔgM/ΔUL43 was constructed by replacing the entire UL43 ORF (genomic sequence 94733-96061) in ΔgM virus with the EGFP expression cassette through homologous recombination. Therefore, UL43 is deleted from the virus genome in addition to the deletion of the majority of UL10 as detailed above. Therefore, ΔgM/ΔUL43 carries both GFP and β-galactosidase reporter gene products for isolation.

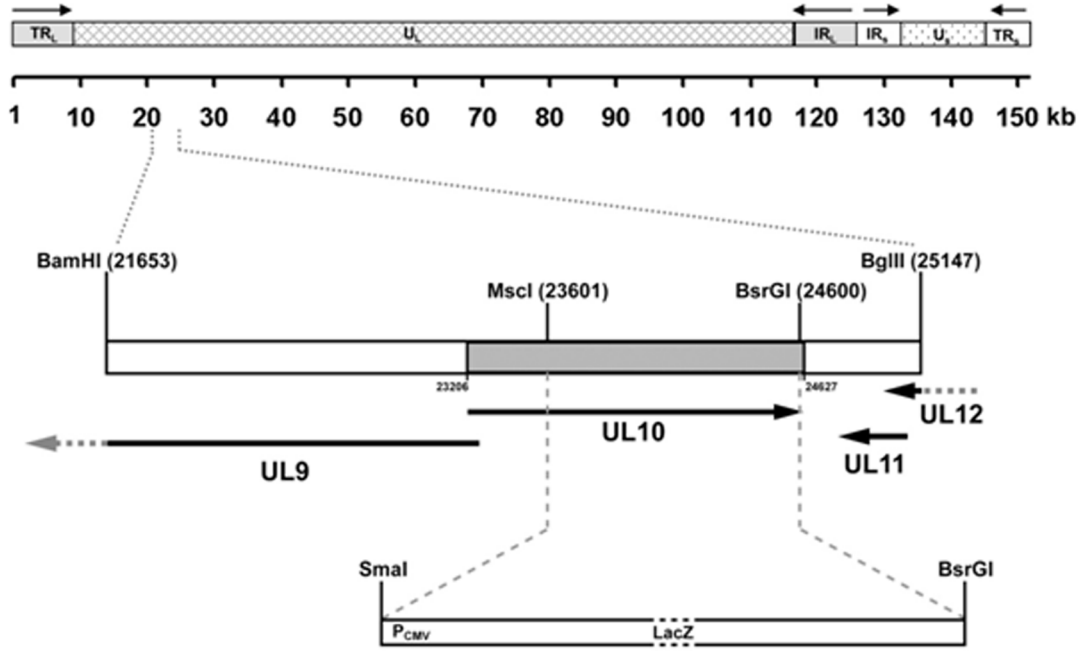

Figure 2.1: Construction of ΔgM virus. A schematic of the HSV-1 genome with relevant restriction sites and ORFs highlighted. The region of UL10 between the indicated MscI and BsrGI restriction enzyme recognition sites in HSV-1 strain SC16 was replaced with a *lacZ* reporter gene, leaving 399bp of UL10 remaining at the 5'-end and 22bp at the 3'-end.

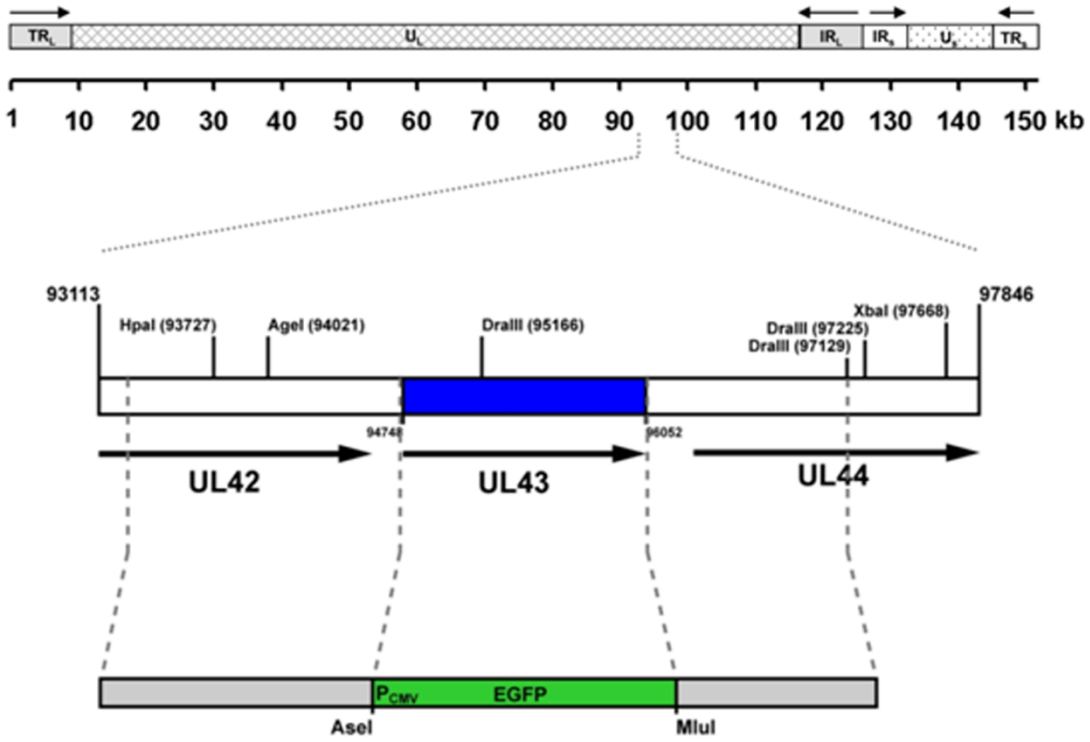

Figure 2.2: Construction of ΔgM/ΔUL43 virus. A schematic of the HSV-1 genome with relevant restriction sites and ORFs highlighted. The region of the indicated AseI and MluI restriction enzyme recognition sites in HSV-1 strain SC16 was replaced with a EGFP expression cassette, resulting the deletion of the entire UL43 gene.

The revertant virus (gMR/ΔUL43) was generated as a control by replacing the EGFP expression cassette with the wild type UL43 fragment (Figure 2.2).

2.2.2 Analysis of viral replication *in vitro*

2.2.2.1 Single time point growth analysis in various cell lines

Thirteen different mammalian cell lines (HT29, HFF, A549, CaCo2, HRT18, 293T, MDCK, COS-7, BHK, Vero, HaCaT, HeLa and SK-NSH) were used to compare the relative single cycle virus replication of the wild type SC16, ΔgM and ΔgM/ΔUL43 viruses. The cells were seeded into six-well plates and the following day infected at 5 PFU/cell at 37 °C for 1 h. The input viruses were removed and the cells were acid washed to inactivate any remaining input viruses. The infected cells were harvested at 26 hpi and infectious titres were determined by plaque assays. The result showed various differences in virus titres among these cell lines. All three viruses replicated poorly in the human neuroblastoma SK-NSH cells and the titres were about 4 logs lower than the other cell lines (Figure 2.3). This level of virus titre could be residual viruses which were not efficiently inactivated by the acid wash and so the results with SK-NSH cells were discounted. All three viruses replicated efficiently in all other cell types with relatively small difference between the viruses. A consistent reduction in titre in the absence of gM and pUL43 expression was observed for HT29 (human colon adenocarcinoma) cells and HaCaT (human keratinocyte) cells where SC16 > ΔgM > ΔgM/ΔUL43. Unexpectedly, the opposite phenotype was observed in CaCo2 (human colorectal adenocarcinoma) and slightly in HeLa (human cervix carcinoma) cells with the titre of SC16 < ΔgM < ΔgM/ΔUL43 (Figure 2.3). For all the other cell lines there was no difference (HFF, A549 and Vero) or there was no obvious trend for the effect of the viral gene mutation(s) on viral growth. However, one potential problem with this approach is that samples were collected at a late time point (26 hpi) but for many cells HSV-1 replication reaches the plateau phase around 14 hpi.

2.2.2.2 Single-step growth analysis of HSV-1 mutant viruses

Based on the single time point growth analysis result, six cell lines were chosen for further analysis. HT29 and HaCaT cells as they demonstrated a consistent reduction in titre in the absence of gM, HFF which showed little difference between the viruses but the cells are human primary diploid cells (foreskin fibroblasts), CaCo2 as they demonstrated a consistent increase in titre in the absence of gM. Furthermore Vero cells were chosen as

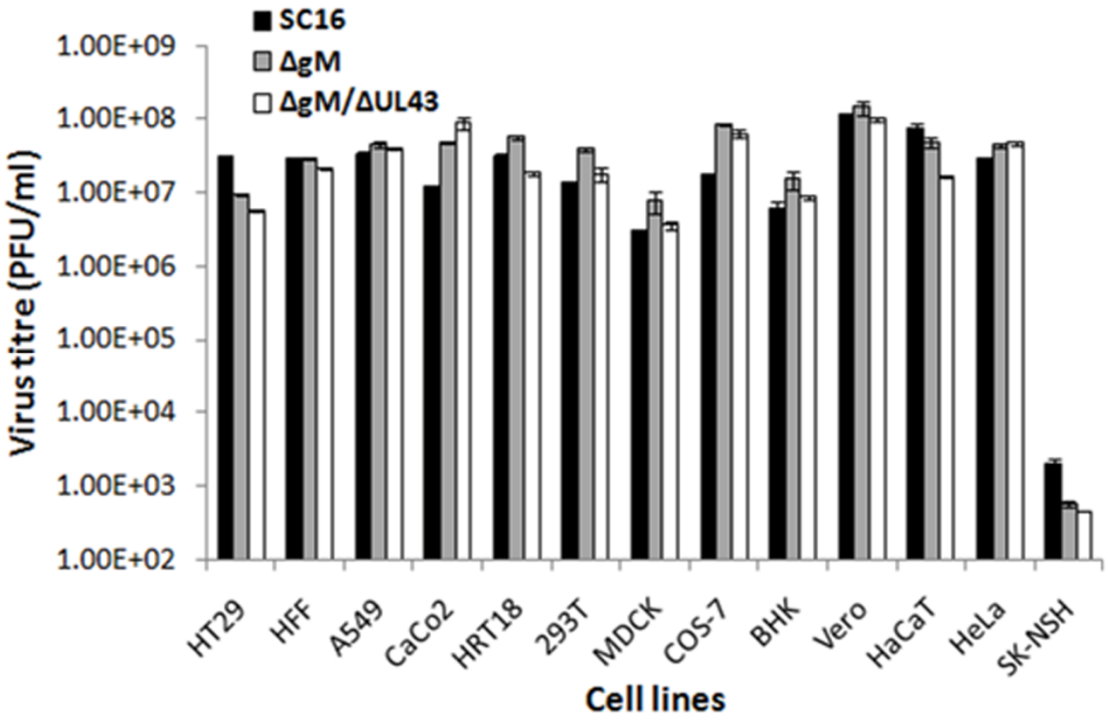

Figure 2.3: Single time point high MOI growth analysis of SC16, ΔgM and ΔgM/ΔUL43 viruses in thirteen cell lines. Cells were seeded into six-well plates at 2.5 x 10^5 cells per well one day prior to being infected at 5 PFU/cell at 37 °C for one hour. The inocula were removed and the cells were acid washed to inactivate remaining input virus. The cells were frozen at -70 °C at 26 hpi and were sonicated after thawing to release progeny viruses. The titres were determined by plaque assay on Vero cell monolayers. The mean titres and standard errors of duplicated samples are shown.

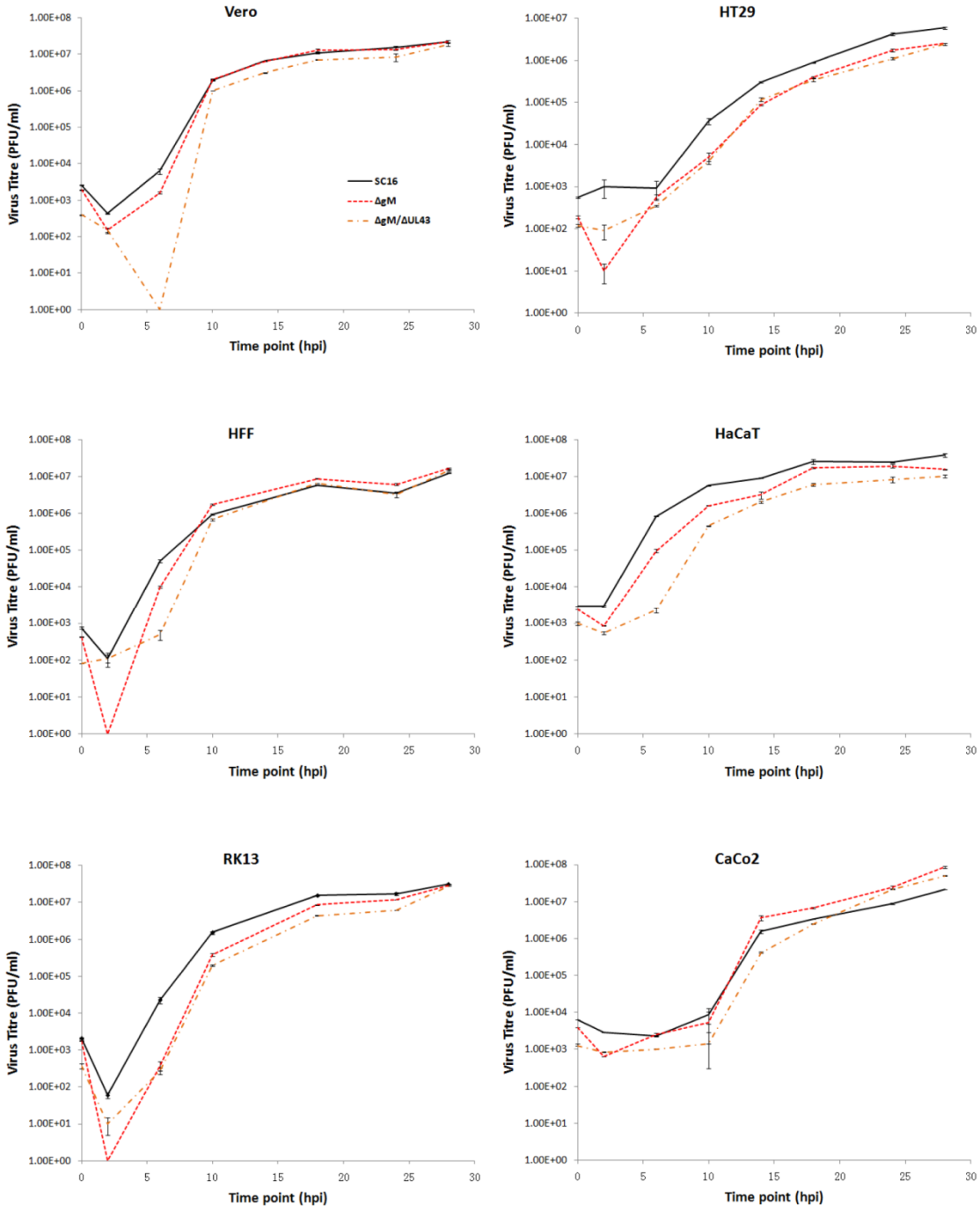

Figure 2.4: Single-step virus growth analysis in Vero, HFF, RK13, HT29, HaCaT and CaCo2 cell lines. The cells were infected at 5 PFU/cell at 37 °C for one hour. The inocula were removed and acid washed to inactivate remaining input virus. Samples were collected at indicated time points by freeze-thaw at -70 °C and sonicated to release progeny virus. The titres were determined by plaque assay on Vero cell monolayers. The mean titres and standard errors of duplicated samples are shown.

they are wildly used in herpesvirus research and another cell line RK13 (rabbit kidney cell) was also chosen as a previous report demonstrated that gM deletion resulted in a significant growth defect in these cells (Leege *et al.*, 2009).

The cells were seeded into six-well plates and the following day infected at 5 PFU/cell at 37 °C for one hour. The virus inocula were removed and acid washed to inactivate residual input viruses. Samples were harvested at various time points and progeny viruses were released by sonication for titration by plaque assay on Vero cell monolayers. As the results shown in Figure 2.4, there was almost no defect in virus growth in Vero or HFF cells as the titres of all the three viruses were almost identical from 10 hpi onwards. Although a relatively large growth defect of HSV-1 gM deletion virus constructed in a strain KOS background was reported in RK13 cells (Leege *et al.*, 2009), the two SC16-based gM deletion viruses used here showed a much smaller defect in replication in RK13 at early time points and the titres reached a similar level as wild type by 26 hpi (Figure 2.4). This may due to the different virus strain used in the study or difference in experimental approach. In the two human cell lines HT29 and HaCaT, the mutant viruses demonstrated a greater defect in replication. Both mutant viruses had lower titres than the wild type during the whole time course. There were no difference between the growth of ΔgM and ΔgM/ΔUL43 in HT29 cells, however, the double deletion virus showed a stronger defect in HaCaT cells. Interestingly, in CaCo2 cells the absence of gM again resulted in increased virus titres than the wild type SC16 at late stages of the growth curve although ΔgM/ΔUL43 only demonstrated this at the final 2 time points (Figure 2.4). However, the reason for this phenotype is currently unknown.

2.2.2.3 Multi-step growth analysis of HSV-1 mutant viruses

The single-step growth kinetics suggests gM and pUL43 may have cell type dependant functions and the deletion of gM alone or together with pUL43 has small effects on infectious virus assembly in certain *in vitro* cell culture models including two human cell lines: HT29 and HaCaT. In order to further investigate the growth defects caused by the deletion of gM and/or pUL43 from the virus, multi-step growth ananlysis of ΔgM and ΔgM/ΔUL43 as well as their gM revertant viruses (gMR, gMR/ΔUL43) were performed in HT29, HaCaT and Vero cells. The gMR/ΔUL43 virus is equivalent to a single ΔUL43 deletion virus.

In HT29 cells, the deletion of pUL43 had very small defects (~ 2-fold) in growth (compare gMR to gMR/ΔUL43, and ΔgM to ΔgM/ΔUL43) (Figure 2.5 A). The single deletion of

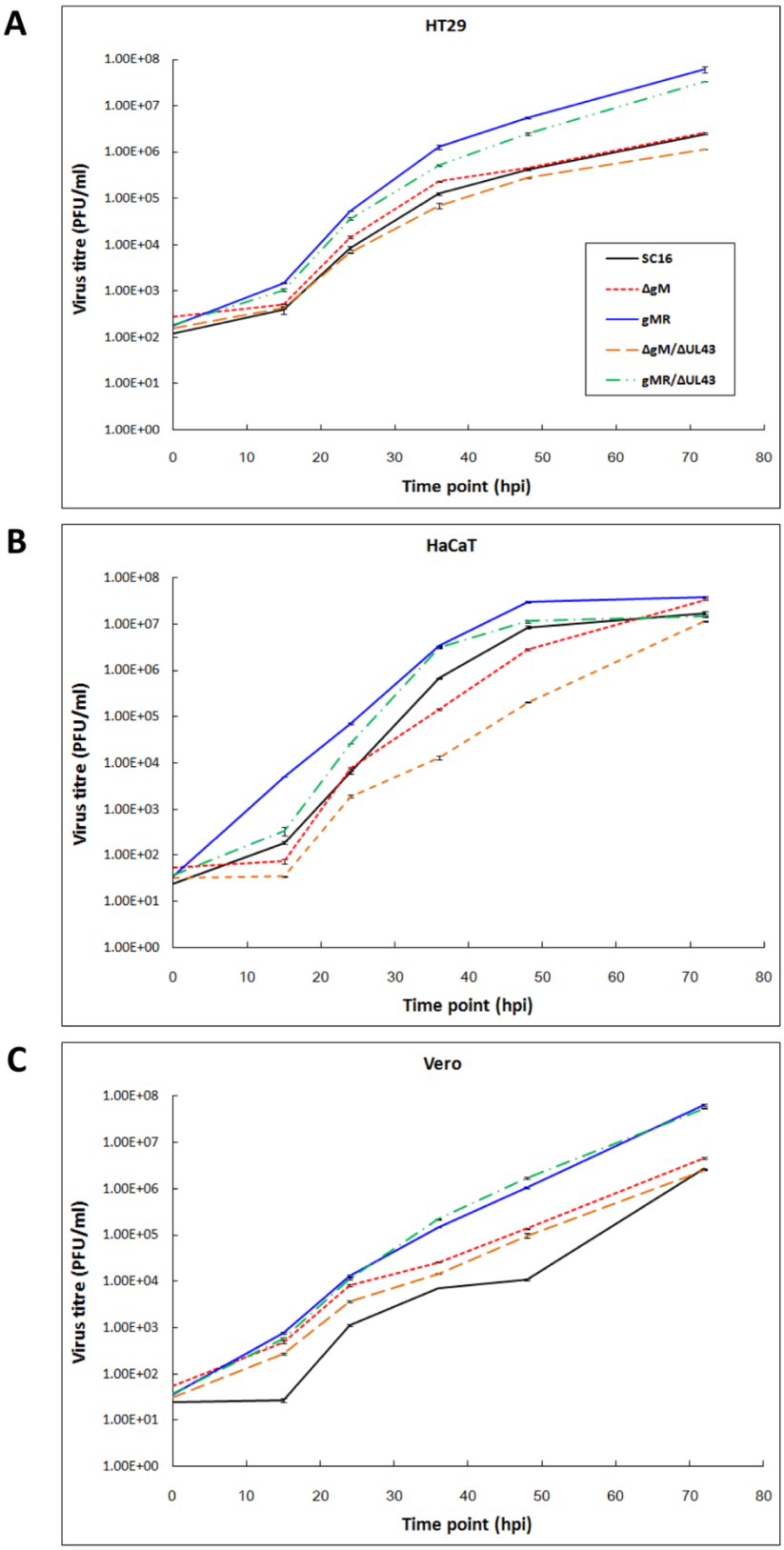

Figure 2.5: Multi-step virus growth analysis. HT29 (A), HaCaT (B) and Vero (C) cells were infected with the indicated viruses at 0.001 PFU/cell at 37 °C for one hour. Samples were collected at the indicated time points and titrated by plaque assay on Vero cell monolayers. The mean titres and standard errors of duplicated samples are shown.

gM showed a defect in viral growth in these cells with 20-30 fold decrease in titre at 72 hpi (comparing ΔgM to gMR, and ΔgM/ΔUL43 compared to gMR/ΔUL43) (Figure 2.5 A). Furthermore, the growth of the virus with gM and pUL43 double deletion had the slowest growth rate with 54-fold lower titre at 72 hpi (comparing ΔgM/ΔUL43 to gMR) (Figure 2.5 A). These results suggest that pUL43 deletion has little or no effect on HSV-1 growth while gM deletion has a relatively greater defect in HSV-1 multi-step replication. In HaCaT cells, the deletion of pUL43 did cause defects in replication as shown comparing the gMR to gMR/ΔUL43, or ΔgM to ΔgM/ΔUL43. The deletion of gM caused larger defects in growth at early stage but the mutant viruses reached a similar level as the revertants at 72 hpi (comparing ΔgM to gMR and ΔgM/ΔUL43 to gMR/ΔUL43) (Figure 2.5 B). Similar to HT29 cells, in Vero cells the single deletion of pUL43 had virtually no effect on virus growth (compare gMR to gMR/ΔUL43, and ΔgM to ΔgM/ΔUL43), while the deletion of gM caused 14-22 fold decrease in titre at the final time point (comparing ΔgM to gMR, and ΔgM/ΔUL43 compared to gMR/ΔUL43) (Figure 2.5 C).

Surprisingly, in these experiments the parental virus strain (SC16) demonstrated a significantly lower replication rate in all cell types than the gMR virus (Figure 2.5 A-C), which should be an equivalent "wild type" virus, while the reasons for this are unclear. The parental SC16 strain is a low passage isolate that is known to have a certain level of heterogeneity in plaque size. As the ΔgM virus is a clone isolate, the revertant gMR virus that was generated from ΔgM is likely to be more isogenic and thus a better control than the parental SC16.

2.2.2.4 SC16 wild type control

As mentioned above HSV-1 strain SC16 is a low passaged isolate that displays heterogeneity in the population as reflected by the various sized plaques (Figure 2.6 A). The parental virus has been passaged during the generation of the mutant and revertant viruses and so that original SC16 parental strain stocks may not be a fair comparison. In order to test the effect of passage on the parental SC16 virus plaque population, Vero cells were infected with SC16 at 0.1 PFU/cell for two passages. As would be expected, the proportion of large plaques increased with each passage (Figure 2.6 A-C). These results suggest that the SC16 population does change during serial passage and it would be more reasonable to use a wild type SC16 that has been subjected to the same procedures as the mutant viruses for a control. Thus the high molecular weight DNA harvested from SC16 infected cells was transfected into Vero cells to generate a virus stock P0 (Figure 2.6 D).

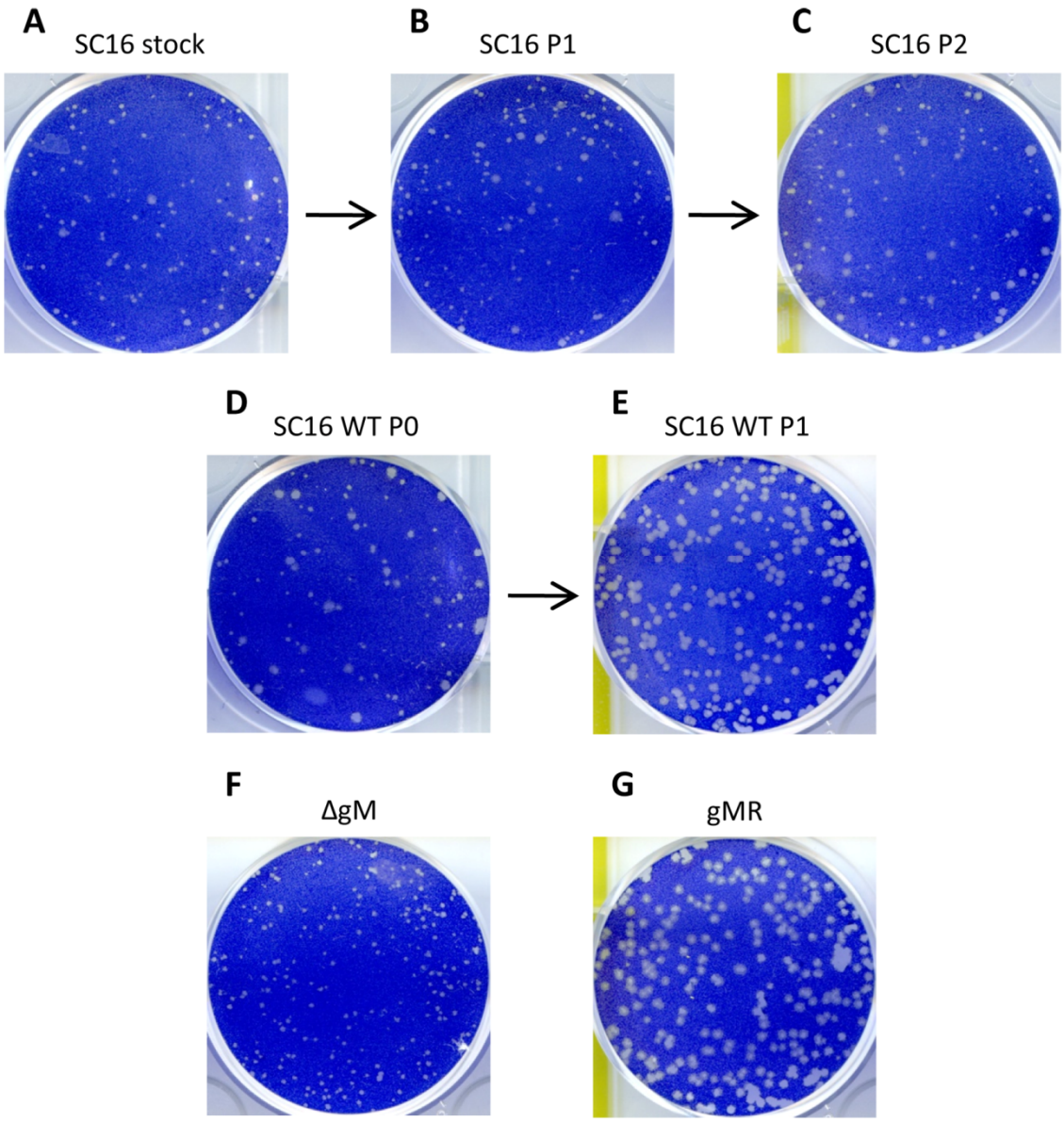

Figure 2.6: Virus plaque sizes on Vero cell monolayer. Vero cells were seeded at 5 x 10^5 cell per well into six-well plate and incubated to form monolayer. The cells were infected with appropriate diluted virus stocks in 0.5 ml per well volume at 37 °C for one hour. Semisolid medium was added for incubation and the cells were fixed and stained three days post infection. (A-C) SC16 virus stocks were passaged twice and the plaques of different passaged virus stocks are shown. (D) High molecular weight DNA was prepared from SC16 infected cells and transfected into BHK cells to generate virus stock used for the plaque assay. (E) The virus stock harvest from D was passaged once and the plaques of the passaged virus stock are shown. (F) ΔgM plaques. (G) gMR plaques.

This virus stock was passaged with infection at 0.1 PFU/cell to generate the virus stock P1 for SC16 control (Figure 2.6 E). This new SC16 "wild type" control demonstrated a much more homogenous plaque size that was virtually the same as gMR (Figure 2.6 E, G), with both showing larger plaques than ΔgM (Figure 2.6 F).

2.2.3 Glycoprotein M in HSV-1 cytoplasmic assembly

2.2.3.1 The effect of gM deletion on virus replication

From the virus growth analysis in vitro, there was little effect observed when pUL43 was deleted in HSV-1. Furthermore while investigating many cell lines does give a broad range of information, it is difficult to draw a conclusion by comparing the results from different cell models. Therefore, further experiments were focused on the function of gM using the HT29 cell line as the one showing the strongest phenotype and the Vero cell line as a control cell line as it has been used widely in published work.

To investigate the effect of gM deletion on viral replication, the ΔgM, gMR and the equivalently treated wild type SC16 viruses were analysed in single- and multi-step growth assays in both cell lines. SC16 and gMR had virtually identical growth properties in both cell lines (Figure 2.7). ΔgM demonstrated a small growth deficit in HT29 cells at high multiplicity of infection (MOI) and showed ~10 fold reduction in titre at 10-14 hours post infection (hpi) compared to the other two viruses, although the difference became smaller (~3-fold) by 24 hpi (Figure 2.7 A). Much greater defects in the growth of ΔgM were observed in HT29 cells at low MOI with up to 37-fold reduction in infectious titre at 36-48 hpi (Figure 2.7 C). At 72 hpi the reduction was about 24-fold, which indicates that the total production of ΔgM virus was about 4% of the two control viruses. In Vero cells there was virtually no difference in the growth properties of ΔgM compared to the control viruses in the single-step growth curve (Figure 2.7 B), comparable to previously published data on the growth properties of an independently generated SC16-based gM deletion virus in Vero cells (Browne et al., 2004). In the case of low MOI infection, ΔgM showed a modest delay in replication kinetics in Vero cells, with 4-8 fold lower titres at 36-48 hpi (Figure 2.7 D). However, different from HT29, the titres of the three viruses were similar at 72 hpi. These data suggest that while the absence of gM has small effect on the assembly of infectious virions in the human cell line HT29, gM expression is necessary for efficient cell-to-cell spread in these cells. Furthermore, gM expression also appears to aid efficient spread in Vero cells.

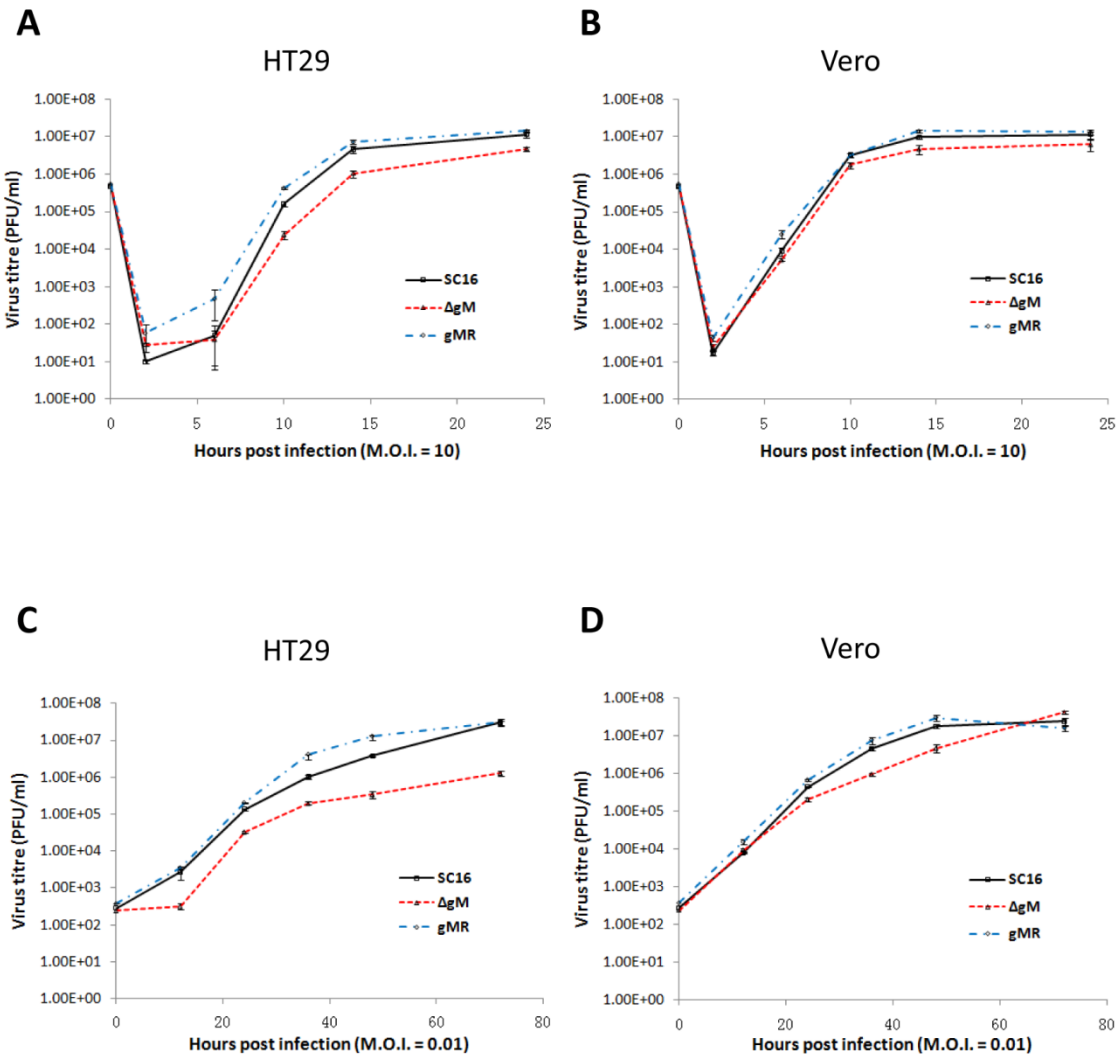

Figure 2.7: Virus growth analysis. Single-step (A, B) and multi-step (C, D) growth analysis at MOI of 10 and 0.01 respectively were performed on HT29 and Vero cells. The mean titres of ΔgM, gMR and wild type SC16 and standard errors are shown (n=3).

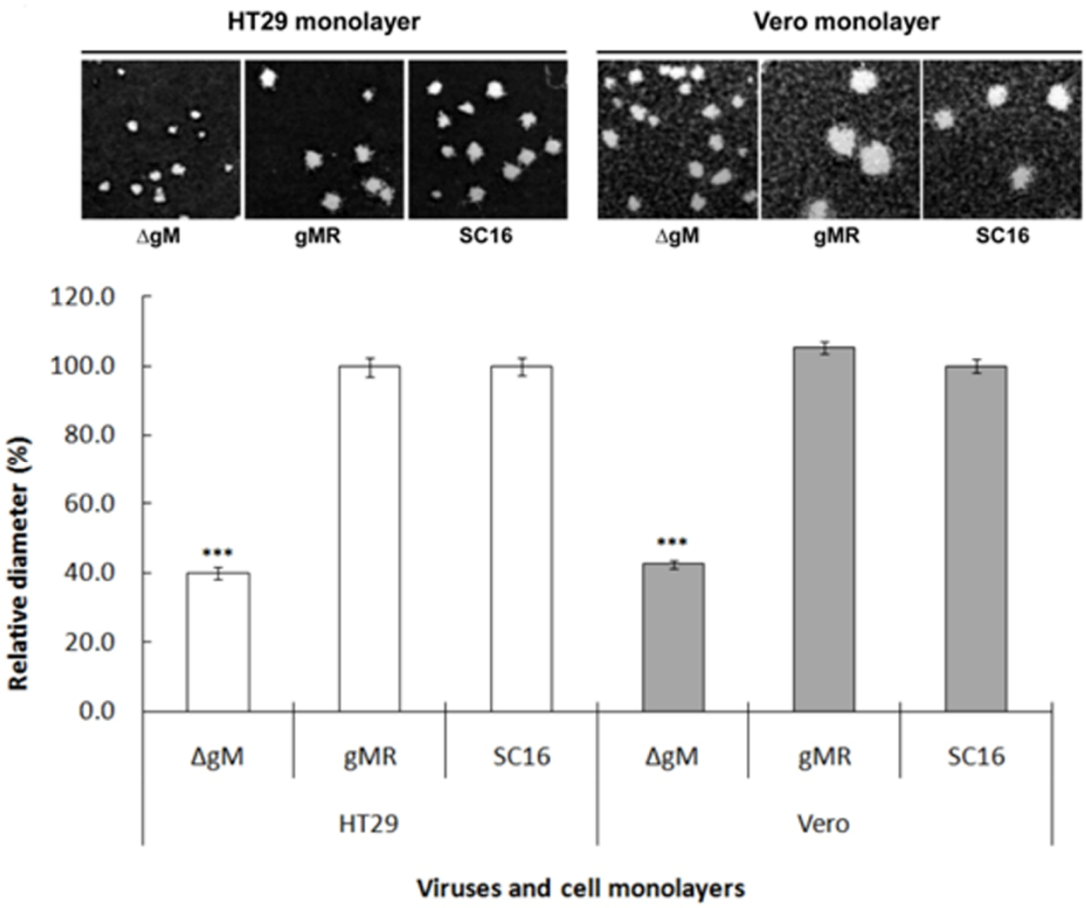

Figure 2.8: Plaque size quantification. The plaques of ΔgM, gMR and wild type SC16 on HT29 and Vero cell monolayer are shown in the upper panel. The relative plaque sizes of ΔgM and gMR were calculated as the percentage of SC16 (set as 100%). The mean relative diameters and standard errors (n=50) are shown. ***: $p < 0.001$ (two-tailed Student's *t*-test).

2.2.3.2 Plaque size and quantification

Defects in cell-to-cell spread can also be determined by analysis of plaque formation under semi-solid media. The size of plaques formed by wild type SC16 and gMR were virtually identical in size in both cell types. However, the ΔgM plaques were significantly smaller on both HT29 and Vero monolayers (Figure 2.8). Quantification data revealed that the ΔgM plaque diameter was reduced by ~60% in both cell types. Taken together with single and multi-step growth analysis, these data suggest defects in cell-to-cell spread in the absence of gM in both cell types.

Given that plaque size and growth kinetics were virtually identical between wild type SC16 and gMR, further experiments were performed on ΔgM and gMR only.

2.2.4 The expression of viral proteins

The expression of a panel of viral proteins in HT29 and Vero cells infected by ΔgM or gMR was analysed by western blot. As expected there was no detectable gM expression in either cell line infected by ΔgM (Figure 2.9). However, a slight reduction in the expression of pUL11 was observed in cells infected with ΔgM, which may be due to the proximity of the UL11 gene to the engineered deletion within the gM gene (UL10). Importantly, the major capsid protein VP5, the major tegument proteins VP16 and VP22, as well as the envelope proteins gB, gC, gD and gH were all expressed at similar levels in cells infected with ΔgM or gMR (Figure 2.9). This result suggests that the loss of gM did not have significant effect on viral gene expression. However, a greater population of the mature forms of gB, gC and gD were observed in Vero cells infected by ΔgM although the reason for this is unclear (Figure 2.9 B). Immunofluorescence analysis also confirmed the loss of gM expression in ΔgM and the regain of gM expression in gMR (Figure 2.10).

2.2.5 gH/L and gD localisation

It has previously been shown that when gD or gH/L is expressed alone by transfection, they localise at the cell surface, while when co-expressed with gM, both gD and gH/L localises mainly at the TGN (Crump *et al.*, 2004). Here the localisation of these glycoproteins in infected cells was examined by immunofluorescence microscopy. In both ΔgM and gMR infected cells, gH/L showed some co-localisation with the Golgi markers GM130 and TGN46 (Figure 2.11). In addition, the amount of gH/L present on the cell surface was greater in ΔgM infected cells compared to gMR (Figure 2.11). Thus it appears that the localisation of gH/L in infected cells at least partially relies on the expression of

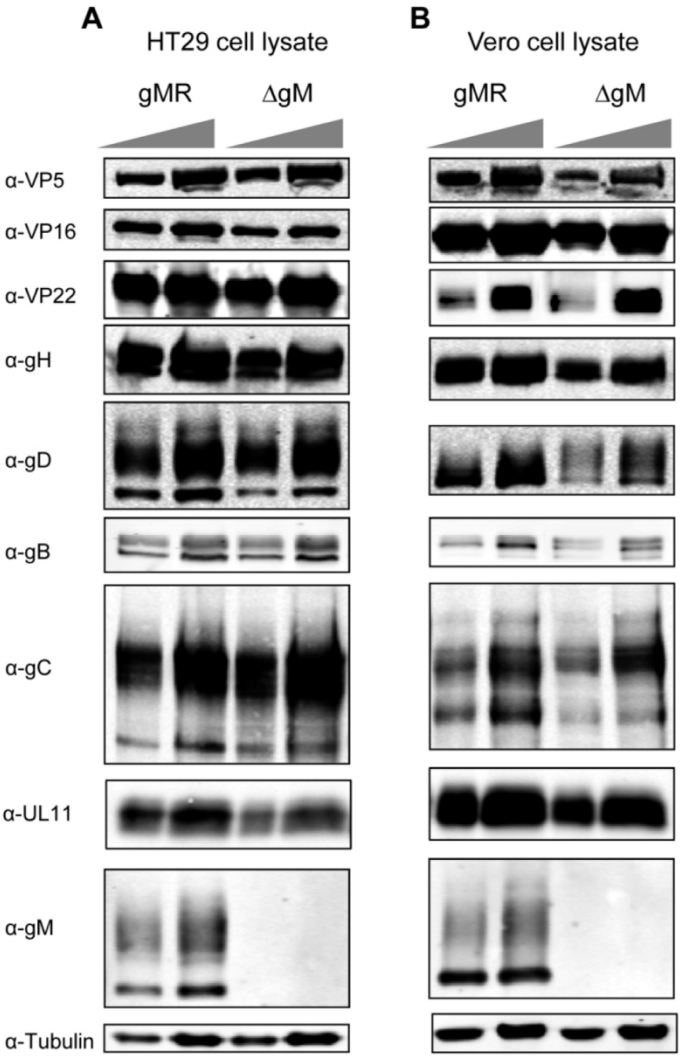

Figure 2.9: Analysis of viral protein expression levels in infected cells. HT29 cells (A) or Vero cells (B) were infected with ΔgM or gMR at an MOI of 10 and harvested at 24 hpi. Two-fold dilutions of cell lysates (indicated by the gray triangles) were loaded and samples were probed with antibodies against HSV-1 proteins. The tubulin signals were used as loading controls.

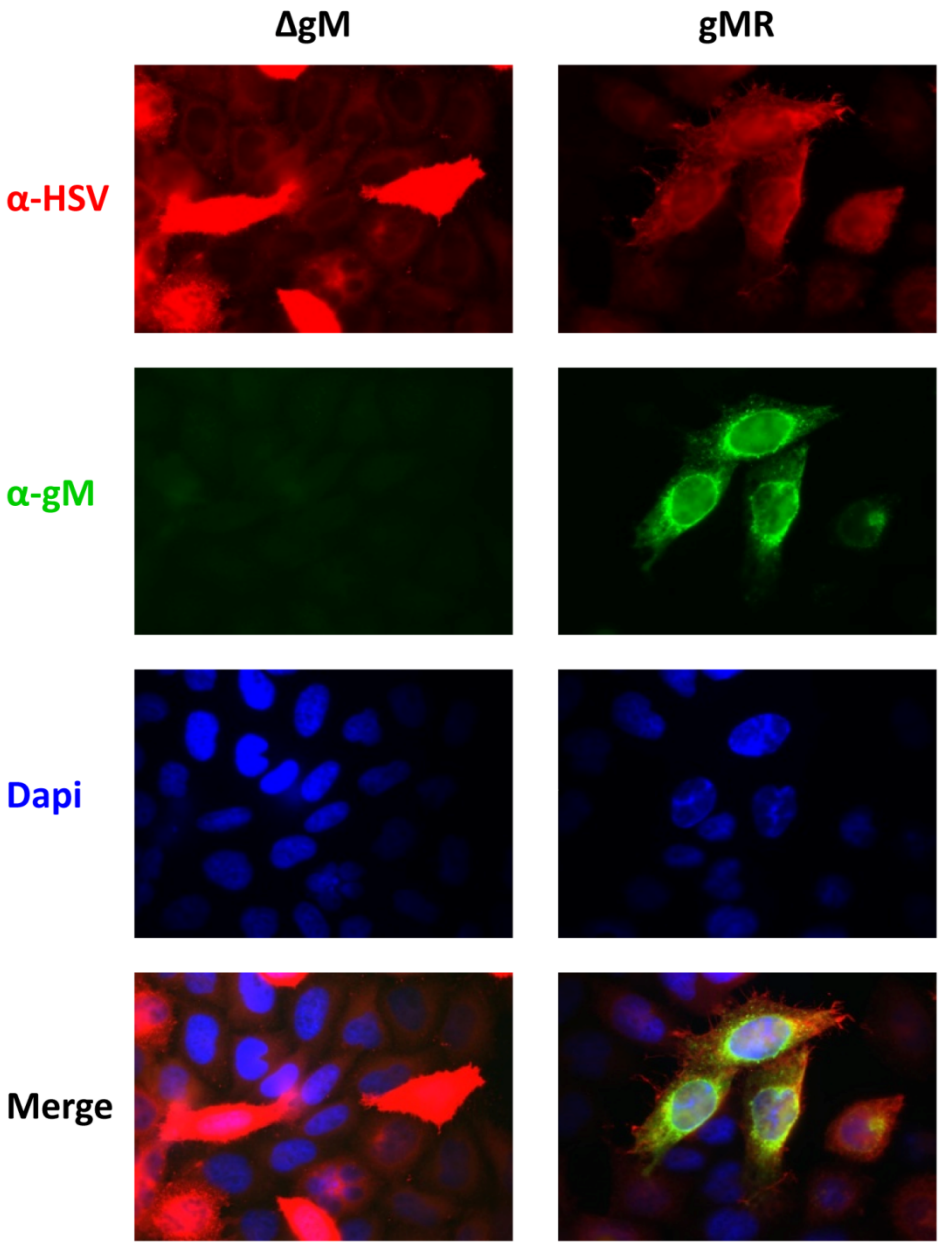

Figure 2.10: Immunofluorescence staining of gM. HeLa cells were seeded on cover slips and infected by HSV-1 wild type SC16, ΔgM or gMR at MOI of 2. The samples were fixed at 14 hpi followed by staining with primary antibodies anti-HSV and anti-gM (CB18). Donkey-anti-rabbit 568 (red) and donkey-anti-mouse 488 (green) (Molecular probes/Invitrogen) were used as secondary antibodies. Pictures were taken with a fluorescent microscope (Olympus IX70) and processed in ImageJ software.

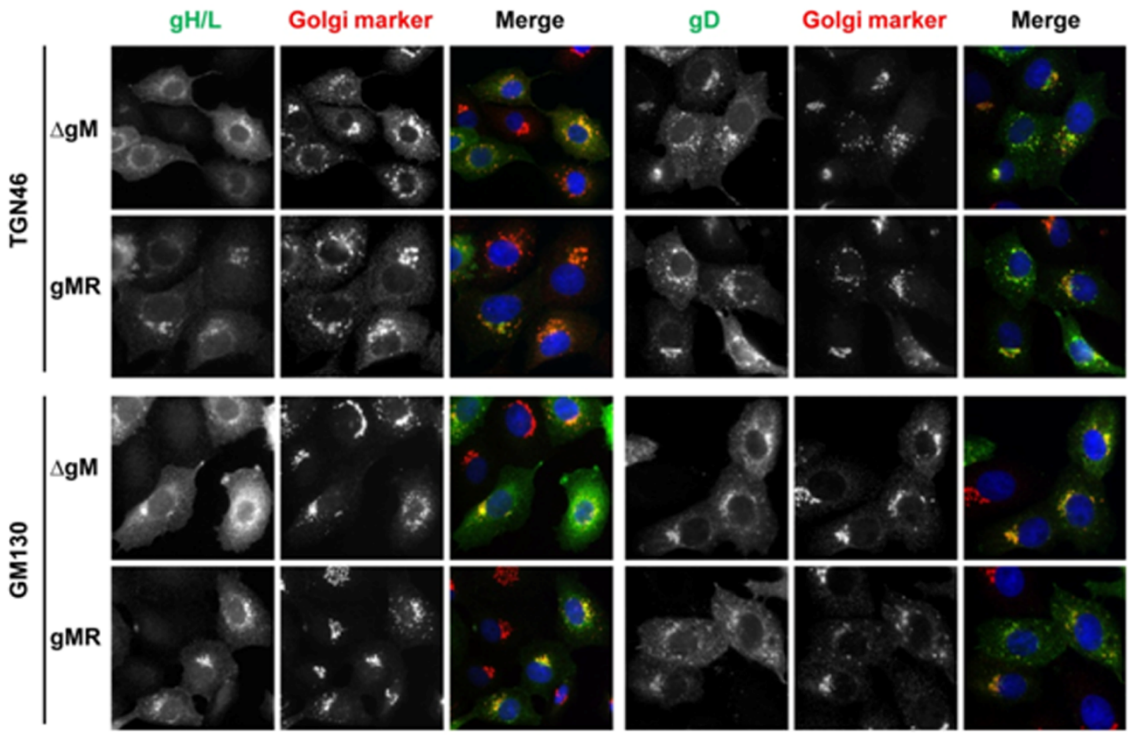

Figure 2.11: gH/L and gD localisation in infected cells. The localisation of gH/L and gD in Vero cells infected with ΔgM or gMR were determined by immunofluorescence microscope. The cells were fixed and stained at 6 hpi. Images were compiled and pseudocoloured with green representing gH/L or gD, red represents Golgi markers TGN46 or GM130 and blue indicating nuclei (DAPI staining).

gM. In contrast, there were no obvious differences in the distribution of gD between ΔgM or gMR infected cells, suggesting gM-independent mechanisms for controlling the sub-cellular localisation of gD during infection (Figure 2.11).

2.2.6 Analysis of the levels of gD and gH/L on the cell surface of infected cells

To further investigate the levels of gH/L present on the cell surface in the presence or absence of gM, infected cells were analysed by flow cytometry. Vero cells were infected with ΔgM or gMR at three different MOI (0.8, 2.0 and 5.0 PFU/cell) and labelled with primary antibody anti-gH/L (LP11) followed by fluorescent secondary antibody labelling at 6 hpi. Signals from 10000 cells were collected for analysis. The mean value of cell surface gH/L and standard error bars are shown (Figure 2.12 A). As expected, for both viruses the cell surface gH/L levels increased with the increase of MOI. Interestingly, the ΔgM infected cells demonstrated higher surface gH/L levels than the gMR infected cells at all three MOI conditions (Figure 2.12 A).

In the above experiment conditions, the increased gH/L on the surface of ΔgM infected cells could be due to greater numbers of virions attached to the cell surface rather than free glycoprotein expressed upon infection. In order to test this, the cell surface gD level was labelled in parallel with gH/L. No significant difference was observed in surface levels of gD in cells infected with either virus. However, an increase in the level of gH/L was observed on the surface of cells infected with ΔgM compared to gMR (Figure 2.12 B). These data suggest that gM plays an important role in controlling the sub-cellular localisation of gH/L and in the absence of gM, gH/L internalisation is inhibited and/or gH/L transport to the cell surface is increased.

2.2.7 Analysis of the internalisation of gD and gH/L in infected cells

To test whether the increased level of gH/L on the plasma membrane was due to the impaired internalisation in the absence of gM, infected cells were incubated with antibodies specific to the extracellular domains of gH/L complex or gD at 37 ºC for one hour prior to fixation. The gH specific antibody LP11 recognises gH in gL dependant manner, while antibody 52S recognise gH in a gL independent manner. It was observed that both of the antibodies were efficiently internalised to cytoplasmic organelles in gMR-infected cells. However, in cells infected with ΔgM, these antibodies remained on the plasma membrane

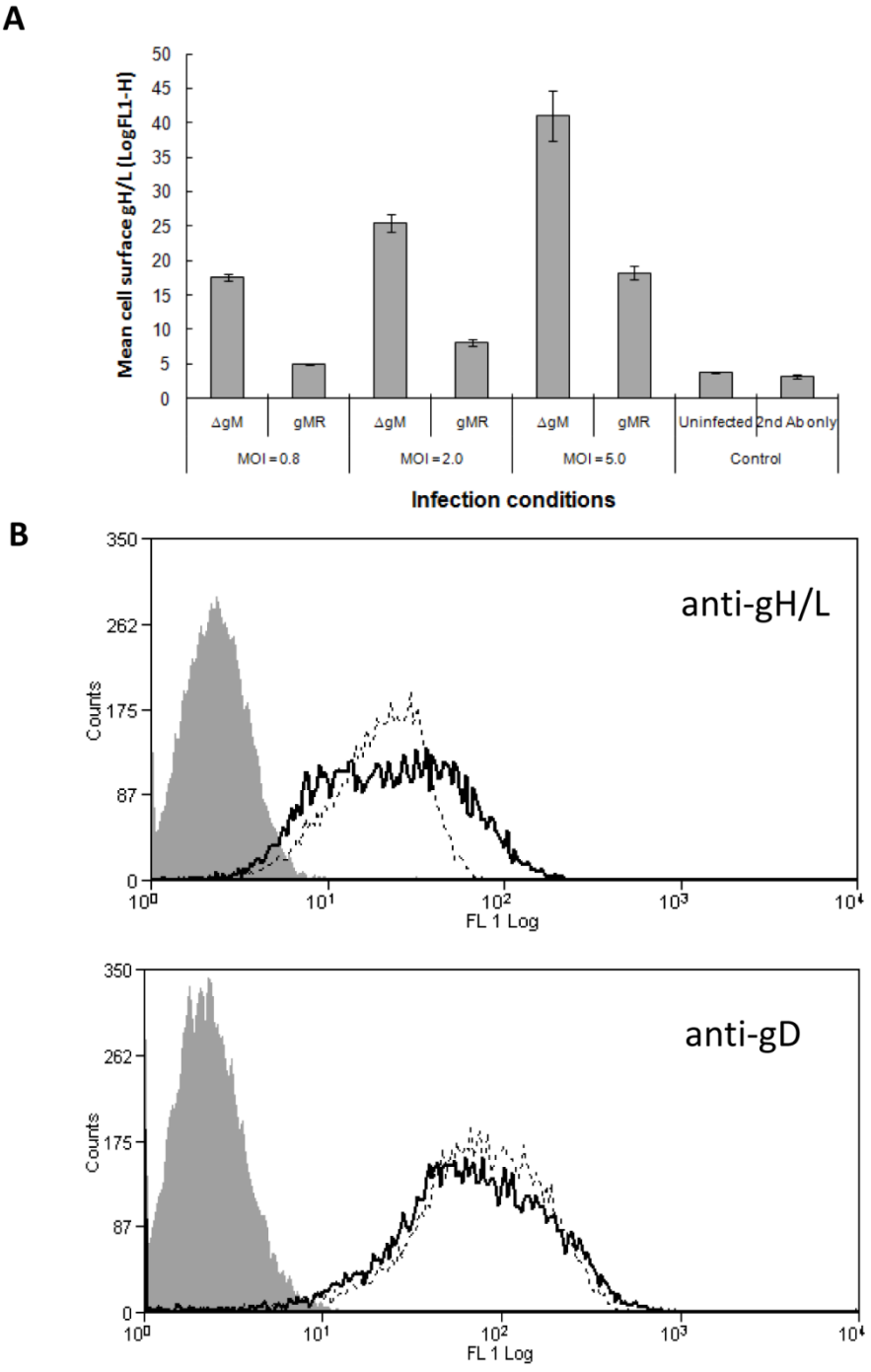

Figure 2.12: Analysis of cell surface gH/L and gD in infected cells by FACS. (A) Vero cells were infected with ΔgM or gMR at 0.8, 2.0 and 5.0 PFU/cell. At 6 hpi, the live cells were incubated with gH/L specific antibody on ice followed by fluorescent secondary antibody labelling. The cell surface fluorescent signals were analysed by FACS. Uninfected cells and infected cells incubated with secondary antibody only were used as the negative controls. (B) Vero cells infected with ΔgM or gMR were separated into two parallel samples at 6 hpi for labelling with gH/L or gD specific antibodies and analysis by FACS. Histograms show the gH/L (upper panel) or gD (lower panel) present on the cell surface of uninfected controls (grey filled), ΔgM infected cells (solid line) and gMR infected cells (dashed line).

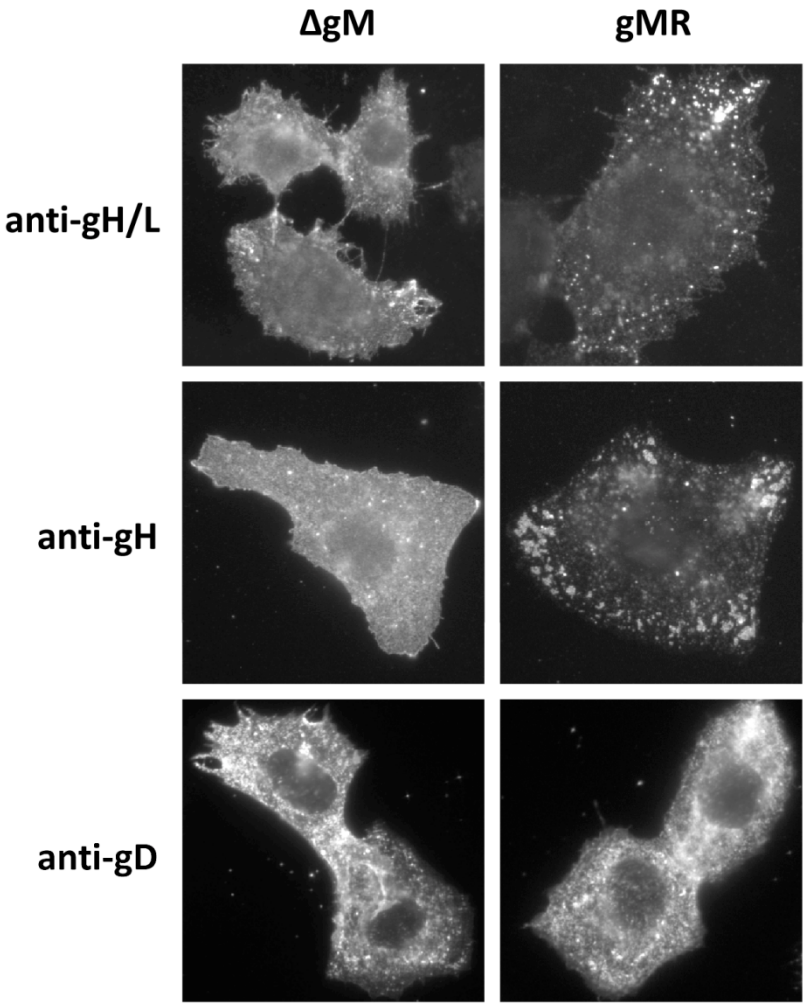

Figure 2.13: Analysis of gD and gH/L internalisation. Vero cells were infected by ΔgM or gMR at 3 PFU/cell. At 6 hpi, cells were incubated with gH/L, gH or gD specific antibodies at 37 ºC for one hour and then fixed and labelled with fluorescent secondary antibodies. Pictures were taken with a fluorescent microscope (Olympus IX70) and processed in ImageJ software.

(Figure 2.13). No obvious differences were observed in the internalisation of a gD specific antibody in cells infected by ΔgM or gMR (Figure 2.13). These data suggest that gM has a specific role in the internalisation of gH/L from the cell surface during HSV-1 infection.

2.2.8 Analysis of virion proteins in purified ΔgM and gMR viruses

Previously it has been demonstrated that gM can cause the internalisation of both gD and gH/L, which suggests a possible role of gM in transporting these envelope proteins from cell surface to the secondary envelopment sites for incorporation to virions (Crump *et al.*, 2004). As observed from section 2.2.6 and 2.2.7, more gH/L is on cell surface and the internalisation of gH/L is impaired in the absence of gM suggesting that the virion incorporation of gH/L might be affected. To analyse whether the deletion of gM had any effect on the incorporation of gH/L and other viral proteins into virions, ΔgM and gMR viruses were purified by Ficoll gradient centrifugation from the media of infected cells. The viral protein content in the purified virus preparations was examined by coomassie blue staining and western blotting.

According to the coomassie blue staining of viruses purified from HT29 cell culture supernatant, the protein profiles of ΔgM and gMR were similar. There are bands at estimate size on the gel showing tegument proteins including VP1/2, VP13/14, VP16 and VP22, the major capsids protein VP5 and various bands indicating the glycoproteins (Figure 2.14 A). Interestingly, with the same amount of PFU (8×10^6) loading, purified ΔgM showed stronger viral protein signals than gMR (Figure 2.14 A). This result suggests that with the same amount of infectious particles the purified ΔgM virus contains more protein content than gMR. Upon analysing a range of PFU it was found that the preparations of ΔgM contained approximately twice the amount of the capsid and tegument proteins than the equivalent PFU of gMR (Figure 2.14). This suggests that the particle-to-PFU ratio is higher for ΔgM and the loss of gM causes virions to be less infectious. When comparing similar levels of capsid (VP5) loading (compare 1.6×10^7 PFU of gMR with 8×10^6 PFU of ΔgM in Figure 2.14), the two viruses harvested from HT29 cells had no significant difference in the levels of tegument proteins VP16 and VP22 or envelope proteins gB and gD. However, a small decrease in gC and a significant decrease in gH were observed in ΔgM virions (Figure 2.14 B). Quantification of signals and normalisation of the data to VP5 levels demonstrated that ΔgM virions contained approximately 6-fold less gH and 3-fold less gC than gMR virions (Figure 2.14 C).

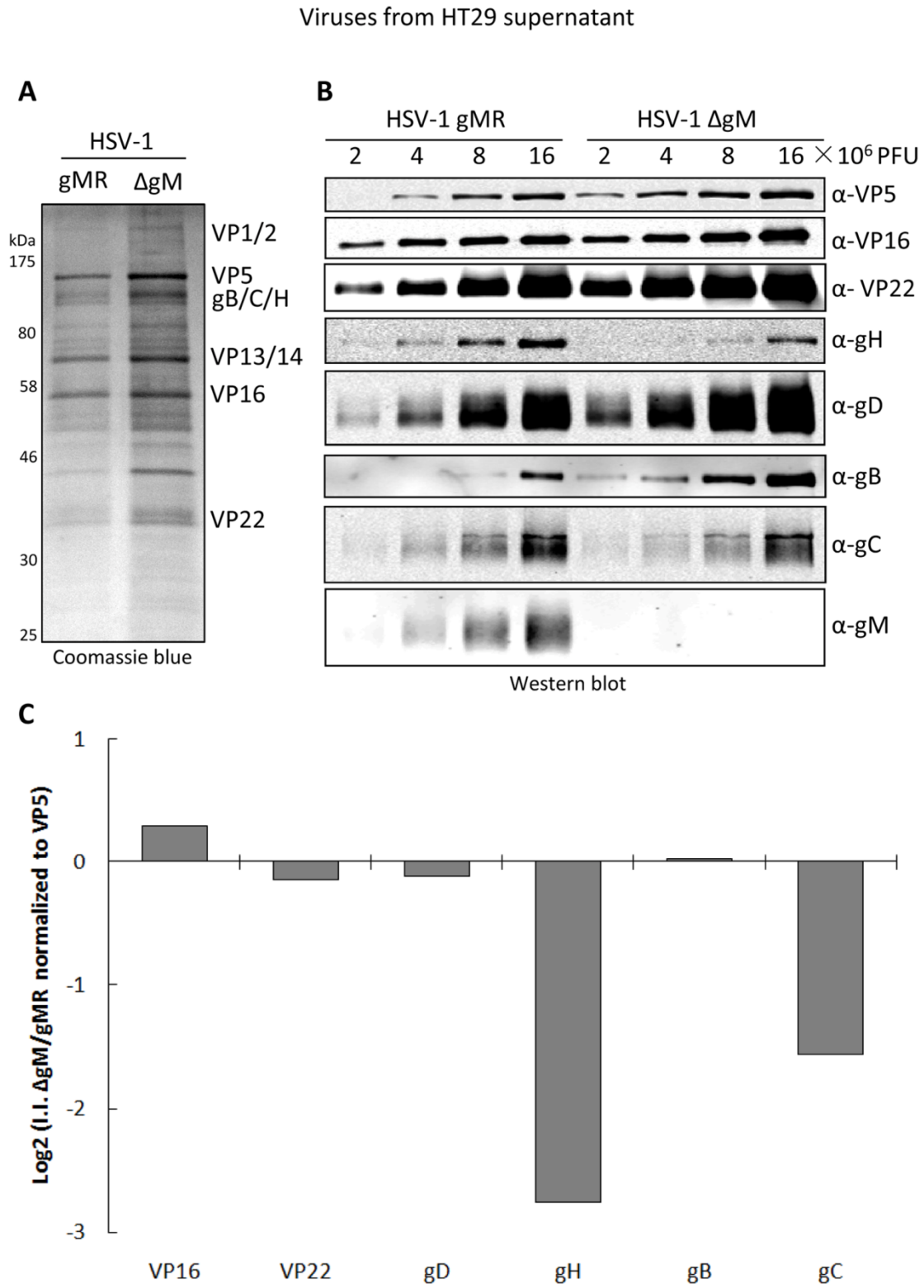

Figure 2.14: Analysis of viral protein incorporation in virions generated by HT29 cells. ΔgM or gMR were purified from the culture supernatant of HT29 cells. 8 x 10^6 PFU purified viruses were separated by SDS-PAGE and stained with coomassie blue* (A). Two-fold dilution series of each virus were analysed by western blotting with antibodies against HSV-1 proteins (B). The integrated intensity (I.I.) values for viral protein signals were normalised to VP5 and the values of $\log_2$ (ΔgM:gMR) after the normalisation are shown (C). * Coomassie blue staining was done by Dr C. Crump.

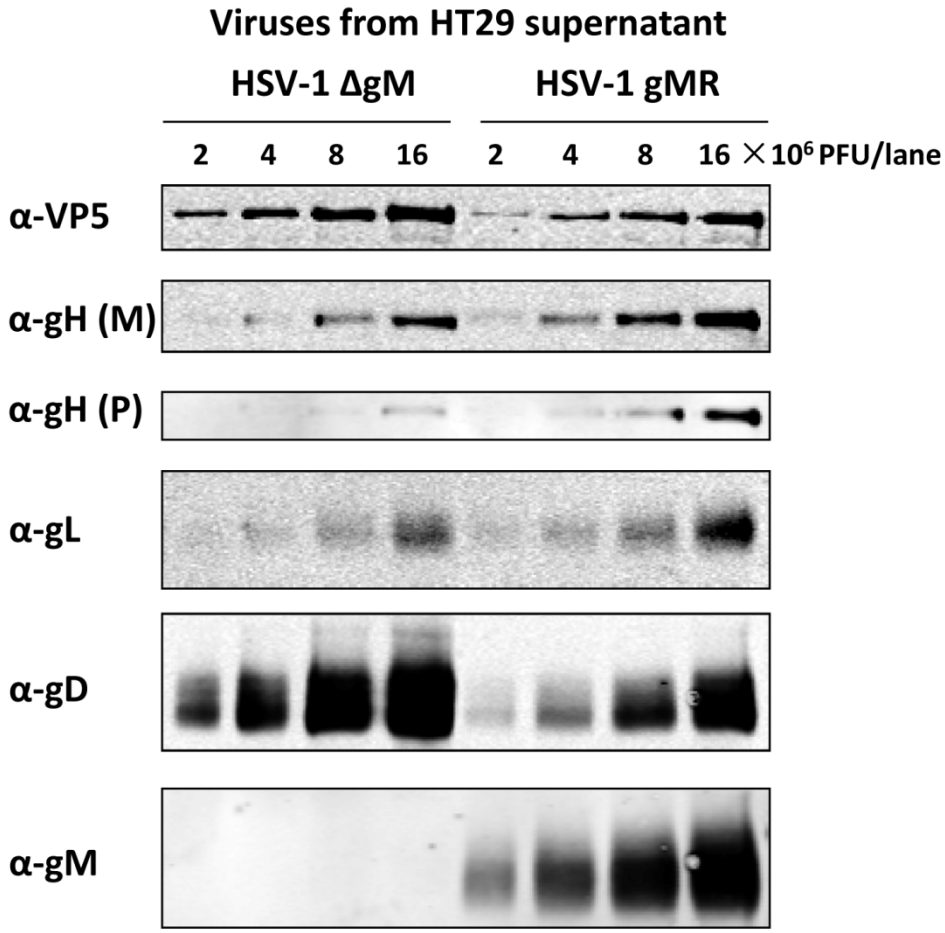

Figure 2.15: Further western blot analysis of viral protein incorporation in virions generated by HT29 cells. ΔgM or gMR were purified from the culture supernatant of HT29 as an independent preparation. Two-fold dilution series of each virus were separated by SDS-PAGE gels and analysed by western blotting with the indicated antibodies. Two gH specific antibodies were used: mouse monoclonal antibody BBH1, α-gH (M), and rabbit polyclonal antibody Shabba, α-gH (P).

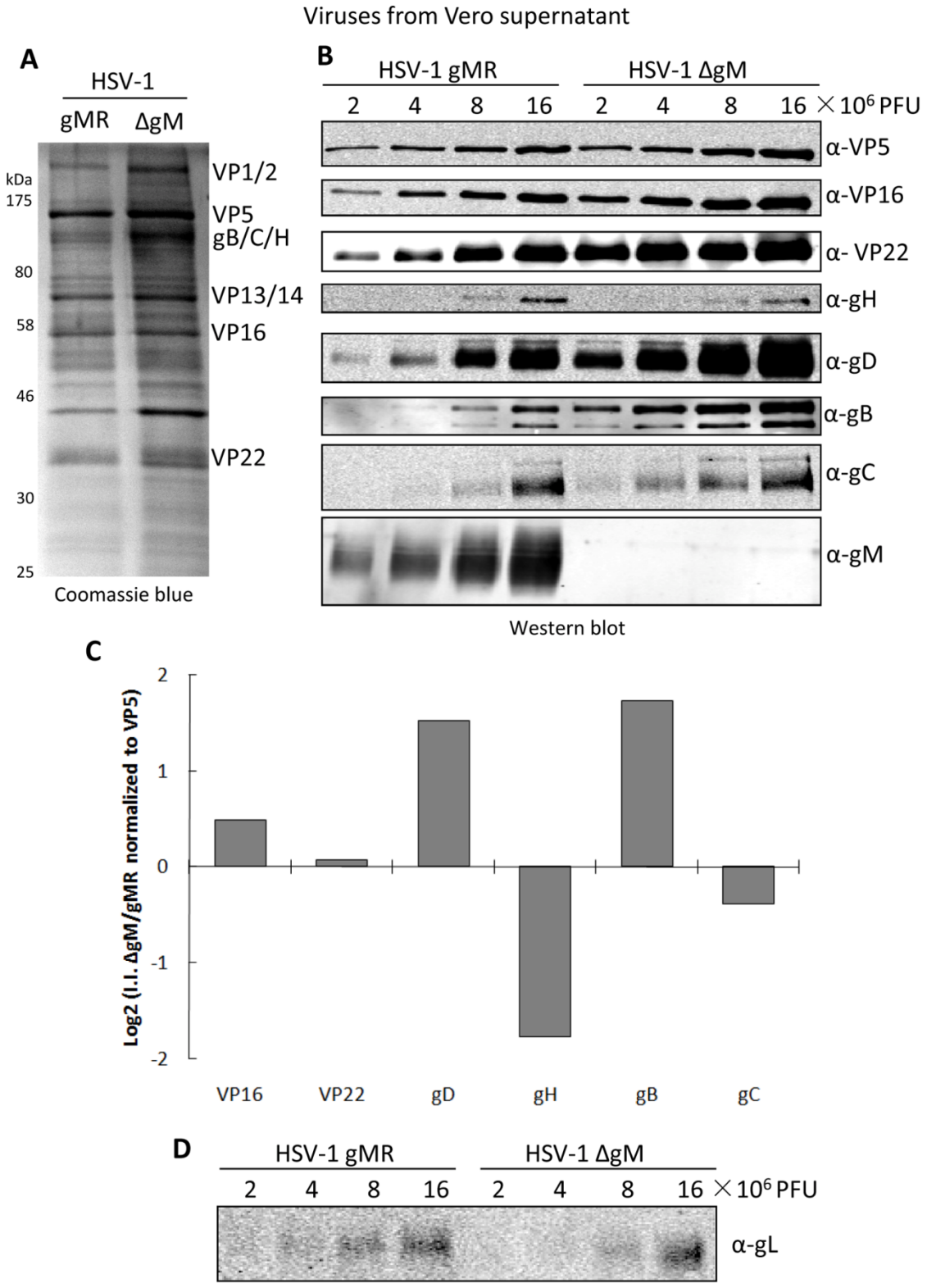

Figure 2.16: Analysis of viral protein incorporation in virions generated by Vero cells. ΔgM or gMR were purified from the culture supernatant of Vero cells. 8 x 10^6 PFU purified viruses were separated by SDS-PAGE and stained with coomassie blue (A). Two-fold dilution series of each virus were analysed by western blotting with antibodies against HSV-1 proteins (B). The integrated intensity (I.I.) values for viral protein signals were normalised to VP5 and the values of $\log_2$ (ΔgM:gMR) after the normalisation are shown (C). The virus samples were also analysed by anti-gL antibody (D). * Coomassie blue staining was done by Dr C. Crump.

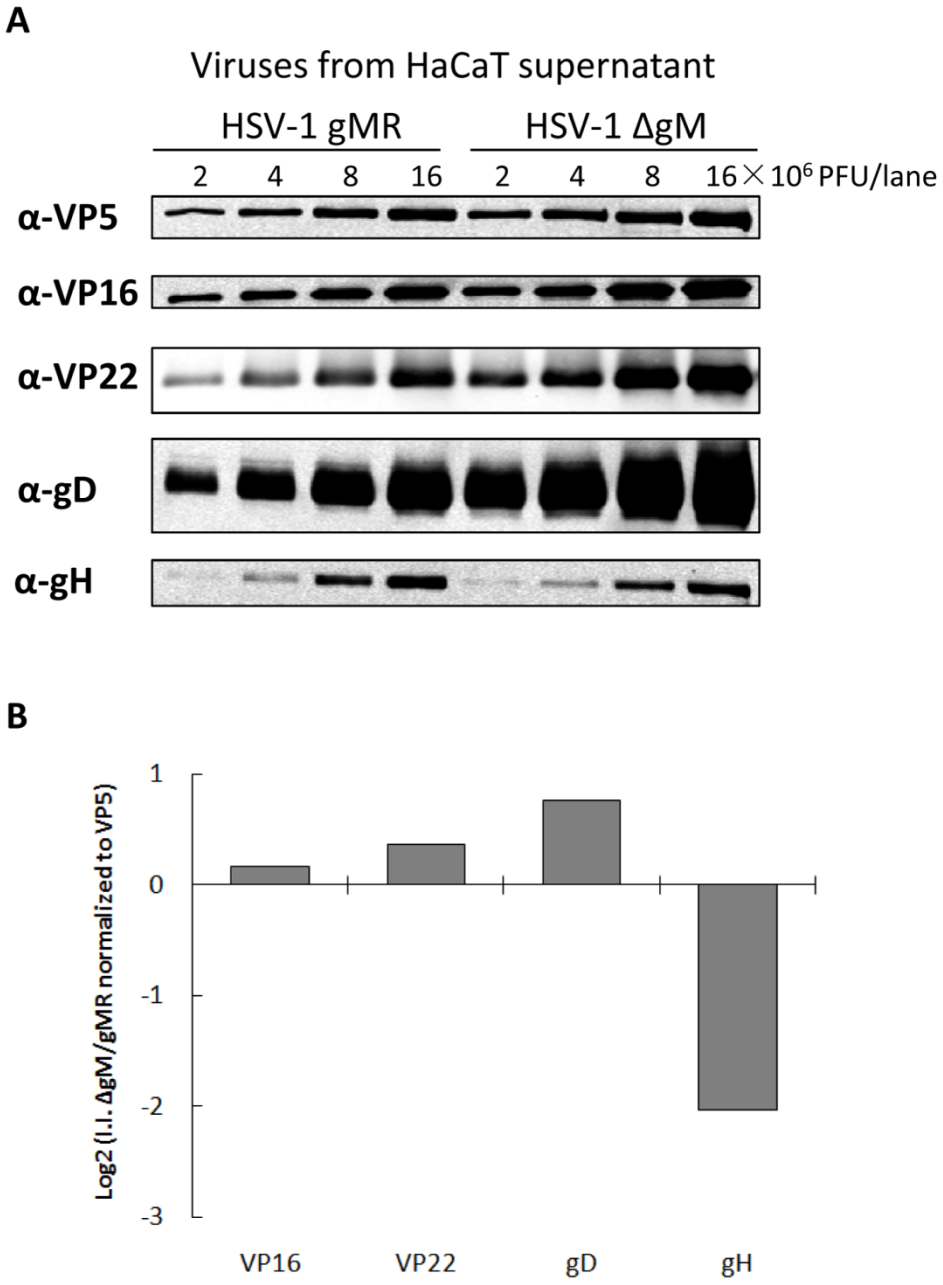

Figure 2.17: Analysis of viral protein incorporation in virions generated by HaCaT cells. (A) Two-fold dilution series of purified ΔgM and gMR were loaded into SDS-PAGE gel as indicated by the PFU amount per lane and analysed by western blotting. (B) The integrated intensity (I.I.) values for all the viral protein signals were normalised to VP5 and the values of $\log_2$ (ΔgM:gMR) after the normalisation are shown.

Western blotting of independent purified virus preparations from HT29 culture supernatant was performed in order to confirm the observation. Both of the anti-gH monoclonal and polyclonal antibodies showed with similar capsid protein VP5 loading, there was lower gH in ΔgM virus (Figure 2.15). Furthermore, the gL content from the purified viruses were also tested and, as expected, the purified ΔgM virus contains less gL. Unfortunately, the anti-gL antibody always gave weak and fuzzy band, thus gL was omitted from the protein band quantification to avoid potential errors (Figure 2.15).

Similarly, ΔgM and gMR viruses produced by Vero cells also had same protein profile according to the coomassie blue staining but ΔgM contains higher protein content (Figure 2.16 A). According to the western blotting, the Vero generated ΔgM and gMR had no significant difference in the incorporation of the tegument proteins VP16 and VP22 between the two viruses, but approximately 3-fold less gH was found in ΔgM than gMR virions (Figure 2.16 B, C). However, unlike virions prepared from HT29 cells, when viruses were prepared from Vero cells there was little difference in the incorporation of gC, and surprisingly ΔgM virions contained 2-3 times more gB and gD than gMR virions (Figure 2.16 B, C). The gL content from the purified viruses were also tested and, as expected, the purified ΔgM virus contains less gL (Figure 2.16 D).

These observations were consistent between independent preparations of purified viruses from both cell types and the gH reductions in ΔgM virions agree with the gL levels observed by western blot (Figure 2.15, 2.16 D). In addition, viruses purified from HaCaT culture supernatant were also investigated by western blotting. It was found that similarly as viruses generated by HT29 and Vero cells, the particle-to-PFU ratio is consistently higher in ΔgM virions and there were similar level of VP16 and VP22 in ΔgM and gMR virions. However, the ΔgM virions contains about 4-fold less gH than gMR (Figure 2.17).

Overall these data suggest gM plays an important role in the efficient incorporation of gH/L into HSV-1 particles, but to a greater extent in HT29 cells than in Vero and HaCaT cells.

2.2.9 Entry kinetics of HSV-1 in the absence of gM

It is widely known that gB, gD and the gH/L complex are essential for HSV-1 entry (Heldwein & Krummenacher, 2008). The decrease of gH/L levels in ΔgM virions observed in section 2.2.8 could alter the entry kinetics of HSV-1. Therefore virus penetration assays were performed to examine the entry rate of HSV-1 with or without gM.

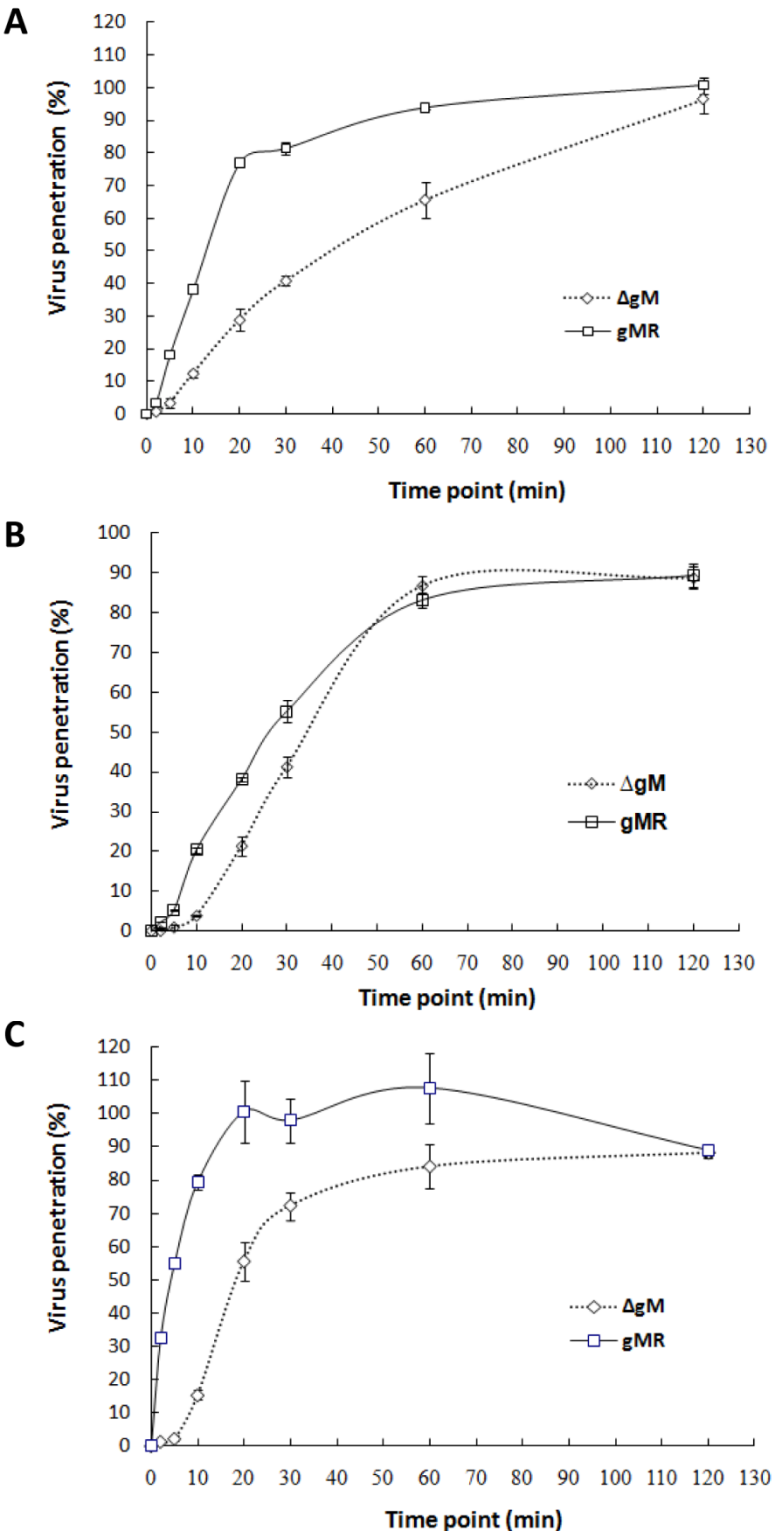

Figure 2.18: Entry assay on three cell lines using ΔgM and gMR working stocks. Appropriate diluted ΔgM and gMR working stocks were incubated on HT29 (A), Vero (B) or HaCaT (C) cell monolayers at 4 °C and then shifted to 37 °C for various times as indicated. Acid wash was applied at each time points and the cells were incubated at semi solid medium for plaque formation. The plaques were counted and the relative penetrations of the viruses were determined by calculating the percentage of plaques formed of the input. The means and standard errors from triplicate experiments are shown.

Standard working stocks of ΔgM and gMR viruses grown in Vero cells were tested for entry kinetics on HT29, Vero and HaCaT cell monolayers (Figure 2.18, A-C). The cells were seeded into six-well plates to form monolayers and incubated with 240 PFU/well of either ΔgM or gMR virus at 4 ºC for 1 hour. The cells were shifted to 37 ºC for virus penetration and acid wash was performed at the various time points to inactivate viruses that had not penetrated into the cells. The percentage of the PFU at each time point of the total input PFU was calculated to determine penetration rates. In HT29 cells, ΔgM demonstrated a significantly delayed penetration rate compared to gMR. For instance, at 20 min time point, the penetration rate of gMR was nearly 80% while it was only ~30% for ΔgM; gMR reach the plateau phase within one hour while it took two hours for the penetration rate of ΔgM to reach the same level (Figure 2.18 A). In Vero cells, ΔgM demonstrated a delayed penetration rate than gMR but the difference between these two viruses was much smaller than in HT29 cells. ΔgM had slower penetration rate than gMR during the initial 30 min but both of these viruses reached the plateau phase within one hour (Figure 2.18 B). In HaCaT cells, both of the viruses had faster penetration rate than on HT29 and Vero cells with steeper slopes for the penetration rate curves. Consistent with the other two cell lines ΔgM also demonstrated a delayed penetration rate. gMR reached a plateau phase within 20 min while ΔgM took 30-60 min in HaCaT cells (Figure 2.18 C). Therefore, for all the three tested cell lines, the deletion of gM caused defects in host cell penetration.

The viruses used in the above experiments were standard working stocks prepared from whole lysate of infected cells and they contain not only viruses but also cell debris, which could cause unexpected effects during the penetration assays. The gradient purified virus stocks contain low level of cellular contamination and the virus content can be determined by both titration and western blotting. Thus penetration assays using purified virus stocks can offer more detailed information. Furthermore, the working stocks used above were prepared from infected Vero cells and as demonstrated in Figure 2.14-2.16, the deletion of gM showed a greater reduction of gH/L in virions generated from HT29 cells compared to Vero cells. Therefore, the ΔgM and gMR viruses purified from Vero and HT29 cells were analysed in penetration assays. On comparison of ΔgM and gMR viruses purified from Vero (Figure 2.19 A) and HT29 (Figure 2.19 B) cells, there was a significant delay in the initial rate of ΔgM entry. It took approximately twice as long for ΔgM to reach 50% entry as it did for gMR (Figure 2.19 A, B). The two viruses harvested from Vero cells obtained an equivalent level of entry by 70 min (Figure 2.19 A). However, for the viruses

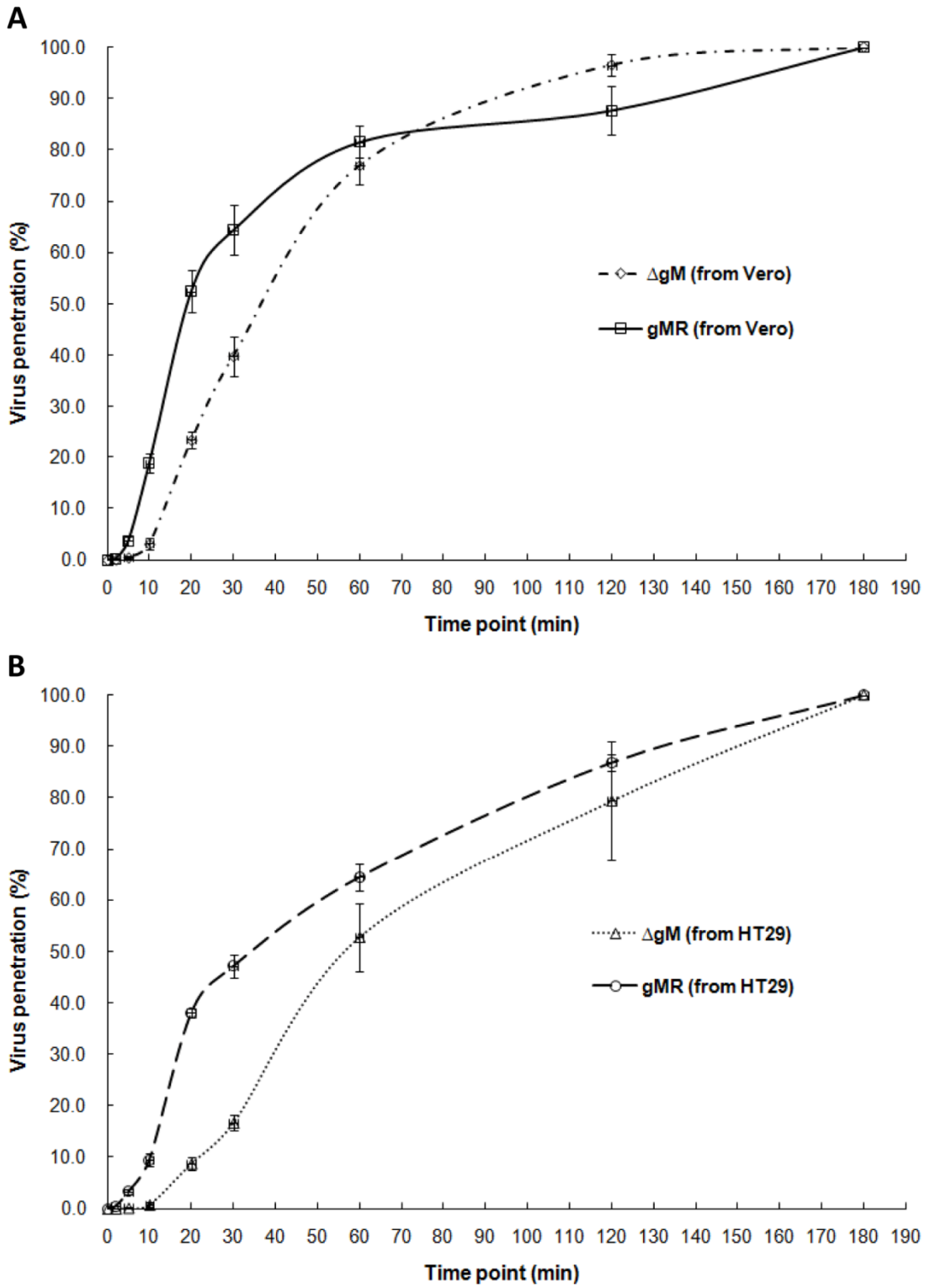

Figure 2.19: Entry assay on Vero cell monolayers using ΔgM and gMR purified viruses. The purified viruses were incubated on Vero monolayers and the entry assays were performed as described in Figure 2.18. The plaques were counted and the relative penetrations of ΔgM and gMR purified from Vero (A) and HT29 (B) culture supernatant were determined. The means and standard errors from triplicate experiments are shown.

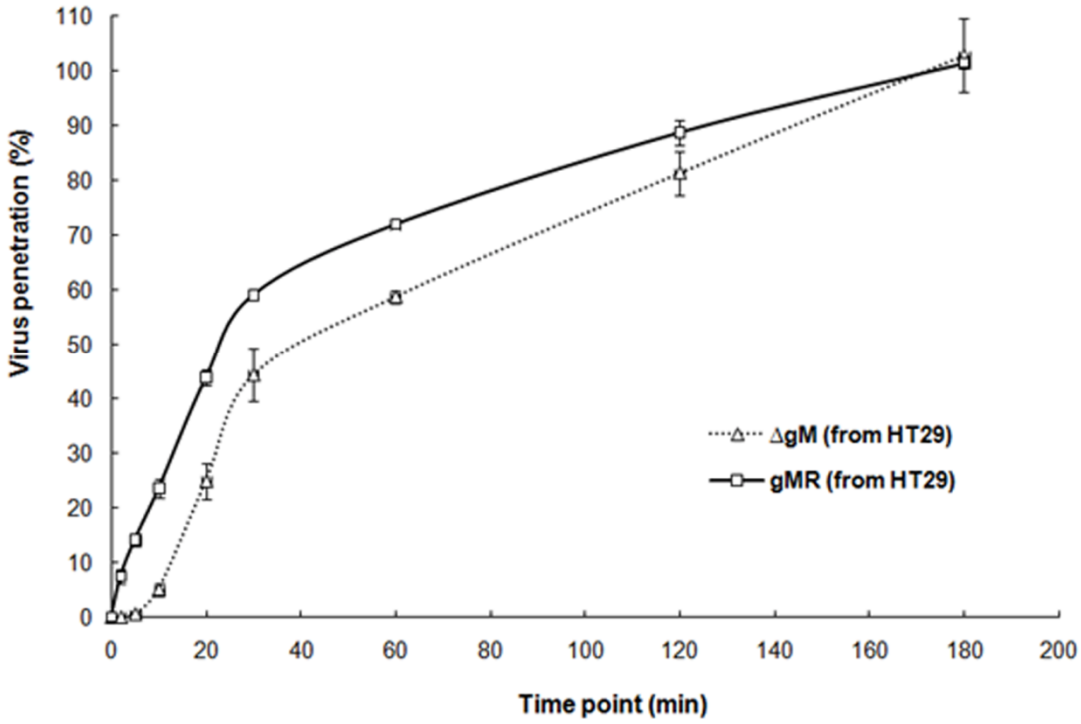

Figure 2.20: Entry assay on HT29 cell monolayers using ΔgM and gMR purified viruses. The entry assay was performed as described in Figure 2.18. The relative penetration rates of ΔgM and gMR purified from HT29 culture supernatant were determined. The means and standard errors from triplicate experiments are shown.

purified from HT29 cells, ΔgM showed a more severely attenuated entry with just ~9% of the virus penetrated into the host cells by 20 min compared to the 38% of gMR and they did not reach an equivalent level until 2 h (Figure 2.19 B). In addition, both of the viruses purified from Vero cells penetrated Vero cells fast than the corresponding virus harvested from HT29 cells. These may be directly related to the different profiles of the viral protein content of the purified viruses from these two cell types (Figure 2.14-2.16). Furthermore, the penetration assay was also performed on HT29 cell monolayers for ΔgM and gMR viruses purified from HT29 cells. Consistent with the other penetration assay results, ΔgM had a delayed penetration rate compared to gMR (Figure 2.20). However, it took both of the viruses three hours to reaching the plateau phase (Figure 2.20), suggesting a generally slower entry of HSV-1 into HT29 cells in these assay conditions.

Taken together, gM deletion causes delayed penetration rate for HSV-1 and this delay in viral entry correlates with the observed reduction of gH/L in ΔgM virions, with more significant delay in entry for ΔgM viruses prepared from HT29 cells, which had the lowest level of gH/L in purified virions.

2.3 Discussion and conclusion

The work described in this chapter is primarily an investigation into the role of gM in HSV-1 assembly. Particular focus was given to the possible role of gM in the targeting of other HSV-1 glycoproteins to virus assembly sites, as previous data from the laboratory had shown gM mediated internalisation and targeting of gD and gH/L in transfection studies. To investigate the function of gM in HSV-1, the gM encoding gene UL10 was deleted from the low passage strain SC16 and the effects of this deletion in infected cells was analysed. As another type III membrane protein, pUL43 may have similar functions as gM, in the initial studies, a gM and pUL43 double deletion virus was also included.

The product of the UL43 gene in HSV-1 was firstly reported and characterised as a protein about 32 kDa in size (Carter *et al.*, 1996). In addition, pUL43 has been predicted to contain multi-transmembrane domains (Klupp *et al.*, 2005) as a type III membrane protein. There were potential implications for regulation of gene expression by antisense transcription of UL43.5, although, pUL43 is one of the least characterised proteins in alphaherpesviruses. Both UL43 and UL43.5 are dispensable for viral replication in HSV-1 in tissue culture (MacLean *et al.*, 1991; Powers *et al.*, 1994). Subsequently it was also shown that the PRV pUL43 is present in the virions but the deletion of UL43 from the viral genome did not

show a significant effect on virus replication (Klupp *et al.*, 2005). However, the expression of PRV UL43 protein in cells inhibited membrane fusion induced by the viral fusion proteins to a similar extent as gM (Klupp *et al.*, 2000), suggesting possibly related functional roles of gM and pUL43 in controlling glycoprotein localisation. Previous data has also shown that the deletion of HSV-1 UL43 protein has no effect in a mouse model (MacLean *et al.*, 1991) and so it is unclear what roles pUL43 may have *in vivo*. In the viral growth assays performed for these studies, no robust phenotype was found. Furthermore, no antibodies were available to investigate pUL43 proteins in infected cells, and so additional studies were not performed on UL43 and its deletion viruses. However, the data collected in a relatively wide range of in vitro cell models for these studies will be informative for future analysis of HSV-1 UL43.

The combined data from the single- and multi-step growth analysis together with the observed plaque sizes suggest that gM is relatively dispensable for the viral assembly but that gM is important for efficient cell-to-cell spread. Analysis of purified virus particles demonstrated a significant reduction in the incorporation of gH/L into ΔgM virions, and a concomitant inhibition of the internalisation of gH/L from the plasma membrane was observed in ΔgM-infected cells. These data are best explained by a functional role of gM in the retrieval of gH/L from the cell surface, and subsequent targeting to sites of secondary envelopment for efficient virion incorporation. However, although internalisation of gH/L appears to be significantly inhibited in the absence of gM, gH/L could still be observed in Golgi/TGN compartments in ΔgM infected cells when the sub-cellular localisation of total gH/L was probed. As all glycoproteins pass through the Golgi on their way from the endoplasmic reticulum (ER) to the plasma membrane, this Golgi/TGN localised gH/L may be newly synthesised protein within the secretory pathway. Furthermore, as infectious particles can still be produced in the absence of gM, this suggests that the pool of gH/L within the secretory pathway must pass through the viral assembly compartment and be present at sufficient concentrations to be incorporated into virions, albeit at a lower level, when gM is deleted. These data suggest that while gM is not essential for newly synthesised gH/L to reach sites of secondary envelopment, gM is necessary for maintaining an appropriate concentration of gH/L within the secondary envelopment compartment for assembling fully infectious particles, by retrieving gH/L molecules that have escaped further down the secretory pathway.

Previously it has been shown that gM and/or the gM/N complex can cause the relocalisation of both gD and gH/L from the plasma membrane to the TGN in

transfection assays. It was therefore surprising that no decrease in the incorporation of gD into ΔgM virions was observed neither the internalisation of cell surface gD in infected cells was affected in the absence of gM. Whilst gM has the capacity to relocalise gD to intracellular compartments in transfected cells, in the context of HSV-1 infection other viral proteins must also be able to control gD localisation. It is currently unclear what performs this function in infected cells, although possible candidates are the gK/pUL20 complex or pUL43.

One of the surprising observations we made during these studies was that more gB and gD were incorporated into ΔgM produced in Vero cells. Upon analysis of the expression of viral proteins there was a greater proportion of higher molecular weight gB, gD and gC species in ΔgM infected compared to gMR infected Vero cells, suggesting more rapid maturation of these glycoproteins in the absence of gM (Figure 2.9). Interestingly, gM has been shown to localise to the ER in infected cells (Baines *et al.*, 2007b; Zhang *et al.*, 2009a). It is therefore conceivable that ER localised gM could retard the exit of glycoproteins from the ER, thereby delaying their processing in the Golgi. This could increase levels of mature glycoproteins in post-Golgi membranes in the absence of gM, leading to enhanced incorporation into virions. However, this appears to be a phenotype specific to Vero cells; there was no observable difference in viral glycoprotein expression patterns between ΔgM and gMR in HT29 cells (Figure 2.9).

Whether gM can control the localisation of other HSV-1 envelope proteins is currently an open question. It is interesting that in HT29 cells less gC is incorporated into virions in the absence of gM. The cytoplasmic domain of HSV-1 gC is only 11 amino acids with no consensus trafficking motifs present. Therefore gC is likely to be localised to the plasma membrane in the absence of other viral proteins. In addition, one of the currently on-going projects in the laboratory where the plasma membrane fraction of ΔgM or gMR infected cells was extracted and subjected to mass spectrometer for analysing the change of plasma membrane proteins under ΔgM or gMR infection. Data has shown that ΔgM infected cells demonstrate higher gC level on cell surface than gMR infected cells (S. Y. K. Lau *et al.* unpublished data). These data suggest gM is indeed important in the efficient internalisation and targeting of gC to viral assembly compartments.

Recently, it has been reported that the absence of gM in the HSV-1 KOS causes an inhibition of virion morphogenesis in the cytoplasm of infected cells (Leege *et al.*, 2009). It is plausible that reduced levels of envelope glycoproteins such as gH/L to assembly compartments could lead to defects in secondary envelopment. Indeed the cytoplasmic

domain of gH has been shown to interact with the major tegument protein VP16 (Gross *et al.*, 2003). Given that gM can also interact with the major tegument protein VP22 (Stylianou *et al.*, 2009) at least two routes of tegument-envelope interaction would be inhibited for ΔgM viruses. However, we observe much smaller effects on the single cycle replication kinetics of HSV-1 lacking gM expression with strain SC16 than was observed for strain KOS (Leege *et al.*, 2009). This may imply that there are mechanisms in SC16 that can compensate for the loss of gM function that are absent from the highly passaged KOS strain. It would also be interesting to determine whether reductions in titre that have been previously observed for gM deletion viruses are due to fewer virus particles being produced or whether similar numbers of virions are made but they are less infectious due to defective envelope protein incorporation.

Overall, data in this chapter demonstrate an important role for HSV-1 gM in gH/L internalisation from the plasma membrane of infected cells and incorporation into mature virions. Although still many questions remain about the mechanisms of the role of this conserved herpesvirus protein gM, this work is the first demonstration of a functional role of gM in viral glycoprotein trafficking in infected cells.

3 Searching for interactions between HSV-1 tegument and human ESCRT proteins

3.1 Introduction

The ESCRT machinery is involved in the pathway for the down regulation of cell surface receptors by controlling their transport and incorporation into the intraluminal vesicles of MVBs, which subsequently fuse with lysosomes to degrade their content (Wollert & Hurley, 2010). The ESCRT proteins were first identified in yeast and this pathway is conserved from yeast to human. There are four ESCRT complexes (ESCRT-0, -I, -II and -III), the VPS4 ATPase complex and many associated proteins. Many studies have shown that ESCRTs are also responsible for the membrane remodelling during retrovirus budding on the cell surface (Morita & Sundquist, 2004) and the cleavage of the membrane neck between daughter cells during cytokinesis (Carlton & Martin-Serrano, 2007; Morita *et al.*, 2007b).

While the use of ESCRTs by retroviruses [reviewed in (Morita & Sundquist, 2004)] and several other families of RNA viruses (Ariumi *et al.*, 2011) has been well established, less is known about the role of ESCRTs in the replication of large complex DNA viruses such as the herpesviruses. Previous studies have shown that the replication of HSV-1 is inhibited by the over expression of dominant-negative VPS4 (Calistri *et al.*, 2007; Crump *et al.*, 2007). It has also been shown that over expressing dominant-negative ESCRT-III proteins inhibits infectious HSV-1 production, which suggests ESCRT-III proteins are important for HSV-1 replication. However, the mechanism by which HSV-1 recruits the ESCRT machinery is unknown, and no direct interaction between HSV-1 proteins and the ESCRT machinery has been reported. ESCRT recruitment by HSV-1 does appear to be different from human immunodeficiency virus (HIV) which interacts with TSG101 and ALIX through late domain motifs to recruit ESCRTs because the disruption of TSG101 and/or ALIX function does not impair HSV-1 replication (Pawliczek & Crump, 2009).

When the tegumented HSV-1 capsids bud into host membrane structures in the cytoplasm, the tegument layer located in between the viral capsid and membrane would seem the most likely to be involved in ESCRT recruitment (by analogy to RNA virus that primarily interact with ESCRT protein via their matrix). In order to identify direct interactions

between HSV-1 viral proteins and ESCRTs, HSV-1 tegument genes were cloned and tested against a panel of ESCRT and ESCRT-associated proteins in yeast two-hybrid (Y2H) assays. Positive hits from interaction screens were analysed using GST pull-down, co-immunoprecipitation and protein co-localisation assays for validation. In addition, experiments were performed to identify short motifs/domains within tegument proteins and ESCRT candidates that are important for their interactions.

3.2 Result

3.2.1 HSV-1 tegument gene cloning and ESCRT plasmids

A panel of ESCRT and ESCRT associated protein in yeast expressing plasmids were provided by J. Martin-Serrano at King's College London. The CC2D1B clone that was included in this library is a variant of the full length protein lacking the C-terminal domain. The CC2D1B full length (CC2D1BFL) clone was obtained by PCR using a human cDNA library as the template. The primers were designed according to the full length CC2D1B gene (Gene ID: 200014) (Table 6.8) and the plasmid was sequenced for confirmation. HD-PTP protein was reported to be functionally related to ALIX and has been shown to be involved in endosomal cargo sorting and multivesicular body morphogenesis. HD-PTP plasmids were not included in the original set of Y2H plasmids and so the appropriate yeast expression plasmids were generated by sub-cloning from pcDNA3-HA-HD-PTP from P.Woodman at University of Manchester (Doyotte *et al.*, 2008).

The yeast strain Y190 used in the screen contains the *lacZ* reporter gene under the control of a Gal4 promoter. The paired plasmids pHB18 and pGBKT7 express the prey and tagged bait respectively. Plasmids derived from pHB18 express the prey fused to the VP16 activation domain (AD) and plasmids derived from pGBKT7 express the bait fused to the Gal4 DNA binding domain (BD). Yeast cells were co-transformed with the pGBKT7- and pHB18- derived plasmids, grown in selective agar plates to form colonies and the report gene product β-gal activity was measured as described later in Chapter 6.

There are 23 HSV-1 tegument proteins that were identified to be component of extracellular virions by mass spectrometry (Loret *et al.*, 2008). Although UL4 was not found in HSV-1 extracellular virions in this study, it was detected in HSV-2 virions (Yamada *et al.*, 1998), and thus it was included in the tegument library construction for Y2H assays. In order to clone the HSV-1 tegument genes into the pHB18 and pGBKT7 plasmids, primers were designed based on the HSV-1 strain 17 genomic sequence (Refseq:

NC_001806) with appropriate restriction enzyme sites to enable insertions of the full length ORFs into plasmid multi-cloning sites. Plasmids containing HSV-1 KOS EcoR I genomic fragments (Goldin *et al.*, 1981) were used as templates during PCR (Table 6.5). As UL48 (VP16) of HSV-1 is a strong transactivator, when fused to the Gal4 DNA binding domain it is likely to cause high levels of auto-activation of reporter genes in the yeast two-hybrid assays. Therefore, a C-terminal activation domain truncated construct (UL48ΔAD) was made to attempt to prevent this auto-activation.

Table 3.1 Sequencing result of HSV-1 tegument gene clones for Y2H.

Tegument gene	Strain 17 size (bp)	Protein sequence differences compared to strain 17
UL4	600	A189T.
UL7	891	Y201H.
UL11	291	A8T.
UL13	1557	R25Q; V35I; A56G; V198A; P422L; C433R.
UL14	660	G131E; G163S; P177H; S194A.
UL16	1122	No amino acid mutation.
UL21	1608	No amino acid mutation.
UL23	1131	N23S; K36E; R89Q; A265T.
UL37	3372	D82A; D153E; M205L; P446A; S1054A; M1071T; A1088V; G1092E.
UL41	1470	R19Q.
UL46	2157	V180A; R304C; N411S; S443R; Ins482P; N502D; T513A.
UL47	2082	T82S; A162D; A532T.
UL48	1473	N13D; T124A.
UL49	906	G29C; S49A; Q51P; G95A; L252I.
UL50	1115	A85S; E162A; A172D; T177P.
UL51	735	A40V; F92L; I177L.
UL55	561	No amino acid mutation.
US2	876	R57Q; T85I; L124Y; D231S; L232H; Y239S; K253I; T254L.
US3	1446	S62G; E63D; C136R; D162Q.
US10	903	ΔLPGSPGLPGSPG; A117D.
US11	450	ΔPRSPREPRSPRE.
RL2 (ICP0)	2328	Sub cloned from plasmid pT7-111-ICP0cDNA containing strain 17 ICP0 cDNA.
UL36ΔPQ	9420	From Dr Crump. PQ repeat was replaced with in frame AflII site. L243M, V279G, $\Delta PPSAD_{352}$, T480M, A527T, N595S, W599R, V1219G, T1315I, H1580D, V1670L, S1700N, L2015I, Q2093H, A2168V, A2171T, V2242A, V2515A, A2520T, P2708L, A2723F, A2831T, A2850T, S2881N, A3030T, G3048R.

All of the clones were verified by sequencing (Table 3.1). In cases of significant protein sequence alterations, at least two independent clones were sequenced for confirmation. Comparison of the sequencing results of these KOS genes to HSV-1 strain 17 demonstrated that only three genes UL16, UL21 and UL55 had no amino acid differences. The other KOS gene sequences are highly similar to strain 17 except for a few single amino acid alterations, short deletions (12 amino acids) in the repeat sequences of US10 and US11, and one amino acid insertion in UL46 (Table 3.1). The nucleotide sequences are shown in the appendix.

Attempts were made to clone ICP4, ICP34.5 and ICP0 from the KOS strain plasmids by PCR using various conditions, however, no optimised condition was found to generate sufficient PCR products. These genes are highly GC rich (>75%) and the PCR reactions produced many non-specific product bands. There was no available plasmid contaning ICP4 and ICP34.5 that could be used for sub-cloning in the lab. Thus these tegument proteins were not included in the screen. Plasmid pT7-111 containing the ICP0 cDNA from strain 17 (from R. Everett) was used to sub-clone ICP0 cDNA into yeast expression plasmids for Y2H assays.

3.2.2 Yeast two-hybrid screen

In order to search for potential interactions between HSV-1 tegument and cellular ESCRT proteins, yeast cells were transformed with all combinations of prey and bait plasmids and tested for β-gal reporter gene activity. Liquid β-gal activity assays were performed using chlorophenol red-β-D-galactopyranoside (CPRG) as substrate and absorbance was measured at 550 nm (OD_{550} nm) in a microplate spectrophotometer (Martin-Serrano *et al.*, 2001).

For any new bait protein fused with a DNA binding domain there is the potential for false positive due to non-specific activation (auto-activation) of the reporter genes. Therefore pGBKT7 tegument constructs were initially tested for auto-activation by co-transfection with empty pHB18. Those constructs with OD_{550} nm > 0.20 were counted as auto-activated and were eliminated from the screen. Among all the constructs tested, pGBKT7-UL7, UL11, UL16, UL21, UL48 and UL48ΔAD constructs showed auto-activation with OD_{550} nm readings greater than 0.20 (Figure 3.1). Thus these six constructs in pGBKT7 were eliminated from the screen. This auto-activation was expected for pGBKT7-UL48 because it is known that the UL48 gene product VP16 is a strong transactivator. However, surprisingly, the pGBKT7-UL48ΔAD construct, which expresses Gal4 DNA binding

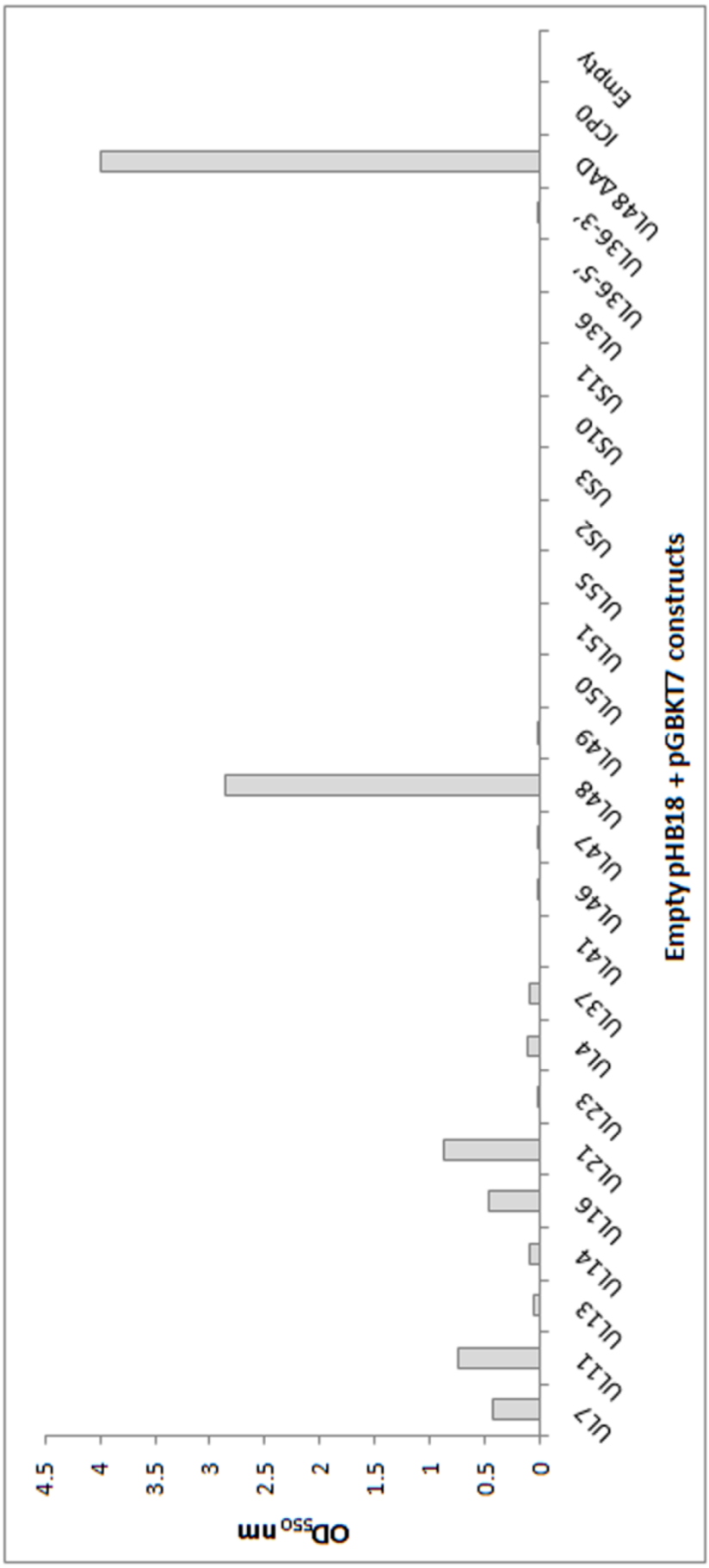

Figure 3.1: Auto-activation test of the HSV-1 tegument pGBKT7 constructs in Y2H system. The pGBKT7 plasmids expressing tegument proteins fused with Gal4 DNA binding domain were co-transfected with empty pHB18 plasmid into yeast cells. The reporter gene β-Gal activity was measured by a colour-change assay using chlorophenolred-β-D-galactopyranoside (CPRG) and OD_{550} nm absorbance units are shown. The auto-activation threshold was set as OD550 nm = 0.20 as shown by the dotted line. The empty pGBKT7 plasmid was used as the negative control.

domain fused with VP16 without its activation domain, also showed strong auto-activation level (Figure 3.1). This was despite previous reports using UL48ΔAD as bait in Y2H assays (Vittone *et al.*, 2005). However the difference in the system used here is the prey plasmid (pHB18) expresses the VP16 activation domain. These observations suggest that the VP16 activation domain may be able to interact with the VP16 core domain thereby causing expression of the reporter gene. In addition, the constructs pGBKT7- UL4, UL13, UL14 and UL37 showed a low level of auto-activation with OD_{550} nm between 0.05 and 0.20 (Figure 3.1). They were included in the screen although they may have relatively higher risk of generating false positive results.

Resulting colonies from leucine/tryptophan dual selection plates were screened for β-gal activity. The interaction between TSG101 and VPS28 has been reported in Y2H assays; therefore the combination of pGBKT7-TSG101 and pHB18-VPS28 was used as a positive control (Martin-Serrano *et al.*, 2003a). The bait plasmid (pGBKT7 derived) and empty pHB18 or the prey plasmid (pHB18 derived) and empty pGBKT7 combination were used as negative controls. The combined results from all these initial Y2H screens are shown when the tegument constructs were used as prey (Figure 3.2 A) and bait (Figure 3.2 B). The potential interactions are illustrated by colour boxes based on the values of OD_{550} nm. The OD_{550} nm values of the negative controls are mostly less than 0.20, so OD_{550} nm values larger than 1.00 give at least 5 fold higher level of the reporter gene expression, which indicates a high stringency for positive interactions. The protein pairs with OD_{550} nm values greater than 1.00 (orange and red colour boxes) were counted as positive hits. Thus orange and red coloured boxes were chosen as the primary candidates for further analysis. A part of these Y2H screen was performed by S. Rauch at King's College London as indicated in the figure.

CHMP4B and Nedd4 both showed positive interactions with many tegument proteins (Figure 3.2 A). While among these positive hits, there may be interesting candidates for further analysis; these data suggest CHMP4B and Nedd4 are generally "sticky" in this Y2H assay system. Therefore the tegument candidates that showed positive interactions with these two ESCRT proteins would need to be further analysed with more stringent methods. Similarly, the tegument protein pUL47 (VP13/14) also showed many positive hits (Figure 3.2 B), which also indicates that pUL47 may be prone to have non-specific interactions when expressed in yeast.

In addition, as shown in Figure 3.2, most of the identified interactions only occurred in one combination of the prey and bait plasmid pair but not the other way around (*e.g.*,

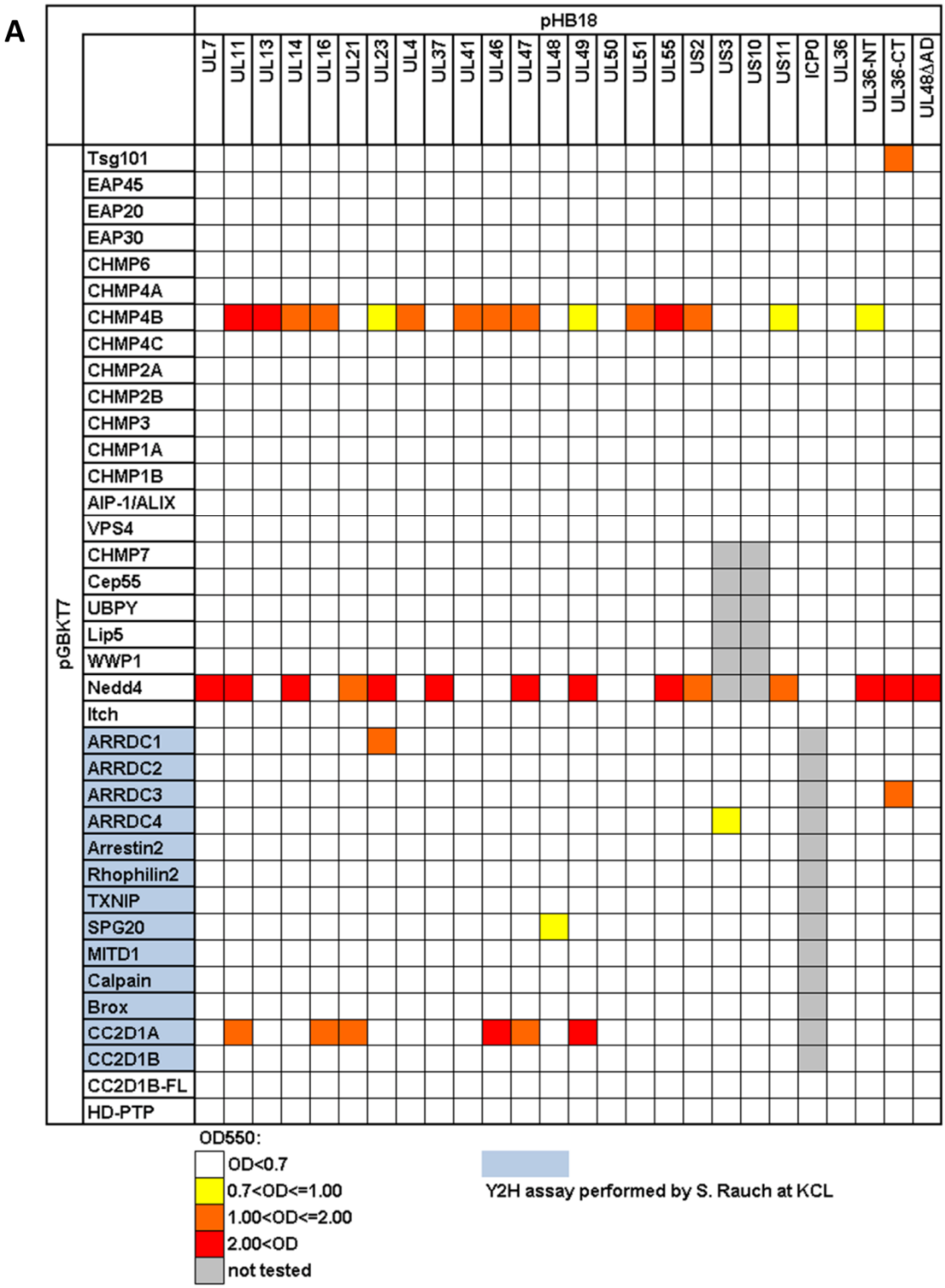

Figure 3.2: Potential interactions between HSV-1 tegument proteins and human ESCRT machinery. Paired plasmids of pHB18 and pGBKT7 were used. For each reaction, 1ug of each plasmid was transformed into competent yeast cells (strain Y190). The yeast cells were selected in leucine and tryptophan drop-out agar plates for three days. For measuring the reporter gene β-Gal activity, the yeast colonies were scrapped off the plates and suspended in 250ul β-Mercaptoethanol and SDS containing working buffer. The β-gal activities were tested by colour-changing assay of CPRG and quantified by measuring OD_{550} nm. The empty pHB18 or pGBKT7 plasmids containing no inserts were used as the negative controls. The interaction of pGBKT7-TSG101 and pHB18-VPS28 was used as the positive control. (to be continued)

B

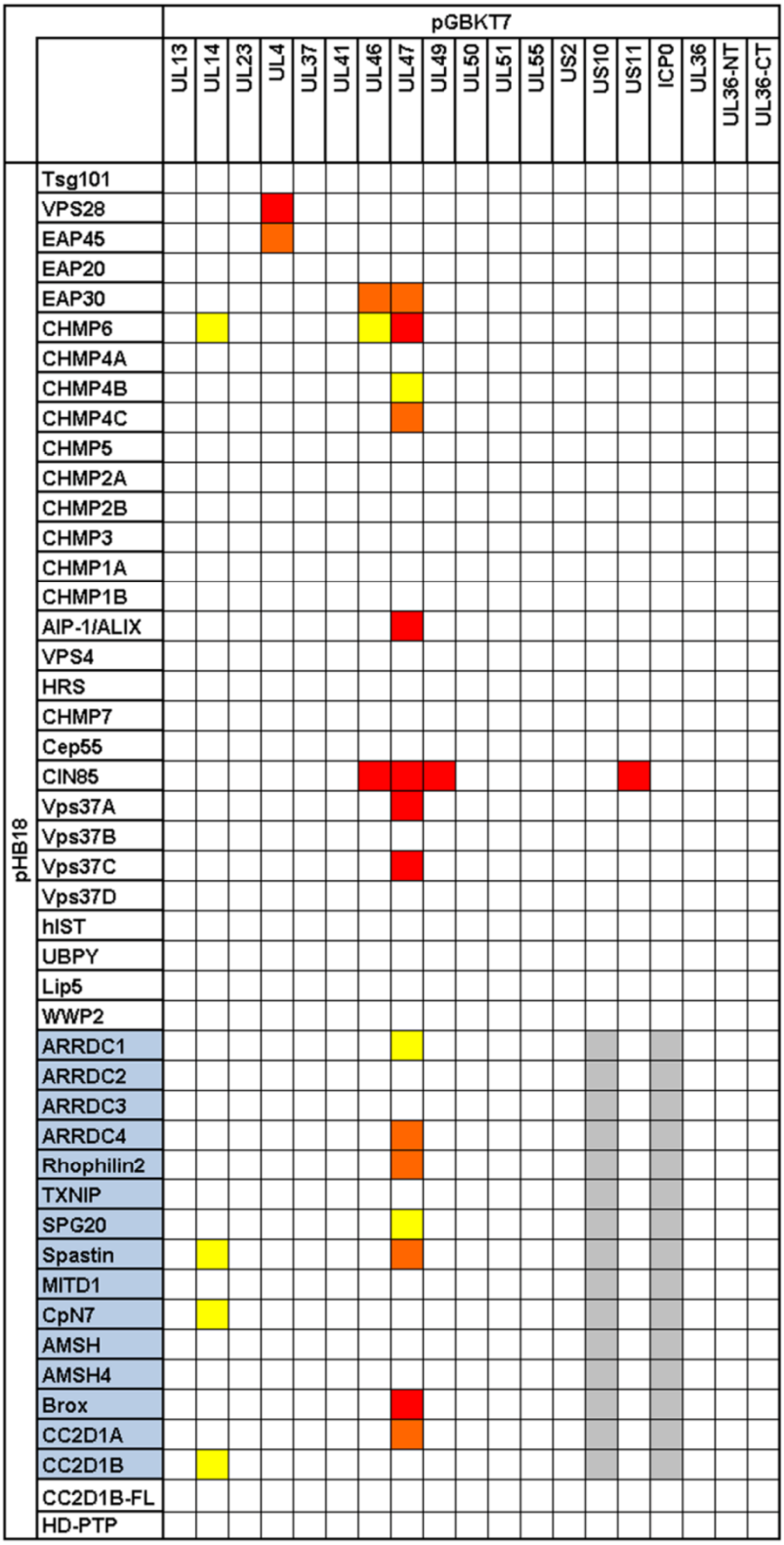

Continued

(A) Potential interactions found when use the ESCRT proteins as bait and HSV-1 tegument proteins as prey. The colour boxes are shown according to the OD_{550} nm values as illustrated at bottom left corner. Y2H assays carried by S. Rauch at KCL are indicated by the blue filled boxes. (B) Potential interactions found when use the HSV-1 tegument protein as bait and ESCRT proteins as prey. The colour coding is the same as described in (A).

UL47 and ALIX). In theory, interaction between two proteins should be reflected in both combinations. However, similar to the published Y2H assays (Vittone *et al.*, 2005), many interactions were usually only demonstrated in one combination but not the other, and unfortunately the reasons for this are unclear. Among all of the positive hits, CC2D1A showed interaction with pUL47 in both combinations (Figure 3.2 A, B), suggesting this interaction is less likely to be an artefact.

All candidates that gave OD_{550} nm > 1.0 in the initial screen (except pGBKT7-CHM4B and pGBKT7-Nedd4 combinations) were re-tested by Y2H assays in triplicate. Consistent with the initial screen result, CIN85 showed reproducible interactions with pUL46 and pUL49 (Figure 3.3 A). pUL47 showed strong interactions with CHMP6, ALIX, CIN85, Vps37A and Vps37C (Figure 3.3 B). However, other potential interactions identified in the initial screen were not reproducible during the repeat assays including the combinations of VPS28 and UL4, EAP45 and UL4, and EAP30 and UL46. Furthermore the interactions between UL36-3' and TSG101 as well as CIN85 and US11 were relatively weak. Although these potential weak interactions might also contribute to the recruitment of ESCRTs by HSV-1, further studies were focused on the candidates that gave the strongest interactions.

Current understanding of ESCRT function in the literature suggests that the CHMP4 proteins of the ESCRT-III complex play the key role in the scission event that separates membrane and so the recruitment of CHMP4A, B and/or C are likely to be crucial for envelopment. Interestingly, several proteins that interact directly or indirectly with CHMP4A/B/C proteins were identified in this study. CHMP6 and ALIX both directly interact with CHMP4A/B/C. CIN85 interacts with ALIX, thus it is potentially linked to the function of CHMP4A/B/C via ALIX. Therefore, CHMP6, ALIX and CIN85 were chosen as ESCRT candidates for further analysis. In addition, among the part of this Y2H screen performed at King's College London, one interesting ESCRT candidate, CC2D1A, showed reproducible interactions with six tegument proteins (pUL11, pUL16, pUL21, pUL46, pUL47 and pUL49) (Figure 3.2 A). It has been reported that CC2D1A directly interacts with CHMP4A/B/C (Tsang *et al.*, 2006), and so CC2D1A was also chosen as a good candidate for further analysis.

Taken together, the Y2H screen identified the following interactions as reproducible and potentially interesting: CHMP6 with pUL47, ALIX with pUL47, CIN85 with pUL46, pUL47 and pUL49, and CC2D1A with pUL11, UL16, UL21, pUL46, pUL47 and pUL49. These interaction candidates were taken forward for further characterisation. The analysis for interacting domain(s) in tegument proteins pUL46, pUL47 and pUL49 as well as

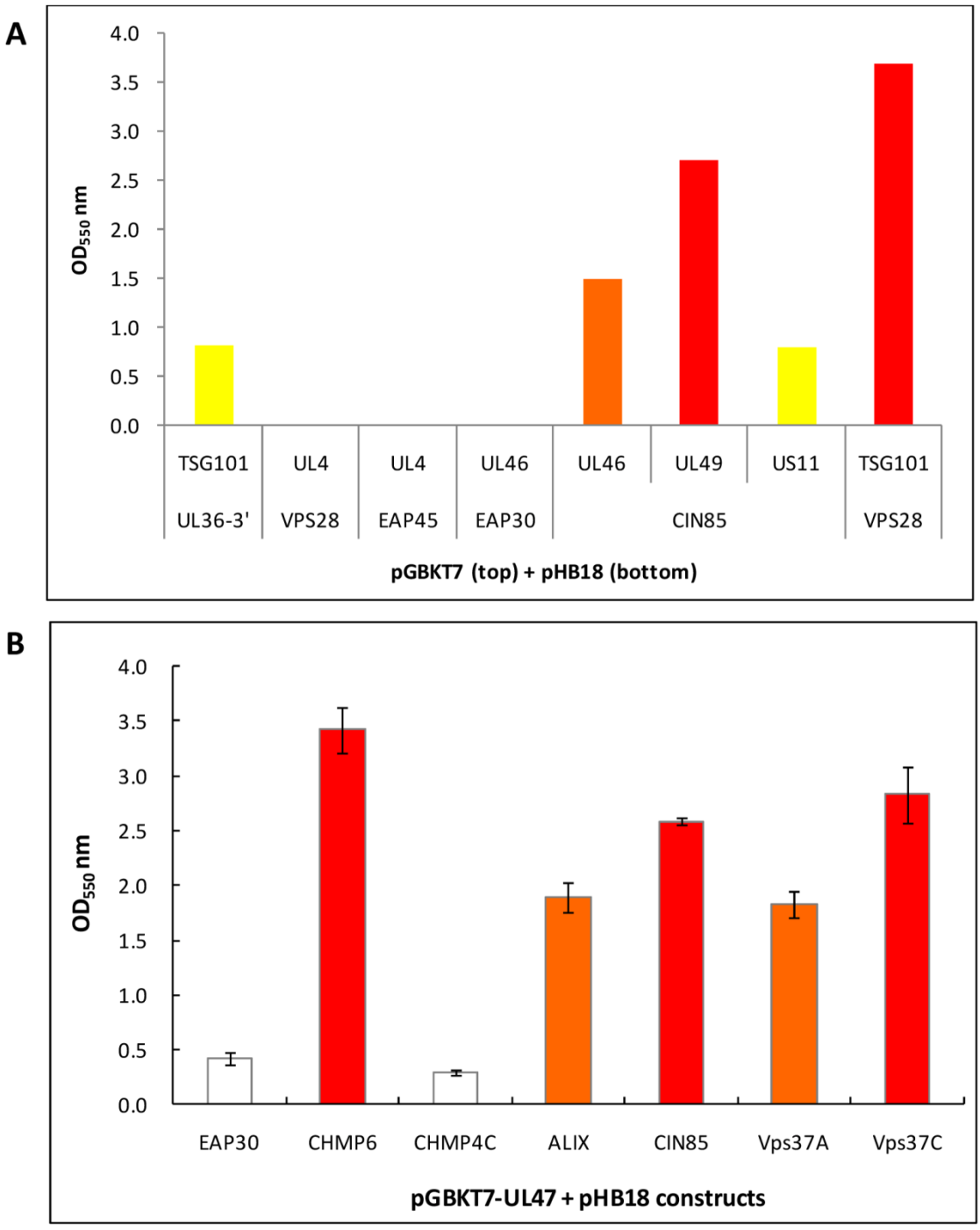

Figure 3.3: Repeat Y2H test of potential interactions with OD_{550} nm > 1.00 from the initial screen. Yeast cells were co-transformed with the indicated combinations of pGBKT7 and pHB18 constructs. The yeast two-hybrid assays were carried out as described in Figure 3.2. The empty pGBKT7 and pHB18 combinations were used as the negative control and the pGBKT7-TSG101 and pHB18-VPS28 combination was used as the positive control. (A) Repeat test of potential interactions (except pUL47) revealed from the initial screen. (B) The repeat assays to confirm potential interactions between the ESCRT candidates and pUL47. The mean OD_{550} nm values and standard errors are shown (n=3).

CIN85 has been performed in this study. The further characterisations of UL11, UL16 and UL21, as well as the search of interaction domain(s) of CC2D1A have been carried out by S. Rauch at King's College London.

3.2.3 Identification of interacting domains

As a first step to characterise the candidates identified from the Y2H screen, the domain(s) or short motif(s) of the tegument proteins that could mediate these interactions were investigated. A series of UL46, UL47 and UL49 domain constructs were generated by PCR using the full length gene as template and cloned into pGBKT7 or pHB18. All of the clones from PCR products were confirmed by sequencing.

3.2.3.1 Interaction domains of pUL47

Primers for twelve constructs were designed initially to generate a series of UL47 domains with about 100 aa truncation by each time from either N- or C-terminus (Figure 3.4 A). In order to reduce the scale of Y2H assays, the twelve pUL47 constructs in pGBKT7 were tested in Y2H assays firstly with one ESCRT candidate pHB18-CHMP6. Other than the full length pUL47, only the construct containing aa 83 to 693 UL47(83-693) demonstrated a strong interaction (Figure 3.4 B). To confirm these data, further Y2H assays were performed to test the interactions of ALIX and CHMP6 with UL47 constructs 1-82, 1-592, 83-693 and 182-693 (Figure 3.5). The construct UL47(1-82) contains the N-terminal region 1-82 missing from the construct UL47(83-693), and thus serves as a control for construct UL47(83-693). The constructs UL47(1-592) and UL47(182-693) were included to confirm that further truncations of about 100 aa from either N-terminus or C-terminus of UL47(83-693) will inhibit the interactions. The results clearly show that only pUL47(83-693) and full length pUL47 interacts with CHMP6 and ALIX, but all other truncated constructs failed to maintain the interactions.

It has previously been shown in the literature that pUL47 (VP13/14) is primarily targeted to the nucleus in transfected (Donnelly & Elliott, 2001) and infected cells (Verhagen *et al.*, 2006b). Furthermore pUL47 exhibits the properties of a protein that shuttles between the nucleus and cytoplasm, mediated by a nuclear localisation signal (NLS) and a nuclear export signal (NES) located in the N- and C-terminal domains of pUL47 respectively (Donnelly & Elliott, 2001; Verhagen *et al.*, 2006a). The truncation analysis conducted so far indicated that the structure of pUL47 is likely to be important for interactions with ESCRT proteins and that the nuclear localisation signal at the N-terminal of the protein is not important for the interaction.

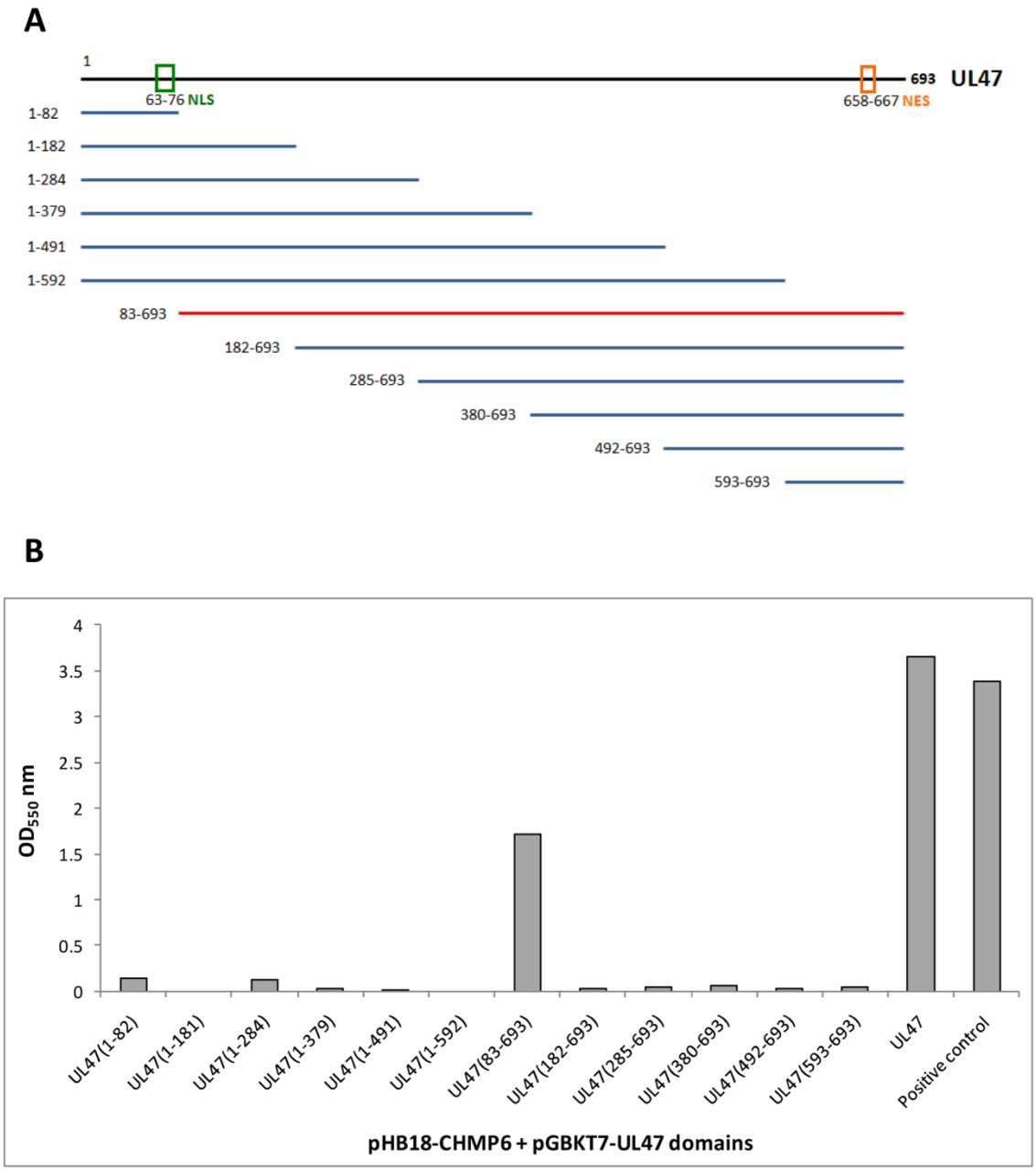

Figure 3.4: UL47 domain constructs and Y2H analysis. (A) Diagram illustrating the twelve UL47 constructs and the aa positions are indicated by the numbers. The top line represents the full length UL47 gene with its nuclear localisation signal at aa position 63-76 and nuclear export signal at aa position 658-667 as indicated. (B) UL47 constructs in pGBKT7 were tested for interactions with pHB18-CHMP6 in Y2H. The Y2H assays were performed as described in Figure 3.2. The pHB18-VPS28 and pGBKT7-TSG101 combination was used as the positive control.

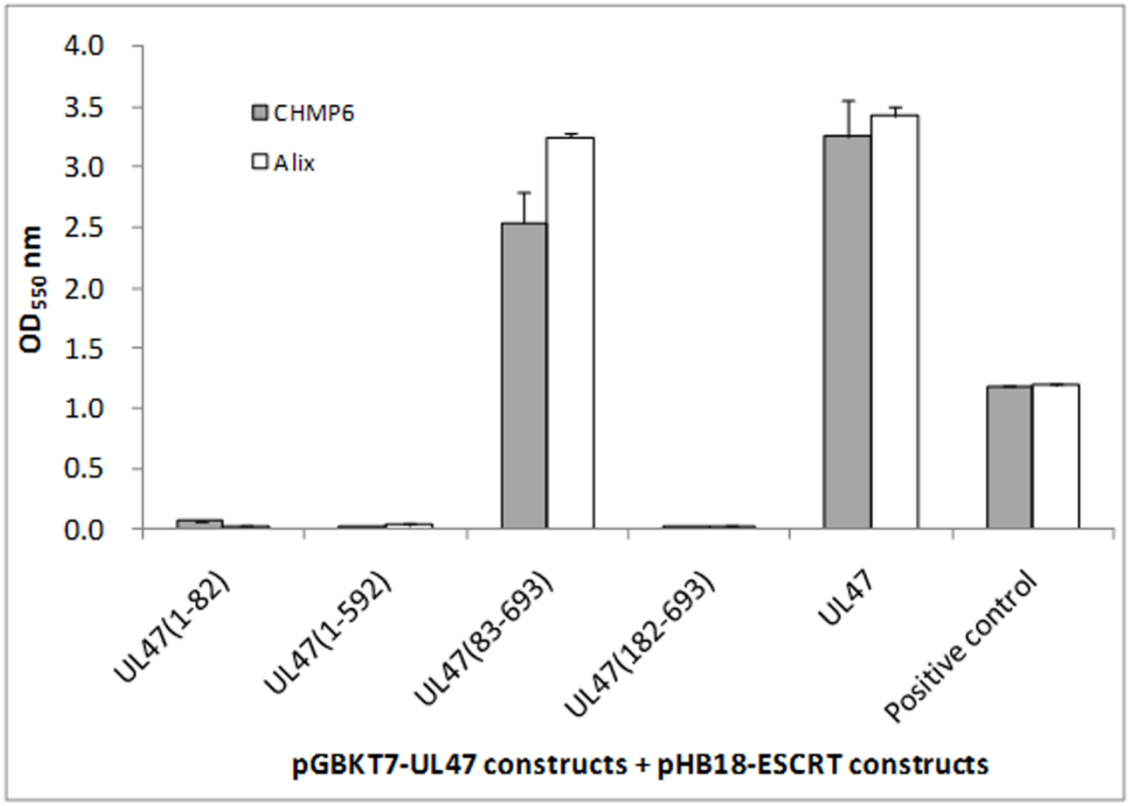

Figure 3.5: Y2H assay of UL47 domain constructs with CHMP6 and ALIX. Competent yeast cells were co-transformed with the indicated UL47 pGBKT7 derived constructs and pHB18-CHMP6 or ALIX. The Y2H assays were performed as described in Figure 3.2. The pHB18-VPS28 and pGBKT7-TSG101 combination was used as the positive control. The mean OD_{550} nm and standard error bars are shown (n=3).

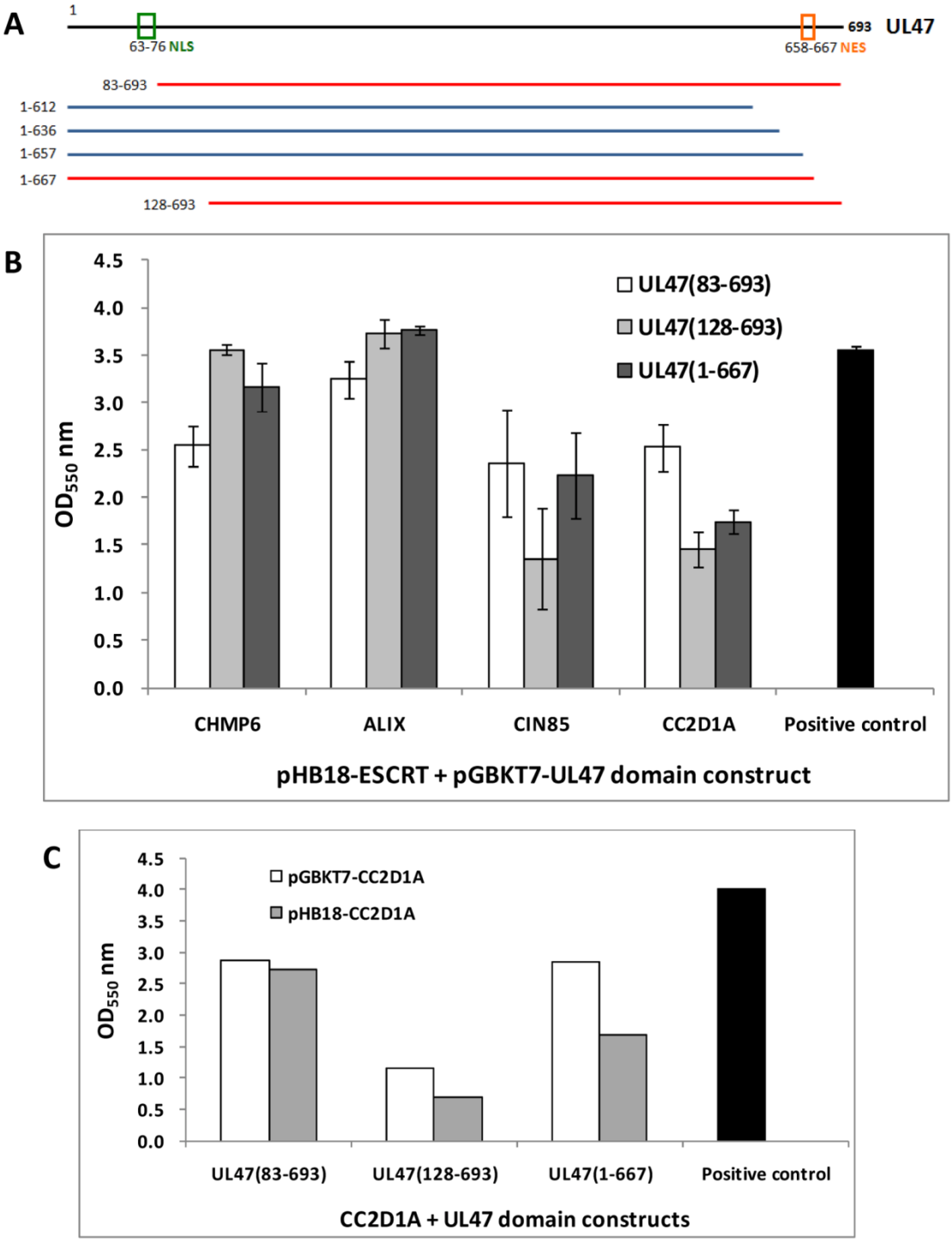

Figure 3.6: Y2H assay of UL47 domain constructs. (A) This diagram illustrates five further domain constructs of UL47. The top line shows the full length UL47 gene as described in Figure 3.4. The aa position of the various truncated constructs are shown. The constructs retaining the interactions with ESCRT proteins are highlighted in red. (B) The pGBKT7-UL47(83-693), UL47(128-693) and UL47(1-667) constructs were tested with the indicated four ESCRT proteins in pHB18 derived plasmids. The Y2H assays were performed as described in Figure 3.2. The mean OD_{550} nm and standard error bars are shown (n=3). (C) Three UL47 constructs UL47(83-693), UL47(128-693) and UL47(1-667) were test against pGBKT7- or pHB18-CC2D1A. The pHB18-VPS28 and pGBKT7-TSG101 combination was used as the positive control.

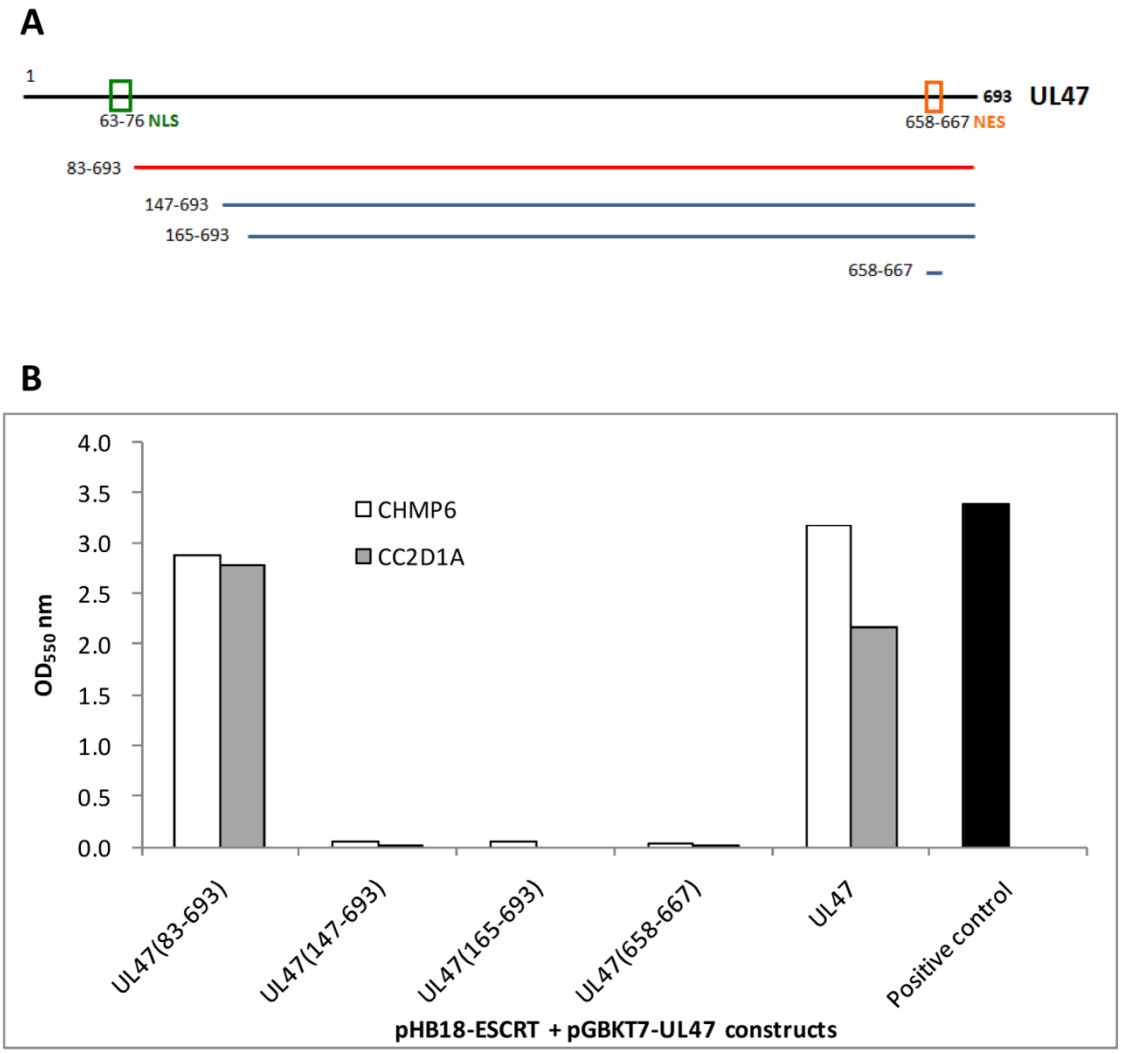

Figure 3.7: Y2H assay of UL47 domain constructs. (A) This diagram illustrates three further domain constructs of UL47. The top line shows the full length UL47 gene as described in Figure 3.4. The aa position of the various truncated constructs are shown at left hand side. The Y2H assays were performed as described in Figure 3.2. (B) The values of OD_{550} nm are shown. The pHB18-VPS28 and pGBKT7-TSG101 combination was used as the positive control.

In order to further narrow down the domain of pUL47 that is important for the interaction and address any role of the NES, five additional UL47 constructs were created (Figure 3.6 A). The constructs were made to truncate further at the N-terminus of UL47(83-693) or C-terminus of the full length UL47. According to the Y2H assays, the construct UL47(1-667) and UL47(128-693) retained interactions with CHMP6, ALIX, CIN85, and CC2D1A (Figure 3.6 B). However, the construct UL47(1-657) lacking the NES (658-667) did not interact with any tested ESCRT proteins. Therefore, UL47(658-667) was constructed (contains only the NES) along with two additional constructs with further truncations UL47(147-693) and UL47(165-693) (Figure 3.7 A). These three constructs were tested against CHMP6 and CC2D1A together with full length UL47 and UL47(83-693) constructs. As the result shown, the further truncation of UL47 from aa 128 to 147 abolished the interactions. Furthermore, the NES fragment construct UL47(658-667) did not show interactions in yeast two-hybrid assays (Figure 3.7 B).

Overall these data suggest a core domain of pUL47 encompassing aa 128-667 appears crucial for all the interactions identified. Although the loss of NES abolished the interaction with CHMP6, ALIX, CIN85 and CC2D1A, the NES alone was not sufficient for any interaction. According to these results, the NLS is not important for the interactions. This suggests a large folded domain or the structure of pUL47 is required for these interactions, and unfortunately no short motif could be identified.

3.2.3.2 Interaction domains of pUL46

In order to search for potential domains that are responsible for the interactions between pUL46 and the ESCRT candidates, similarly to pUL47, a series of truncation constructs of pUL46 were generated by PCR and cloned into pGBKT7 and pHB18. All of the clones from PCR products were confirmed by sequencing. Six domain constructs were cloned of approximately 200 aa in length (Figure 3.8 A).

The pGBKT7-CC2D1A showed positive interaction with full length UL46 construct pHB18-UL46 in the initial Y2H screen (Figure 3.2 A). In this same bait and prey plasmid combination, among the six UL46 constructs, CC2D1A showed positive interaction with the domain construct UL46(357-718) with OD_{550} nm > 1.0 (Figure 3.8 B). Therefore, this domain of UL46 contains a potential CC2D1A interacting site. Interestingly, the construct UL46(1-193) also showed an interaction that almost reached OD_{550} nm threshold (1.0) for positive interactions, suggesting there could be two interacting sites. However, these results need to be treated with caution. Additionally, the OD_{550} nm values of the domain

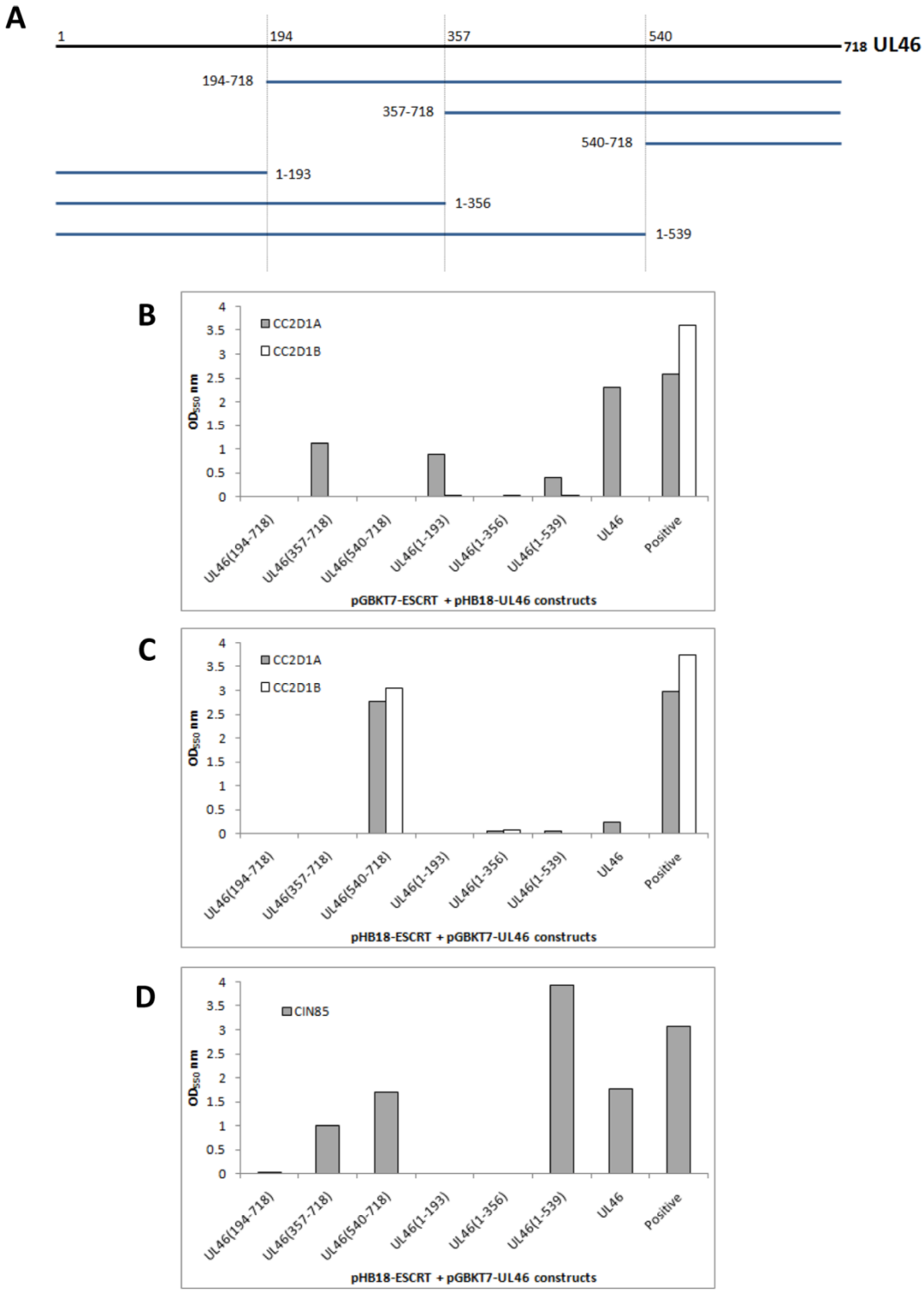

Figure 3.8: Domain constructs of UL46 and Y2H assays. (A) This diagram illustrates the six domain constructs of UL46. The top line represents the full length UL46 with the numbers indicating the amino acid positions. (B) Y2H assay of the six UL46 domain constructs in pHB18 and pGBKT7-CC2D1A and –CC2D1B. (C) Y2H assay of the six UL46 domain constructs in pGBKT7 and pHB18-CC2D1A and –CC2D1B. (D) Y2H assay of the six UL46 domain constructs in pGBKT7 and pHB18-CIN85. The Y2H assays were performed as described in Figure 3.2. The pHB18-VPS28 and pGBKT7-TSG101 combination was used as the positive control.

constructs are only half the values of the full length UL46, which suggests the fully folded pUL46 protein is required for optimal CC2D1A interaction. In agreement with the initial screen results, CC2D1B did not show any interactions with either the full length pUL46 or any truncated protein (Figure 3.8 B).

Interestingly, positive interactions were detected by Y2H assays for the UL46 construct pGBKT7-UL46(540-718) with both pHB18-CC2D1A and pHB18-CC2D1B. However, in this prey-bait combination, neither of pHB18-CC2D1A or pHB18-CC2D1B showed positive interactions with the full length UL46 protein (Figure 3.8 C). In addition, the pHB18-CIN85 protein also showed interaction with pGBKT7-UL46(540-718) (Figure 3.8 D), suggesting the pGBKT7-UL46(540-718) construct may be general "sticky" in Y2H assays.

Apart from the UL46(540-718) construct described above, the pHB18-CIN85 also showed positive interactions with constructs pGBKT7-UL46(357-718) and pGBKT7-UL46(1-539) (Figure 3.8 D). This result suggests the interaction domain for CIN85 may reside in the aa 357-539 region although further characterisation will be necessary.

3.2.3.3 Interaction domains of pUL49

Two domain constructs of pUL49 were made to contain the N or C-terminal region of full length pUL49 (Figure 3.9 A). The ESCRT associated proteins CC2D1A and CIN85 showed positive interactions with full length pUL49 in the original screen (Figure 3.2). Thus the pGBKT7-CC2D1A and pHB18-CIN85 were tested against the domain constructs of pHB18-UL49 and pGBKT7-UL49 in yeast two-hybrid assays respectively. The interactions between full length pUL49 and these two proteins were reproducible, although no positive interactions could be detected for the truncated pUL49 constructs (Figure 3.9 B, C). This result suggests that the structure of pUL49 could be important for interactions with both CC2D1A and CIN85, although it is possible that the interacting domain may be located in the middle region of the full length protein and neither of the constructs retains an intact functional interacting domain.

3.2.4 Validation of the HSV-1 tegument-ESCRT interactions

Yeast two-hybrid assays are an efficient screening strategy to search potential interactions between two proteins. The prey and bait proteins are cloned into plasmids that fuse the proteins of interest to a DNA binding domain and a transactivation domain respectively. During the assay, the fusion proteins are overexpressed in yeast cells and the products of

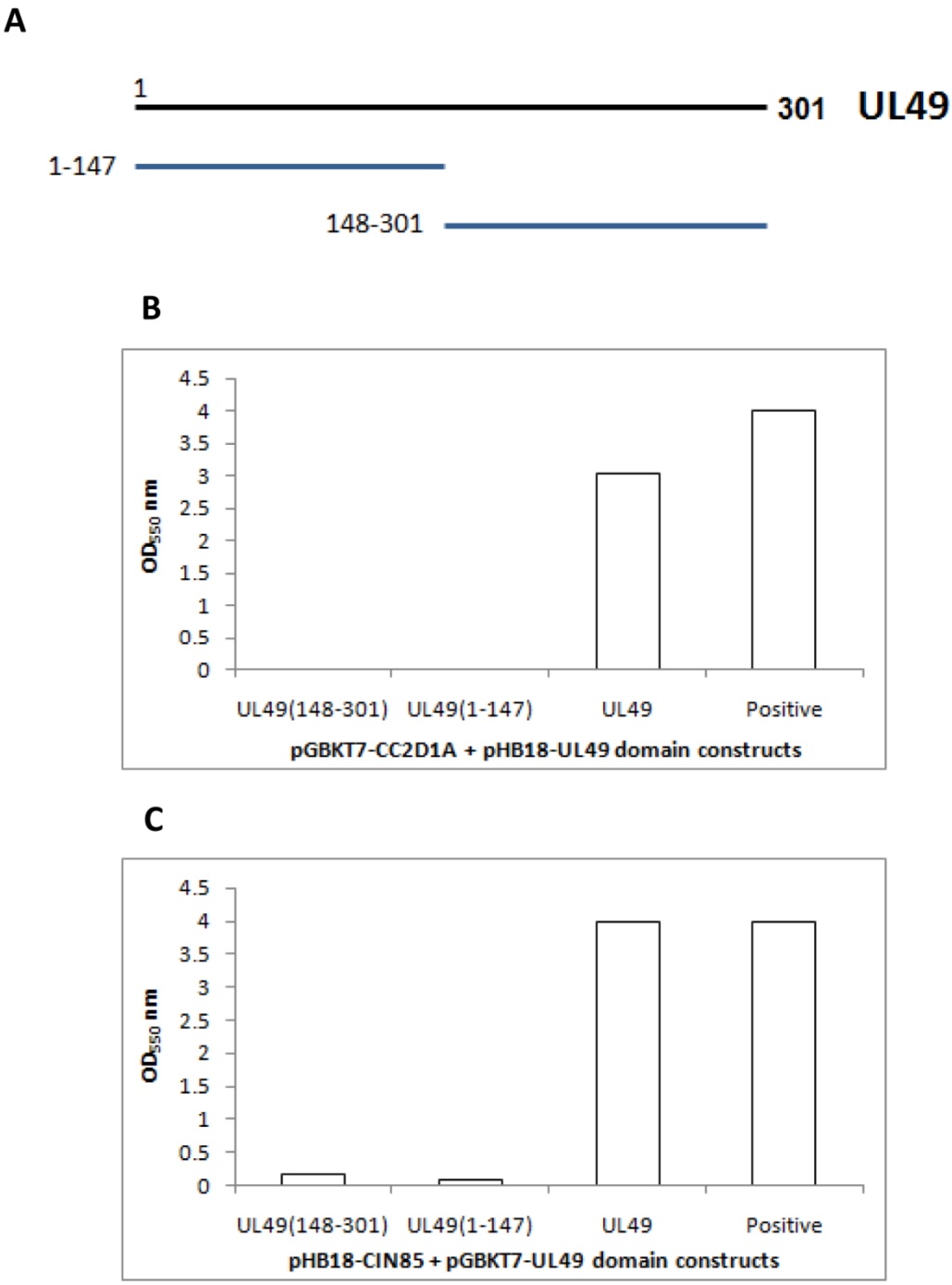

Figure 3.9: Domain constructs of UL49 and Y2H assays. (A) This diagram illustrates the two domain constructs of UL49. The top line represents the full length UL49 with the numbers indicating amino acid positions. (B) Y2H assay of the two UL49 domain constructs in pHB18 and pGBKT7-CC2D1A. (C) Y2H assay of the two UL49 domain constructs in pHB18 and pGBKT7-CIN85.

downstream reporter genes are used as an indirect indicator for positive interactions. The major disadvantage of yeast two-hybrid assays is the relatively high frequency of false positive/false negative results. The proportion of the protein interactions identified by Y2H that agree with other methods may be as low as 30% (Deane *et al.*, 2002). Therefore, it is important to use alternative and independent assays to validate the candidate interactions that arise from yeast two-hybrid assays.

3.2.4.1 Interactions of HSV-1 pUL47 with CHMP6 and ALIX

According to the Y2H results, both CHMP6 and ALIX showed reproducible interactions with pUL47, both full length protein as well as the N-terminal truncated pUL47 lacking the first 81 to 127 aa. To investigate whether the interactions occur in mammalian cells, GST pull-down assays were performed. The UL47 gene was sub-cloned into pEGFP-C2 to express N-terminal GFP tagged pUL47 in mammalian cells. Due to the presence of a nuclear localisation signal (NLS) at the N-terminus of pUL47 (aa 63-76) (Donnelly & Elliott, 2001), pUL47 was found to mainly localise to the cell nucleus in transfected cells (Figure 3.10 A, B). This is likely to result in a significant loss of the GFP-pUL47 protein during the cell lysate preparation when the cell nuclei are removed by centrifugation. Therefore the N-terminally truncated pUL47 (aa 83-693), which lacks the NLS was also sub-cloned into pEGFPC2. GFP-pUL47(83-693) demonstrated much stronger signals in the cytoplasm of transfected cells (Figure 3.10 B).

For the GST pull-down assays, 293T cells were transfected with plasmid expressing GST tagged ALIX or CHMP6 together with plasmid expressing GFP tagged pUL47 or pUL47(83-693). In the control samples, the GST tagged constructs were co-transfected with plasmid expressing GFP only, and the GFP tagged constructs were co-transfected with plasmid expressing GST only. Cell lysates were prepared at 48 h post transfection and small portions of the lysates were retained to test protein expression levels. The rest of the lysates were incubated with glutathione Sepharose beads for GST binding. The beads were harvested by centrifugation and washed. The GFP signals in the bead fractions were tested by western blotting using a GFP specific antibody.

According to the analysis of the beads fraction samples, there were no background signals detected in the control samples. The GST tagged ALIX or CHMP6 did not show interactions with GFP only, neither did the GFP tagged pUL47 or pUL47(83-693) show interactions with GST only (Figure 3.10 C). GFP tagged pUL47(83-693) was successfully pulled down by GST tagged ALIX and CHMP6 (Figure 3.10 C). This result suggests

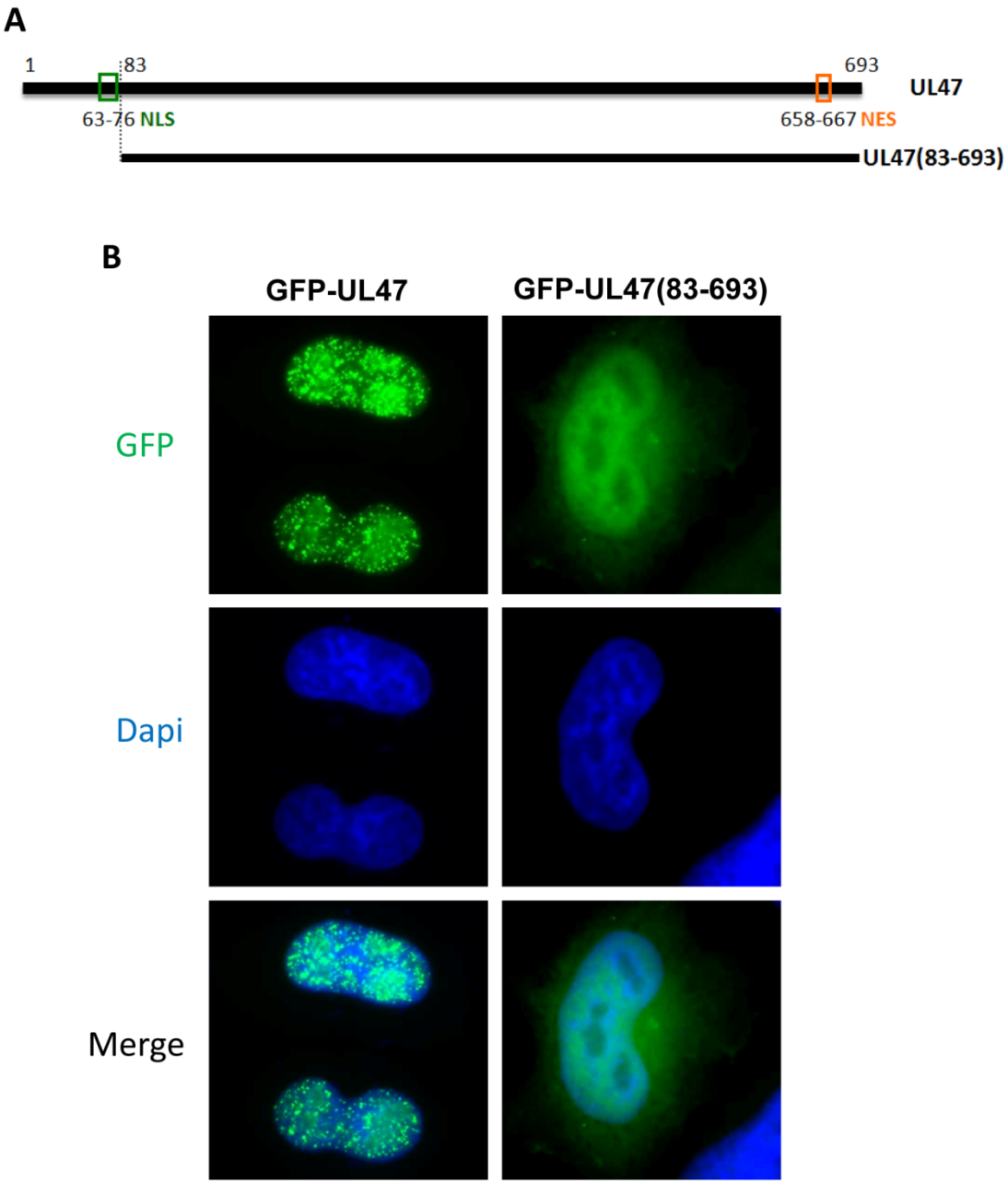

Figure 3.10: GST pull-down assay of pUL47 and pUL47(83-693) with ALIX and CHMP6. (A) Illustration of full length UL47 and UL47(83-693) with the numbers indicating amino acid positions. (B) GFP tagged full length UL47 and the truncated UL47(83-693) plasmids were transfected into HeLa cells. The samples were fixed at 24 h post transfection, and were embedded in ProLong Gold+Dapi. The samples were imaged on an Olympus IX70 microscope with a 60x oil immersion lens and a Retiga 2000R ccd camera. Images were acquired with the Q capture Pro software and processed with ImageJ. (C) GST pull-down assay of GFP tagged pUL47 or pUL47 (83-693) with GST tagged ALIX or CHMP6. The indicated plasmids were co-transfected into 293T cells. The plasmids contain GFP or GST were used as the negative controls. After 48 h post transfection, cells were harvested and cell lysates were prepared. Glutathione-sepharose beads were added into the lysate for GST binding at 4 °C for 3 h. The beads were spun down, washed three times and samples were analysed by western blotting. The GFP signals detected from the pull-down and lysate samples are shown.

C

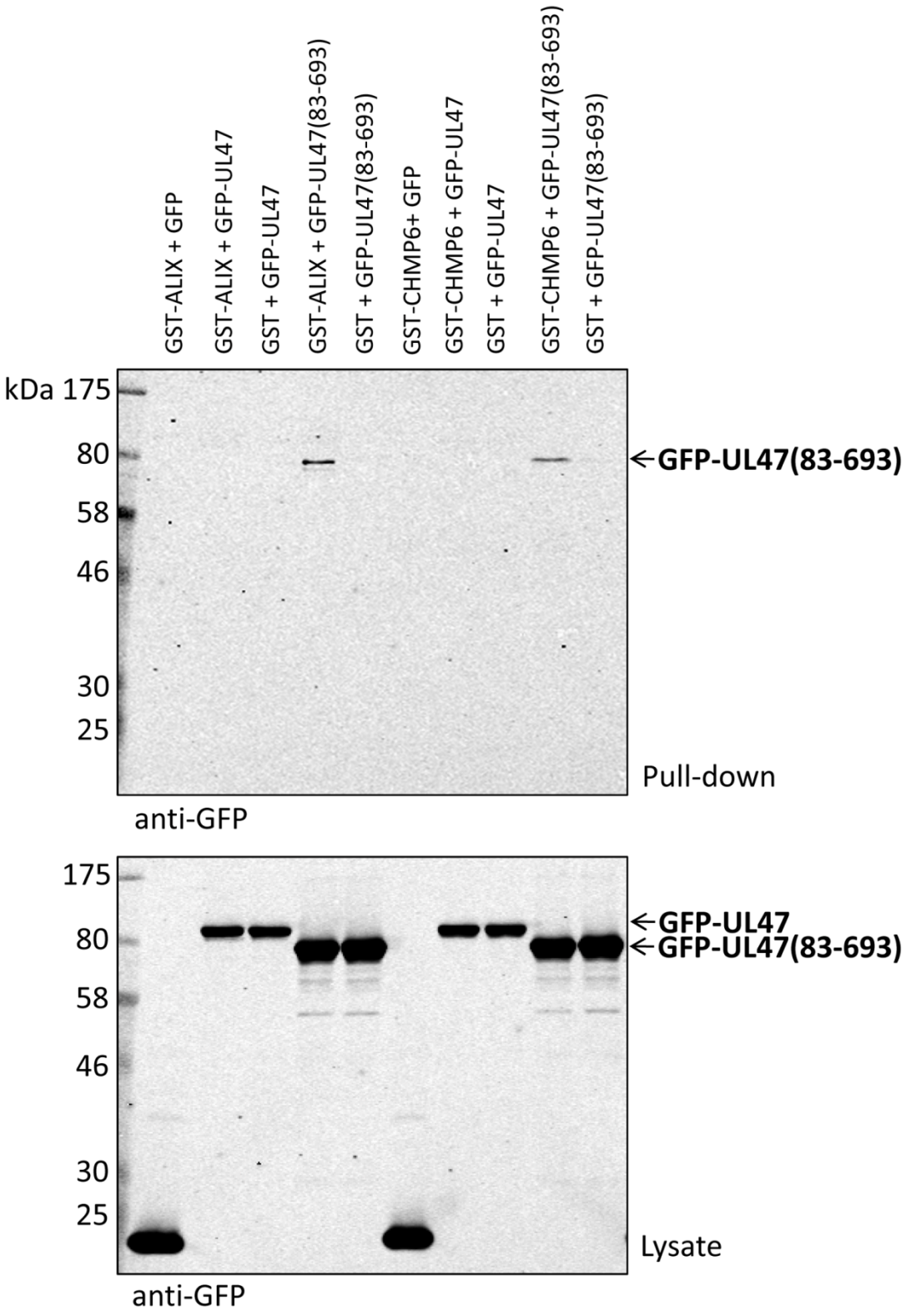
GST-ALIX + GFP
GST-ALIX + GFP-UL47
GST + GFP-UL47
GST-ALIX + GFP-UL47(83-693)
GST + GFP-UL47(83-693)
GST-CHMP6+ GFP
GST-CHMP6 + GFP-UL47
GST + GFP-UL47
GST-CHMP6 + GFP-UL47(83-693)
GST + GFP-UL47(83-693)
kDa 175
80
58
46
30
25
←GFP-UL47(83-693)
Pull-down
anti-GFP
175
80
58
46
30
25
←GFP-UL47
←GFP-UL47(83-693)
Lysate
anti-GFP

pUL47(83-693) does indeed interact with both ALIX and CHMP6 in mammalian cells. However, there were no detectable signals of GFP-pUL47 from the GST-ALIX or GST-CHMP6 pull-down samples. This could be due to the lower level of full length GFP-pUL47 protein present in the lysates.

All of the GFP tagged proteins and GFP only control samples showed the protein bands at expected sizes (Figure 3.10 C, lysate). The levels of GFP tagged pUL47 full length protein presenting in the lysates were significantly lower than the GFP tagged pUL47(83-693) (Figure 3.10 C, lysate). This agrees with the cellular localisation of the two proteins (Figure 3.10 B) and that a higher proportion of the cell nucleus localised pUL47 may be lost during the removal of cell nuclei during lysate preparation.

3.2.4.2 Interactions of tegument protein with CIN85

3.2.4.2.1 GST pull-down

CIN85, Cbl-interacting protein of 85 kDa, was firstly identified as a novel adaptor protein which is likely to be involved in the EGF receptor-mediated signalling cascade (Take *et al.*, 2000). CIN85 contains three SH3 domains within the N-terminal region, a proline-rich domain in the middle and a C-terminal coiled-coil domain (Figure 3.11 A). CIN85 has been subsequently reported to interact with ALIX (Schmidt *et al.*, 2004). In the GST pull-down assay, when GST tagged ALIX and GFP tagged CIN85 were co-expressed in mammalian cells, GFP-CIN85 could be efficiently pulled down by GST-ALIX (Figure 3.11 B). This result agrees with the reported interaction between ALIX and CIN85.

In order to confirm the interactions between CIN85 and pUL46, pUL47, pUL49 and US11 observed in yeast two-hybrid assays (Figure 3.2 B), CIN85 was sub-cloned from pHB18-CIN85 into pCAG-GST to express GST tagged full length CIN85. In order to investigate the domains of CIN85 that may mediate interactions, primers (Chapter 6) were designed for PCR to generate five truncated constructs: N-terminal three SH3 domains (SH3), middle proline-rich domain (PR), C-terminal coiled-coil domain (CC), CIN85 lacking the coiled-coil domain (ΔCC) and one lacking the three SH3 domains (PRC) (Figure 3.11 A). All the PCR products were confirmed by sequencing.

The indicated five GST tagged CIN85 domain constructs and the full length construct were co-expressed with GFP tagged pUL46 or pUL49 in 293T cells. Cell lysates were prepared at round 48 h post transfection and incubated with glutathione Sepharose beads. The cell lysates were tested for protein expression levels and the beads fraction were tested for GFP signals. As the result shows, the constructs without the SH3 domains (PR, CC

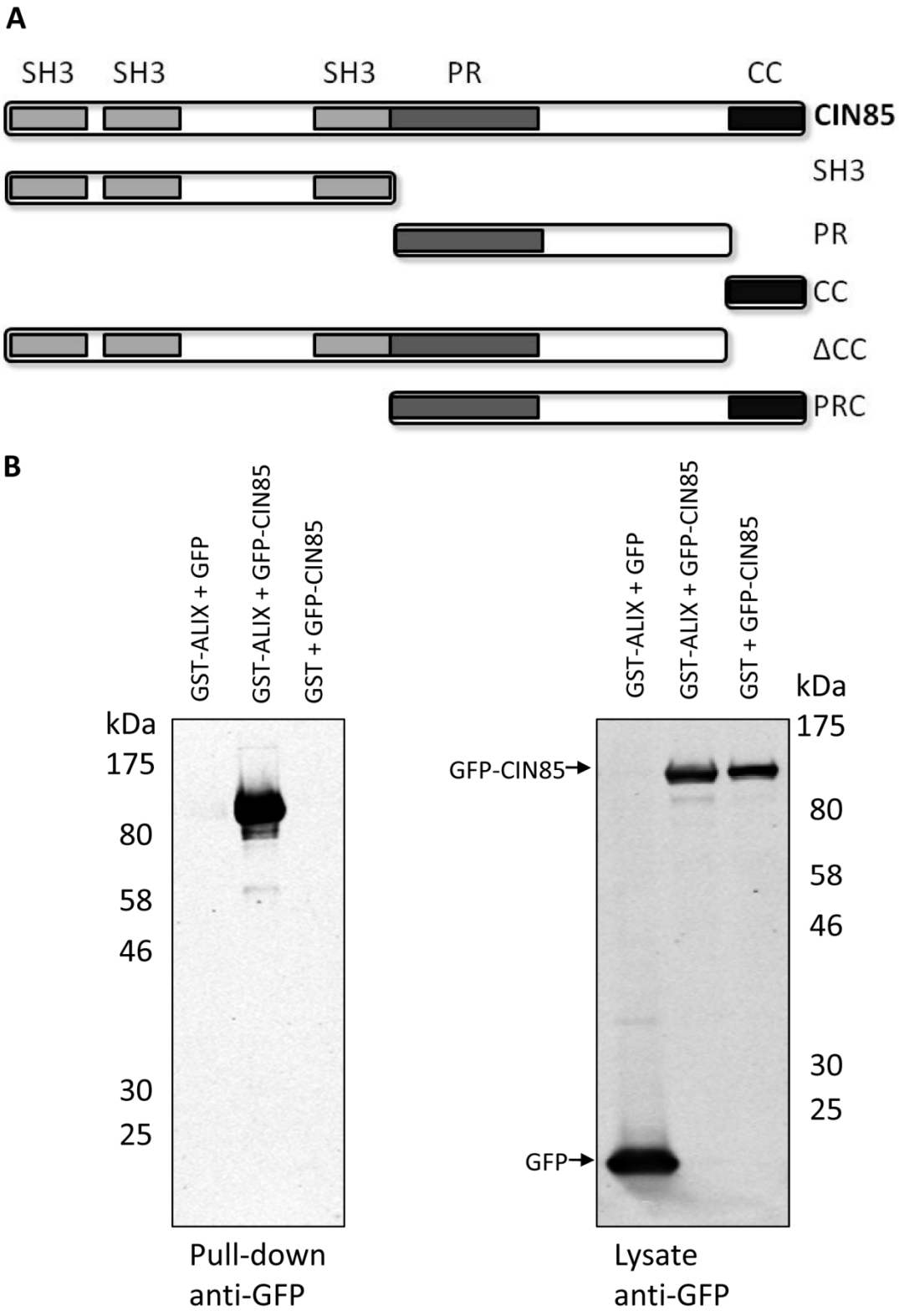

Figure 3.11: CIN85 domain constructs and GST pull-down assays. (A) Diagram of CIN85 domains. Five truncated constructs containing different domain(s) were created and named as SH3, PR, CC, ΔCC and PRC. (B) GST pull-down assay of GST-ALIX and GFP-CIN85. The GST-ALIX + GFP and GST + GFP-CIN85 combinations were used as negative controls. The GFP signals detected from the pull-down and lysate samples are shown. (to be continued)

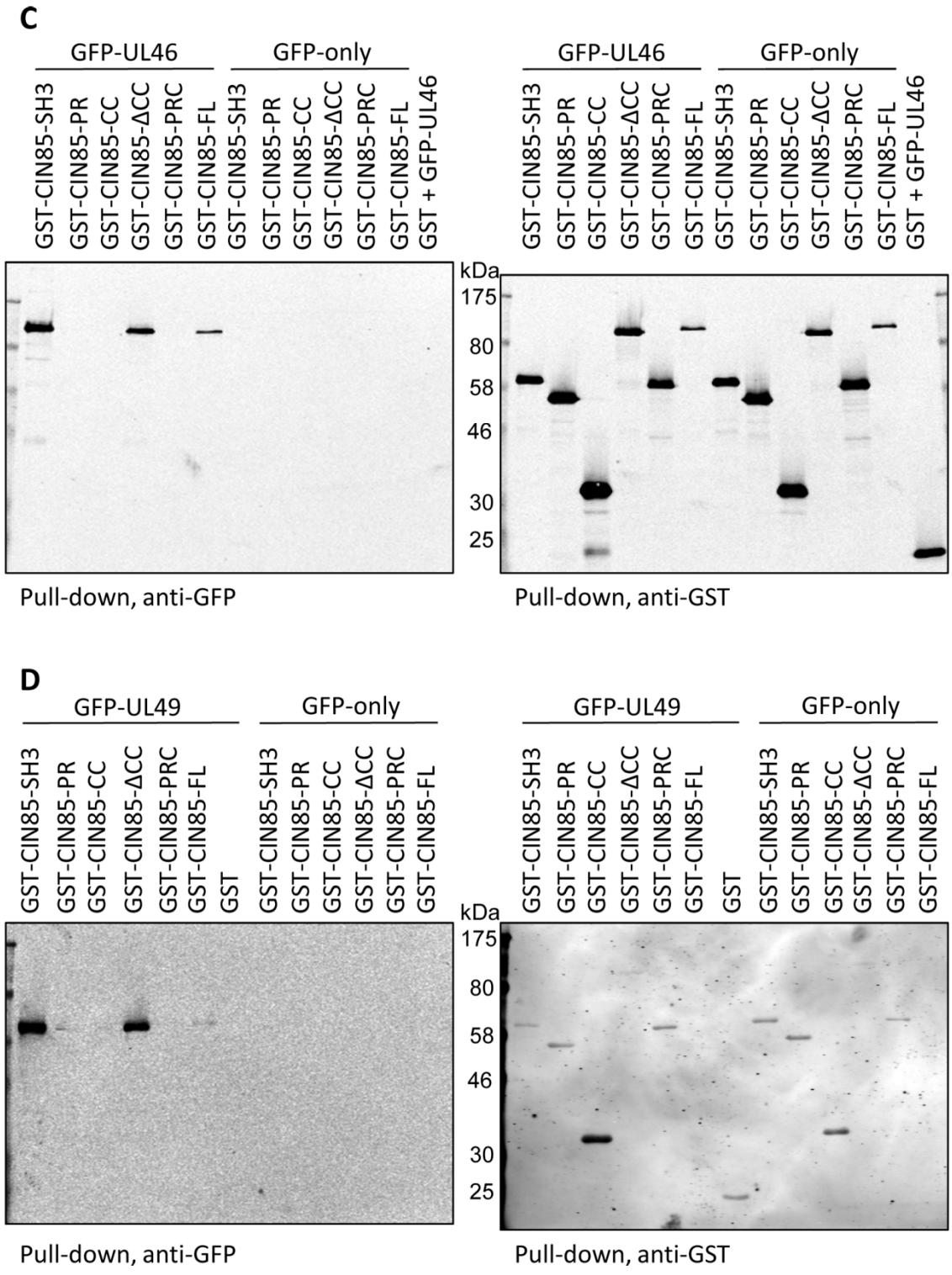

Continued:

(C) GST pull-down of GFP-pUL46 by CIN85 constructs. 293T cells were co-transfected with GFP-UL46 and the indicated GST tagged CIN85 constructs. GST pull-down was performed using glutathione-sepharose beads and the GFP and GST signals detected from the pull-down samples are shown. (D) GST pull-down of GFP-pUL49 by CIN85 constructs. The assay was performed as described above and the GFP and GST signals detected from the pull-down samples are shown. (to be continued)

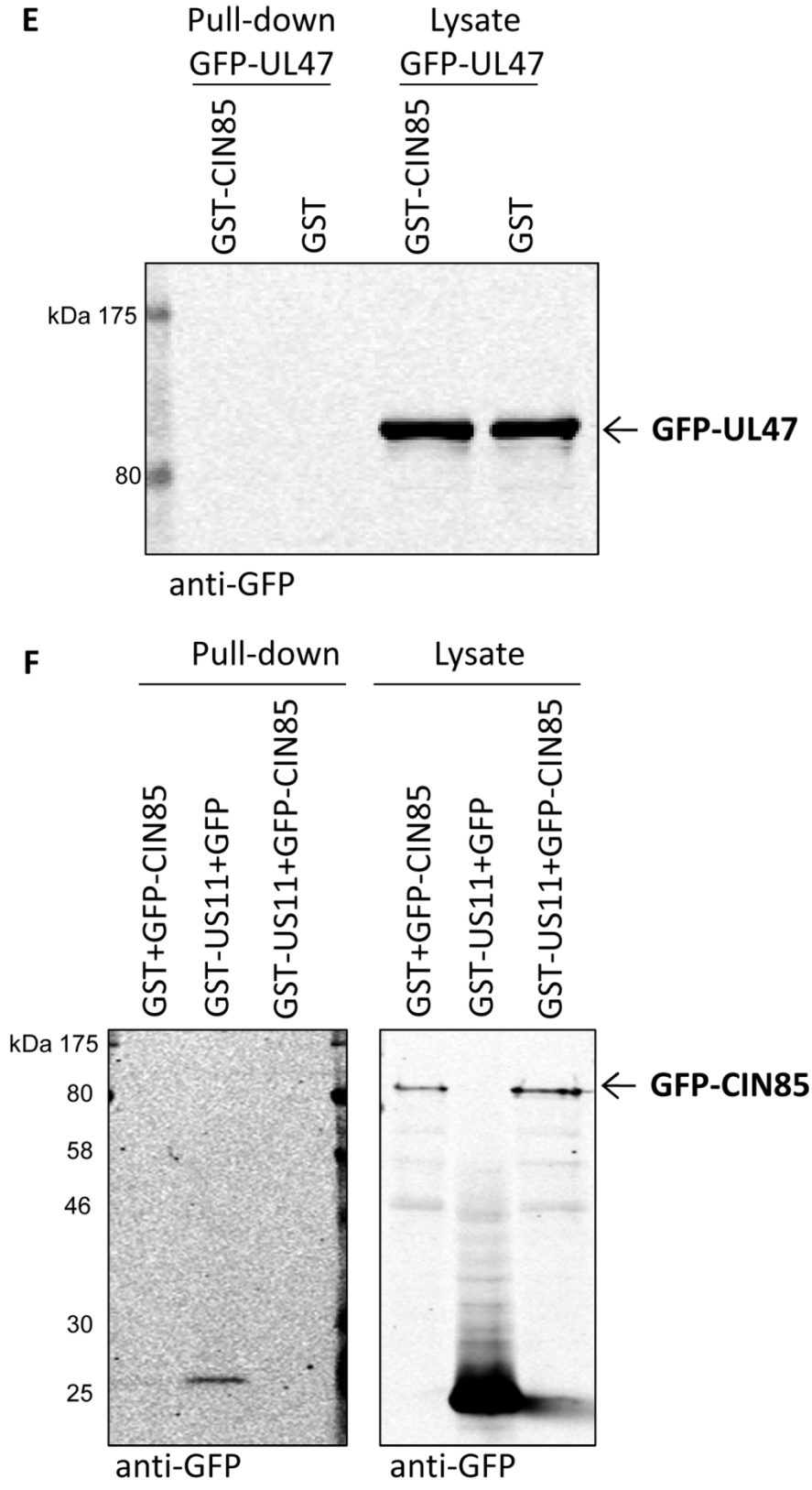

Continued:

(E) GST pull-down of GFP-pUL47 by CIN85. The assay was performed as described above and the GFP signals detected from the pull-down and lysate samples are shown. (F) GST pull-down of GFP-CIN85 by GST-pUS11. The assay was performed as described above and the GFP signals detected from the pull-down and lysate samples are shown.

and PRC) did not interact with the tegument proteins, while GST-CIN85 full length as well as the SH3 domain containing constructs (SH3 and ΔCC) were able to pull down both GFP tagged pUL46 (Figure 3.11 C) and pUL49 (Figure 3.11 D). However, the pull-down signals of pUL46 and pUL49 from the full length CIN85 were weaker than the domain constructs (Figure 3.11 C, D). This may be due to the lower expression level of GST-CIN85 than the domain constructs (Figure 3.11 C, D). In contrast, there was no detectable signal of GFP-UL47 observed from the GST pull-down samples (Figure 3.11 E). Further, there may be relatively weak interaction between CIN85 and pUS11; however, GFP-tagged CIN85 was not pulled down by the GST tagged pUS11 protein (Figure 3.11 F).

Taken together, these results suggest that overexpressed CIN85 interacts with pUL46 and pUL49 in mammalian cells. In addition, the N-terminal SH3 domains are important for the interactions between CIN85 and these two tegument proteins. However, the interactions of pUL47 and pUS11 with CIN85 may be false positive hits from the Y2H assays.

3.2.4.2.2 Protein co-localisation assay

A convenient method to determine whether two proteins interact with each other is to examine their co-localisation in transfected cells by fluorescence microscopy, where the proteins are tagged with different fluorescent proteins and co-expressed in mammalian cells. If different proteins have specific localisations within cells, then interaction between the proteins can be evaluated by examining their co-localisation upon co-expression. One disadvantage to this approach is that interactions cannot be determined if both proteins have the same localisation independent of each other, e.g. soluble cytoplasmic localisation. Based on the result from GST pull-down assays, the SH3 and PRC domains of CIN85 were cloned into pEGFPC2 plasmid, and pUL46, pUL47 and pUL49 were tagged with mCherry in mammalian expressing plasmids. The GFP tagged CIN85 constructs were co-transfected with the mCherry tagged tegument constructs into HeLa cells, and ~24 h post transfection, the samples were fixed and examined by fluorescence microscopy. GFP tagged CIN85-SH3 domain demonstrated good co-localisation signals with Cherry-pUL46 and Cherry-pUL49, whereas GFP-PRC or GFP alone did not show any co-localisation with either pUL46 or pUL49 (Figure 3.12 A, B). However, no co-localisation of Cherry-pUL47 could be observed with the CIN85 domain constructs (Figure 3.12 C). The GFP tagged CIN85 SH3 and PRC domain constructs were co-expressed with Cherry only for further control conditions. As expected, there were no co-localisation signals in these control samples (Figure 3.12 D).

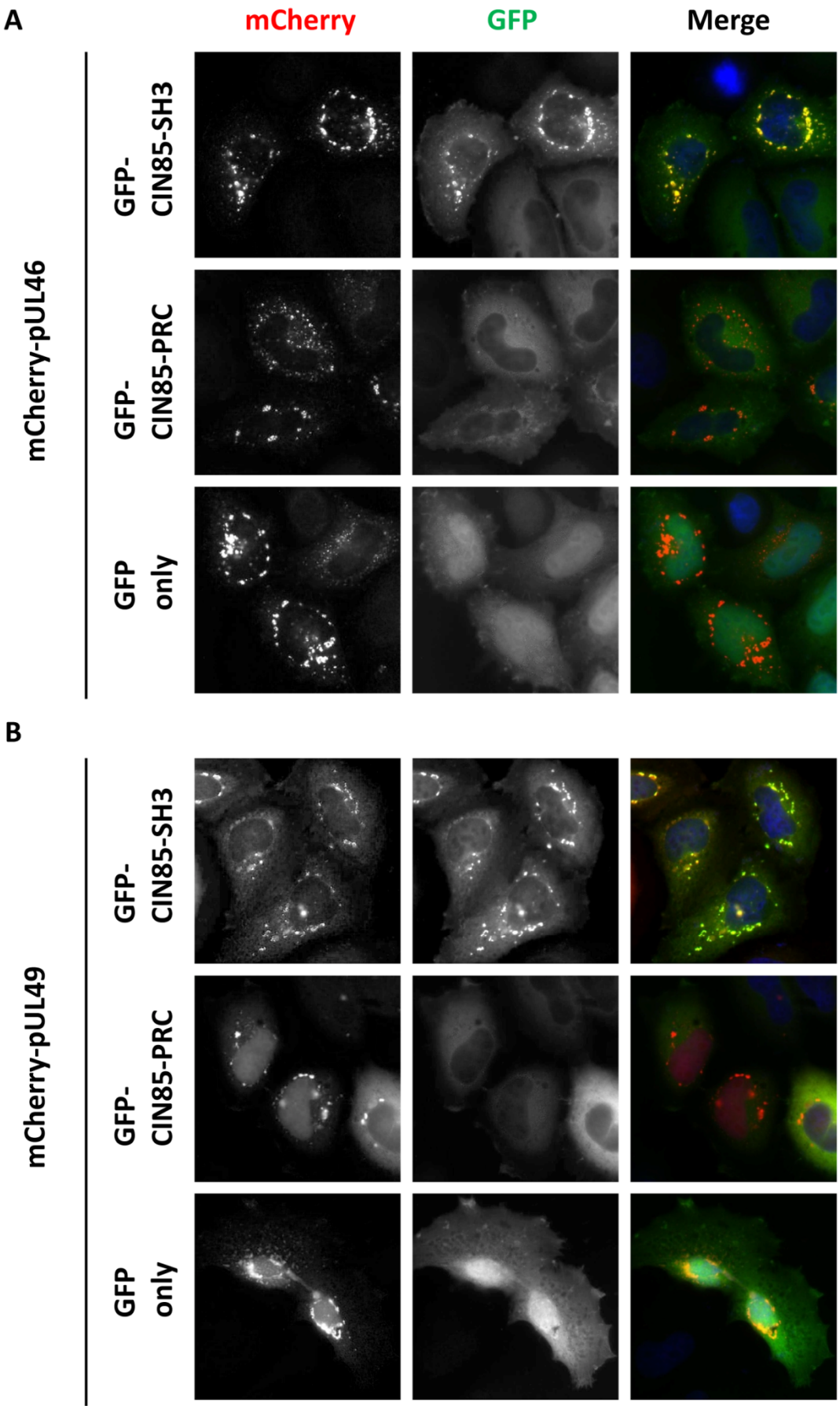
A
mCherry
GFP
Merge
mCherry-pUL46
GFP-CIN85-SH3
GFP-CIN85-PRC
GFP only
B
mCherry-pUL49
GFP-CIN85-SH3
GFP-CIN85-PRC
GFP only

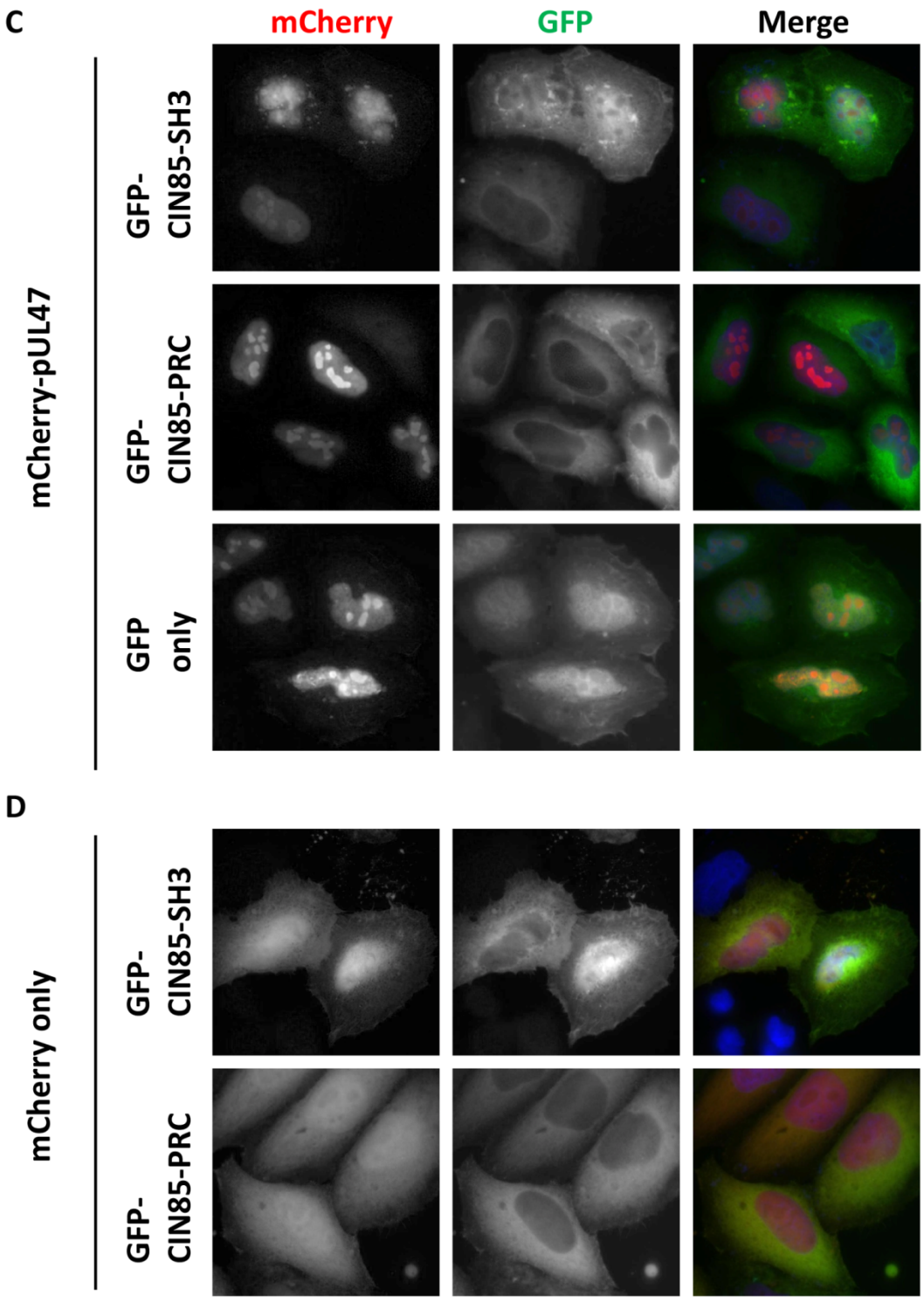

Figure 3.12: Protein co-localisation assay of CIN85 domain constructs and tegument proteins. The Cherry tagged tegument protein pUL46 (A), pUL49 (B) and pUL47 (C) were co-expressed in HeLa cells with GFP tagged CIN85 SH3 or PRC domain. The mCherry and GFP only plasmids were used as the negative controls. The cells were fixed at 27 h post transfection and examined by fluorescence microscopy. The images were obtained and processed in ImageJ software and pseudo-coloured in green, red and blue for the GFP, mCherry and DAPI channels respectively.

These results agree with the data from GST pull-down assays, and further confirmed that the interactions of CIN85 with pUL46 and pUL49 are likely to be genuine and the SH3 domains of CIN85 are required for these interactions. However, these data further confirmed that the interaction of CIN85 and pUL47 is likely to be a false positive result from the Y2H assays.

3.2.4.2.3 Co-immunoprecipitation

The above results suggest direct interactions occur between CIN85 and pUL46 as well as CIN85 and pUL49. However, so far all assays have been performed with individual proteins and not in the context of viral infection. In order to further examine the interactions between CIN85 and tegument proteins in infected cells, co-immunoprecipitation (co-IP) analyses were performed in HSV-1 infected cells. HeLa cells were infected at 5 PFU/cell and harvested at 24 hpi for lysate preparation. Mock infected cells were used as controls. The lysates were incubated with anti-CIN85 antibody for ~5 h followed by incubation of protein A-Sepharose beads. The beads were harvested by centrifugation, washed three times and the samples were analysed by western blotting. pUL49 (VP22) was clearly observed in the anti-CIN85 precipitated sample but not in the control (Figure 3.13 A), indicating that CIN85 binds to pUL49 in infected cells. However, it should be noted that additional controls using an irrelevant antibody in the co-IP and blotting for pUL49 would be required to confirm this result. As a control, the anti-CIN85 antibody precipitated sample was also blotted by anti-VP16 (pUL48) specific antibody. Interestingly, VP16 was also pulled down by anti-CIN85 antibody (Figure 3.13 B), although there was no interaction observed between CIN85 and pUL48 from the initial Y2H screen (Figure 3.2 A). The immunoprecipitates were also blotted with anti-VP13/14 (pUL47) and there were no detectable signal of pUL47 further confirming CIN85 and pUL47 do not interact (Figure 3.13 C). The viral proteins VP22, VP16 and VP13/14 were detected from the infected cell lysate but not from the uninfected control as expected (Figure 3.13 A-C). Unfortunately, no pUL46 specific antibody was available in the lab and so it could not be tested whether pUL46 interacts with CIN85 in infected cells.

One of the interesting results described above is the potential interaction between CIN85 and VP16 revealed by co-IP (Figure 3.13 B). VP16 (pUL48) is a major tegument protein and perhaps it has interactions with host cellular proteins that are important for HSV-1 assembly. However, due to the strong auto-activation in yeast two-hybrid assays, pUL48 could not be tested in the assay as a bait protein in pGBKT7. Therefore some potential interactions between VP16 and ESCRT proteins could be missed in the screen. Previous

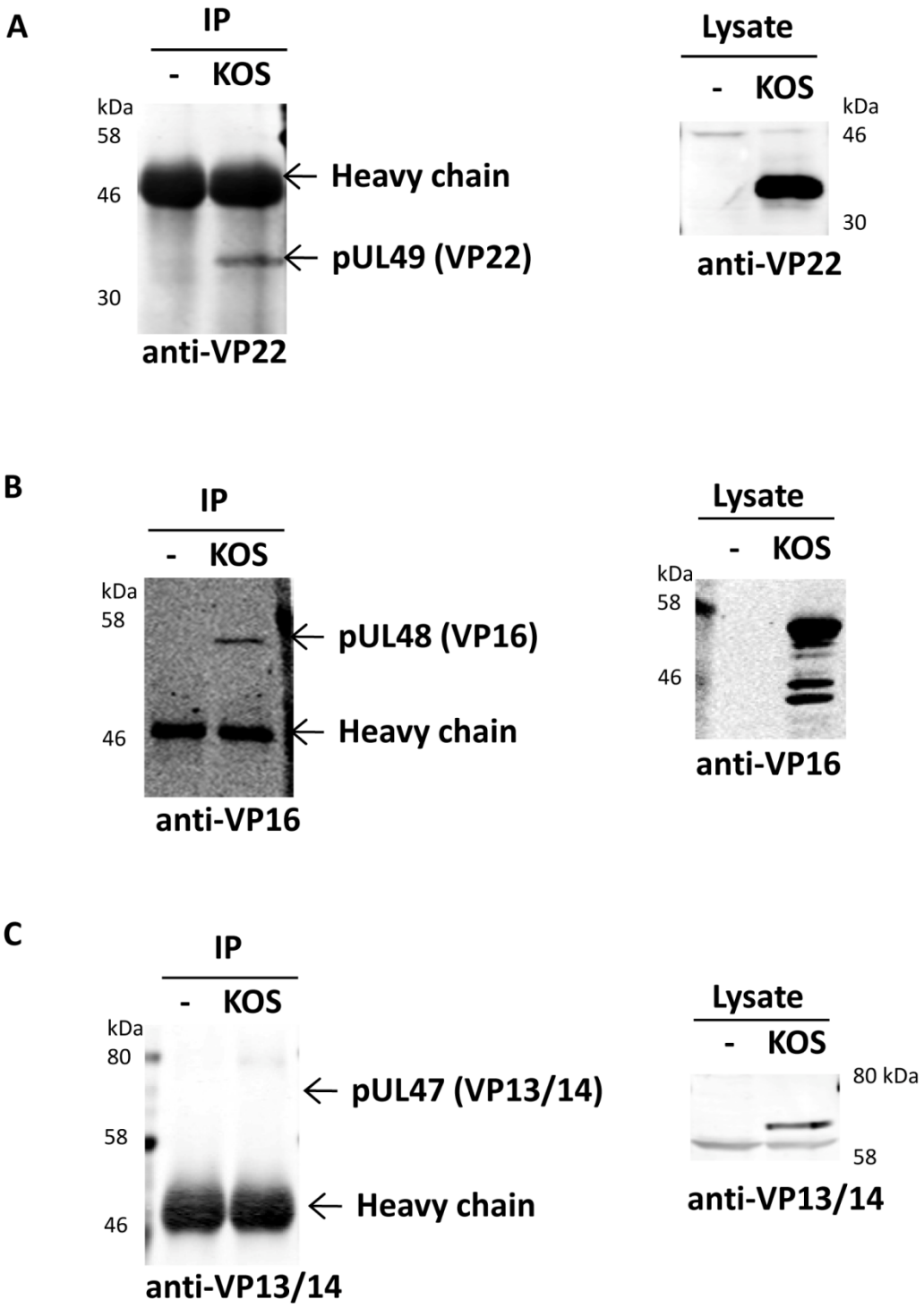

Figure 3.13: Co-immunoprecipitation of CIN85 and tegument proteins. HeLa cells were seeded into T75 flask and infected at 5 PFU/cell one day later. At 24 hpi, cells were harvested for co-immunoprecipitation. Cell lysates were prepared and incubated with anti-CIN85 antibody followed by protein A-Sepharose. The beads fractions were resolved by SDS-PAGE and examined by western blotting with anti-pUL49 (VP22) (A) or anti-pUL48 (VP16) (B) or anti-pUL47 (VP13/14) (C) antibodies. Uninfected cell lysates were used as the negative control. The viral proteins in the lysate samples were detected by western blotting and shown in corresponding panels.

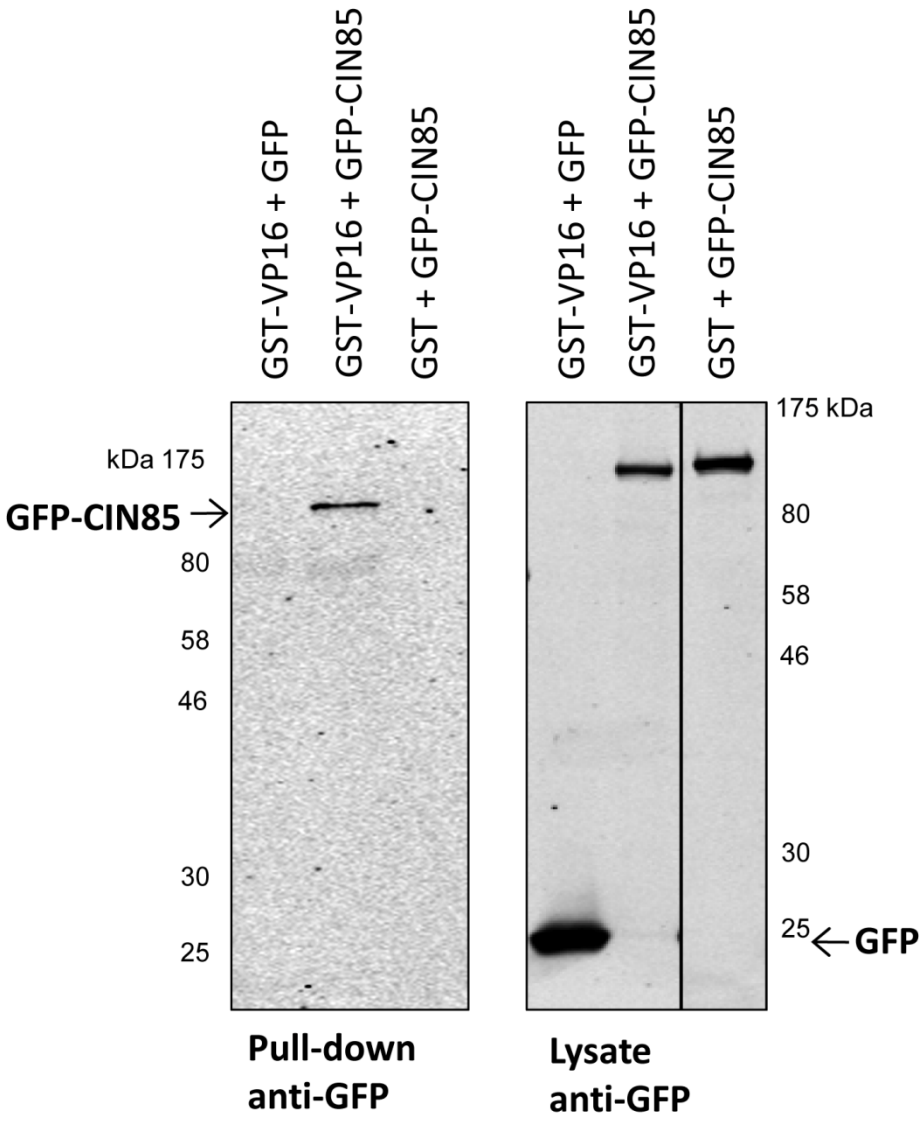

Figure 3.14: GST pull-down of CIN85 with pUL48 (VP16). The assay was performed as described above and the GFP signals detected from the pull-down and lysate samples are shown.

reported data have shown that tegument protein VP16 interacts with pUL49 (VP22) (Hafezi *et al.*, 2005) and pUL46 (Vittone *et al.*, 2005). Thus the VP16 signal observed from the anti-CIN85 immunoprecipitates could be indirect via interaction(s) of pUL48 with pUL49 and/or pUL46, or through other unknown viral proteins that bind to CIN85. Hence, to further analyse whether there is a direct interaction between CIN85 and VP16, GST pull-down assay were performed. 293T cells were co-transfected with GST tagged VP16 and GFP tagged CIN85 plasmid, or GST and GFP only as negative controls. The GFP tagged CIN85 protein was clearly detected in the GST-VP16 pull-down sample and there was no binding of GST-VP16 to GFP only or GFP-CIN85 to GST only in the control samples (Figure 3.14). This result suggests that CIN85 can indeed directly interact with VP16.

3.2.4.3 Interactions of tegument proteins with CC2D1A and CC2D1B

3.2.4.3.1 GST pull-down

From the yeast two-hybrid screen assays performed by S. Rauch at King's College London, CC2D1A showed specific interactions with six HSV-1 tegument proteins (Figure 3.2). CC2D1A has been previously reported to interact with ESCRT-III protein CHMP4A, CHMP4B and CHMP4C according to Y2H assays (Tsang *et al.*, 2006), thus CC2D1A is potentially a pathway for HSV-1 to recruit CHMP4A/B/C proteins. CC2D1A has a homologous protein CC2D1B that may have similar functions as CC2D1A. Therefore, CC2D1B was also included for further analysis.

GST pull-down assays were performed to test whether CC2D1A and CC2D1B directly interact with CHMP4 proteins. All of three YFP tagged CHMP4 isoforms were pulled down by both GST tagged CC2D1A and CC2D1B (Figure 3.15). Among the three YFP tagged CHMP4 proteins, CC2D1A and CC2D1B showed the strongest binding to YFP-CHMP4C and weakest binding to YFP-CHMP4A. Protein bands at estimated sizes were detected from the cell lysates suggesting YFP control and YFP tagged CHMP4 proteins were all expressed. However, the YFP tagged CHMP4A/B/C showed cleavage products suggesting a level of instability. Taken together, these results are in agreement with the previously reported interactions between CC2D1A and CHMP4A, CHMP4B and CHMP4C identified by Y2H assays (Tsang *et al.*, 2006) and further confirm the direct interactions of CC2D1B with all three human CHMP4 proteins in mammalian cells.

In the initial Y2H screen with HSV-1 tegument proteins, CC2D1A showed interactions with six HSV-1 tegument proteins: pUL11, pUL16, pUL21, pUL46, pUL47 and pUL49

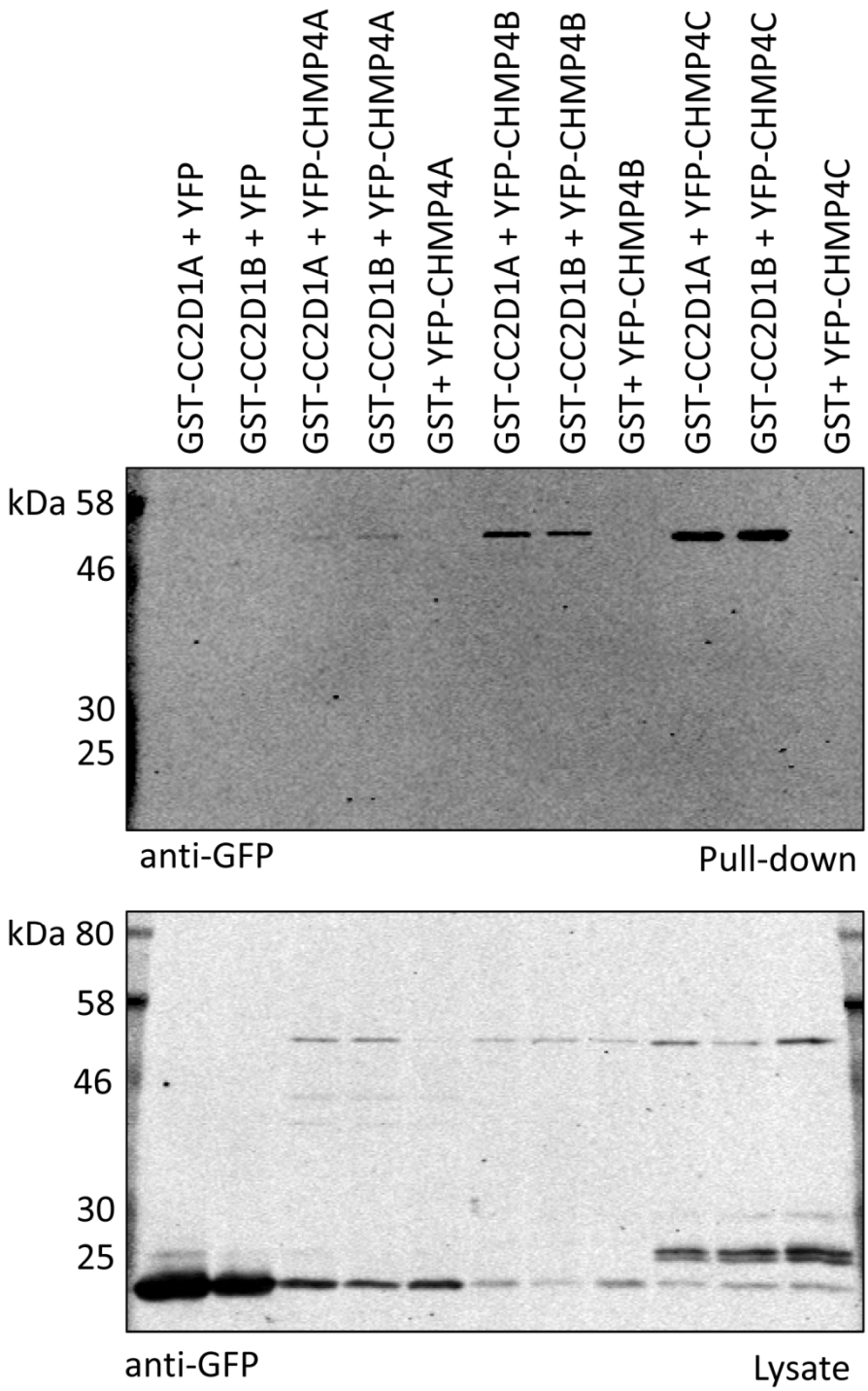

Figure 3.15: GST pull-down of YFP-CHMP4 proteins by CC2D1A and CC2D1B. 293T cells were seeded into six-well plates at density of 6 x 10^5 cells per well one day before transfection. The GST tagged CC2D1A or CC2D1B plasmids were co-transfected with the indicated YFP tagged CHMP4A, CHMP4B or CHMP4C plasmids. The GST or GFP only plasmids were used as negative controls. 48 h post transfection, the cells were harvested to prepare lysates and subjected to GST pull-down assay. The GFP signals of the pull-down and lysate samples are shown.

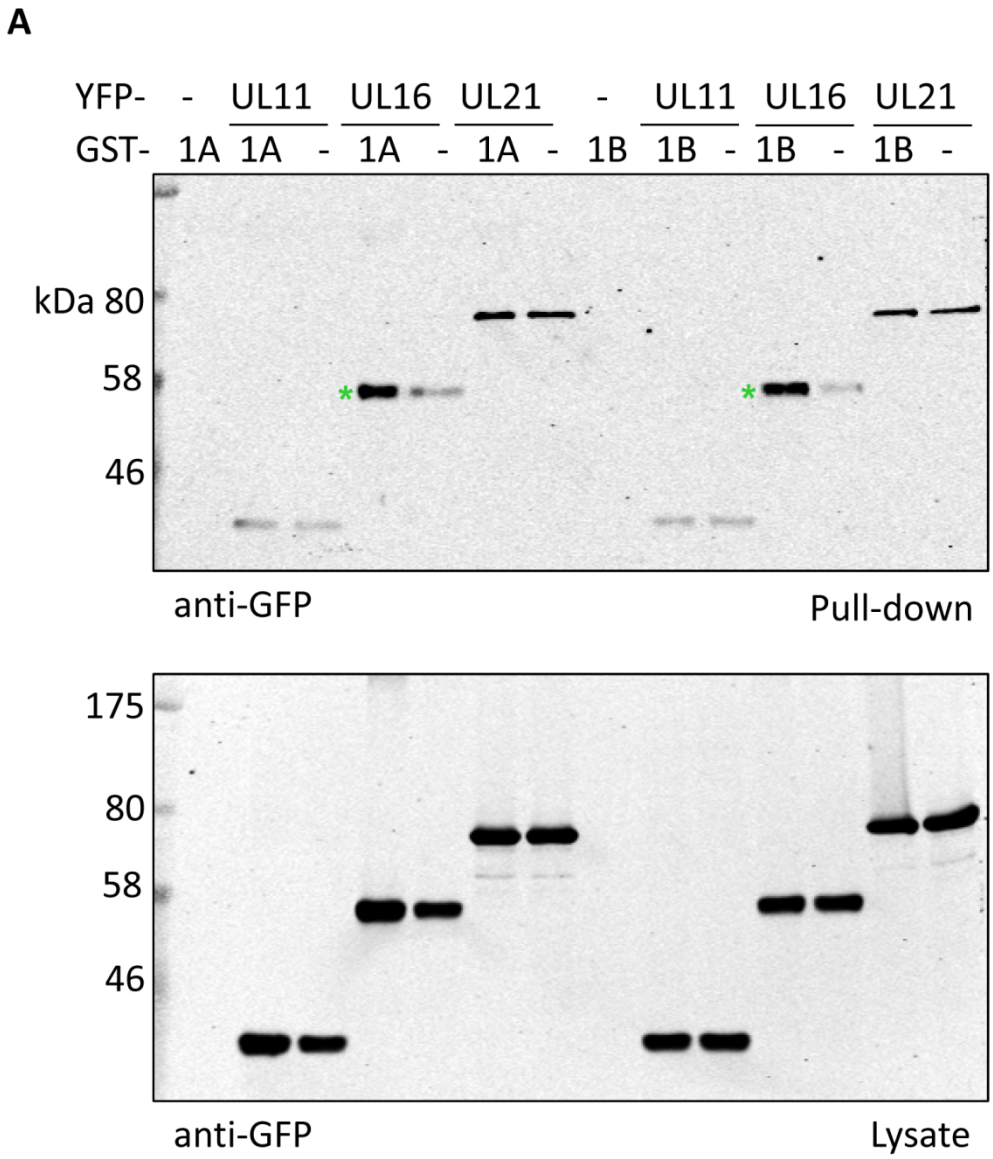

Figure 3.16: GST pull-down of YFP/GFP tagged tegument proteins by GST-CC2D1A and CC2D1B. 293T cells were seeded into six-well plates at density of 6 X 10^5 cells per well one day before transfection. The GST tagged CC2D1A (1A) or CC2D1B (1B) plasmids were co-transfected with the indicated GFP/YFP tagged tegument plasmids. The GST or GFP only plasmids were used as negative controls. 48 h post transfection, the cells were harvested to prepare lysates and subjected to GST pull-down assay. The GFP signals of the pull-down and lysates are shown. The positive interactions above non-specific binding are indicated by the green stars.

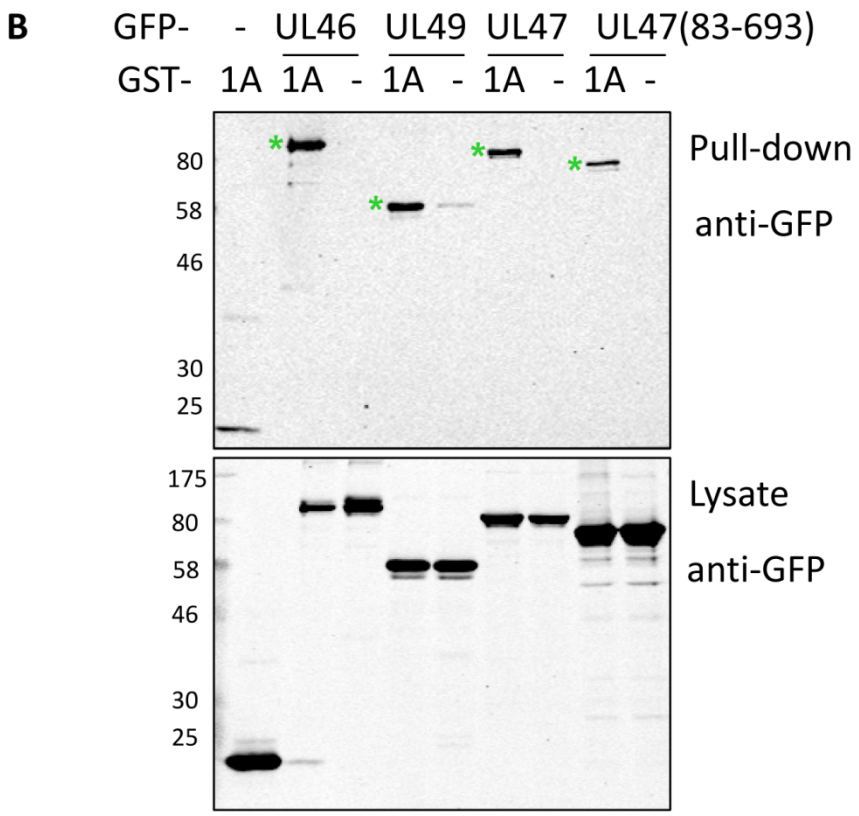
B
GFP- - UL46 UL49 UL47 UL47(83-693)
GST- 1A 1A - 1A - 1A - 1A -
80
58
46
30
25
Pull-down
anti-GFP
175
80
58
46
30
25
Lysate
anti-GFP

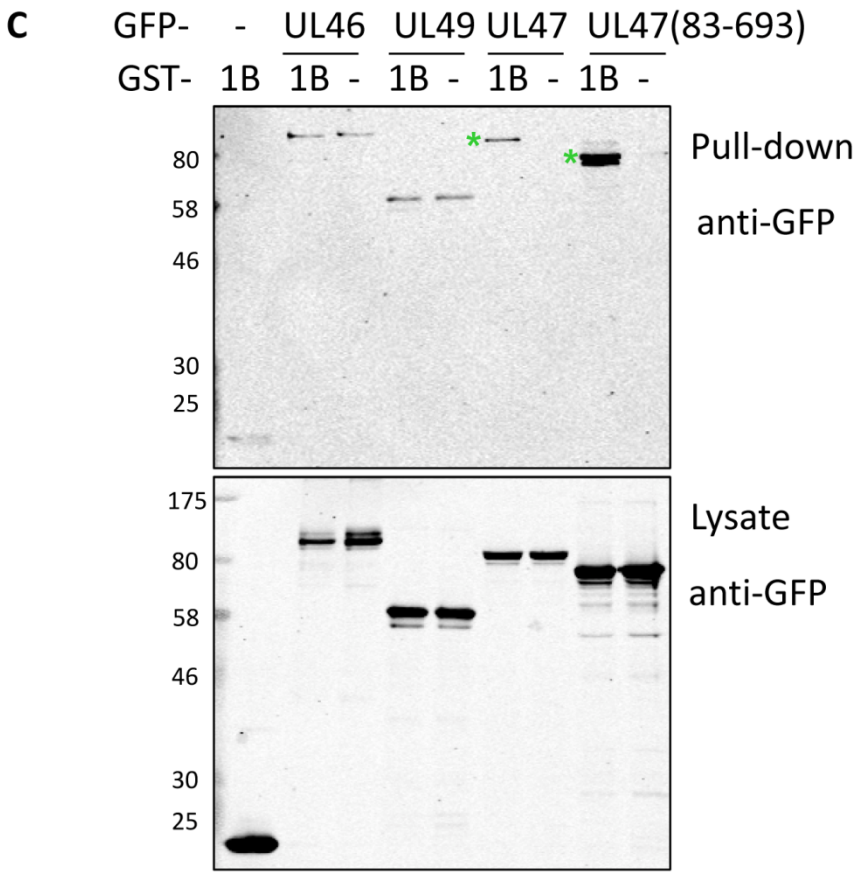
C
GFP- - UL46 UL49 UL47 UL47(83-693)
GST- 1B 1B - 1B - 1B - 1B -
80
58
46
30
25
Pull-down
anti-GFP
175
80
58
46
30
25
Lysate
anti-GFP

(Figure 3.2). While the homologous protein of CC2D1A, CC2D1B failed to show any interactions with HSV-1 tegument proteins in the initial Y2H screen. It was noticed that the CC2D1B clone used in the assays was shorter than expected. This CC2D1B clone is missing 309 aa from the N-terminus and has a different sequence at the C-terminus. The full length CC2D1B (CC2D1B-FL) clone was obtained by PCR using total cDNA from human cells as template (the sequence is shown in the appendix). Surprisingly, the CC2D1B-FL also showed no positive interactions with tegument proteins in Y2H assays. However, due to the possibility for homologous protein to have overlapping functions, and relatively high level of false negative result from yeast two-hybrid assays, it was considered worthwhile to further analyse the interactions of both CC2D1A and full length CC2D1B with HSV-1 tegument proteins. To do so, GST pull-down assays were performed from lysate of cells expressing YFP/GFP tagged pUL11, 16, 21, 46, 47 and 49 with GST tagged CC2D1A or CC2D1B.

GST tagged CC2D1A demonstrated interactions with GFP/YFP tagged pUL16 (Figure 3.16 A), pUL46, pUL47 and pUL49 (Figure 3.16 B), and GST tagged CC2D1B interacted with GFP/YFP tagged pUL16 (Figure 3.16 A) and pUL47 (Figure 3.16 C), within all these samples demonstrating either no background signals for GST only control or the sample signals were clearly higher than the background. In addition, GST tagged CC2D1A and CC2D1B both interacts with GFP tagged pUL47(83-693) (Figure 3.16 B, C) in agreement with the Y2H data (Figure 3.6 B, C). However, the GFP tagged pUL11 and pUL21 appear to bind to GST under the conditions used, thus these interactions could not be confirmed here (Figure 3.16 A). Furthermore, GST tagged CC2D1B did not show any interaction with GFP tagged pUL46 and pUL49 above background binding to GST controls (Figure 3.16 C). In agreement with these results, GST pull-down assays performed by S. Rauch at King's College London have demonstrated that CC2D1A interacted with HA-tagged pUL16, 21, 46, 47 and 49 and CC2D1B interacted with HA tagged pUL47 (S. Rauch, unpublished data).

3.2.4.3.2 Co-immunoprecipitation

Co-immunoprecipitation assays were performed to investigate whether CC2D1A and CC2D1B interact with the identified tegument candidate proteins in infected cells. Procedures were followed as described in section 3.2.4.2.3 using anti-CC2D1A and anti-CC2D1B antibodies. The protein A-Sepharose beads fractions were subjected to western blotting and tested by anti-pUL49 (VP22), anti-pUL48 (VP16), and pUL47 (VP13/14) and

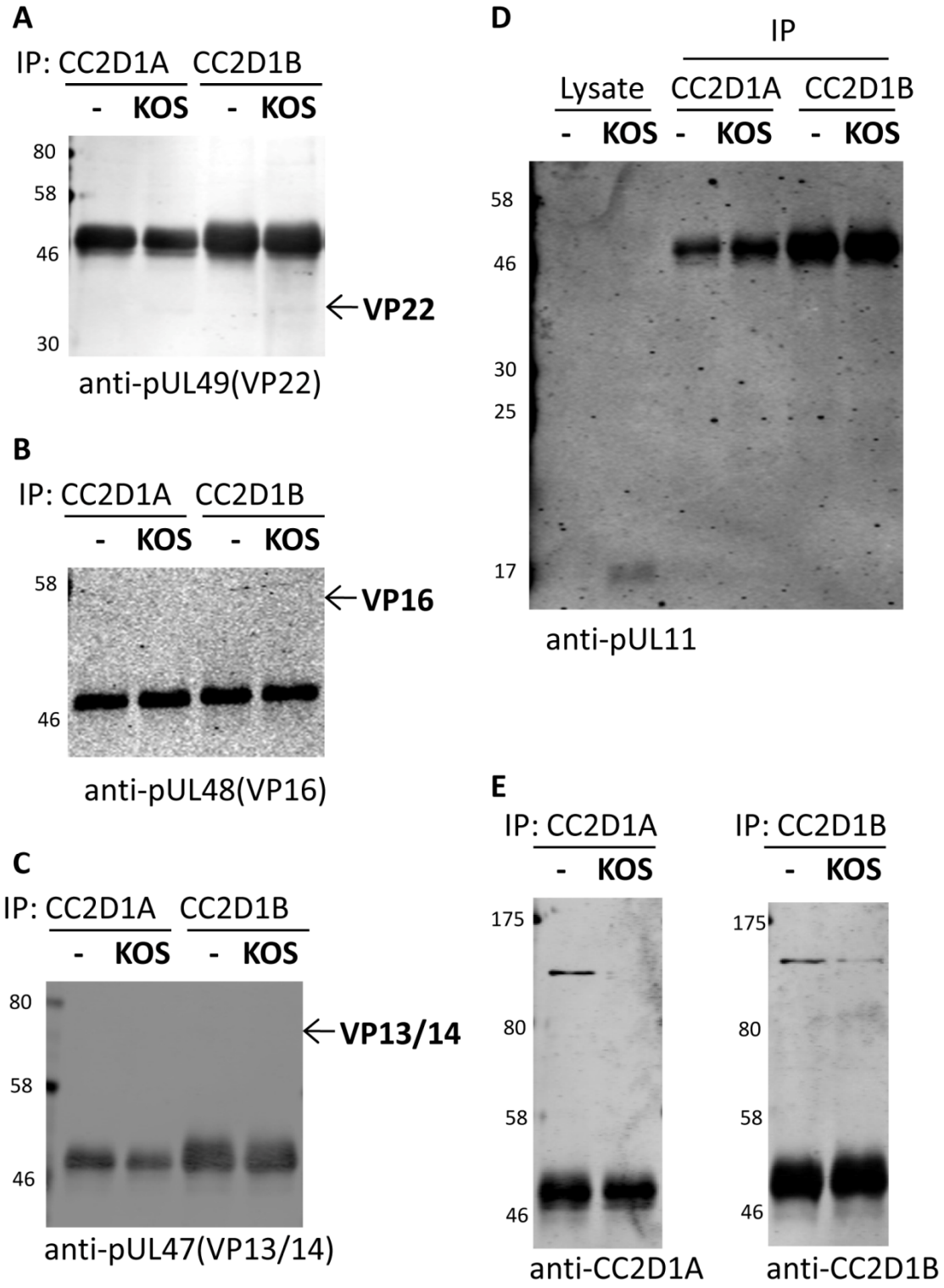

Figure 3.17: Co-immunoprecipitation of CC2D1A/1B and tegument proteins. HSV-1 infected HeLa cells lysates were prepared as described in Figure 3.13 and were incubated with anti-CC2D1A or anti-CC2D1B antibody followed by protein A-Sepharose. The beads fractions were resolved by SDS-PAGE and examined by western blotting with anti-pUL49 (VP22) (A), anti-pUL48 (VP16) (B), anti-pUL47 (VP13/14) (C) or anti-pUL11 (D) antibody. Uninfected cell lysates were used as the negative control. Except the pUL11 signals in infected cell lysate (D), the viral proteins in the lysate samples are shown in Figure 3.13. The beads fractions were also examined with anti-CC2D1A or anti-CC2D1B antibodies (E).

anti-pUL11 antibodies. As the results shown in Figure 3.17 A-D, there was no detectable signal from any of the immunoprecipitate samples. The expression levels of VP22, VP16 and VP13/14 in infected cell lysates are shown in Figure 3.13 (experiments performed with same lysate samples) and pUL11 band was detected from the lysate at ~17 kDa (Figure 3.17 D). The endogenous CC2D1A and CC2D1B precipitated were tested using anti-CC2D1A and anti-CC2D1B respectively (Figure 3.17 E). Surprisingly, the antibody precipitation efficiency was lower in infected cells than the mock control. This, presumably, could be due to the inhibition of protein expression by viral host-cell shutoff, or protein degradation upon infection. These data suggest there were no detectable interactions between CC2D1A/1B and the viral tegument proteins that could be observed with this approach. This, however, could be due to the low levels of CC2D1A/1B precipitated by the antibodies, or the interactions between CC2D1A/1B and tegument proteins are of a relatively low efficiency and are disrupted during the washing of the IP samples. Optimisation of these experiments would be required to further analyse the interactions of these HSV-1 tegument proteins and endogenous CC2D1A or CC2D1B, although time constraint prevented this from being pursued further.

Unfortunately, there were no anti-pUL16, anti-pUL21 or anti-pUL46 antibodies available for this analysis. It would be interesting to test the immunoprecipitates to examine whether these tegument candidates were precipitated by the CC2D1A and/or CC2D1B antibodies.

3.2.4.3.3 CC2D1A and CC2D1B stable cell lines and virion incorporation

Although the co-IP assays did not support direct interactions between endogenous CC2D1A/1B and tegument proteins under the conditions tested, the Y2H and GST pull-down data in the previous sections, as well as additional data from our collaborator at King's College London, suggest that these proteins do directly interact. Close contacting between cellular proteins and viral proteins could lead to the cellular proteins being incorporated into the virions. ESCRT components have been previously observed in purified HSV-1 preparation (Pawliczek & Crump, 2009). In the following studies, the virion incorporation of tagged CC2D1A and CC2D1B proteins has been examined in human keratinocyte HaCaT cells.

The HaCaT cell lines stably expressing YFP tagged CC2D1A and CC2D1B were generated by retroviral transduction, using a VSV-G pseudotyped murine leukemia virus (MLV) system. Stable cell populations were selected and maintained in puromycine. The CC2D1B plasmid used was the C-terminal truncated variant of the full length protein. The YFP

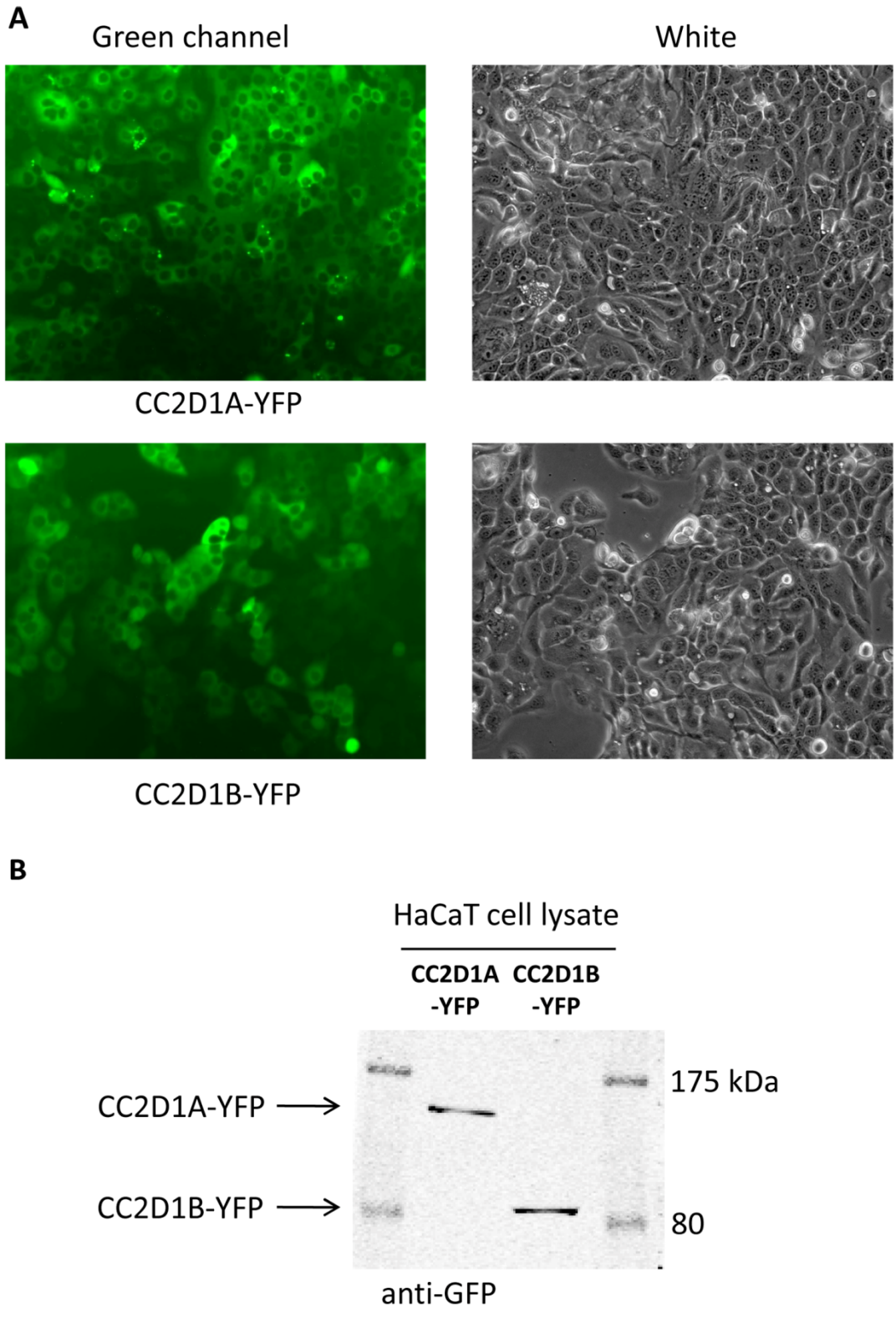

Figure 3.18: HaCaT stable cell line expressing CC2D1A-YFP or CC2D1B-YFP. (A) Fluorescence and phase-contrast images of stable cell populations. (B) HaCaT cell lysates were prepared and tested by western blotting using anti-GFP antibody to further confirm the over expressed CC2D1A-YFP (~ 130 kDa) and CC2D1B-YFP (~ 89 kDa) signals.

signals in HaCaT cells could be detected by both fluorescence microscopy (Figure 3.18 A) and GFP antibody in western blotting (Figure 3.18 B). The over expression levels of the two tagged protein were similar.

As a first step to examine whether the YFP tagged CC2D1A and/or CC2D1B are incorporated into HSV-1 virions, the cells were infected by HSV-1 strain KOS and virions in the culture supernatant were partially purified by centrifugation through a 33.3% sucrose cushion. The virion samples were subjected to western blotting and GFP antibody was used to detect the YFP-CC2D1A and YFP-CC2D1B signals. YFP-CC2D1A signals were detected in the virus samples harvested from the cells stably expressing YFP-CC2D1A and the protein band was at the same size as the YFP-CC2D1A band detected from the lysate sample. However, no YFP signals were observed in the viruses produced by YFP-CC2D1B over expressing cells (Figure 3.19 A top panel). In addition, it has been previously shown that CHMP2B is incorporated into HSV-1 virions (Pawliczek & Crump, 2009). Consistently with the reported data, CHMP2B was detected in the viruses purified from the two cell lines and the levels detected from the two viruses were similar (Figure 3.19 middle panel). A potential caveat to this approach is the viral cytopathic effect (CPE) can cause lysis of cells, which might lead to contamination of virus samples with cellular factors. To monitor this, tubulin was used as an indicator for potential cellular protein contamination. As the result shows tubulin was only detected from the cell lysate (Figure 3.19 A bottom panel), which implies little or no cellular component contamination of the virus preparation. The viral capsid signals in the sucrose purified viruses from the two stable cell lines were also shown by western blotting and the two virus preparations had similar levels of VP5 (Figure 3.19 B).

Thus these data suggest that YFP-CC2D1A is incorporated into HSV-1 KOS virions, but not YFP-CC2D1B. However, CC2D1B-YFP might also be incorporated into the virions, but of a much lower level. To test this, viruses could be harvested from a greater number of cells, or other methods, such as density gradient purification, could be performed to generated more concentrated virus stocks for further testing. Additionally, virus sucrose cushion "purification" is not as stringent as gradient purification. Although there was no tubulin signal in the virion samples, there might be some other cellular contaminations. Thus Ficoll gradient purification was performed to obtain higher purity virus stocks for western blotting analysis.

HaCaT cells over expressing YFP-CC2D1A or YFP-CC2D1B were infected with HSV-1 strain KOS at 0.01 PFU per cell. After three days of incubation, the cell culture

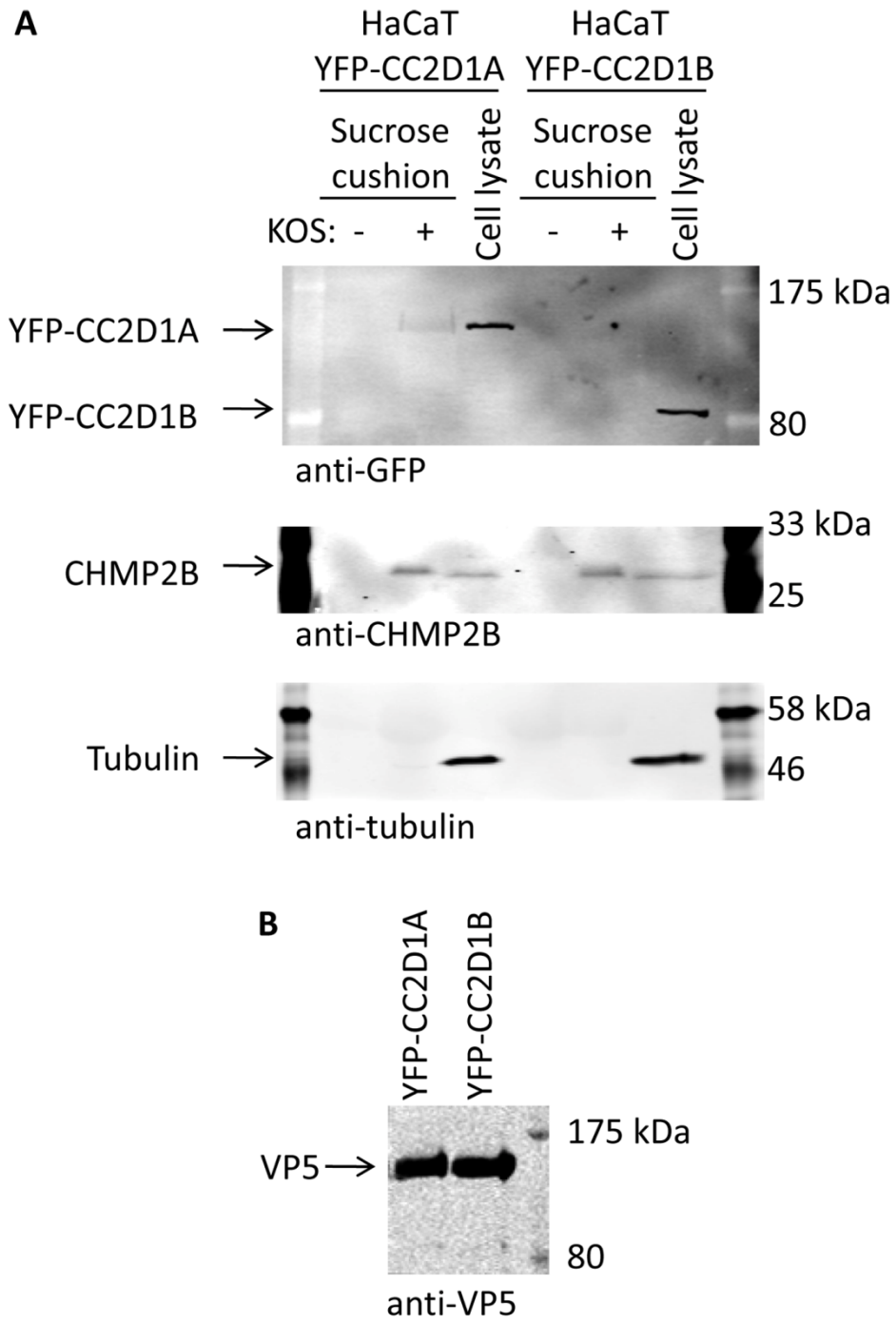

Figure 3.19: YFP-CC2D1A and YFP-CC2D1B in sucrose cushion purified HSV-1. (A) HaCaT cells stably over expressing YFP-CC2D1A or YFP-CC2D1B were seeded into T75 flasks at 4 x 10^6 cells per flask one day before infection. The cells were infected with HSV-1 strain KOS at 10 PFU per cell in 2 ml DMEM culture medium at 37 ºC for one hour. The inocula were removed and 10 ml medium per flask was added after the cells were washed in PBS. The culture supernatant was collected at 24 hpi and the cell debris was removed by centrifugation at 1800 rpm at 4 ºC for 10 min. The supernatant was overlaid onto 33.3% sucrose cushion and the viruses were harvested by centrifugation at 35000 rpm at 4 ºC for 90 min. The supernatant from uninfected HaCaT cells were used as control. YFP, CHMP2B and tubulin signals were tested for all the samples. (B) The viral capsid protein (VP5) signals were tested for the sucrose cushion purified KOS from the two HaCaT stable cell lines.

supernatant was harvested and cell debris was removed by low speed centrifuge. The viruses were harvested by ultracentrifugation and overlaid onto 5-15% Ficoll gradient for purification. The visible virus band located near the middle of the gradient was harvested, virion pelleted by ultracentrifugation and then resuspended in a small volumn of PBS and stored at -70 °C. The infectious titres were determined by plaque assays on Vero cell monolayers. The purified viruses were loaded at 4 x 10^8 PFU per lane in SDS-PAGE gel for western blotting. There was strong YFP-CC2D1A signal detected from the viruses harvested from the HaCaT cells stably express YFP-CC2D1A. The detected band is at the same position as the YFP-CC2D1A signal from the cell lysate sample. However, there was no YFP-CC2D1B signal detected from the viruses generated by YFP-CC2D1B expressing HaCaT cells (Figure 3.20 A, upper panel).

In addition, it has been previously shown that VPS4A is incorporated into HSV-1 virions (Pawliczek & Crump, 2009). As expected, VPS4A was detected from the two purified viruses and the levels in the two purified viruses were similar (Figure 3.20 A, lower panel). However, there was no VPS4A signal detected from the cell lysate samples, which may due to the protein concentration of the cell lysates being too low.

The purified virus samples were also tested with an anti-CC2D1B antibody. Surprisingly, the anti-CC2D1B detected the presence of YFP-CC2D1B in the virion preparation purified from cells expressing YFP-CC2D1B (Figure 3.20 B), despite the fact that the GFP antibody did not detect any signal in this sample (Figure 3.20 A, upper panel). This might be due to the anti-CC2D1B antibody being more efficient than anti-GFP in detecting YFP-CC2D1B. No band at the size of YFP-CC2D1B could be detected in virions purified from YFP-CC2D1A expressing cells. However, faint bands at ~100 kDa were detected in both purified viruses by the anti-CC2D1B, which could represent full length endogenous CC2D1B (predicted size ~94 kDa). Analysis of VP5 showed that the loading of the two viruses were similar (Figure 3.20, C). Overall, these data suggest that both YFP-CC2D1A and YFP-CC2D1B are incorporated into HSV-1 virions, while YFP-CC2D1B was only incorporated at a low level. As a further step, it will be interesting to test whether the endogenous CC2D1A and CC2D1B proteins are incorporated into the virions during viral replication.

3.2.4.3.4 Virion incorporation of endogenous CC2D1A and CC2D1B

In order to investigate whether the endogenous CC2D1A and CC2D1B are incorporated into HSV-1 virions, anti-CC2D1A and anti-CC2D1B antibodies were used to detect

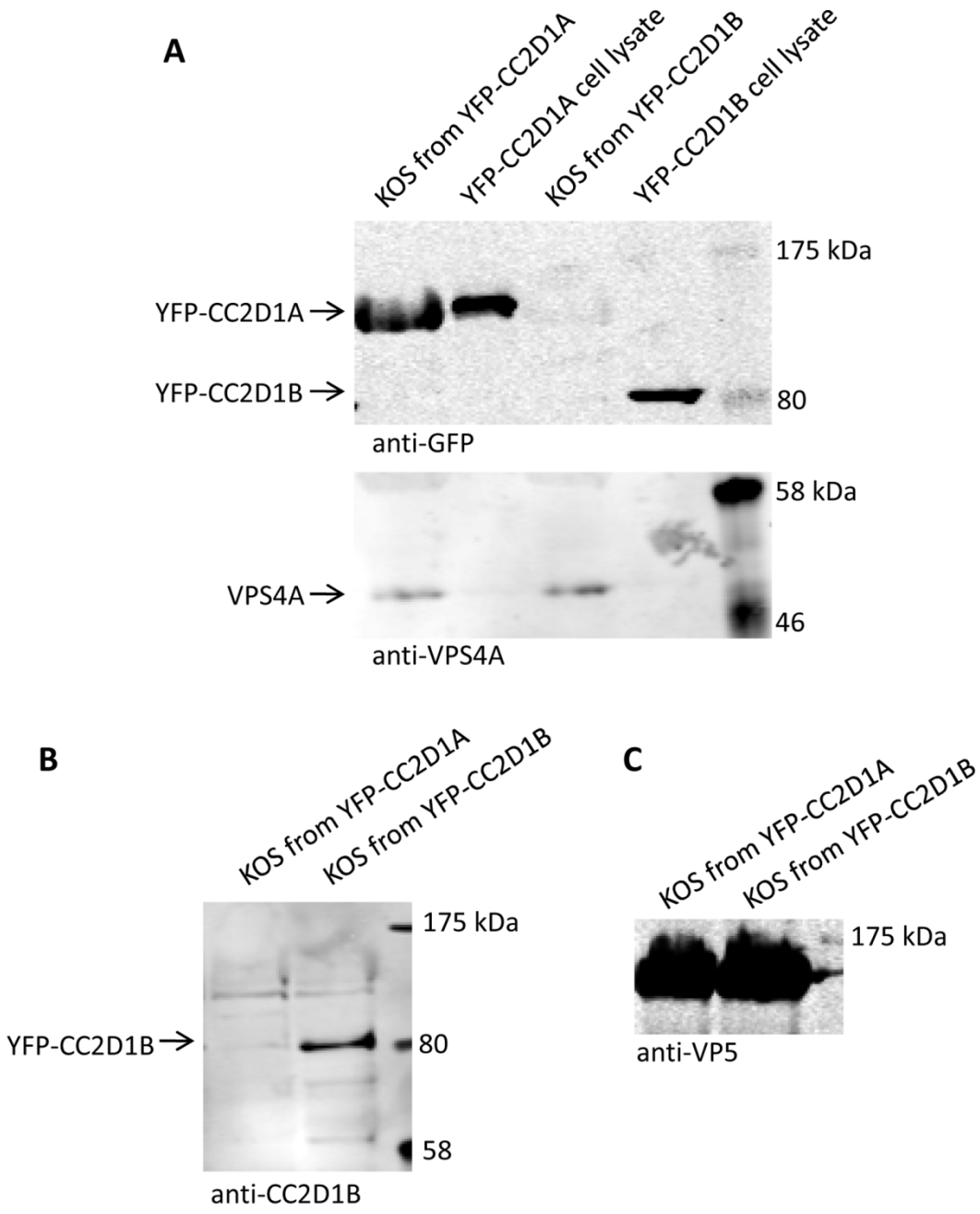

Figure 3.20: Virion incorporation of YFP-CC2D1A and YFP-CC2D1B in HSV-1. HaCaT cells stably expressing YFP tagged CC2D1A or CC2D1B proteins were infected with HSV-1 strain KOS at 0.01 PFU per cell. After incubation at 37 ºC for three days, the culture supernatant was collected and the cell debris was removed by centrifugation at 1200 rpm at 4 ºC for 20 min. The viruses from the supernatant were harvested by ultracentrifugation at 16000 rpm at 4 ºC for 2 h. The virus pellets were resuspended in 1% BSA/PBS solution, carefully overlaid onto 5-15% Ficoll gradient and centrifuged at 12000 rpm at 4 ºC for 1.5 h. The virus band was harvested, virion pelleted by centrifuged at 20000 rpm at 4 ºC for 2 h and the virus pellets were resuspended in PBS. The titres were determined by plaque assays on Vero cell monolayer. 4 x 10^8 PFU of the viruses were loaded per lane of SDS-PAGE gels for western blotting. Lysates of HaCaT stable cell lines were included for reference. Anti-GFP and anti-VPS4A antibodies were used to detect CC2D1A-YFP/CC2D1B-YFP and VPS4A singles respectively (A). Anti-CC2D1B was used to detect CC2D1B-YFP (B) and the viral capsid protein VP5 was detected by anti-VP5 antibody (C).

signals from purified virus stocks. Using the anti-CC2D1A antibody, both the YFP-tagged CC2D1A and the endogenous CC2D1A protein can be detected from the YFP-CC2D1A stable expressing HaCaT cell line, as well as from the purified KOS virions generated by this cell line. Further, another HSV-1 strain SC16 generated by two human cell lines (HaCaT and HT29) also showed endogenous CC2D1A signals (Figure 3.21 A). These data suggest that endogenous CC2D1A is indeed incorporated in HSV-1 virions.

Similarly, CC2D1B specific antibody was also used to test whether the endogenous CC2D1B is incorporated into HSV-1 virions. HSV-1 strain KOS and SC16 were harvested from different human cell lines (HT29 and HaCaT) and purified through 5-15% Ficoll gradient as described above. As the results show, there is weak signal from 1.4 x 10^9 PFU of SC16 while the signal was barely detectable from 1 x 10^8 PFU of KOS sample (Figure 3.21 B). This result implies that the endogenous CC2D1B is incorporated into HSV-1 virions, and while it is difficult to compare signals from two different antibodies, these data together with the observation using YFP-CC2D1B expressing cells suggest less CC2D1B is presented in virions than CC2D1A.

3.3 Discussion and conclusion

In order to identify direct interactions between the viral and cellular ESCRT proteins, a Y2H screen was performed. Twenty-two tegument genes were cloned from HSV-1 strain KOS and the sequence results showed certain amino acid changes compare to strain 17. These changes including amino acid point mutations, short deletions in the repeat region of the viral genome and one amino acid insertion. In all, the differences between the different strains were minor.

From the Y2H screen results, the tegument proteins US3 and US10 showed toxicity to yeasts. The amount of yeast colonies generated was generally much lower than the other samples. In these instances, some of the Y2H results were not obtained as there were not enough yeast cells for accurate measurement and these proteins are shown in Figure 3.2 as grey-coloured boxes. ICP0 has not been tested in the screen part performed at King's College London and they are also shown by the grey-coloured boxes. In the initial screen result, some proteins such as CHMP4B and Nedd4 appear to be 'sticky' in this system, as they had many positive interactions with tegument proteins, suggesting generally non-specific interactions.

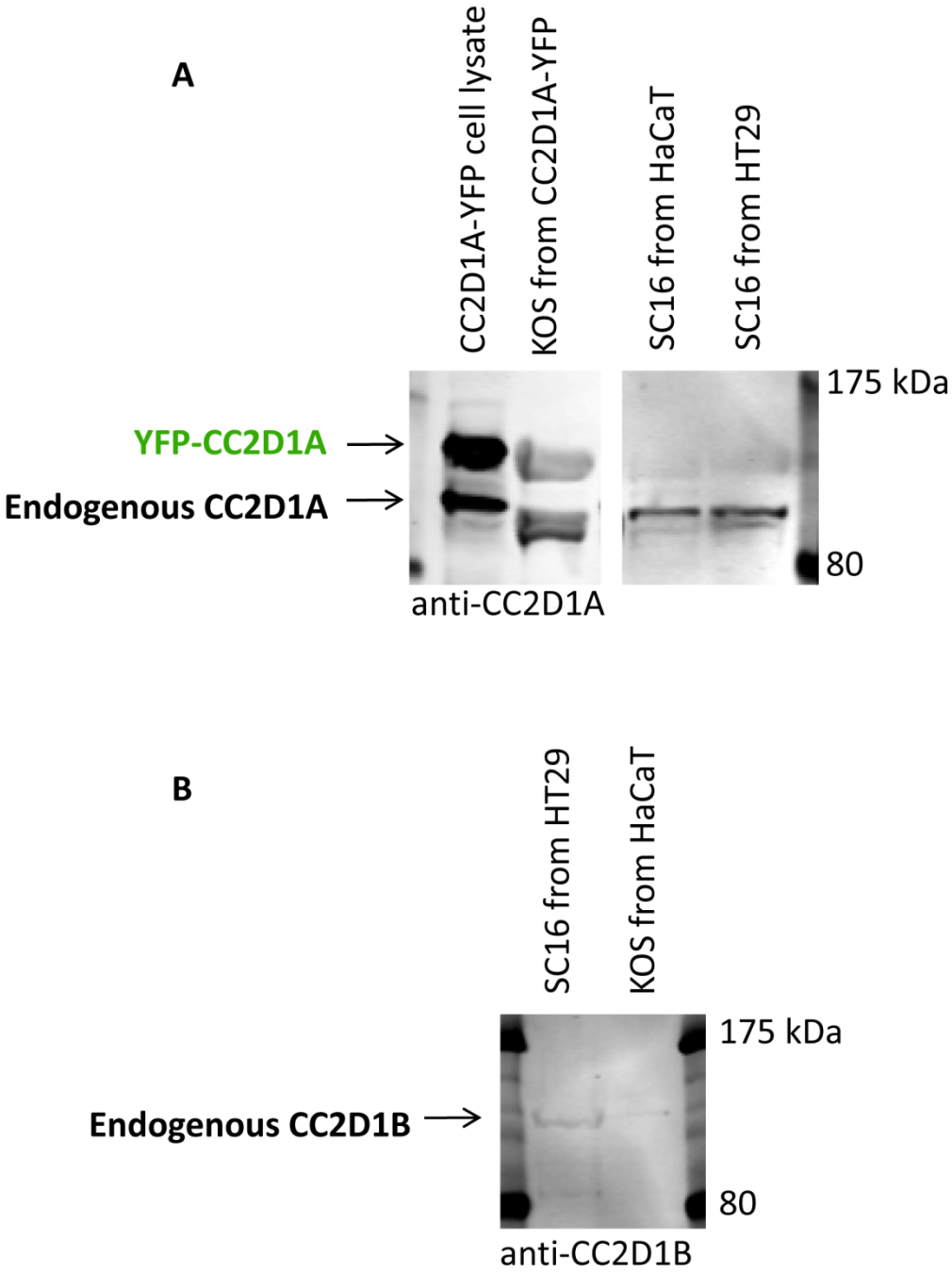

Figure 3.21: Endogenous CC2D1A and CC2D1B in HSV-1 purified virions. (A) HSV-1 strain KOS purified from HaCaT cells stably express YFP-CC2D1A, and strain SC16 purified from normal HaCaT and HT29 cells were loaded to SDS-PAGE at 4 x 10^8 PFU per lane for western blotting using anti-CC2D1A antibody. The expected positions of YFP tagged CC2D1A and endogenous CC2D1A protein bands are indicated. (B) 1.4 x 10^9 PFU of SC16 purified from HT29 cells and 1 x 10^8 PFU of KOS purified from HaCaT cells were loaded to SDS-PAGE for western blotting using anti-CC2D1B antibody. The expected position of endogenous CC2D1B is indicated.

Although ESCRT-0, I, II and III complexes are important for the MVB pathway in the cells, they are not all essential for HSV-1 assembly. During the forming of intraluminal vesicles in MVB pathway, membrane deformation requires the functions of ESCRT-0, I and II to recruit the ubiquitin labelled cargos and initiate the bud forming, while the viral structure proteins are likely to drive the initial membrane deformation thus becoming independent of the function of ESCRT-0, I and II complexes. In addition, previous reported data has demonstrated that the disruption of ESCRT-I complex did not affect HSV-1 production (Pawliczek & Crump, 2009). Thus among the positive hits, the interactions between HSV-1 tegument and ESCRT-III related proteins were the primary focus and these candidates were investigated by other methods. The interactions between pUL47 and CHMP6, ALIX and CC2D1A were reproducible in GST pull-down assays. The interactions of CC2D1A with other tegument proteins pUL16, pUL46, and pUL49 were also confirmed in GST pull-down assays. CC2D1B is a homologous protein of CC2D1A and these two proteins are proposed to have similar functions in cells. Surprisingly, there were no positive interactions found between CC2D1B and tegument proteins in Y2H assays. This may be due to poor expression of CC2D1B in yeast cells, or the overexpressed protein is either somehow not stable or misfolded. However, direct interactions between pUL47 and pUL16 with CC2D1B were observed in GST pull-down assays using mammalian cells. These data suggest that similar as CC2D1A, CC2D1B maybe directly interact with HSV-1 tegument proteins.

After identifying new interactions between the virus and ESCRT/ESCRT associated proteins, attempts were made to search domains that are important for the interactions. For pUL47 it was found that the N-terminal 127 aa, including the NLS, were dispensable for interactions with CHMP6, ALIX, CIN85 and CC2D1A. Furthermore, the NES region near the C-terminus of pUL47 is required for these interactions because while the C-terminal 26 aa of pUL47 downstream of the NES were dispensable, the truncation of pUL47 region beyond the NES resulted in the loss of interactions in Y2H assays (Figure 3.4 - 3.7). In addition, some evidence was obtained for possible interacting domains in pUL46 for CIN85 and CC2D1A/1B (Figure 3.8), while for pUL49, neither of the domain constructs tested showed interactions with CC2D1A or CIN85 (Figure 3.9). Different from short late domain motifs (usually contain 4 amino acid) identified in retroviruses that interact with ESCRT proteins, so far no such short motifs could be found from HSV-1 tegument proteins and large folded domains appear to be necessary. There is no information available about the structures of the HSV-1 tegument proteins in question.

Hence, protein structure prediction based on aa sequencing may offer helpful information for further analysis and domain constructs design in the future.

The investigation of interacting domains in CIN85 revealed that the N-terminal SH3 domains were important for interactions with pUL46 and pUL49. Both pUL46 and pUL49 are relatively proline rich (9.9% and 12.6% respectively) and contain multiple potential SH3 binding motifs (PxxP). It would be interesting to perform further experiment to study which SH3 domain (or short motif) is responsible for the interactions between CIN85 and these proteins.

Furthermore, the interaction between CIN85 and pUL49 (VP22) was confirmed by co-IP in infected cells. The result suggests that a direct interaction between pUL49 and CIN85 does occur in infected cells. In addition, despite not showing positive hits in the Y2H assays, VP16 demonstrated an interaction with CIN85 in both GST pull-down and co-IP assays. This result adds further information to the complex interactions between tegument proteins and ESCRTs, some of which may not be revealed by the Y2H screen. However, the control samples for the co-IP experiments presented in this thesis could have been improved by using a control antibody in addition to the controls using uninfected cell lysates (Figure 3.13 and 3.17).

The involvement of cellular ESCRT proteins in HSV-1 assembly might lead to their virion incorporation as previously reported from the laboratory for some ESCRT-III and VPS4 proteins (Pawliczek & Crump, 2009). The data presented in this thesis now show virion incorporation of the ESCRT associated CC2D1A and CC2D1B proteins quite clearly for both YFP tagged and endogenous CC2D1A (Figure 3.19 - 3.21), while the incorporation of both forms of CC2D1B appears to be much lower. These data offer further evidence for close contact/interactions between CC2D1A/1B and HSV-1. In addition, there were no CIN85 signals detected in purified HSV-1 samples, which could be due to low incorporation level, or the CIN85 antibody is not efficient enough. Moreover, the virus might interact with CIN85 in order to establish the link to ALIX to recruit ESCRT, therefore the interaction with CIN85 occurs at a relatively early stage during secondary assembly, which could possibly result in low level of (or no) incorporation. Future construction of stable cells overexpressing GFP-CIN85 and examine HSV-1 virions generated by these cells may address this question.

Over all in this chapter, ESCRT and tegument candidates were chosen according to the Y2H screen result. Some interactions observed from Y2H were confirmed by other

methods such as GST pull-down, protein co-localisation and co-IP assays. The ESCRT associated protein CC2D1A and CC2D1B were found to be incorporated into the HSV-1 extracellular virions. These results demonstrate that there are direct interactions between the tegument and ESCRT/ESCRT associated proteins. The interactions may play important roles in recruiting ESCRT machinery. Further experiments to examine the effect of depleting ESCRT/ESCRT associated proteins on viral replication are detailed in the following chapter.

4 The effect of depleting ESCRT and ESCRT associated proteins on HSV-1 replication

4.1 Introduction

During the HSV-1 life cycle, mature virus particles are formed by the budding of tegumented capsids into membrane compartments in the cytoplasm of the host cell. This event results in a double-membrane structure, where the inner membrane is the viral envelope, and the mature enveloped virus particle is contained in a transport vesicle formed by the outer membrane. During the formation of virus containing vesicles, the separation of the inner and outer membranes requires membrane scission.

The ESCRT machinery has been identified as being involved in several events which require membrane scission. This machinery has four major complexes (ESCRT-0, I, II and III) and VPS4 ATPase. The ESCRT-III proteins polymerise into ring filaments and are thought to directly mediate the membrane scission event at sites of membrane deformation (Wollert *et al.*, 2009). VPS4 ATPase is the only energy providing complex and is responsible for recycling ESCRT-III proteins after the separation of membrane is completed (Babst *et al.*, 1998). It has been previously reported that HSV-1 replication requires the function of VPS4 ATPase (Crump *et al.*, 2007). Additionally, previous data have shown that HSV-1 replication requires the function of the ESCRT III complex as overexpression of dominant negative ESCRT III proteins inhibited the production of infectious HSV-1 (Pawliczek & Crump, 2009). Among the eleven CHMP proteins (CHMP1A/B, 2A/B, 3, 4A/B/C, 5, 6 and 7) of the human ESCRT-III complex, there is evidence that the CHMP4 isoforms drive the actual membrane scission event. For example, CHMP4A and CHMP4B proteins can form circular arrays and cause plasma membrane deformation (Hanson *et al.*, 2008) and the *S. cerevisiae* ESCRT III protein Snf-7 (the yeast homologue protein of human CHMP4A/B/C) has been shown to be essential for membrane scission *in vitro* (Wollert & Hurley, 2010). These reported data suggest that the key step in the separation of membranes during inducing vesicle/virus particle formation is the recruitment and activation of CHMP4 proteins.

Previous data from the laboratory has shown that overexpression of dominant negative CHMP4A/B/C proteins inhibited HSV-1 production (Pawliczek & Crump, 2009). However, the expression of dominant negative ESCRT III protein is thought to affect the entire protein complex and may not give information on the specific role of individual CHMP proteins, and the role of endogenous CHMP4 proteins in HSV-1 replication had not been described. In this chapter, HSV-1 replication was investigated in cells depleted of all three isoforms of CHMP4. Further investigations were carried out to study the role of the proteins identified in Chapter 3 that interact with HSV-1 tegument proteins and may mediate the recruitment of CHMP4A/B/C. These ESCRT and ESCRT associated proteins are ALIX, CHMP6, CIN85 and CC2D1A/1B that were identified to interact with HSV-1 tegument proteins by yeast two-hybrid screening and validated by several methods (see Chapter 3). ALIX, CHMP6 and CC2D1A/B have all been shown to directly interact with CHMP4 proteins (McCullough *et al.*, 2008; Teis *et al.*, 2008; Tsang *et al.*, 2006) and are thus potential pathways for the virus to recruit the membrane scission activity of the ESCRT machinery. CIN85 has been shown to interact with ALIX, and so it is another potential route for CHMP4A/B/C recruitment, albeit via ALIX.

It was hypothesised that HSV-1 may recruit the ESCRT machinery via these direct interactions, and therefore if these cellular factors are removed or depleted from the host cells, viral replication would be affected. However, it has been previously shown that the depletion of ALIX or CHMP6 did not significantly affect HSV-1 production [T. Pawliczek PhD thesis 2010 and (Pawliczek & Crump, 2009)]. Therefore, there is likely to be functional redundancy between these pathways. The effect of depleting CIN85 and CC2D1A/1B on HSV-1 production was investigated initially, and then further experiments were conducted to determine the effect of several combined depletions of these proteins.

Additionally, in the Y2H screen demonstrated in Chapter 3, the HSV-1 tegument protein pUL47 was found to interact with many ESCRT and ESCRT associated proteins. While several of these interactions may be false positives, it is possible to inhibit all these potential interactions between pUL47 and ESCRTs by removing the UL47 gene from the virus genome. This strategy would result in HSV-1 having fewer possible pathways available to recruit the ESCRT machinery and thus could make the virus more sensitive to the depletion of other ESCRT proteins. Hence, a UL47 deletion virus (ΔUL47) was created and the replication of ΔUL47 was analysed in cells with depletion of certain ESCRT and ESCRT associated proteins using siRNA.

Finally an alternative pathway beyond the candidates identified from the yeast two-hybrid screen in Chapter 3 was explored. ALIX has been shown to interact with CHMP4 isoforms via its Bro1 domain (Meckes & Wills, 2007). Related Bro1 domains are also present in other mammalian proteins, and they could serve as alternative routes for the recruitment of ESCRT III. One of these Bro1 domain containing proteins, HD-PTP, although it did not show interactions with tegument proteins in the yeast two-hybrid screen, has been reported to be required in endosomal cargo sorting and multivesicular body morphogenesis (Doyotte *et al.*, 2008). Therefore the effect of depleting HD-PTP on HSV-1 replication was investigated.

4.2 Results

4.2.1 HSV-1 replication in CHMP4A/B/C depleted cells

Among the eleven CHMP proteins in the ESCRT III complex, CHMP4A/B/C proteins are the most important components for membrane scission events. In this section, the requirement for endogenous CHMP4A/B/C in HSV-1 replication has been investigated by siRNA depletion and the ultrastructures of the infected cells were examined by transmission electron microscopy (TEM).

Previous studies in the laboratory have demonstrated that siRNA depletion of all three CHMP4 isoforms is highly toxic for HeLa cells, resulting in cell death before assays of viral replication could be performed. However, more recently it was observed that 293T cells are less sensitive to the loss of ESCRT function and remain viable for long enough to assay viral replication. 293T cells were transfected twice consecutively with CHMP4A/B/C siRNA oligonucleotides to knockdown endogenous protein expression. 48 h after the second transfection, cells were infected with HSV-1 strain KOS at 10 PFU/cell and the production of infectious viruses from a single round of viral replication was determined by plaque assay. In cells with simultaneous CHMP4A/B/C depletion, HSV-1 production is inhibited by more than 100 fold compared to the controls (Figure 4.1 A). The expression levels of CHMP4A, CHMP4B and CHMP4C were tested in western blotting using anti-CHMP4A, anti-CHMP4B and anti-CHMP4C antibodies. The endogenous expression of the three CHMP4 proteins was reduced in CHMP4A/B/C siRNA treated cells, while the expression levels were not affected by the control siRNA ConX (Figure 4.1 B). The tubulin signals were at a similar level indicating there were similar amount of cells in different samples at the time of infection.

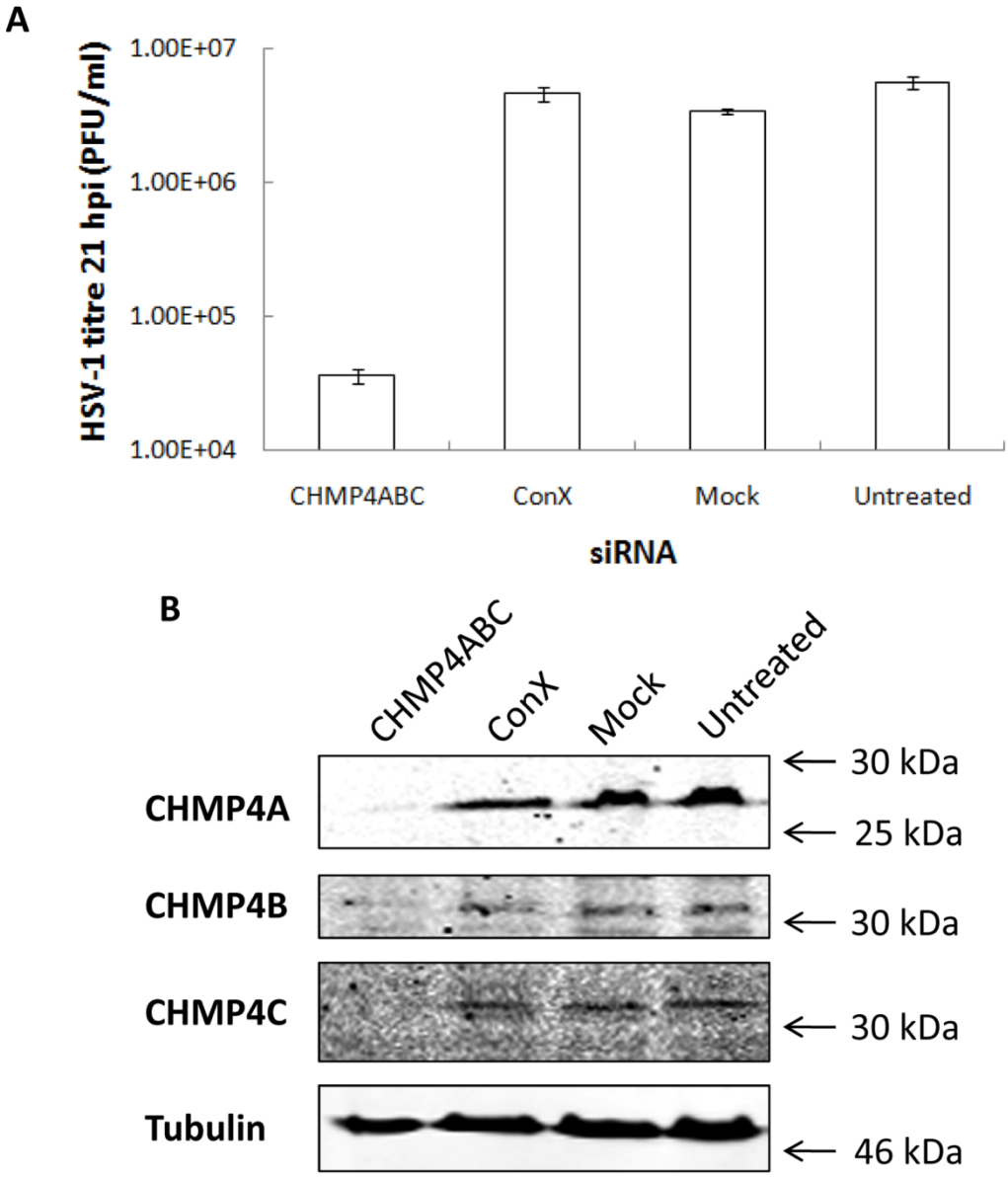

Figure 4.1: HSV-1 replication is inhibited by the depletion of CHMP4A/B/C. 293T cells were seeded into six-well plates at density of 4 x 10^5 cells per well. The first transfection was performed 2 h post seeding. Around 48 h after the first transfection, the cells were split into new plates and 2 h later the second transfection was performed. The cells were infected with HSV-1 strain KOS at 10 PFU/cell at 48 h post the second transfection. The infected cell samples were collected at 24 hpi by freezing at -70℃. The parallel uninfected cell samples were harvested for cell lysate preparation for western blotting. Tubulin signals in the samples were used as the loading control. (A) The progeny viruses produced in the cells were released by sonication. The infectious virus titres were determined by plaque assays on Vero cell monolayers. The mean titres and standard error bars from triplicate samples are shown. (B) The expression levels of endogenous CHMP4A, CHMP4B and CHMP4C in CHMP4A/B/C triple depleted cells and the control samples.

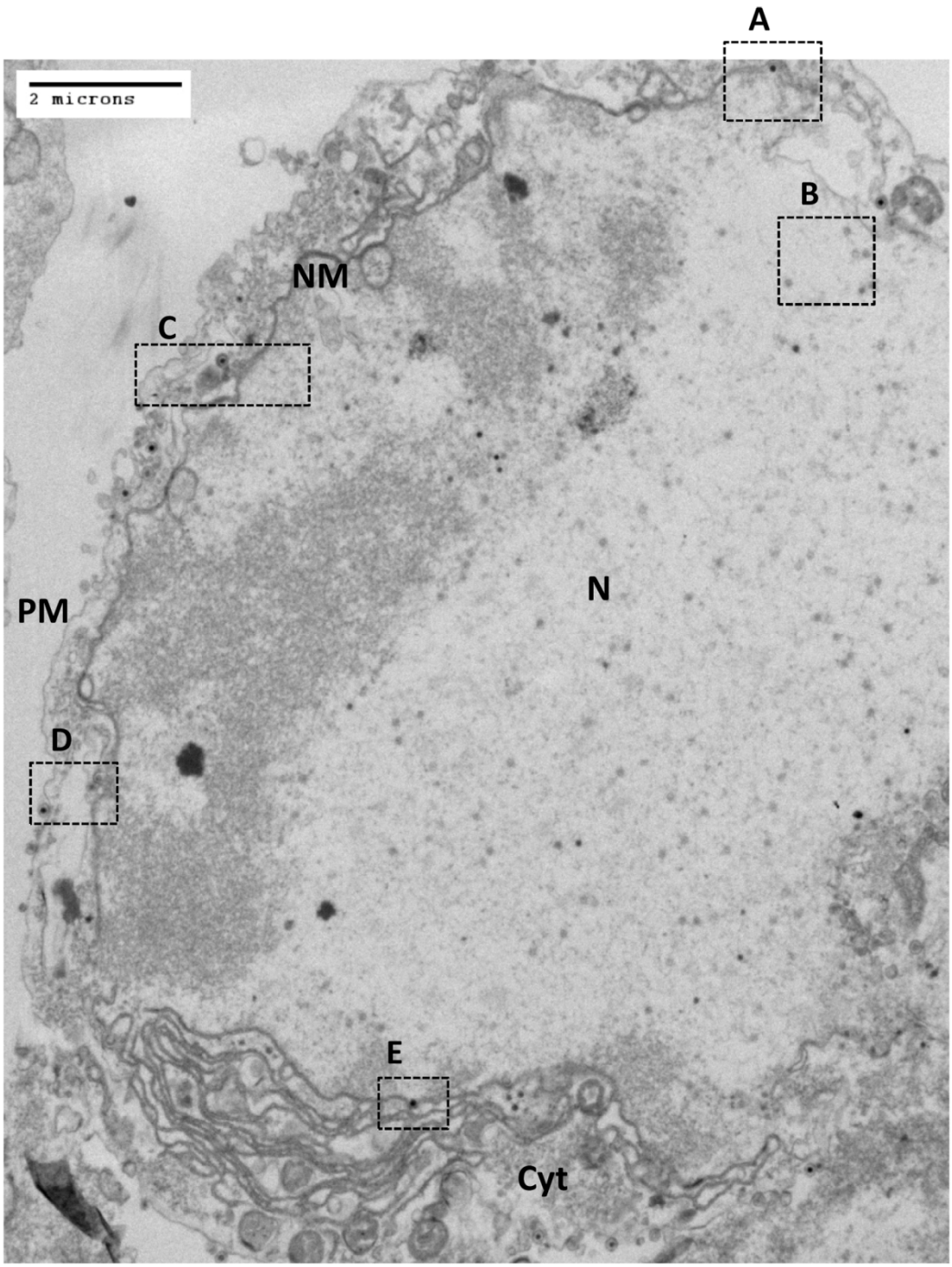

Figure 4.2: Ultrastructure of ConX siRNA treated cells infected with HSV-1. 293T cells were treated with two rounds of siRNA as described in the legend of Figure 4.1. The cells were infected with HSV-1 strain KOS at 5 PFU/cell at 48 h post the second siRNA transfection. The infected cells were fixed at 16 hpi in 2% glutaraldehyde in 0.1M HEPES buffer (pH 7.4) on ice and subjected to preparation for TEM by Dr J. Skepper (Multi Imaging Unit of Physiology Development and Neuroscience, University of Cambridge). The images were obtained using a FEI Philips CM100 TEM with a digital camera. An image of the ConX treated cells showing the major events in viral life cycle highlighted by the dot line boxes in the cell. More details of the structures are shown by the enlarged pictures (A-E). N: nucleus. NM: nuclear membrane. NC: nuclear capsid. Cyt: cytoplasm. PM: plasma membrane. CC: cytoplasmic capsid. ECV: extracellular virion. PE: primary envelopment. SE: secondary envelopment.

Figure 4.2

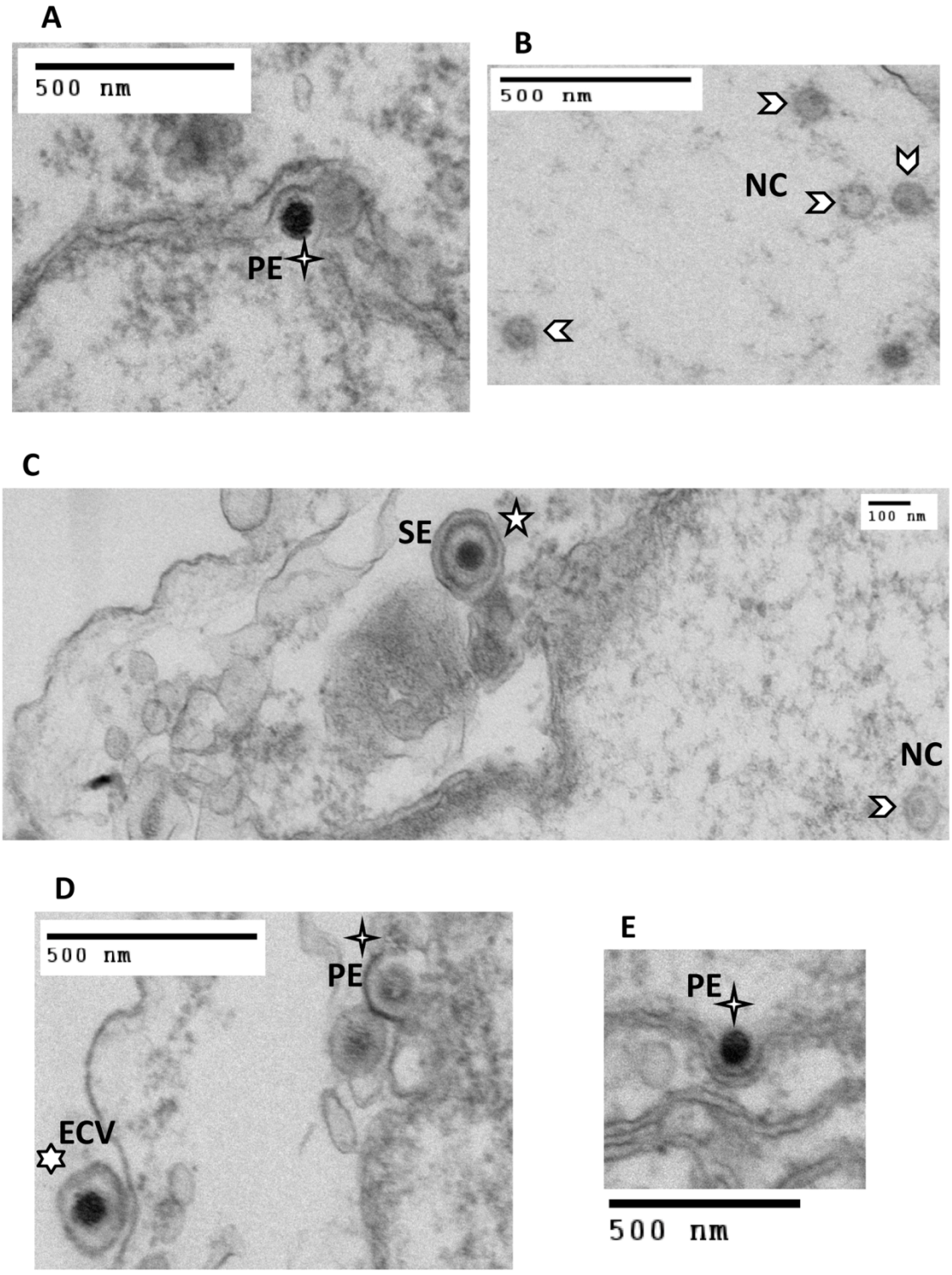

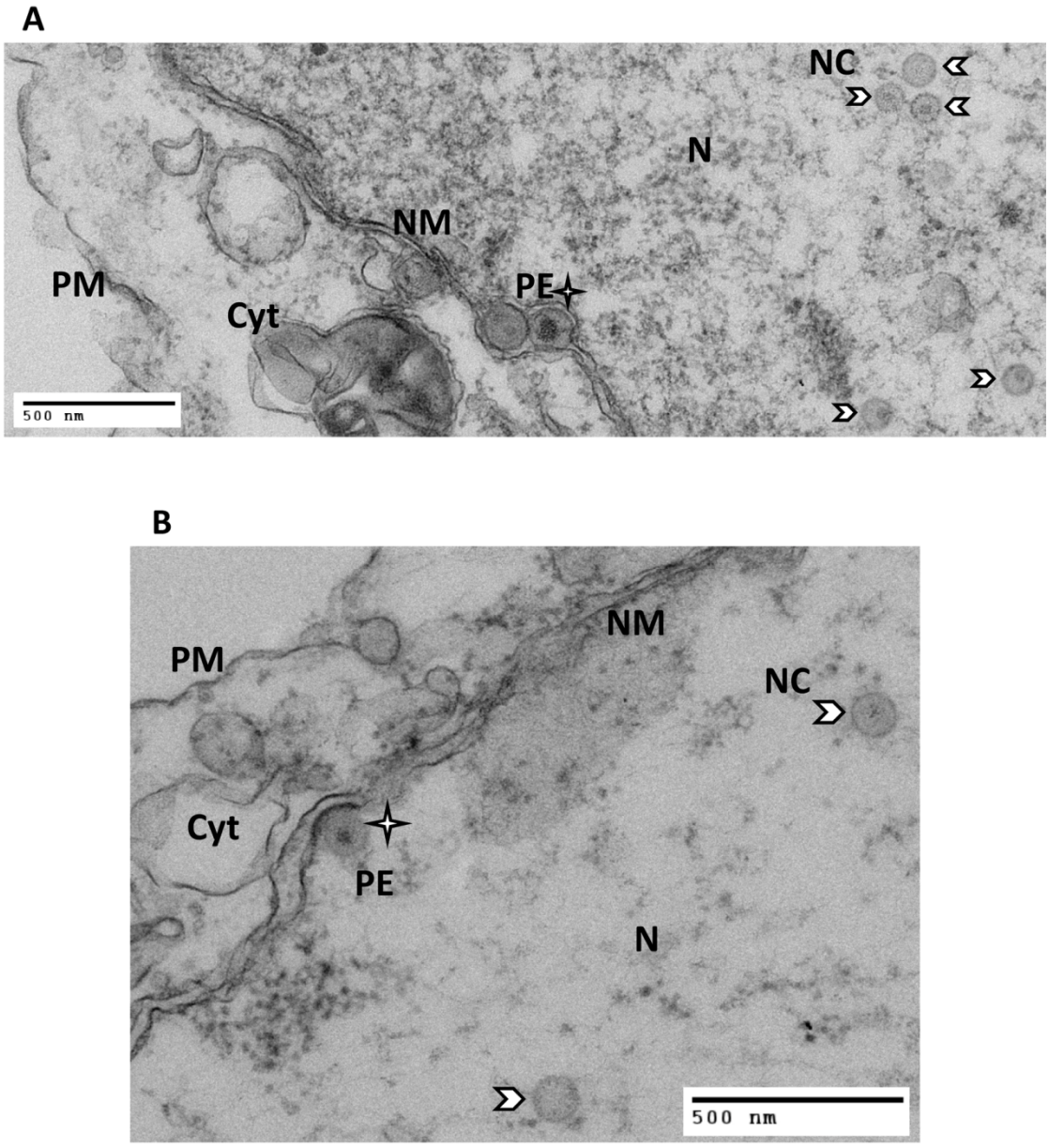

Figure 4.3: Ultrastructure of CHMP4A/B/C triple depleted cells infected with HSV-1. The samples were prepared as described in Figure 4.2. N: nucleus. NM: nuclear membrane. NC: nuclear capsid. Cyt: cytoplasm. PM: plasma membrane. CC: cytoplasmic capsid. ECV: extracellular virion. PE: primary envelopment. SE: secondary envelopment.

Figure 4.3

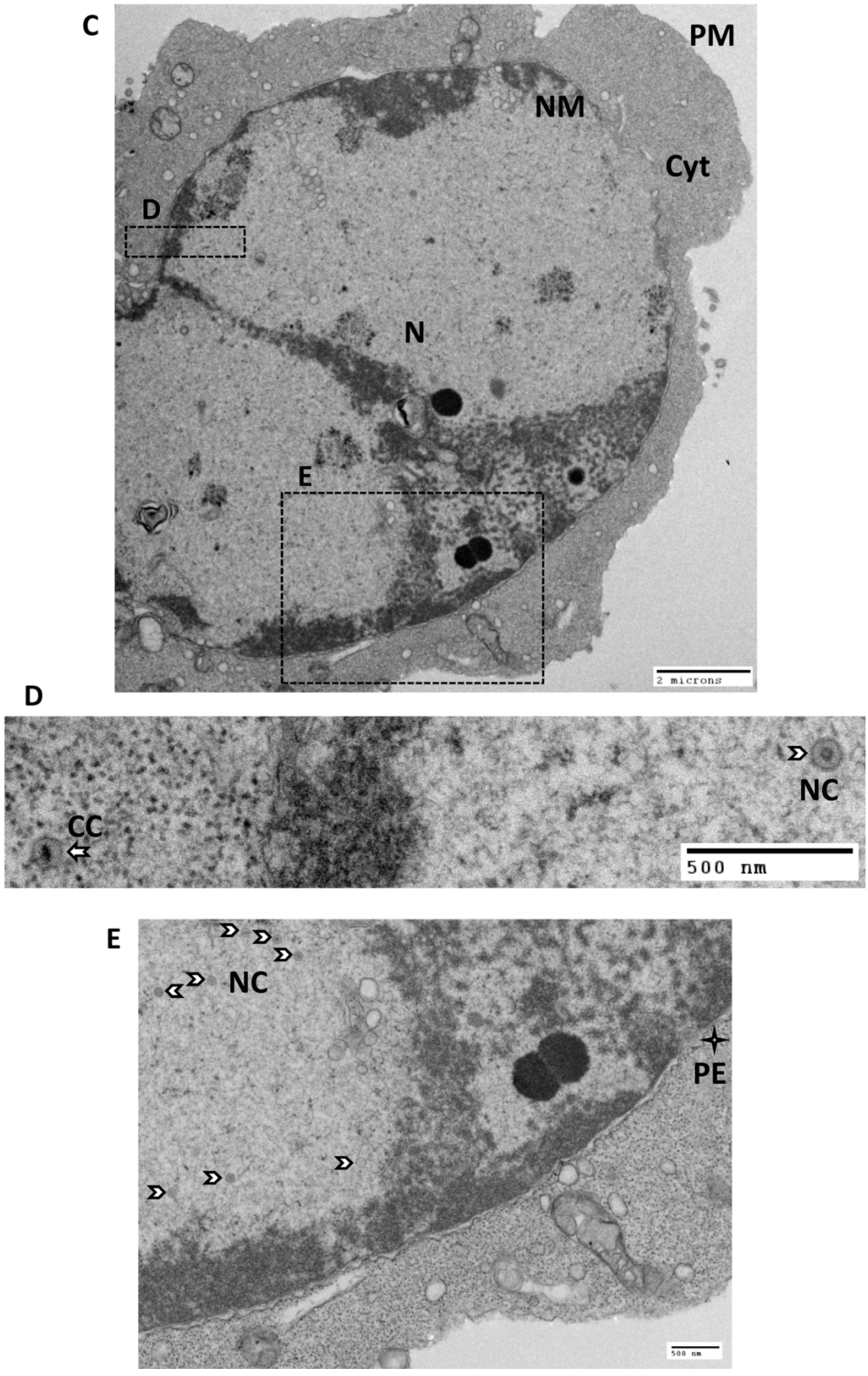

Figure 4.3

F

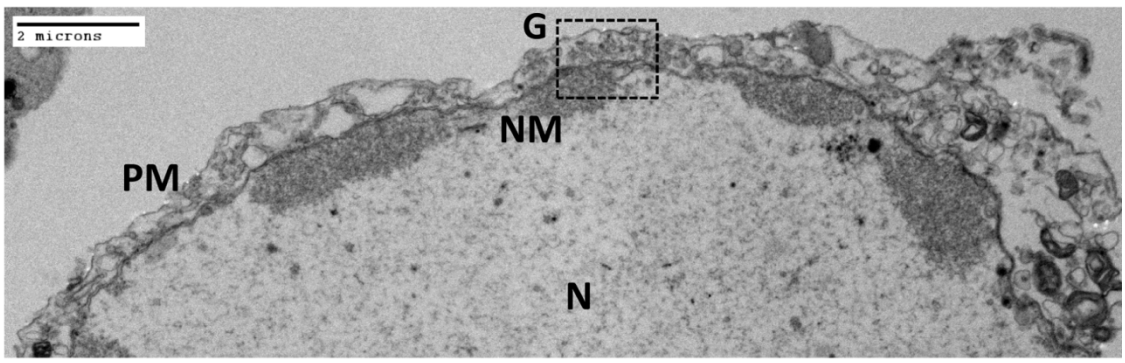

G

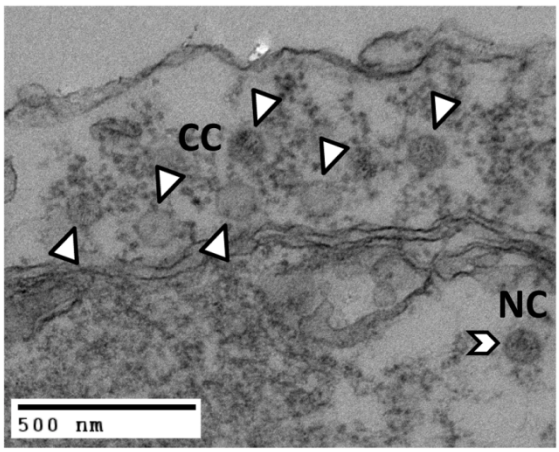

H

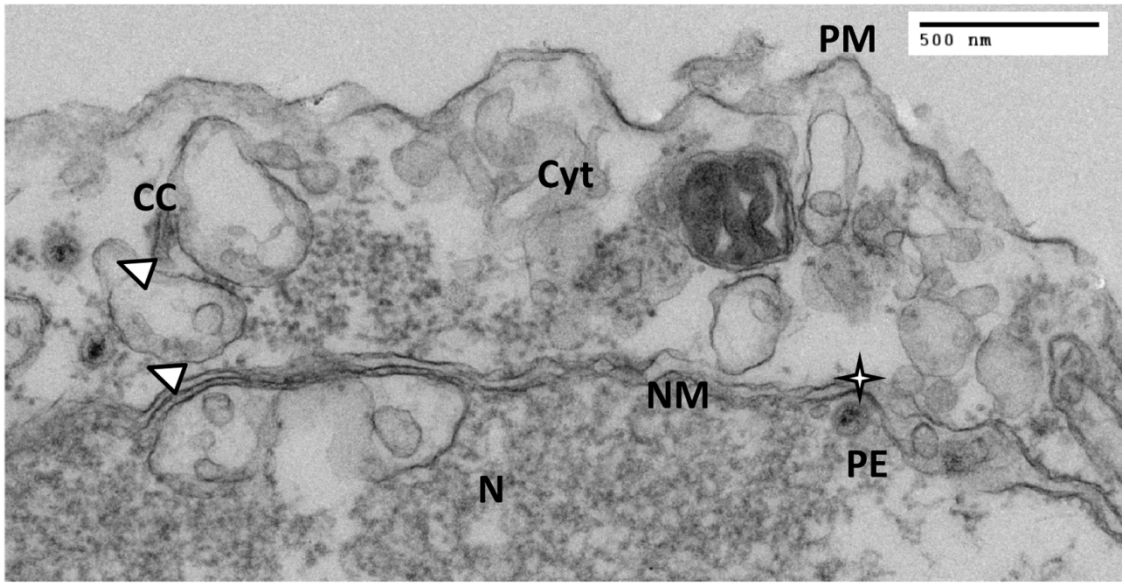

The infected cell samples were also examined by TEM. Figure 4.2 shows a representative image obtained from the ConX treated control sample demonstrating the nucleus (N), nuclear membrane (NM), cytoplasm (Cyt) and plasma membrane (PM). All stages of the viral replication cycles were observed in ConX siRNA treated cells including nuclear capsids (NC), primary envelopment (PE), secondary envelopment (SE) and extracellular virions (ECV) (Figure 4.2 A-E). The PE stages show the capsids in the cell nucleus enveloped by the inner nuclear membrane (Figure 4.2 A, D, E). The secondary envelopment stage is shown when the viral capsid has budded into a membrane compartment in the cytoplasm to form mature virus particles (Figure 4.2 C).

In the CHMP4A/B/C depleted cells, nuclear capsids and primary envelopment events could be readily observed, with examples of all three types of A, B and C capsids in the nucleoplasm (Figure 4.3 A, B, E). However, there was virtually no extracellular virus particles observed and no secondary envelopment events could be detected in the cytoplasm of infected cells. Furthermore, higher levels of free cytoplasmic capsids (CC) were observed in the CHMP4A/B/C depleted cells (Figure 4.3 C-H). These results suggest that the secondary envelopment of HSV-1 is inhibited in the absence of CHMP4A/B/C proteins while the early stages of the viral life cycle such as genome replication, capsid assembly and nuclear egress remain largely unaffected. Additionally, these data demonstrated that siRNA mediated depletion of endogenous CHMP4 function leads to a strong inhibition of HSV-1 replication, suggesting that depletion of cellular pathways utilised by HSV-1 to recruit CHMP4A/B/C using siRNA may demonstrate a similar phenotype.

4.2.2 The effect of CIN85 knockdown on HSV-1 replication

CIN85 is a Cbl-interacting protein which has previously been shown to interact with ALIX (Usami *et al.*, 2007). Thus CIN85 could indirectly link to the function of CHMP4A/B/C via ALIX. As described in Chapter 3, CIN85 showed interactions with pUL46, pUL47 and pUL49 in the yeast two-hybrid screen and the interactions with pUL46 and pUL49 were further validated in GST pull-down and protein co-localisation assays. In addition, the CIN85 specific antibody could co-immunoprecipitate tegument protein pUL49 (VP22) and pUL48 (VP16) in infected cell lysate. These data imply that there are direct interactions between CIN85 and HSV-1 tegument proteins in host cells during infection and HSV-1 could recruit CHMP4A/B/C by CIN85 via its interaction with ALIX.

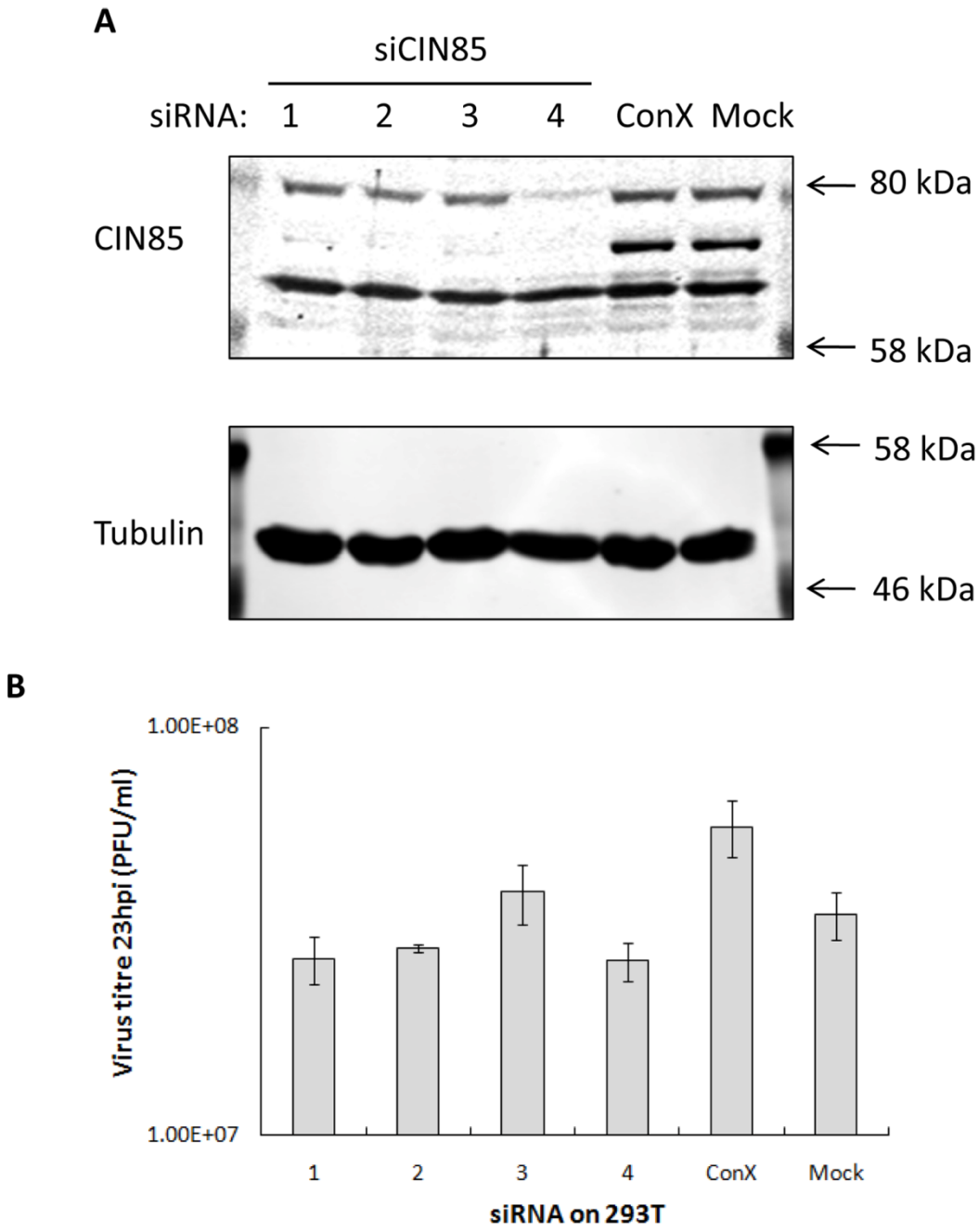

Figure 4.4: Effect of depletion of CIN85 by siRNA on HSV-1 replication. 293T cells were transfected with four independent siRNA oligonucleotides against the human CIN85 gene. The non-targeting siRNA ConX treated cells and mock transfected cells were used as controls. (A) Uninfected cell samples were harvested at 74 h post siRNA transfection and analysed by western blotting. Anti-CIN85 antibody was used to detect the CIN85 expression levels in the different treated samples. Tubulin signals were used for loading control. (B) Cells were infected by HSV-1 strain KOS at 10 PFU per cell at 72 h post siRNA transfection. Infected cells were harvested at 23 h post infection, sonicated and frozen-thawed once to release infectious progeny viruses. The infectious virus titres were determined by plaque assay on Vero cell monolayers. The mean titres and error bars of triplicate samples are shown.

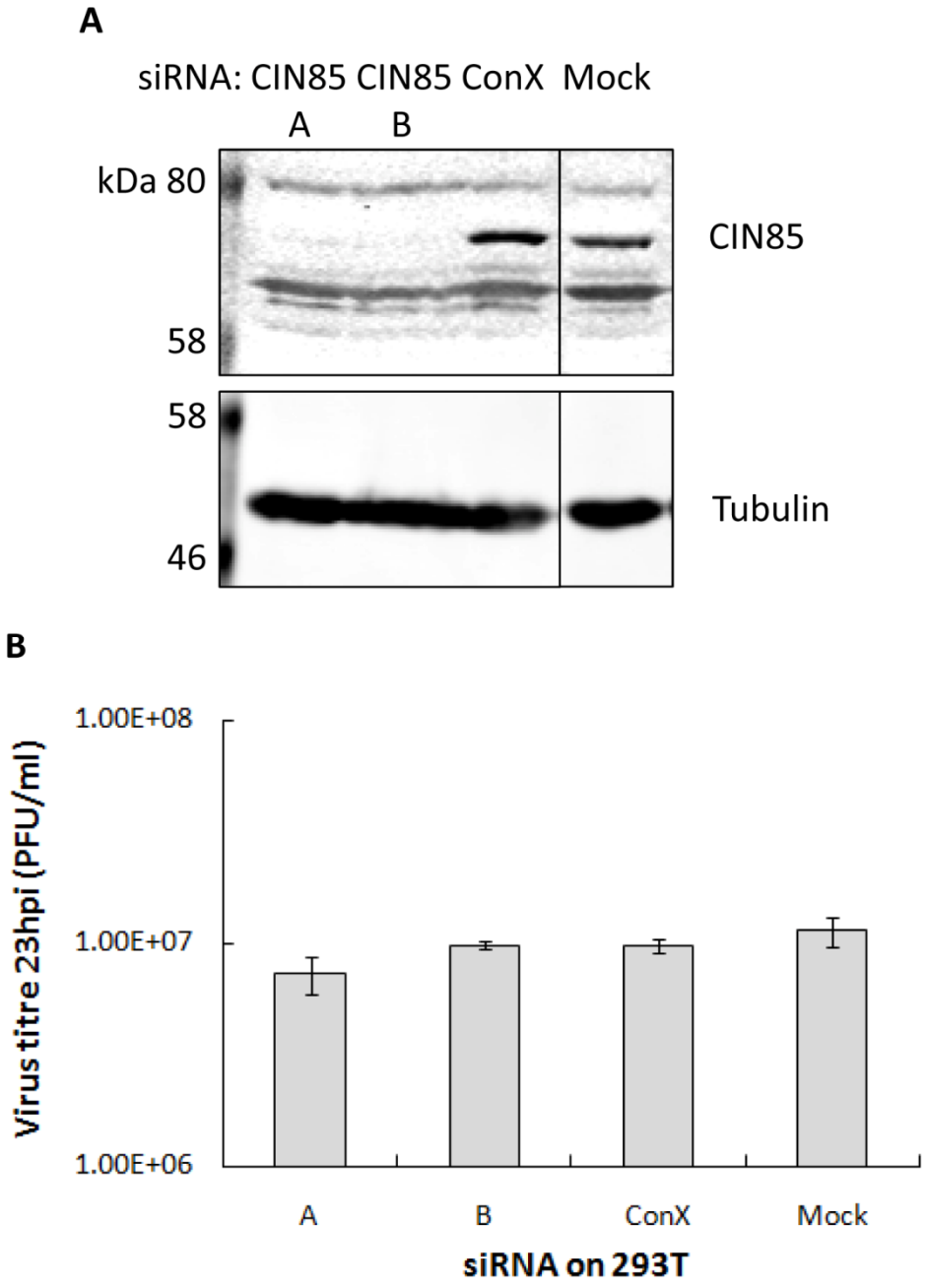

Figure 4.5: Effect of depletion of CIN85 by combined siRNA oligonucleotides on HSV-1 replication. 293T cells were transfected with a mixture of four siRNA oligonucleotides targeting CIN85. The non-targeting siRNA ConX treated cells and mock transfected cells were used as controls. (A) The endogenous CIN85 expression levels in different samples are tested by western blotting. The tubulin levels were used as the loading control. The signals were from the same blot but the irrelevant lanes were cut out. A and B indicate the duplicates of CIN85 siRNA treated samples. (B) Cells were infected by HSV-1 strain KOS and collected as described above. The average titres and error bars of triplicate samples are shown.

To further investigate the function of CIN85 in HSV-1 viral replication. siRNA was used to knockdown CIN85 expression in cells and infectious virus production was tested by plaque assay. Endogenous CIN85 expression was significantly depleted in 293T cells using any of the four individual oligonucleotides tested (Figure 4.4 A), while the expression levels of CIN85 in ConX and mock treated cells were comparable. The depletion of CIN85 caused little cytotoxicity as the tubulin levels in the samples were all similar (Figure 4.4 A). However, in CIN85 depleted cells the viral replication was at comparable levels to the control samples (Figure 4.4 B). Thus CIN85 depletion did not have a significant effect on HSV-1 replication.

According to the western blotting result shown in Figure 4.4 A, the expression of endogenous CIN85 is significantly inhibited in cells treated with single CIN85 siRNA oligonucleotide. However, it is conceivable that low levels of CIN85 protein remain in the cells which are not detectable by western blotting, and that these levels of CIN85 might be sufficient for the virus to recruit the ESCRT machinery efficiently. Single siRNA oligonucleotides only targets one region of a gene while the silencing efficiency could be improved by combining multiple siRNA oligonucleotides to target several regions of a specific gene. Thus the cells were treated with a mixture of the four individual CIN85 siRNA oligonucleotides and the virus production from these cells was tested. Similarly as single siRNA oligonucleotide treated samples, the expression level of CIN85 was efficiently depleted by the mixture of four siRNA oligonucleotides in two independent samples. The cells were viable and the tubulin levels in the different samples were equivalent (Figure 4.5 A). However, in the CIN85 siRNA mixture treated cells, the virus replicated as well as in the control cells (Figure 4.5 B). Thus transient silencing of CIN85 expression by single or multiple siRNA oligonucleotide(s) did not have a significant effect on HSV-1 replication.

4.2.3 HSV-1 replication in CC2D1A or CC2D1B depleted cells

In Chapter 3, CC2D1A showed interactions with HSV-1 tegument proteins pUL11, pUL16, pUL21, pUL46, pUL47 and pUL49. The interactions between CC2D1A and pUL16, pUL46, pUL47 and pUL49 have been validated by GST pull-down assays. CC2D1A has a homologous protein called CC2D1B, which shares ~50% amino acid identity with CC2D1A (Hadjighassem *et al.*, 2011). According to GST pull-down data, CC2D1B interacts with pUL16 and pUL47, although these interactions were not identified in the original Y2H assays. It has been reported that CC2D1A interacts with the CHMP4

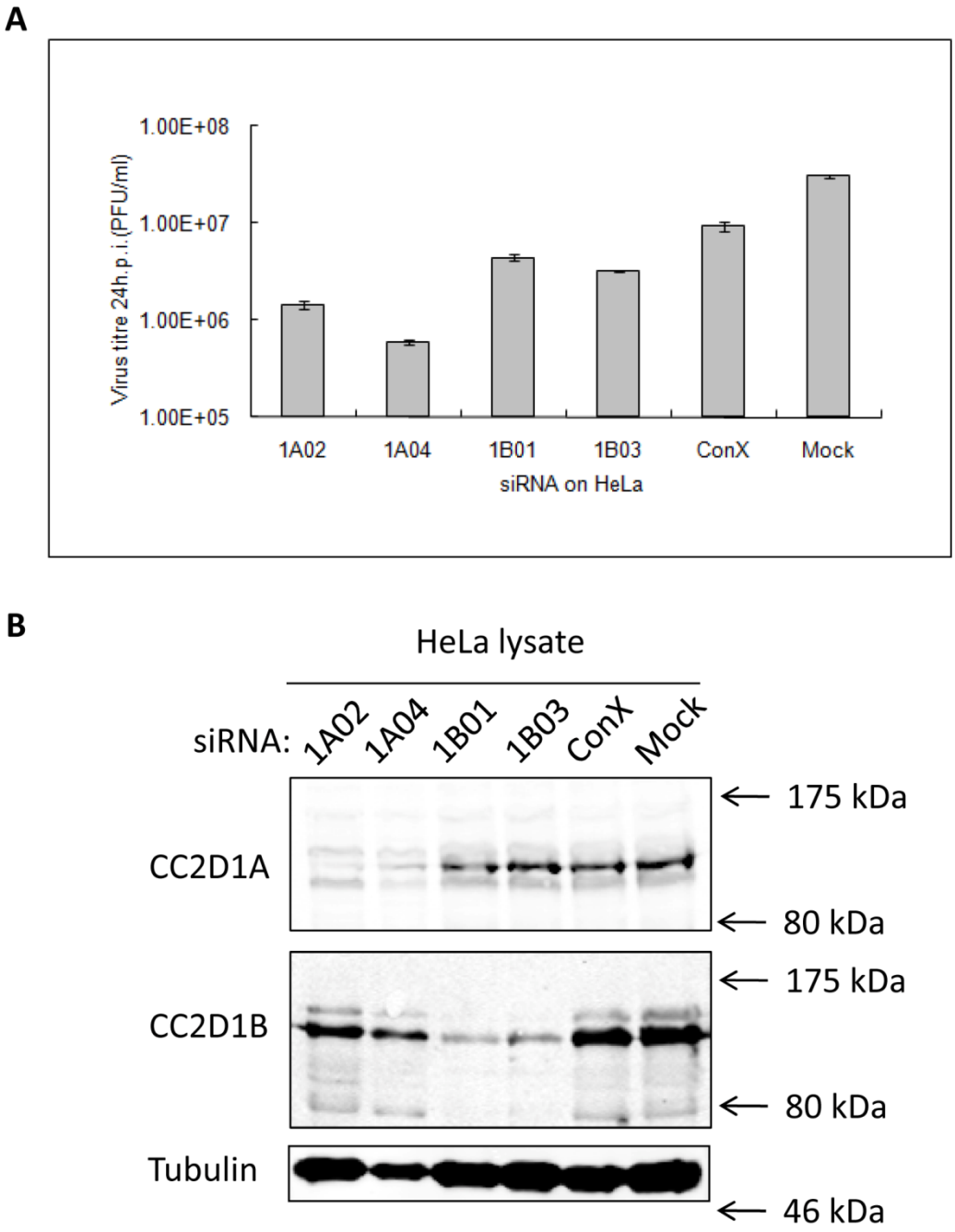

Figure 4.6: HSV-1 replication in HeLa cells with CC2D1A or CC2D1B depleted by siRNA. HeLa cells were seeded into six-well plates at 1 x 10^5 cells per well one day before siRNA transfection. The cells were transfected with siRNA oligonucleotides against CC2D1A (1A02 and 1A04), oligonucleotides against CC2D1B (1B01 and 1B03), the control siRNA ConX or mock treated. (A) The cells were infected with HSV-1 strain KOS at 10 PFU per cell at 66 h post transfection. At 24 hpi the infected cell samples were harvested and the progeny viruses were released by sonication. The infectious virus titres were determined by plaque assay on Vero cell monolayers. The mean titre and standard error bars from triplicate samples are shown. (B) Uninfected cell samples were harvested at 70 h post transfection for cell lysate preparation for western blotting. The endogenous expression levels of CC2D1A and CC2D1B are shown. The tubulin signals were used as a loading control and an indication for cell viability.

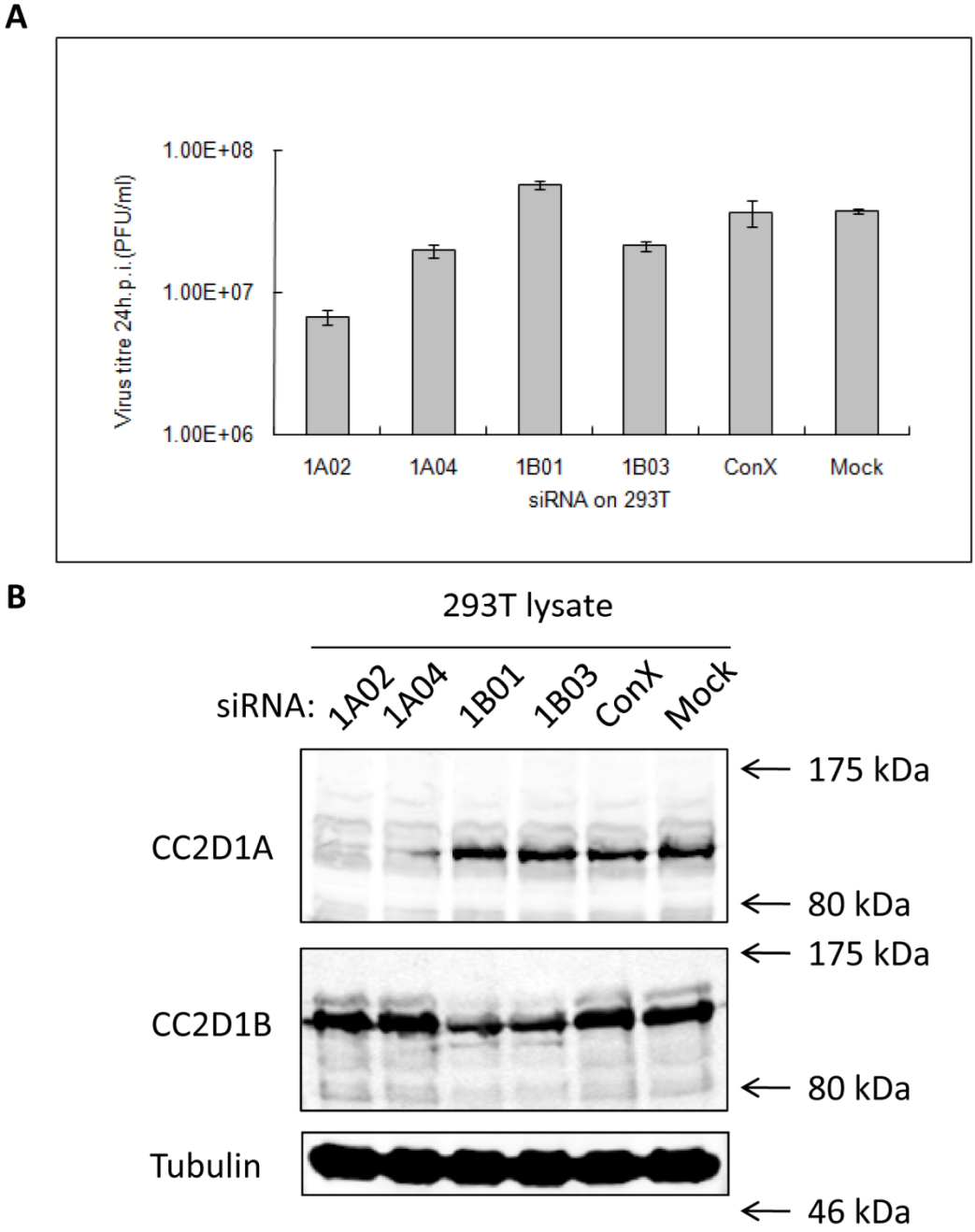

Figure 4.7: HSV-1 replication in 293T cells with CC2D1A or CC2D1B depleted by siRNA. 293T cells were seeded into six-well plates at 2 x 10^5 cells per well one day before siRNA transfection. The samples were treated and processed as described in Figure 4.6.

proteins of the ESCRT III complex (Tsang *et al.*, 2006), which implies that the virus may be able to recruit ESCRT III via the direct interaction with CC2D1A and/or CC2D1B. Therefore, the ability of HSV-1 to replicate in cells depleted of these proteins was investigated.

HeLa cells were transfected with two independent siRNA oligonucleotides against CC2D1A and CC2D1B respectively. The cell samples were infected with HSV-1 strain KOS at 10 PFU/cell at 66 h post transfection and harvested at 24 hpi. The infectious titres were determined by plaque assays on Vero cell monolayers. Cells treated with the CC2D1A siRNA 1A02 generated approximately 6-fold lower infectious virus particles compare to the ConX control, whereas the 1A04 treated cells produced a 16-fold lower viral titre. However, the depletion of CC2D1B from the host cells did not have a significant effect on virus replication compared to ConX treated cells (Figure 4.6 A). The efficiency of siRNA mediated protein depletion was analysed by western blotting. Both endogenous CC2D1A and CC2D1B were depleted in HeLa cells, although there were low levels of both proteins detected in the siRNA treated samples. The depletion level of CC2D1A appeared better than CC2D1B although the 1A04 oligonucleotide showed some level of cytotoxicity in HeLa cells as the tubulin signal was lower than the control samples (Figure 4.6 B).

Different cell lines may respond differently to siRNA in both protein depletion level and cytotoxicity. Therefore, similar experiments were also performed in 293T cells. The CC2D1A siRNA 1A02 treated cells generated about 5 fold lower infectious virus particles compared to the ConX control. However, the 1A04 treated cells demonstrated almost the same titre as the control (Figure 4.7 A, B). Similarly as in HeLa cells, the CC2D1B depletion did not have a significant effect on HSV-1 replication in 293T cells (Figure 4.7 A). According to the western blotting data, the depletion of CC2D1A by 1A02 oligo was as efficient as observed in HeLa cells, while the 1A04 oligonucleotide appeared to be less efficient in 293T cells than in HeLa cells (Figure 4.7 B). The depletion level of CC2D1B was not very efficient as there were still relatively high levels of signals detected from both 1B01 and 1B03 siRNA treated cells, although the levels were lower than the control samples (Figure 4.7 B). Different from HeLa cells, there was no significant cytotoxicity observed in 293T cells as the tubulin levels from all samples were similar to the controls (Figure 4.7 B). Due to the lower cytotoxicity and other siRNA experiments conducted with this cell line, 293T cells were chosen as the model for further siRNA analysis.

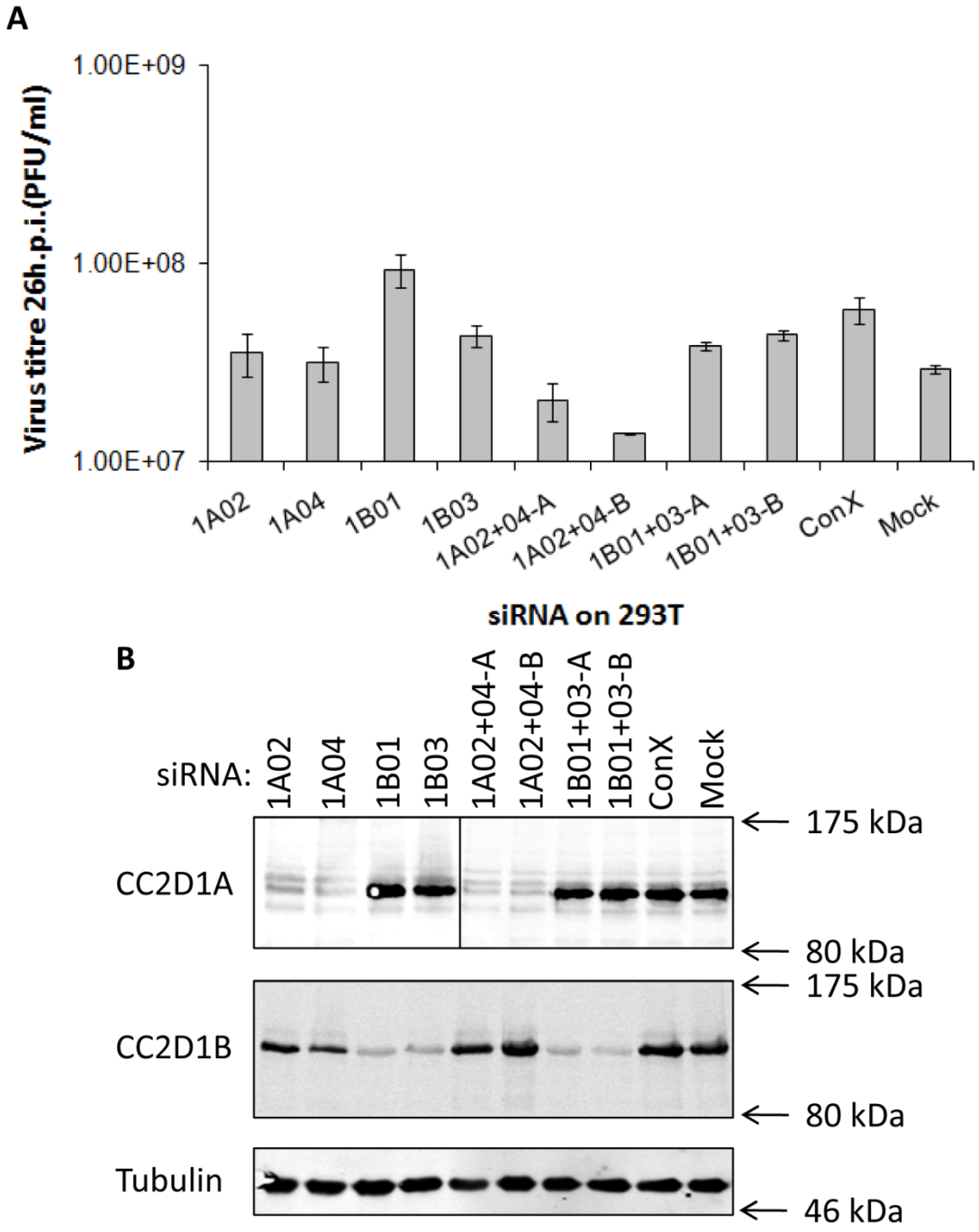

Figure 4.8: HSV-1 replication in 293T cells with CC2D1A or CC2D1B depleted using combined siRNA oligonucleotides. 293T cells were seeded into six-well plates at 2 x 10^5 cells per well one day before siRNA transfection of the stated combinations. Cells were infected with HSV-1 strain KOS at 10 PFU at 69 h post transfection. (A) The infected cell samples were harvested at 26 hpi and titrated on Vero monolayers. The mean titres and standard error bars of triplicate samples are shown. (B) Uninfected cell samples were harvested at 72 h post transfection for cell lysate preparation for western blotting. The endogenous CC2D1A and CC2D1B expression levels in the cell samples are shown, and tubulin was used as the loading control.

HSV-1 replication was also examined in cells with CC2D1A and CC2D1B depleted by a mixture of two siRNA oligonucleotides. Compared to the ConX treated control, the virus titres of CC2D1A single siRNA treated samples were about 2 fold lower (Figure 4.8 A, sample 1A02, 1A04), while the titres of the mixed CC2D1A siRNA treated samples were about 3-4 fold lower (Figure 4.8 A, samples 1A02+04-A/-B). However, there was little effect on viral replication when CC2D1B was depleted from the host cells (Figure 4.8 A). The depletion levels of CC2D1A and CC2D1B by single or mixed siRNA oligonucleotides were both efficient and similar according to the western blotting data (Figure 4.8 B). There was little difference in the levels of tubulin for any sample, indicating little or no cytotoxicity from any siRNA treatment (Figure 4.8 B).

The data described above suggested only minor effects on HSV-1 replication when depleting CC2D1A and virtually no effect when depleting CC2D1B. However, these experiments were performed with only a single round of siRNA transfection. In all the above cases, a certain level of CC2D1A or CC2D1B could be detected in the siRNA treated samples and it is conceivable that these low levels of endogenous protein could be sufficient for HSV-1 replication. Therefore similar experiments were performed in cells with prolonged depletion of CC2D1A and CC2D1B using two rounds of transfection with single (Figure 4.9 A, B) or combined (Figure 4.9 C, D) siRNA oligonucleotides. The cells with prolonged depletion of CC2D1A showed a three to five fold reduction in infectious virus production in cells treated with two rounds of siRNA 1A02 (Figure 4.9 A, sample 1A0202), or one round of 1A02 followed by a second round with 1A04 (Figure 4.9 A, sample 1A0204). However cells treated with two rounds of 1A04 (Figure 4.9 A, sample 1A0404), one round of 1A04 followed by 1A02 (Figure 4.9 A, sample 1A0402) or two rounds of the combined 1A02 and 1A04 (Figure 4.9 C, sample 1A02+04-A, B) showed very minor effects on HSV-1 titre, despite all CC2D1A siRNA treatment showing efficient depletions of the endogenous protein by western blotting (Figure 4.9 B, D).

Prolonged depletion of CC2D1B did not appear to significantly affect HSV-1 replication in any combination of siRNA treatment (Figure 4.9 A, C). However, while CC2D1B levels were efficiently reduced, the depletion of CC2D1B was not as robust as CC2D1A. Taken together, this data suggest that the prolonged depletion of CC2D1A or CC2D1B individually from host cells does not cause a significant inhibition of HSV-1 replication. Small effects on infectious viral production were observed when CC2D1A was depleted from the host cells. However, these observations were not always reproducible, although it is possible that there was a more efficient depletion of CC2D1A in the samples showing a

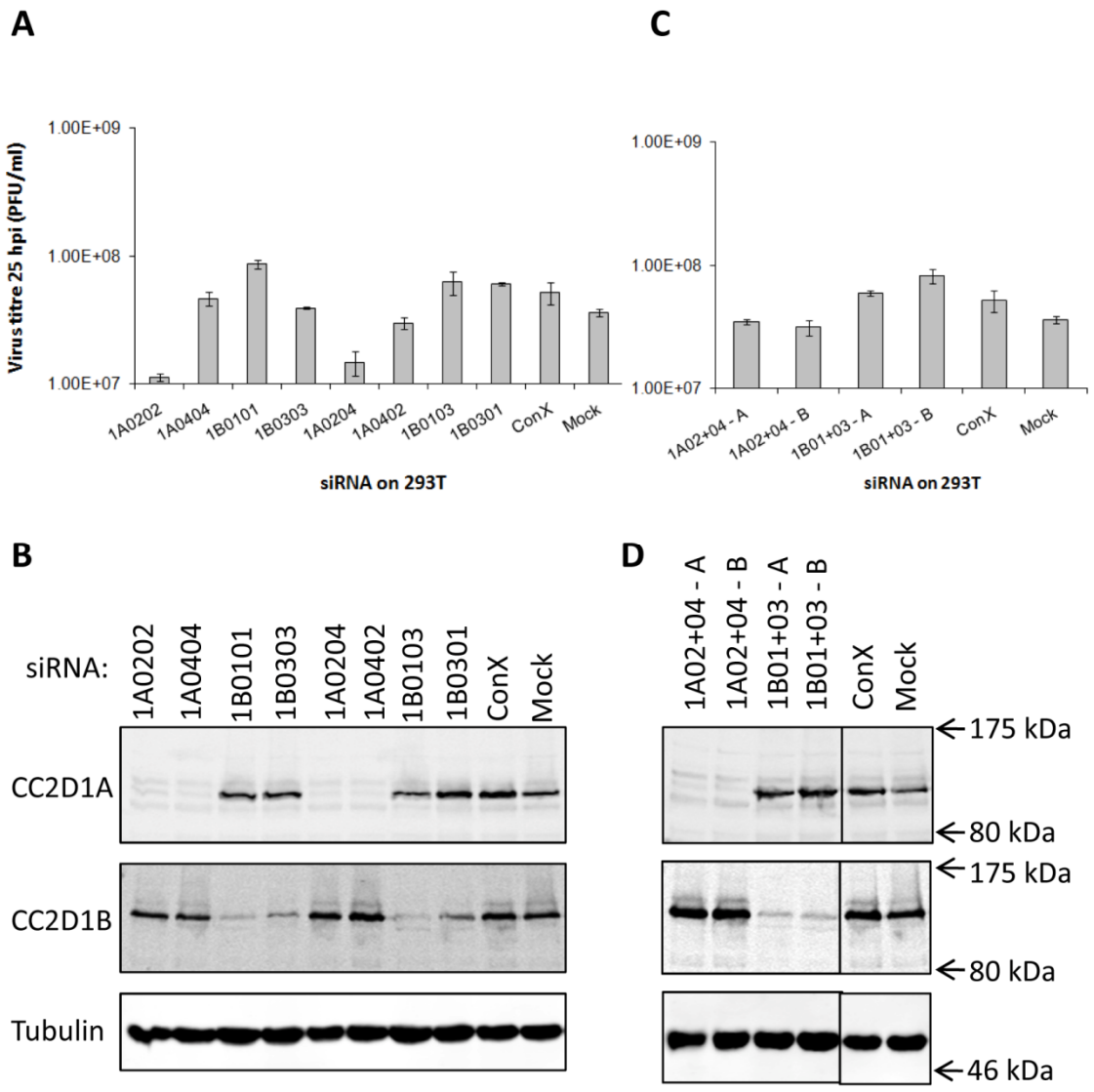

Figure 4.9: HSV-1 replication in 293T cells with prolonged depletion of CC2D1A or CC2D1B. 293T cells were seeded into six-well plates at 2 x 10^5 cells per well one day before siRNA transfection. The second siRNA transfection was performed 48 h post the first transfection. The cells were infected with HSV-1 strain KOS 48 h post the second transfection and the infected cell samples were harvested at 25 hpi for titration. The mean titres and standard error bars are all from triplicate samples. (A) Virus titres from cells treated with single siRNA oligonucleotide. The two rounds of siRNA transfections are indicated by the labels. For example, 1A0204 indicates the cells were transfected with siRNA oligonucleotide 1A02 for the first time and 1A04 for the second time. (B) The depletion levels of CC2D1A and CC2D1B were determined by western blotting. (C) Virus titres of cells treated with combined siRNA oligonucleotides as indicated by the labels. For example, 1A02+04-A and 1A02+04-B are duplicated samples of the same condition where cells were transfected with 1A02 and 1A04 siRNA oligonucleotide mixture twice. (D) The depletion levels of CC2D1A and CC2D1B by western blotting. The results are from the same blot with irrelevant lanes removed.

greater inhibition of HSV-1 replication, but this was not detectable due to insufficient sensitivity of the western blotting.

4.2.4 HSV-1 replication in cells depleted of multiple ESCRT associated proteins

The data presented in sections 4.2.2 and 4.2.3 has demonstrated that the single depletion of CIN85, CC2D1A or CC2D1B does not have a significant effect on HSV-1 replication. However, a direct interaction of the HSV-1 tegument protein with ALIX could serve as an alternative route for the recruitment of ESCRT III. The retrovirus HIV-1 has previously been shown to recruit the ESCRT machinery via an interaction of Gag with ALIX in a manner that was dependant on the ability of ALIX to bind to CHMP4 proteins. Despite the fact that depletion of ALIX has previously been shown to have no effect on HSV-1 replication (Pawliczek & Crump, 2009), it is conceivable that HSV-1 can make use of multiple redundant pathways to recruit the ESCRT III membrane scission machinery. Therefore it may be necessary to simultaneous deplete multiple ESCRT candidates in order to block the recruitment of ESCRT III by HSV-1, particularly the pathways capable of directly recruiting CHMP4A/B/C proteins.

Triple depletions of ALIX together with CC2D1A and CC2D1B, and CIN85 together with CC2D1A and CC2D1B, were performed to test whether inhibiting the CIN85/ALIX and CC2D1A/1B pathways in parallel could block HSV-1 replication. Surprisingly, virus titres produced by cells with either triple depletion were not reduced compared to the control cells (Figure 4.10 A). Western blotting was used to test the depletion levels of the proteins. The expression of the targeted proteins was significantly reduced although there was some detectable protein expression remaining in siRNA treated cells. This suggests the depletion was not efficient when three independent siRNA oligonucleotides were mixed, which results in a 3-fold lower concentration of each individual siRNA oligonucleotide (Figure 4.10 B). The tubulin signals from the control samples were lower than the triple depletion cells, which could have masked some effect of the triple depletion (Figure 4.10 B). Quantification data show there was 2-3 fold difference in tubulin between the samples and the controls (Appendix). Therefore, as the tubulin signals were relatively comparable, there is unlikely to be a significant difference due to this sample loading variation. Thus neither of the two triple depletion combinations appeared to block the ability of HSV-1 to recruit ESCRT III function. This suggests there may be some additional pathways for the virus to hijack the ESCRT machinery through other interactions.

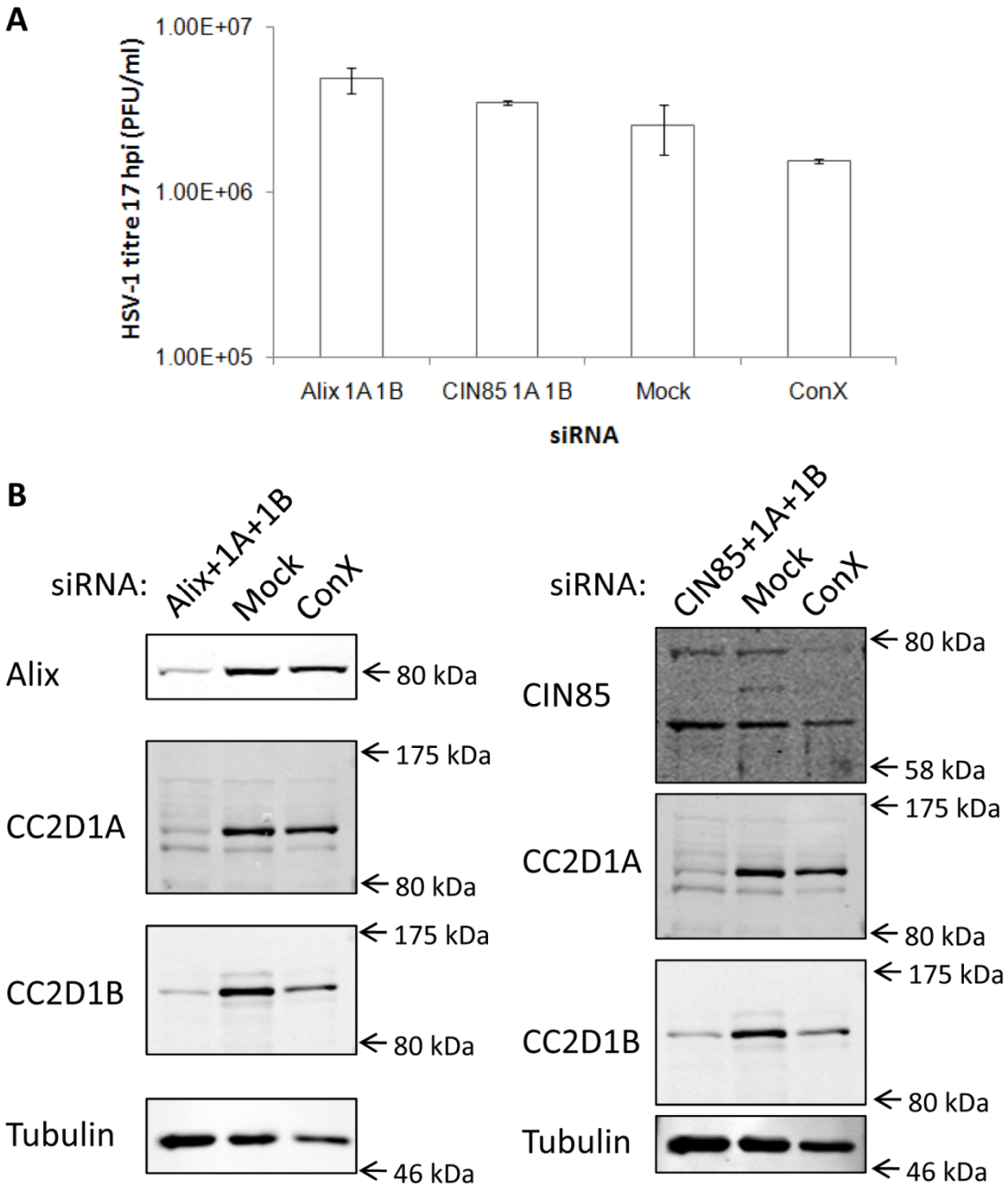

Figure 4.10: HSV-1 replication in cells with combined depletion of ALIX or CIN85 together with CC2D1A and CC2D1B. 293T cells were seeded into six-well plates at 2 x 10^5 cells per well medium one day before the first siRNA transfection. 24 h later, the cells were split into new plates and the second siRNA transfection performed 48 h post the first transfection. At 48 h post the second transfection, the cells were infected with HSV-1 strain KOS at 10 PFU/cell. Parallel uninfected cell samples were harvested for western blotting to test the depletion levels. (A) Mean virus infectious titres and standard error bars from triplicate samples are shown. (B) The endogenous protein expression levels in the cell samples. ALIX, CC2D1A and CC2D1B triple depleted cells were blotted with anti-ALIX, anti-CC2D1A and anti-CC2D1B antibodies. CIN85, CC2D1A and CC2D1B triple depleted cells were blotted with anti-CIN85, anti-CC2D1A and anti-CC2D1B antibodies. The tubulin signals were used as the sample loading control.

4.2.5 Construction of HSV-1 ΔUL47 and its replication in ESCRT depleted cells

4.2.5.1 HSV-1 ΔUL47 construction

HSV-1 tegument protein pUL47 (VP13/14) showed interactions with many ESCRT and ESCRT associate proteins in the initial Y2H screen presented in Chapter 3. Although some of the interactions appeared to be false positive (such as the interaction between pUL47 and CIN85), some interactions were confirmed by other methods (such as the interaction between pUL47 and ALIX). Although it has been previously reported that pUL47 is not essential for HSV-1 in tissue culture (Barker & Roizman, 1990; Zhang & McKnight, 1993), these results imply that pUL47 might be involved in multiple pathways for the recruitment of the ESCRT machinery by HSV-1. As demonstrated by the data in the previous sections of this chapter, viral replication was not significantly affected by single, double or triple depletion of certain ESCRT proteins, and so there are likely to be more redundant pathways for the virus to recruit the ESCRT machinery. All the potential interactions of pUL47 and ESCRT proteins would be inhibited by removing the UL47 gene from the viral genome. This should restrict the number of pathways available to HSV-1 to recruit the ESCRT machinery, and possibly make the virus more sensitive to the depletion of ESCRT proteins. Following this hypothesis, HSV-1 ΔUL47 virus was created by two-step red-mediated recombination to replace the UL47 gene with the tdTomato gene (Tischer *et al.*, 2010; Tischer *et al.*, 2006). Western blotting demonstrated that ΔUL47 infected cells, lack pUL47 expression while the viral capsid protein VP5 expression was at a similar level as in the WT virus infected cells (Figure 4.11 A). Viral plaques showed fluorescent signals of tdTomato in cells infected with ΔUL47 (Figure 4.11 B). In single-step viral growth curve analysis, the viral replication kinetics is similar and both the ΔUL47 and parental wild type viruses reached the plateau phase at around 14 hpi. However, ΔUL47 showed a small defect with an approximately 3-5 fold lower titres than the wild type virus at all time points (Figure 4.11 C).

4.2.5.2 Viral replication of ΔUL47 in ESCRT depleted cells

Double depletion of CC2D1A and CC2D1B

CC2D1A and CC2D1B are homologous proteins and they may share overlapping cellular functions. Therefore these proteins could have a certain level of redundancy between them and depletion of either CC2D1A or CC2D1B alone might not be sufficient to block the

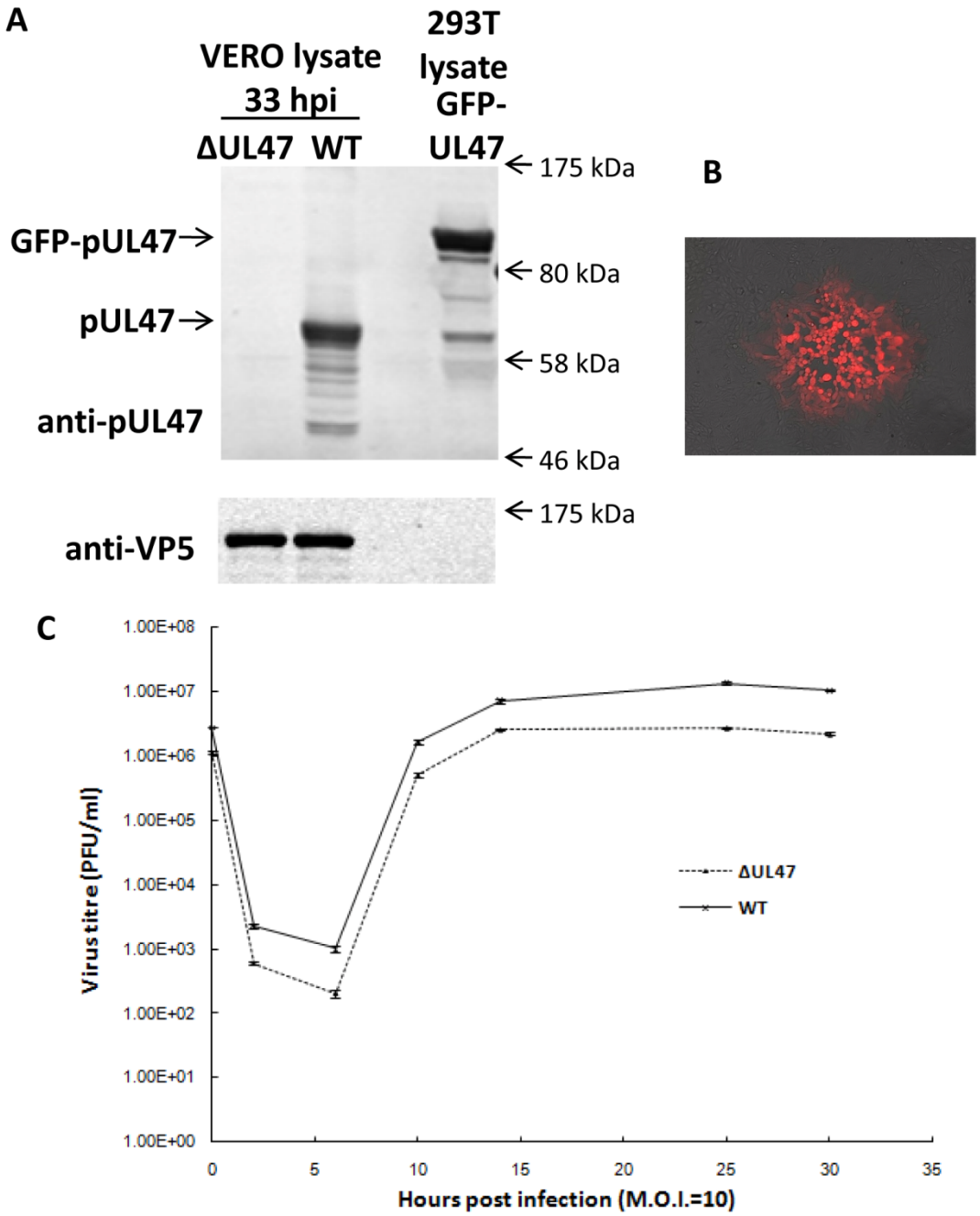

Figure 4.11: HSV-1 UL47 deletion virus. The UL47 gene was replaced by a similar sized reporter gene tdTomato in KOS BAC using two-step red-mediated recombination. (A) Vero cells were infected with either ΔUL47 or wild type KOS (WT) virus. At 33 hpi the cells were harvested and the pUL47 expression levels in host cell lysates were tested by western blotting. VP13/14 (pUL47) specific antibody was used and the lysate from 293T cells overexpressing GFP tagged pUL47 was used as a control. The HSV-1 major capsid protein VP5 signal was used as a loading control between the WT and ΔUL47 viruses. (B) A fluorescent virus plaque of ΔUL47 showing tdTomato expression in infected cells. (C) Single-step virus growth curve. Vero cells were infected with either ΔUL47 or WT virus at 10 PFU/cell at 37 ℃ for one hour. Unabsorbed viruses were inactivated by acid wash and the cells were incubated 37 ℃. At the time points shown cells were freeze-thawed and sonicated. The virus titres were determined by plaque assay on Vero cell monolayers. The mean virus titres and standard error bars are shown (n=3).

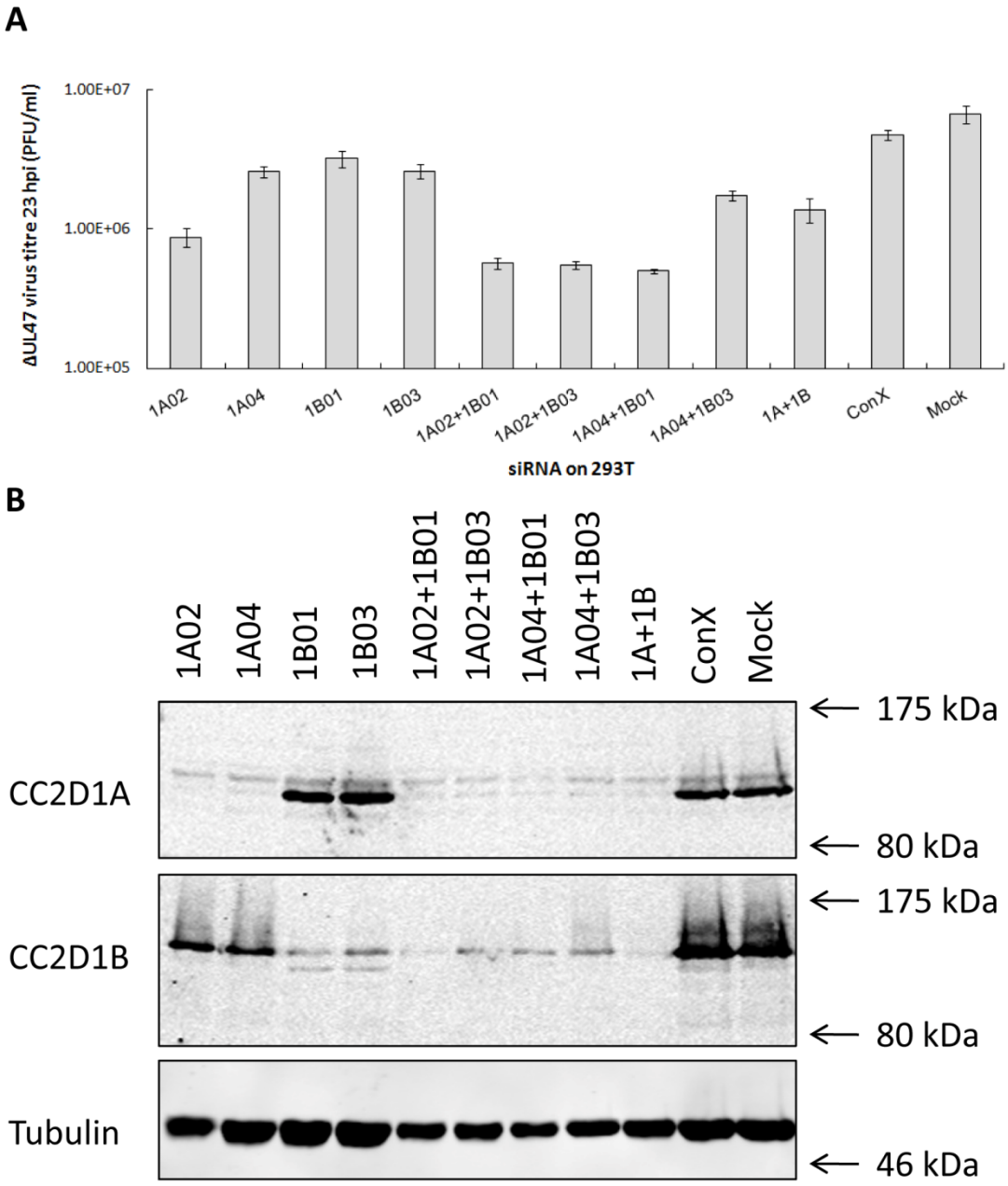

Figure 4.12: ΔUL47 replication in cells with combined depletion of CC2D1A and CC2D1B. 293T cells were seeded into six-well plates at 2 x 10^5 cells per well one day before the siRNA transfection. The siRNA oligonucleotides used for the 1A+1B sample were an equal mixture of 1A02, 1A04, 1B01 and 1B03. At 72 h post transfection, the cells were infected with HSV-1 virus at 10 PFU/cell. Parallel uninfected cell samples were harvested for western blotting to test the depletion levels of CC2D1A and CC2D1B. The infected cell samples were collected at 23 hpi and titrated on Vero cell monolayer. (A) Mean virus titres and standard error bars from triplicate samples are shown. (B) The depletion levels of CC2D1A and CC2D1B and the tubulin in the samples were determined by western blotting.

activity. Additionally, compared to wild type HSV-1, the mutant virus lacking pUL47 has less available pathways to recruit the ESCRT machinery. Therefore, the replication of ΔUL47 is more likely to be inhibited by the depletion of CC2D1A and CC2D1B. Thus simultaneous depletions of CC2D1A and CC2D1B from 293T cells were performed and the replication of ΔUL47 was investigated in these cells. The cells were treated with single or combined siRNA oligonucleotide(s) as indicated. The production of ΔUL47 from 1A02 treated cells was about 5-fold lower than the ConX siRNA treated control. 1A04 oligonucleotide treated cells and CC2D1B single depleted cells had similar virus productions compared to the controls. Virus titres from cells treated with combinations of CC2D1A and CC2D1B siRNA oligonucleotides were 3-9 fold lower than the ConX siRNA treated control. However the treatment of cells with 1A02 or double depletions showed varying levels of cytotoxicity according to the tubulin signals and so these data must be treated with caution (Figure 4.12 A). Nevertheless there was a consistent inhibition of HSV-1 ΔUL47 replication by silencing CC2D1A and CC2D1B together. Western blotting demonstrated efficient reductions in expression levels of these two proteins in siRNA treated cells compared to control cells (Figure 4.12 B). Overall these data suggest CC2D1A single depletion may have small effects on ΔUL47 replication, while the CC2D1A and CC2D1B double depletion has a synergistic effect on ΔUL47 replication. However, the inhibition of interactions related to pUL47 together with CC2D1A/1B did not entirely block the pathways for the virus to recruit the ESCRT machinery.

Triple depletion of CC2D1A/1B and CIN85

The removal of gene UL47 from the virus genome results in inhibiting of all the potential interactions between pUL47 and cellular proteins. However, ESCRT candidates such as CC2D1A/1B and CIN85 are still able to interact with HSV-1 via other tegument proteins. Thus in order to inhibit as many pathways as possible to block the viral recruitment of ESCRT by the tegument, combined siRNA depletion were performed to silence CIN85 together with CC2D1A/1B in cells and the replication of the ΔUL47 virus was analysed. Unfortunately, the triple depletion of CIN85 and CC2D1A/1B did not have a significant effect on HSV-1 replication. The production of both the wild type and ΔUL47 viruses from a single round of infection in the triple depletion cells was only approximately 2 fold lower than the controls (Figure 4.13 A). When compared to the wild type virus, ΔUL47 virus had lower virus yields (5-7 fold lower) from cells with or without siRNA depletion (Figure 4.13 A). Western blotting shows that CIN85, CC2D1A and CC2D1B were all depleted efficiently. The depletion of CIN85 was very efficient and there were no

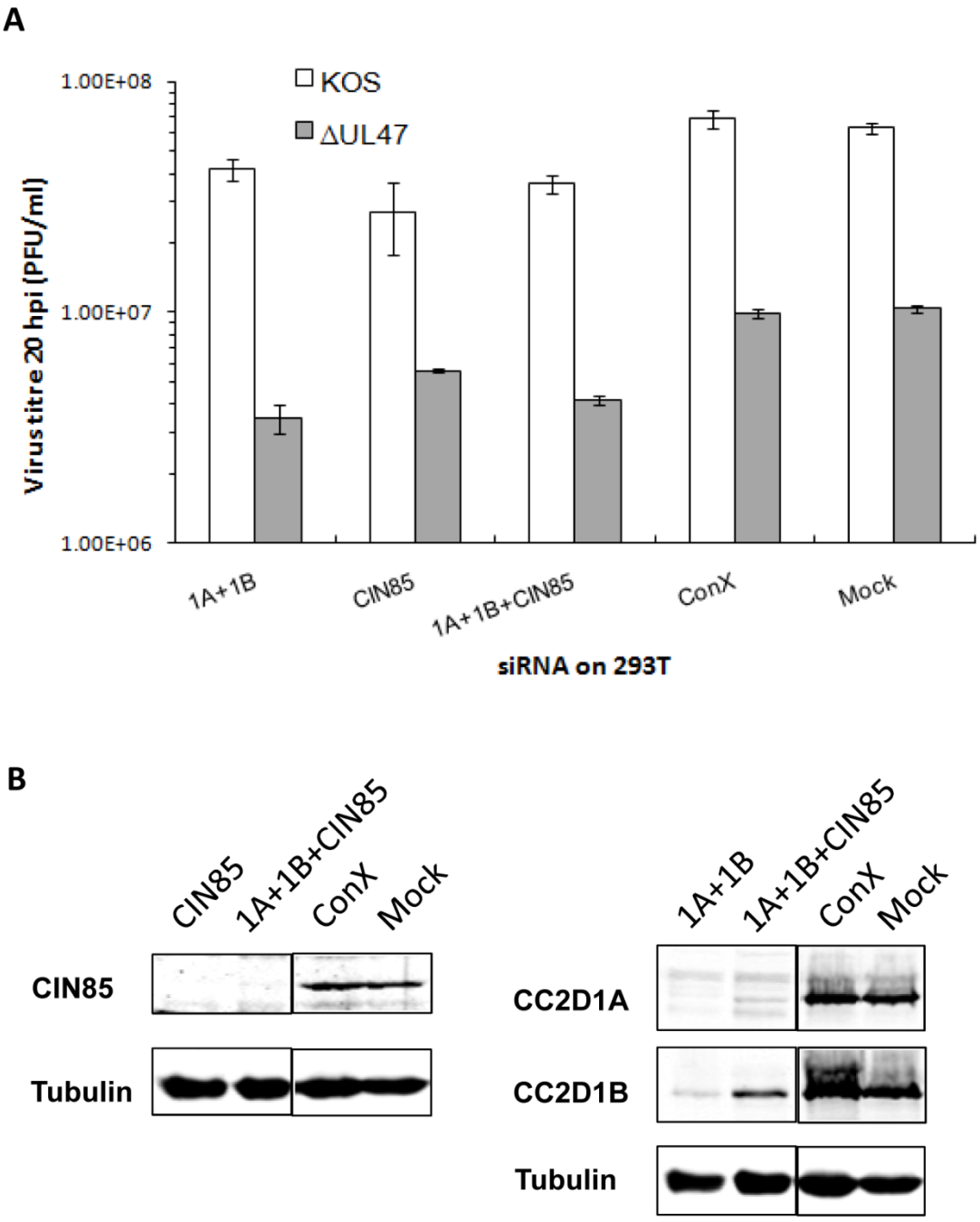

Figure 4.13: HSV-1 wild type and ΔUL47 viral replication in cells with CIN85 single depletion, CC2D1A/1B double depletion and CIN85, CC2D1A/1B triple depletion. 293T cells were transfected with two rounds of individual or combined siRNA as described before. The cells were infected with either wild type HSV-1 strain KOS, or the ΔUL47 virus at 10 PFU/cell. The infected cell samples were collected at 20 hpi and the titres were determined by plaque assays on Vero cell monolayers. (A) The virus titres of KOS or ΔUL47 infected samples. The mean virus titres and standard error bars are shown (n=3). (B) The protein depletion levels of CIN85, CC2D1A and CC2D1B. The tubulin signals were used as the sample loading control.

detectable signals of CIN85 from either the CIN85 single or triple depletion samples (Figure 4.13 B left panel). CC2D1A was also efficiently depleted in cells treated with siRNA targeting CC2D1A + CC2D1B, or CC2D1A + CC2D1B + CIN85, although a faint band was detectable in the triple depletion sample. However, the protein depletion levels of CC2D1B were not as efficient as the other two proteins, especially in the triple depletion cells, where there were relatively high levels of CC2D1B detected in the cell lysate, although they were lower than the control samples (Figure 4.13 B right panel). Thus the combination of removing pUL47 from the virus and the triple depletion of CIN85 and CC2D1A/1B from the host cell did not completely block the viral recruitment of the ESCRT machinery. However, it cannot be ruled out that the remaining protein expression in the triple depletion cells was sufficient to allow ESCRT III recruitment by HSV-1.

Depletion of CHMP6 and HD-PTP

Some other ESCRT recruiting pathways which may be hijacked by HSV-1 were also explored. CHMP6 belongs to the ESCRT III complex and can be the initiating event for the formation of CHMP4A/B/C filaments on membranes (Wollert *et al.*, 2009). Thus interaction between a HSV-1 viral protein and CHMP6 could play role in recruiting CHMP4A/B/C proteins. From the Y2H data, CHMP6 interacts with pUL47 and this interaction was confirmed by GST pull-down assay. Additionally, the ESCRT interacting protein HD-PTP shares structural similarities with ALIX and contains a Bro1 domain that can interact with CHMP4 isoforms. Therefore HD-PTP could be an alternative pathway for the virus to recruit CHMP4A/B/C although no interactions between HSV-1 tegument protein and HD-PTP were observed in Y2H assays. In order to study these alternative pathways for recruiting CHMP4A/B/C, replication of wild type and ΔUL47 HSV-1 were analysed in cells depleted of HD-PTP and HD-PTP together with CHMP6. In HD-PTP single depleted cells, both of the wild type and the ΔUL47 virus replicated to a similar level as in control cells (Figure 4.14 A). Thus HD-PTP single depletion did not affect HSV-1 replication. The virus yields from cells with double depletion of HD-PTP and CHMP6 were approximately 7 fold lower than the control cells. The reduction in virus production caused by HD-PTP and CHMP6 depletion for both the wild type and the ΔUL47 virus were similar. However, a certain level of cytotoxicity was observed when double depletion of CHMP6 and HD-PTP was performed. The tubulin level of this sample was lower than the controls (Figure 4.14 B), suggesting that the effect of double depletion of CHMP6 and HD-PTP on HSV-1 replication may be due to general cytotoxicity. Western blotting

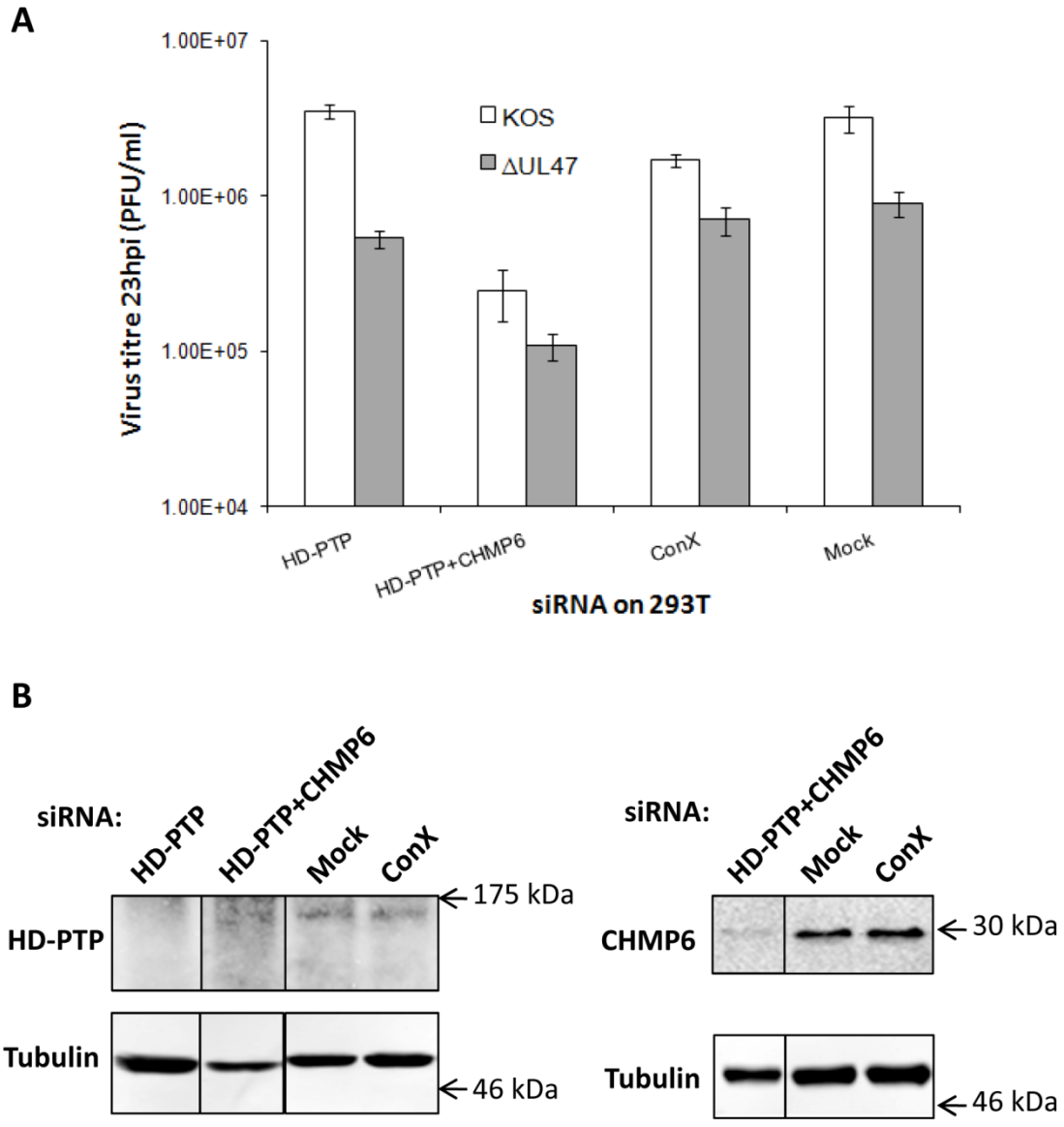

Figure 4.14: HSV-1 wild type and ΔUL47 viral replication in cells depleted of HD-PTP and CHMP6. 293T cells were transfected with one round of individual or combined siRNA as described before. The cells were infected with either wild type HSV-1 strain KOS, or the ΔUL47 virus at 10 PFU/cell. The infected cell samples were collected at 23 hpi and the titres were determined by plaque assays on Vero cell monolayers. (A) The virus titres of KOS or ΔUL47 infected samples. The mean virus titres and standard error bars are shown (n=3). (B) The protein depletion levels of HD-PTP and CHMP6 and tubulin levels were determined by western blotting.

demonstrated both CHMP6 and HD-PTP were depleted in siRNA treated cells, although the HD-PTP antibody gave poor signal levels (Figure 4.14 B).

Overall, there data suggest the removal of pUL47 from HSV-1 does not make the virus significantly more sensitive to the depletion of ESCRT and ESCRT associated proteins. However, ΔUL47 replication is somewhat attenuated compared to the wild type virus in tissue culture, which suggests that the loss of pUL47 causes defects in viral assembly. These defects may be due to the removal of the interactions between pUL47 and ESCRT and/or ESCRT associated proteins.

4.3 Discussion and conclusion

Depletion of all three isoforms of CHMP4 caused a dramatic reduction of HSV-1 infectious virus production by over 100 fold (Figure 4.1). These data further confirm the requirement of the ESCRT machinery in HSV-1 replication and indicate a specific function of CHMP4A/B/C. According to the ultrastructure observed by TEM, the formation of viral capsids in the nucleus was indistinguishable between CHMP4A/B/C depleted and control cells. This suggests that the initial stages of viral infection were not affected by the depletion of CHMP4A/B/C proteins, including the attachment to the cell surface, viral entry, capsid delivery and viral genome import to the nucleus, viral gene expression and capsid assembly. In addition, there were many primary envelopment events observed in the CHMP4A/B/C depleted cells, suggesting that nuclear egress of capsids was not affected by the removal of CHMP4A/B/C functions. The relatively high level of free capsid observed in the cytoplasm of CHMP4A/B/C depleted cells implies a defect in the secondary envelopment stage, which blocked the viral life cycle and inhibited the formation of mature virus particles. These data together with previous published work suggest that HSV-1 secondary envelopment requires the membrane scission activity of CHMP4A/B/C. Surprisingly no partially wrapped capsid structures were observed in the cytoplasm of CHMP4A/B/C depleted cells despite the fact that membrane associated capsids were observed in dominant negative VPS4 expressing cells previously (Crump *et al.*, 2007). However, it should be noted that dominant negative VPS4 expression inhibits the ESCRT machinery at a later stage than the removal of CHMP4 proteins, possibly explaining this discrepancy. Furthermore, capsids extensively associated with membranes were relatively rare in the cytoplasm of VPS4 dominant negative cells and may have been identified in CHMP4A/B/C depleted samples upon analysis of a greater number of cells.

Further experiment could be performed to examine the viral early and late gene expression in the CHMP4A/B/C depleted cells to further confirm the inhibition of the virus replication is not due to abnormal gene expression. In addition to comparing the tubulin levels, the cell viability under siRNA treat could be monitored by other methods, such as FACS.

The recruitment of CHMP4A/B/C to sites of viral assembly could be achieved via direct interactions between viral proteins and CHMP4A/B/C, or by interaction with other cellular proteins that bind CHMP4A/B/C. Several CHMP4A/B/C interacting proteins have been identified in mammalian cells and many have been shown to interact with HSV-1 tegument in this thesis. Therefore there are many potential pathways for HSV-1 to recruit this essential membrane scission machinery. Of these, CHMP6, ALIX, and CC2D1A/1B all directly interact with CHMP4A/B/C, while CIN85 may be able to recruit CHMP4A/B/C via the interaction with ALIX. The roles of each of these CHMP4 associated protein in HSV-1 replication was analysed by depleting the endogenous cellular protein by siRNA. The depletion of CIN85 did not have a significant effect on HSV-1 production, in agreement with previous reported data showing that the depletion of ALIX did not affect HSV-1 production (Pawliczek & Crump, 2009). Therefore the CIN85-ALIX-CHMP4A/B/C pathway is not essential for the viral replication in isolation. However, it may be one of multiple parallel pathways available to HSV-1 for the recruitment of CHMP4A/B/C.

Investigation of the homologous proteins CC2D1A and CC2D1B gave somewhat varying data. As shown in Chapter 3, the virion incorporation of CC2D1A is higher than that of CC2D1B, which indicates that more CC2D1A is associated with structural proteins of the virus than CC2D1B. Accordingly the result in this chapter suggest a greater role of CC2D1A than CC2D1B in HSV-1 replication with virus titres always being lower in CC2D1A depleted cells than CC2D1B depleted cells (Figure 4.6-4.9). However, the effects of CC2D1A depletions were always mild, and furthermore despite similar, CC2D1A in cells treated with two independent siRNA oligonucleotides (1A02 and 1A04) the viral replication was only reduced in one condition (1A02) (Figure 4.9, 4.12). This could suggest possible off-target effects of this siRNA oligonucleotide, although it cannot be ruled out that a more efficient depletion of CC2D1A was achieved with the siRNA 1A02 oligonucleotide treatment, but the enhanced depletion by this oligonucleotide could not be observed due to a lack of sensitivity of the western blotting assay. Despite the observed virion incorporation of CC2D1B, albeit of a low level, detected from the purified HSV-1

in Chapter 3, the depletion of CC2D1B did not show significant effect on HSV-1 production. This would suggest any role of CC2D1B in the viral replication as being dispensable or redundant.

Depleting multiple proteins simultaneously by combined siRNA treatment makes it possible to block several cellular pathways at the same time. However, the simultaneous depletion of ALIX or CIN85 together with CC2D1A and CC2D1B did not have an effect on HSV-1 production. However, in the simultaneous depletion assays, in order to keep the same total amount of siRNA, each individual siRNA oligonucleotide amount was reduced. Thus in the combined siRNA treated samples, the depletion of individual protein was usually not as efficient as in the single siRNA treated cells. Therefore, the lack of effect on HSV-1 could have been due to the residual level of the targeted proteins remaining in the cells.

In addition to ALIX, CC2D1A/1B and CHMP6, other cellular proteins containing Bro1 domains, such as HD-PTP, are known to interact with CHMP4 proteins, and so HD-PTP was also investigated. The simultaneous depletion of CHMP6 and HD-PTP had a small effect on HSV-1 replication, suggesting these are also possibly pathways for the recruitment of CHMP4 by HSV-1. It would be interesting to test whether the simultaneous depletion of ALIX, CHMP6 and HD-PTP affects the HSV-1 replication. However, when inhibiting these three pathways, there are still CC2D1A and CC2D1B to be considered, which may be sufficient to enable the virus to recruit CHMP4A/B/C proteins. Therefore, depletion of all five cellular proteins may be necessary to inhibit HSV-1 replication. However, it is virtually impossible to achieve with current technology.

Among the siRNA combinations tested, only the triple depletion of the ESCRT-III CHMP4A, CHMP4B and CHMP4C proteins strongly inhibited HSV-1 replication, while other siRNA single or combined depletions only demonstrated mild or insignificant effects on HSV-1 replication. These data suggest that HSV-1 virus employs many parallel pathways to hijack the ESCRT machinery and specifically the CHMP4A/B/C components. However, among the combined double or triple depletion siRNA experiments, the efficiency of depletion of each individual protein is lower. It is not known what amount of each cellular protein is required for activity in HSV-1 infected cells. Hence in the cases of mild or insignificant effect, it is difficult to fully assess the inhibition of functions of those proteins.

In order to inhibit as many potential parallel pathways as possible, mutant virus lacking certain viral proteins could be another strategy in addition to the siRNA depletion. From the data presented in Chapter 3, the tegument protein pUL47 showed many potential interactions in the yeast two-hybrid screen, thus a ΔUL47 virus was created to inhibit those potential pUL47 related interactions. However, as shown in Figure 4.13 and 4.14, this mutant virus was no more sensitive than the wild type virus to the depletions of ESCRT protein(s) that have been tested. This result suggests that, apart from the interactions of pUL47 and the depleted cellular proteins, there are likely to be even more pathways for the virus to recruit the ESCRT machinery.

Further work could be carried out to try to remove more non-essential tegument proteins, such as pUL11, pUL16, pUL21, pUL46 or pUL49, from the virus to inhibit further pathways for the viral recruitment of ESCRT. This strategy could be combined with depletion of ESCRT associated proteins to attempt to block the viral replication. However, it is possible that there are yet further redundant pathways to recruit ESCRTs by essential tegument proteins, such as VP16 and VP1/2. These essential proteins cannot be removed from the virus without complementing cell lines in order to grow virus stocks increasing the difficulty of studying the effect of any cellular proteins that may interact with these tegument proteins on the viral replication. During the initial Y2H screening, the major tegument protein pUL36 (VP1/2) showed potential interaction with TSG101, which could be another additional pathway for HSV-1 to recruit the ESCRT machinery, although viral replication has been reported to be insensitive to TSG101 depletion (Pawliczek & Crump, 2009). Furthermore, HSV-1 VP1/2 contains two PTAP ($PSAP_{390}$, $PTAP_{2828}$), one YPXL ($YPYL_{221}$) and one PPXY ($PPTY_{2867}$) type late motifs, and another essential tegument protein VP16 also contains a PPXY ($PPLY_{38}$) motif. These motifs could potentially interact with ESCRT proteins in a similar way to retroviral Gag protein for recruiting the ESCRT-III membrane scission machinery. In addition, siRNA transient knockdown of cellular proteins may have short-comings for studying the function of the proteins involved, as any residual protein might be sufficient for the function, especially when multiple proteins need to be targeted simultaneously. Furthermore, it is often technically not possible to simultaneously knockdown many cellular proteins at the same time without affecting cell viability.

Although informative, it must be taken into account that the data presented in this chapter is analysis of HSV-1 replication in cell culture. It is clear from many studies that highly conserved viral proteins are often dispensable for replication in cell culture, but they are

essential *in vivo*. Therefore it would be intriguing to analyse HSV-1 replication in transgenic mice lacking certain ESCRT or ESCRT associated protein to investigate the relative importance of these multiple pathways of ESCRT recruitment HSV-1 appears to have evolved using the *in vivo* model systems.

In this chapter, several possible pathways for the virus to hijack ESCRTs were explored. According to the data presented, we hypothesised that HSV-1 has evolved multiple parallel pathways to hijack the ESCRT machinery. All of these pathways presumably converge on the recruitment and activation of the CHMP4A/B/C proteins because the simultaneous depletion of CHMP4A/B/C from host cells significantly inhibited HSV-1 replication (Figure 4.15).

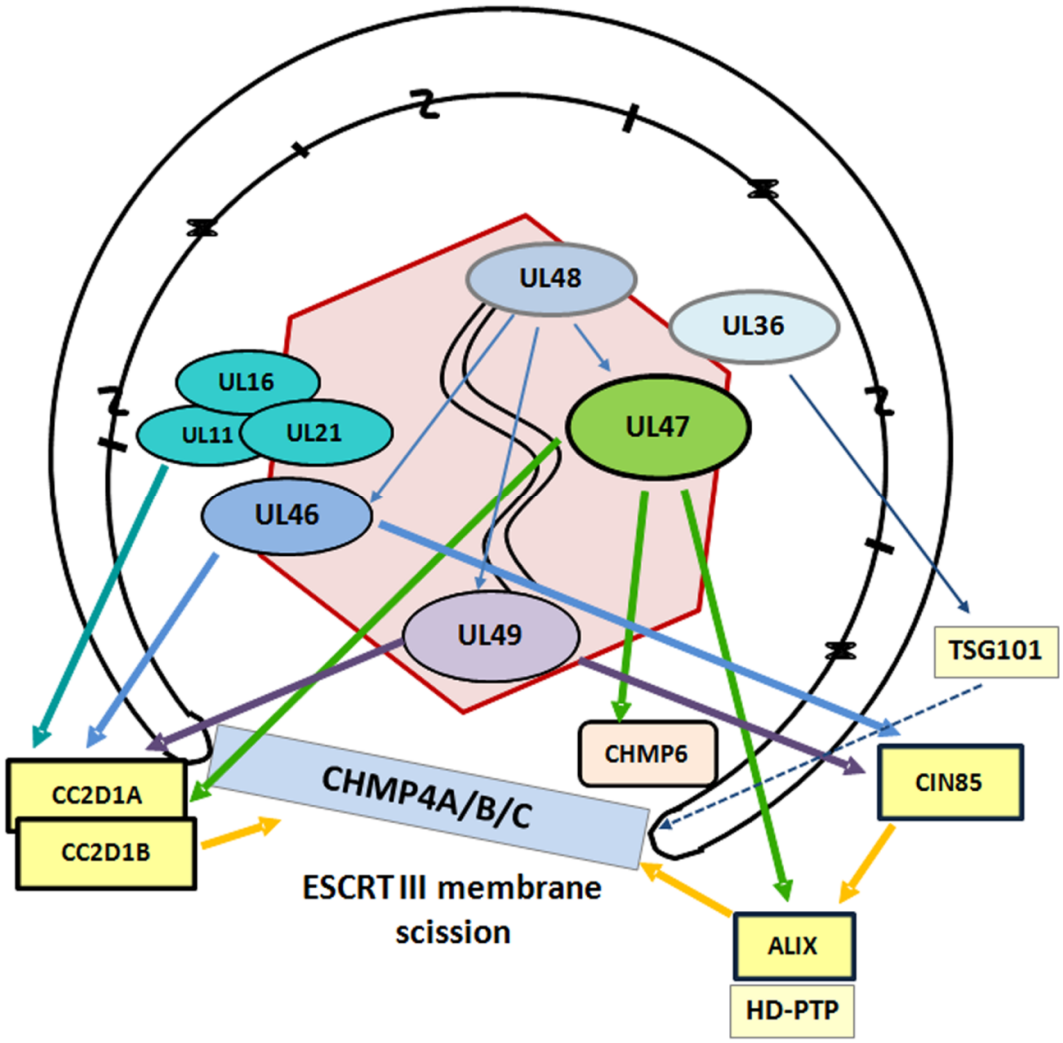

Figure 4.15: Diagram of HSV-1 secondary envelopment and the potential recruitment of ESCRT machinery.

5 Discussion and Future Work

5.1 Glycoprotein M

5.1.1 Phenotypes of previous published alphaherpesviruses with gM deletion

In PRV, deletion of gM resulted in replication to approximately 50-fold lower titres, smaller plaques and reduced penetration kinetics (Brack *et al.*, 1999; Dijkstra *et al.*, 1996; Kopp *et al.*, 2004). Simultaneous deletion of gM together with the gE/gI complex or UL11 caused severe defects in viral replication with large accumulations of unenveloped capsids in the cytoplasm suggesting a partially redundant or synergistic role for gM in secondary envelopment (Kopp *et al.*, 2004; Leege *et al.*, 2009). Similarly to PRV, simultaneous deletion of gM and UL11 in HSV-1 strain KOS showed much more pronounced defects in viral growth, plaque size and cytoplasmic assembly, suggesting a synergistic role of gM and UL11 in HSV-1 cytoplasmic assembly (Leege *et al.*, 2009). Deletion of gM in EHV-1 caused an approximately 100-fold reduction in viral titres, smaller plaques, reduced penetration kinetics and defects in secondary envelopment (Osterrieder *et al.*, 1996; Seyboldt *et al.*, 2000). Deletion of gM in EHV-4 also caused large reductions in virus replication and plaque size, although only a marginal delay in penetration and no obvious defects in cytoplasmic envelopment were observed (Ziegler *et al.*, 2005). In BHV-1, deletion of gM caused delayed penetration of virions into cells, impaired release of infectious virus and smaller plaques (Konig *et al.*, 2002). In VZV, deletion of gM was also shown to cause reductions in plaque size and cell to cell spread (Yamagishi *et al.*, 2008). Taken together, all these gM deletion studies suggest a role for gM in penetration/cell-cell spread and the efficient production of infectious virus particles, as well as with a possible redundant role in the cytoplasmic envelopment process. Data presented in this thesis are in agreement with the reported data of replication kinetics, plaque size and penetration rate. Furthermore, the observation of the impaired incorporation of gH/L into mature virions provides an explanation for defects in penetration.

5.1.2 HSV-1 glycoprotein incorporation during secondary envelopment

As a large and complex virus, the assembly of a mature virion involves more than fifty viral proteins of which sixteen are transmembrane proteins. All of these proteins need to be localised at the correct site for virion incorporation and cellular mis-localisation of these membrane proteins could result in defects in incorporation, and virus particles that have obtained immature envelope proteins during secondary assembly may be defective. It is currently unknown that whether the viral glycoproteins need to be transported to the plasma membrane and then internalised for virion incorporation, or they can be incorporated during the secretion when newly synthesised, or a combination of both. The virus has an advantage to have secondary assembly at early endosomal related membrane structures, as the membrane proteins are expressed at different time and modified at different rates and an endosomal compartment could be a better site to accumulate different mature proteins as they may rapidly exit the TGN. Furthermore, the recycling endosomes may be more likely than early endosomes to be involved in the secondary envelopment. In addition, there are perhaps some virus induced hybrid endosomes-like compartments which could be potential sites for secondary envelopment.

Data presented in Chapter 2 have demonstrated that in the absence of gM, the incorporation of gH/L into HSV-1 virions was impaired. However, certain low levels of gH/L are still incorporated and the production of infectious particles were only mildly affected according to the single-step grow curves (Figure 2.4 and 2.7). Since the internalisation of gH/L is considerably inhibited due to the loss of gM function, this result suggests that gH/L may be incorporated into the virion during the secretory pathway before arrival at the plasma membrane, although at a reduced level.

5.1.3 Viral proteins with potential redundancy with gM

Both gD and gH/L complex are essential envelope proteins and yet do not contain known cellular targeting motifs. Presumably, the efficient targeting of these envelopes relies on the function of other viral proteins. Previously reported data from the laboratory have demonstrated that gM is able to relocalise both gD and gH/L from the plasma membrane to interacellular TGN-like compartments in transfection assays (Crump *et al.*, 2004). Data presented in this thesis has shown that in the absence of gM the internalisation of gH/L from host cell surface was inhibited and the gH/L in purified virions decreased. However, in the absence of gM, the cellular localisation and virion incorporation of gD were not

affected. One possible explanation for this phenotype of gD is that there may be gM independent mechanisms in controlling the localisation of gD. Other viral type III membrane proteins including gK/UL20 and pUL43 may possibly play a similar role as gM. These are the only other type III membrane proteins expressed by HSV-1 and, similarly to gM, they have been shown to inhibit cell-cell fusion induced by the viral entry proteins of HSV-1 or PRV (Avitabile *et al.*, 2004; Klupp *et al.*, 2005). These data suggest that gK/pUL20 and pUL43 may also be able to remove viral glycoproteins from the cell surface and could potentially localise them to virus assembly sites. Another possible reason could be that in HSV-1 lytic infection the internalisation mediated by other viral proteins targeting gD to the viral assembly site is dispensable due to the large quantities of gD being synthesised, which could saturate all the compartments of the secretory/endocytic pathways.

5.1.4 Early involvement of gM in the nuclear membrane

It has been previously shown that when expressed in transfection assays, gM is mainly localised at TGN (Crump *et al.*, 2004). Interestingly, HSV-1 gM has been shown to localise to the nuclear membrane, particularly to large invaginations in the nuclear membrane at early times post infection, and also to be present in primary enveloped particles (Baines *et al.*, 2007a; Zhang *et al.*, 2009a). These data suggest a possible role for gM in primary envelopment, although details of what function gM may have during this stage of HSV-1 assembly are currently unknown. Given recent data showing a role of gH/L or gB, in the fusion of primary enveloped particles with the outer nuclear membrane, this raises the intriguing possibility of gM-mediated targeting of glycoproteins (especially gH/L) to the nuclear membrane (Farnsworth *et al.*, 2007).

5.1.5 gM and pUL49.5

It has been demonstrated in this thesis that the efficient incorporation of HSV-1 gH/L into virions is gM dependent. Without the function of gM, the internalisation of gH/L from the cell surface is impaired and more gH/L is localised on the cell surface, suggesting gM is able to alter the cellular trafficking and localisation of gH/L. Like many other HSV-1 proteins, gM may interact with certain viral and cellular proteins to perform its function. One example is the gM-interacting viral protein, pUL49.5, which is a type I transmembrane protein consisting of 99 aa (in some herpesviruses pUL49.5 is termed gN as it is glycosylated). In several herpesviruses, gM has been shown to form a disulphide bond linked complex with gN/pUL49.5, which is also conserved throughout the

Herpesviridae (Barnett et al., 1992). These include pseudorabies virus (PRV) (Jons *et al.*, 1998), HHV-8 (Koyano *et al.*, 2003), EBV (Lake *et al.*, 1998), bovine herpesvirus type 1 (BHV-1) (Lipinska *et al.*, 2006; Wu *et al.*, 1998), human cytomegalovirus (HCMV) (Mach *et al.*, 2000), and equine herpesvirus 1 (EHV-1) (Rudolph *et al.*, 2002).

In spite of the high conservation, the function(s) of gM, gN/pUL49.5 or the complex formed by these two proteins are not entirely clear. It has been reported that the incorporation of PRV gM into virions is independent of gN, but not vice versa, suggesting gM can function in the absence of gN in this virus (Jons *et al.*, 1998). Furthermore, the deletion of pUL49.5 in HSV-1 demonstrates a milder phenotype than deletion of gM, implying possible functions of HSV-1 gM that are independent of pUL49.5 (Adams *et al.*, 1998; MacLean *et al.*, 1993). There is evidence that gN/pUL49.5 has functions independent of gM, as it has been shown that pUL49.5 is able to inhibit the transporter associated with antigen processing (TAP) transport for MHC class-I peptide loading (Verweij *et al.*, 2011).

Therefore, it will be interesting to investigate the effect of pUL49.5 deletion on gM expression and gH/L incorporation into HSV-1 virions.

5.1.6 gM function and immune evasion

Upon viral infection, the host immune system could recognise the infected cells and induce a series of immune responses to counteract the infection and the subsequent viral spreading. The retrieval of viral protein(s) from host cell surface by gM could reduce the exposure of these viral proteins on cell surface to antibodies. This function of gM represents a potentially interesting strategy for immune evasion.

5.1.7 gM function and host cellular proteins

There may also be a function of gM in host cellular proteins relocalisation. In the reported transfection assays, gM appears to be able to target a broad range of membrane proteins, including a cellular protein, to intracellular compartments (Crump *et al.*, 2004). Furthermore, it has been observed that gM is able to relocalised tetherin (BST-2) in a similar fashion (H. Zenner unpublished data). Tetherin has been reported to counteract HIV by the tethering of the virion on the cell surface (Neil *et al.*, 2008). In addition, it has been shown that the herpesvirus, KSHV, down-regulates tetherin through viral protein mediated ubiquitination. This raises the interesting question of whether gM is able to cause

relocalisation of proteins such as tetherin and result in a viral counteraction against this host "anti-viral" factor.

5.1.8 Future studies

5.1.8.1 Interactions between the cytoplasmic tails of gM and gH/L

In Chapter 2, it has been shown that without the function of gM, the incorporation of gH/L into HSV-1 virions is impaired. This result implies a potential interaction between these two glycoproteins. Unfortunately, as gM is a hydrophobic protein with multi-transmembrane domains, it has been difficult to investigate direct interactions between gM and gH/L. However, an alternative approach will be to examine whether certain domains of gM and gH/L interact with each other. This could be accomplished by cloning the cytoplasmic tails/loops into yeast two-hybrid plasmids to examine potential interactions. However, the hypothesised interaction between gM and gH/L could also be indirect and mediated by other viral/cellular proteins. Therefore, to test whether gM could be immunoprecipitated by anti-gH/L antibody, or vise versa, and to make use of chemical cross-linkers could be sensible approaches for testing the interaction between gM and gH/L.

5.1.8.2 gH incorporation in individual virion

The lower amount of gH/L present in the purified virion samples was shown by western blotting (Figure 2.14-2.16), and this approach reveals the total gH/L level in the whole purified virion population. However this approach provides no conclusive evidence about the gH/L incorporation in each individual virion. The total gH/L decrease in virions could be the results of two situations. One is each individual virions has a lower level of gH/L incorporation, the other is there are more defective particles with no gH/L while there is a small population of virions that have a normal gH/L incorporation level. To test this, high resolution microscopy techniques to examine fluorescence labelled individual virion could possibly reveal the answer.

5.1.8.3 Further investigation about gC and gD sub-cellular localisation

It has been shown that gC plays a role in the initial host entry by binding to heparin sulphate. The decreased level of gC observed in ΔgM purified from HT29 cells (Figure 2.14) implies that the efficient incorporation of gC may also be related to the function of gM, although the effect on gC is at a lower level than gH/L. To address this hypothesis,

similar experiments could be performed to examine cell surface gC level by FACS and the internalisation of gC specific antibodies in the presence and absence of gM.

In addition, it would be interesting to examine the effect on gC and gD sub-cellular with deletion/mutation in gK, pUL20 or pUL43, or the combinations of gM deletion and these deletions/mutations.

5.2 ESCRT and HSV-1

5.2.1 The interactions identified between HSV-1 and host cells

The Y2H screen result presented in this chapter contains many potentially interesting candidates for future work. The cellular protein candidates that were identified are not only associated with the ESCRT machinery but also involved in many other functions. For example, the ESCRT associated protein CIN85 interacts with E3 ligase Cbl and acts as an adaptor protein in the regulation of endocytosis and lysosomal degradation of ligand-induced receptor, including epidermal growth factor receptor (EGFR) (Soubeyran *et al.*, 2002). CIN85 is also likely to play a role in actin dynamics as it directly interacts with F-actin and induces bundling of actin filaments (Gaidos *et al.*, 2007). Further it has been shown that CIN85 binds to AMAP1 and the interaction is important for the invasive activities of breast cancer cells (Nam *et al.*, 2007). Thus the interactions identified in this study are important not only in analysing ESCRT machinery recruitment, but may also shed light on other facets regarding viral-host cell interactions.

5.2.2 Mammalian ESCRTs – not all needed

It has been known that ESCRT-0, I, II complexes are involved in the ubiquitinated cargo recognition and the membrane bud initiation during ILV formation. ESCRT-III complex polymerises into ring filaments and carries out the membrane scission, while the VPS4 ATPase provides energy to recycle the ESCRT-III proteins [reviewed in (Raiborg & Stenmark, 2009)]. However, there is evidence that different cargos show different requirement of the ESCRT complexes in mammalian cells. For example, the sorting of ubiquitinated ferroportin via the MVB pathway requires ESCRT-I, II and III as shown by the inhibition of down-regulation of ferroportin by depletion of TSG101, EAP20 and CHMP6 (De Domenico *et al.*, 2007). Surprisingly, however, the depletion of ESCRT-II did not affect the down-regulation of ubiquitinated major histocompatibility complex (MHC) class I or the degradation of epidermal growth factor (Bowers *et al.*, 2006). This "cargo"

specific function of ESCRT complex subsets in mammalian cells is also reflected by the different requirement of ESCRTs during the membrane scission events in different viruses. For instance, the budding of HIV-1 requires ESCRT-I and III complexes, while it is independent of ESCRT-II. Whilst, the budding of avian sarcoma virus does require ESCRT-II (Pincetic *et al.*, 2008). Additionally, it has been shown that ESCRT-III components CHMP4s and CHMP2s are required but not CHMP3 or CHMP6 (Langelier *et al.*, 2006; Martin-Serrano & Neil, 2011; Martin-Serrano *et al.*, 2003a; Morita *et al.*, 2011). All of the reported virus budding/assembly events which involve membrane separation require the function of ESCRT-III and VPS4 ATPase, while the upstream recruiting pathways appear to vary greatly among different viruses. The yeast two-hybrid screen results and the validation experiments shown in Chapter 3 suggest that HSV-1 is able to interact with multiple proteins to recruit the ESCRT (especially ESCRT-III) machinery. Electron microscopy and siRNA results presented in this thesis have shown that HSV-1 requires CHMP4 proteins to accomplish the membrane separation process, and has revealed possible several routes for viral recruitment of CHMP4s.

Taken together, these different requirements of ESCRT component implies that the membrane deformation and scission reactions that occur during the life cycle of various viruses are different from the topologically related MVB pathway, and the abscission event at the end of cytokinesis. While the result, the ESCRT-III based membrane scission, is the same, many options appear to be available for the viruses to achieve this goal.

5.2.3 Functional redundancy in recruiting ESCRT by HSV-1

Although the depletion of some ESCRT components, such as ALIX and CHMP6, did not show significant effect on HSV-1 replication, it cannot be ruled out that HSV-1 does interact with these proteins in infected cells, as the virus could utilise these interactions among the many parallel pathways with a redundant fashion. This strategy potentially makes the virus able to cope with many different host cellular conditions (*e.g.*, the replication in cells that do not express certain ESCRT components, or mutations occuring in certain viral protein involved in ESCRT recruitment). In addition, data presented in this thesis have shown at least four pathways, ALIX, CHMP6, CIN85 (via ALIX) and CC2D1A/1B, that could be available to HSV-1 for the recruitment of CHMP4 proteins for membrane scission during secondary envelopment. As several other candidates were revealed from the yeast two-hybrid screen, the interactions between HSV-1 tegument and

ESCRT/ESCRT associated proteins may be even more complex than the four presented pathways.

Furthermore, the viral glycoprotein tails presented at the cytoplasmic side of the assembly membrane compartment may also play roles in recruiting ESCRT proteins for mature virion formation. It has been shown that tegument proteins are able to self-assemble in a process independent of capsid to form L-particles, which consist of tegument and envelope, but no capsid (Fuchs *et al.*, 2002). As the formation of these L-particles also requires the same membrane deformation and scission events, this is a strong evidence for the involvement of tegument and/or envelope proteins in ESCRT recruitment, but not capsid proteins.

In addition, it has been shown that human T cell leukemia virus type I (HTLV-I) Gag interacts with Nedd4 ubiquitin ligase family members and hijacks the ESCRT machinery, presumably through the ubiquitin interacting domain of the ESCRT-I complex (Martin-Serrano & Neil, 2011). Potentially, HSV-1 could also hijack the ESCRT machinery via these upstream ubiquitin ligases. Unfortunately, the Nedd4 protein tested in yeast two-hybrid screen showed many positive interactions, which are likely due to its non-specific binding when expressed in yeast cells. It is possible that HSV-1 may have direct interactions with Nedd4, although it is not revealed by the study in this thesis. This could add even more complexity to the recruitment of ESCRT machinery by HSV-1.

5.2.4 Avoiding lysosomes after ESCRT recruitment

The ESCRT machinery involvement is located on the plasma membrane during both HIV budding and cytokinesis. However, HSV-1 secondary envelopment, where virus particle containing vesicles are formed, and the formation of MVBs that are ILVs containing vesicles, both occur in the cytoplasm and share many topological similarities. The final stage of the cellular MVB pathway is the fusion of MVBs with lysosomes for protein degradation. In addition, there is evidence for ESCRT machinery being involved in autophagy (Lee *et al.*, 2007; Rusten *et al.*, 2007), which also leads to the degradation of cellular components by fusion with lysosomes. It has been previously reported that the depletion of TSG101 (an ESCRT-I component) inhibits the down-regulation of epidermal growth factor receptor (EGFR) while it causes sustained downstream activation by EGF, suggesting the initial sorting of EGFR from the cell surface is inhibited due to the loss of TSG101 function (Hewitt *et al.*, 2002). However, the depletion of CHMP3 (an ESCRT-III component) did not affect the endocytosis but caused the accumulation of EGFR in

significantly smaller MVBs. This suggests the possible functional involvement of CHMP3 in the fusion of MVBs with lysosomes (Bache *et al.*, 2006). Therefore, it is plausible to hypothesise that there is a close link between ESCRT and lysosome. This raises the interesting question how the virions containing vesicles escape the potential fusion with lysosomes and complete the transport to the cell surface for release. Presumably, HSV-1 encodes activities to prevent the fusion of virus containing vesicles with lysosomes. However, what viral protein(s) may be involved is currently unknown.

5.2.5 Possible involvement for ESCRT at primary envelopment

Another intriguing question is whether the ESCRT machinery could be involved in the primary envelopment stage, which also requires membrane separation. However, no research work on ESCRT function at the nuclear membrane has been reported. ESCRT components are soluble proteins presenting in cytoplasm and presumably these proteins could also be recruited to nuclear membrane for membrane deformation and scission. In addition, some of the tegument proteins are presented in the cell nucleus and there is evidence that certain tegument proteins (such as VP16) are presented in the primary enveloped virions (Naldinho-Souto *et al.*, 2006). These tegument proteins could potentially play a role in assisting primary envelopment through the interactions with ESCRTs if they are presented at the nuclear membrane. However, a role of ESCRTs in nuclear egress may be unlikely because no defects in perinuclear particle envelopment were observed in VPS4 dominant-negative expressing cells (Crump *et al.*, 2007).

On the other hand, some viruses use different strategies to complete the membrane scission. Since VPS4 is the only energy providing complex of ESCRT machinery required for membrane scission, the ESCRT-dependence of virus budding is usually characterised by whether the viruses have the ability to complete the budding process in cells with overexpression of dominant-negative VPS4. Interestingly, Influenza virus budding has been shown to be VPS4 independent (Bruce *et al.*, 2009). The fact that there are viruses independent of VPS4 activity/ESCRT machinery suggesting either the presence of alternative pathways, or virus budding process independent of cellular assistance. For example, it has been shown that Influenza virus encodes a viral protein called M2, that appears to mediate the membrane scission during budding (Rossman *et al.*, 2010). By analogy to Influenza virus, HSV-1 could also encode viral protein(s) to mediate membrane scission during the primary envelopment stage without the assistance of ESCRT machinery. Which HSV-1 proteins could accomplish such membrane scission is unknown.

Candidates could be pUL31, pUL34 and pUS3, proteins known to be involved in nuclear egress of HSV-1.

5.2.6 Future studies

5.2.6.1 Triple deletion virus

As a complex virus, HSV-1 often has significant functional redundancy. The siRNA experiments performed to deplete certain combinations of CIN85, CC2D1A/1B, ALIX and HD-PTP did not show significant inhibition of virus replication. Presumably, there is a highly complex level of functional redundancy involved in the ESCRT machinery recruitment. From the yeast two-hybrid screen, tegument proteins pUL46, pUL47 and pUL49 showed interactions with several ESCRT proteins (Figure 3.2). The attempt was made to delete pUL47 aiming at making the virus more sensitive to siRNA depletion of certain ESCRT protein(s). While the ΔUL47 virus did show a small defect in replication, it appeared no more sensitive to the siRNA depletions than wild type HSV-1. Therefore, further approaches could be explored to simultaneously delete multiple tegument proteins and examine the virus replication in cells with ESCRT depletion(s). This kind of approach might be able to avoid the complex functional redundancy and reveal more confident information about the requirement of certain ESCRT/ESCRT associated proteins by HSV-1.

5.2.6.2 Searching for potential HSV-1 L domain motif(s)

It has been shown that HSV-1 viral proteins contain many potential L-domain motifs of the known type: PTAP, PPXY and YPXnL (Pawliczek & Crump, 2009). Intriguingly, it has been previously reported that different L-domain motifs can be exchanged between different viruses. For example, the L-domain motif of Rous sarcoma virus (RSV, a retrovirus that causes sarcoma in chicken) could be replaced with the HIV L-domain motif in the Gag protein (Parent *et al.*, 1995). Therefore, it will be very interesting to continue the searching for potential novel L-domain motifs from HSV-1 tegument proteins, such as pUL46, and examine the function of these motifs when they are presenting in other viruses, such as HIV-1.

5.2.6.3 Immunoelectron microscopy

It has been shown in this thesis that the ESCRT associate proteins CC2D1A and CC2D1B directly interacts with HSV-1 tegument proteins and they are present in purified virions.

As a further step to the studies performed, immunoelectron microscopy could be employed to examine whether the identified ESCRT/ESCRT associated proteins co-localise with the secondary envelopment and its closely related events.

This thesis presents the new observations of gM-dependant gH/L sub-cellular localisation in host cells and the direct interactions between HSV-1 tegument and ESCRT/ESCRT associated proteins. These observations are related to HSV-1 secondary envelopment and opens up many interesting questions for further studies in order to develop the current understanding of HSV-1 secondary assembly further. In summary, the results presented in this thesis show that the efficient incorporation of gH/L relies on the function of gM and that HSV-1 has evolved multiple parallel pathways to hijack the membrane scission event mediated by CHMP4 proteins to facilitate the viral replication.

6 Materials and Methods

6.1 Materials

6.1.1 Mammalian cell lines

The cells were grown in Dulbecco's modified Eagle's medium (DMEM), Glasgow Minimum Essential Medium (GMEM) or RPMI supplemented with 10% fetal calf serum (FCS), 2 mM L-glutamine, 100 U/ml penicillin, and 100 μg/ml streptomycin. Cell lines used in this thesis are listed in Table 6.1.

Table 6.1 Cell lines.

Name	Description
293T	Highly transfectable human cell line derived from the 293 human embryonic kidney (HEK) cell line by insertion of the temperature sensitive gene for SV40 T antigen (American Type Culture Collection (ATCC)).
A549	Human alveolar epithelial cell line derived from lung carcinomatous tissue from a 58-year-old Caucasian male (Giard *et al.*, 1973).
BHK	Syrian hamster fibroblast cell line obtained from an unusually rapidly growing primary culture of new-born hamster kidney tissue (Nature 203: 1355-1357, 1964).
Caco-2	Human colorectal adenocarcinoma. The cells can be polarized under certain conditions (Hidalgo *et al.*, 1989).
COS-7	African green monkey fibroblast-like cell line containing SV40 viral DNA and expressing the SV40 T antigen (ATCC).
HaCaT	Spontaneously immortalised human keratinocyte cell line (Boukamp *et al.*, 1988).
HeLa	Immortal human cell line isolated from an aggressive glandular cervical cancer of a patient called Henrietta Lacks in 1951 as the first *in vitro* continuous human cell line (Masters, 2002).
HFF	Human foreskin fibroblasts. They are adherent primary cells at relatively early passages.
HRT-18	Human ileocecal colorectal adenocarcinoma. The HRT-18 line is identical to the HCT-8 cell line (ATCC).
HT29	Human colon adenocarcinoma adherent cells purchased from the European Collection of Cell Cultures (ECACC). It was isolated from a primary tumour in a 44-year-old Caucasian female.
MDCK	Dog kidney cell line derived from a kidney of an apparently normal adult female cocker spaniel (ATCC).
RK13	Rabbit kidney cell line (ATCC).
SK-N-SH	Human neuroblastoma cell line (ATCC).
Vero	African green monkey cell line isolated from the kidney of a healthy animal (ATCC).

6.1.2 Yeast

Saccharomyces cerevisiae strain Y190 used for yeast two-hybrid assay was from Dr J. Martin-Serrano at King's College London.

6.1.3 *Escherichia coli*

Escherichia coli strain DH5α was used for transformation during cloning.

Escherichia coli strain GS1783 use for two-step markerless red recombination was from G. Smith at Northwestern University (Tischer *et al.*, 2010).

6.1.4 HSV-1 viruses

HSV-1 wild type and mutant viruses used in this thesis are listed in Table 6.2.

Table 6.2 HSV-1 viruses.

Name	Description
SC16	A clinical isolate from a recurrent lesion with a low passage history in laboratory (Hill *et al.*, 1975).
KOS	A clinical isolate of HSV-1 with a high passage history from human oral lesions (Smith, 1964).
KΔUL36	HSV-1 mutant derived from strain KOS with a partial deletion of the UL36 ORF that expresses only a small N-terminal region of pUL36. This virus does not replicate in cells without expressing pUL36 (Desai, 2000).
ΔgM*	Created in this study. HSV-1 mutant derived from strain SC16 with the gM gene UL10 replaced by *lacZ* reporter gene.
gMR*	Created in this study. The *lacZ* reporter gene in ΔgM was replaced with the wild type UL10 fragment.
ΔgM/ΔUL43*	Created in this study. HSV-1 double mutant derived from ΔgM with the gM gene UL10 replaced by *lacZ* reporter gene and UL43 gene replaced by EGFP expression cassette.
gMR/ΔUL43*	Created in this study. The *lacZ* reporter gene in ΔgM/ΔUL43 was replaced with the wild type UL10.
ΔUL47	Created in this study. HSV-1 mutant derived from strain KOS with the UL47 gene replaced by tdTomato reporter gene, using the two-step Red-mediated recombination method (Tischer *et al.*, 2010; Tischer *et al.*, 2006).

* viruses created by C. Crump and S. Bell.

6.1.5 Antibodies

Primary antibodies used for Western blot (WB), immunofluorescence microscopy (IF), Fluorescence Activated Cell Sorting (FACS) and Co-immunoprecipitate (Co-IP) are shown in Table 6.3 and 6.4 for cellular proteins and viral proteins respectively. Primary antibodies were either purchased from the indicated companies, developed in the laboratory or kindly provided by Gillian Elliott (Imperial College London), J. Martin-Serrano (King's College London), Wesley I. Sundquist (University of Utah), J. Paul Luzio (Cambridge Institute for Medical Research), Gary Cohen (University of Pennsylvania), Tony Minson and Helena Browne (University of Cambridge). Secondary antibodies used: Alexa Fluor® 680 goat anti-rat (Invitrogen, A21096, 1:20000), LI-COR IRDye 680 goat anti-rabbit, 800CW

donkey anti-rabbit, 800CW goat anti-mouse (LI-COR Biosciences, 926-32221, 926-32213, 926-32210, 1:20000).

Table 6.3 Primary antibodies against cellular proteins.

Antigen	Name	Source	Species	Application
Actin	AC-40	Sigma	Mouse	WB, 1:2000
ALIX	UT325	W. I. Sundquist	Rabbit	WB, 1:1000
CC2D1A	ab70375	Abcam	Rabbit	WB, 1:1000
CC2D1B	sc-134634	Santa Cruz Biotechnology	Rabbit	WB, 1:200
CHMP2B	ab33174	Abcam	Rabbit	WB, 1:200
CHMP4A	sc-67229	Santa Cruz Biotechnology	Rabbit	WB, 1:250
CHMP4B	sc-82556	Santa Cruz Biotechnology	Rabbit	WB, 1:100
CHMP4C	-	J. Martin-Serrano	Mouse	WB, 1:20
CHMP6	-	J. Paul Luzio	Rabbit	WB, 1:1000
CIN85	AB8225	Millipore	Rabbit	WB, 1:5000; IP, 1:100
dsRed	632496	Clontech	Rabbit	WB, 1:1000
HD-PTP	sc-55205	Santa Cruz Biotechnology	Goat	WB, 1:200
GFP/YFP	JL-8	Clontech	Mouse	WB, 1:5000
GM130	-	BD Biosciences	Mouse	IF, 1:100
GST	sc-459	Santa Cruz Biotechnology	Rabbit	WB, 1:1000
Tubulin α	MCA77G	AbD Serotec	Rat	WB, 1:2000
TGN46	-	AbD Serotec	Sheep	IF, 1:200
VPS4A	UT289	W. I. Sundquist	Rabbit	WB, 1:500

Table 6.4 Primary antibodies against viral proteins.

Antigen	Name	Source	Species	Application
gB	R69	G. Cohen and R. Eisenberg	Rabbit	WB, 1:6000
gC	ab6509	Abcam	Mouse	WB, 1:1000
gD	LP2	T. Minson	Mouse	IF, 1:3; FACS, 1:2
	LP14	T. Minson	Mouse	WB, 1:10
gH	BBH1	H. Browne	Mouse	WB, 1:10
	Shabba	H. Browne (Desai *et al.*, 1988)	Rabbit	WB, 1:200
	LP11	T. Minson	Mouse	IF, 1:3; FACS, 1:2
	52S	(Showalter *et al.*, 1981)	Mouse	IF, 1:3
gL	CHL28	G. Cohen (Cairns *et al.*, 2006)	Mouse	WB, 1:500
gM	anti-gM-B	H. Browne	Rabbit	WB, 1:1000
	CB18	C. Crump and S. Bell	Mouse	IF, 1:3
HSV-1	B0114	DAKO	Rabbit	IF, 1:1000
pUL11	-	T. Mettenleiter	Rabbit	WB, 1:50000
VP1/2	CB2	C. Crump and S. Bell	Mouse	WB, 1:2
VP5	ab6508	Abcam	Mouse	WB, 1:1000
VP13/14	-	G. Elliott	Rabbit	WB, 1:3000
VP16	LP1	T. Minson	Mouse	WB, 1:50
VP22	AGV30	G. Elliott	Rabbit	WB, 1:2000

6.1.6 Bacterial artificial chromosome

The bacterial artificial chromosome (BAC) containing HSV-1 strain KOS genome used in the two-step markerless red recombination was from David A. Leib (Gierasch *et al.*, 2006).

6.1.7 Plasmids

The plasmids used in this thesis are listed in Table 6.5.

Table 6.5 Plasmids.

Name	Selection marker	Application and description
pHB18	Ampicillin	Yeast two-hybrid assay. Expresses a protein of interest (pray) and VP16 activation domain fusion protein in yeasts.
pGBKT7	Kanamycin	Yeast two-hybrid assay. Expresses a protein of interest (bait) and Gal4 DNA binding domain fusion protein in yeasts.
pCAG-GST	Ampicillin	GST pull-down assay. Expresses N-terminal tagged GST fusion proteins in mammalian cells.
pEGFP-N1	Kanamycin	Expresses C-terminal tagged GFP fusion proteins in mammalian cells.
pEGFP-C2	Kanamycin	Espresses N-terminal tagged GFP fusion proteins in mammalian cells.
pSG124 (A)	Ampicillin	Template used for UL37 and UL41 in PCR for cloning.
pSG10 (D)	Ampicillin	Template used for UL7, UL11, UL13 and UL14 in PCR for cloning.
pSG28 (EK)	Ampicillin	Template used for UL55 and ICP4 (RS1) in PCR for cloning.
pSG 16 (G)	Ampicillin	Template used for UL16 and UL21 in PCR for cloning.
pSG 25 (H)	Ampicillin	Template used for US2, US3, US10 and US11 in PCR for cloning.
pSG 22 (I)	Ampicillin	Template used for UL46, UL47, UL48, UL49, UL50 and UL51 in PCR for cloning.
pSG 1 (JK)	Ampicillin	Template used for ICP34.5 (RL1) in PCR for cloning.
pSG 87 (N)	Ampicillin	Template used for UL23 in PCR for cloning.
pT7-111-ICP0cDNA	Ampicillin	For ICP0 subcloning. Template used for ICP0 in PCR for cloning.
pHIT VSV-G	Ampicillin	Retroviral transduction system used for establishing stable cell lines. Plasmids Encoding vesicular stomatitis virus G protein (VSV-G) envelope, MLV Gag-pol and YFP tagged CC2D1A and CC2D1B (Carlton *et al.*, 2008).
pHIT60 Gag-pol	Ampicillin	
pCMS28-YFP-CC2D1A	Ampicillin	
pCMS28-YFP-CC2D1B	Ampicillin	
pEP-tdTomato-in	Kanamycin	Template used for recombination sites flanked kanamycin gene in PCR for creating HSV-1 ΔUL47 virus by replacing UL47 codons 1-479by tdTomato reporter gene.
pGS403	Ampicillin	Used to remove bacterial backbone from BAC during the Two-step Red-mediated recombination for markerless mutant virus construction. Contains a gene encoding Cre recombinase under HCMV promoter. This enzyme is a type I topoisomerase that catalyses site-specific recombination of DNA between LoxP sites.

6.1.8 Primers

Table 6.6 Primers for tegument cloning.

Name	Sequence (with restriction enzyme sites underlined)	Restriction enzyme
UL4	5'-CTGAGAATTCGCCACCATGTCCAATCCACAGACGAC-3'	*Eco*RI
	5'-CTGACTCGAGTCA GGACCCCAAAAGTTTGTCTG-3'	*Xho*I
UL7	5'-CTGAGAATTCGCCACC ATGGCCGCCGCGACGGC-3'	*Eco*RI
	5'-CTGACTCGAGTCA ACAAAACTGATAAAACAGCG-3'	*Xho*I
UL11	5'-CTGAGAATTCGCCACC ATGGGCCTCTCGTTCTCCG-3'	*Eco*RI
	5'-CTGACTCGAGTCA TTCGCTATCGGACATGGGG-3'	*Xho*I
UL13	5'-CTGAGAATTCGCCACC ATGGATGAGTCCCGCAGAC-3'	*Eco*RI
	5'-CTGAGGATCCTCA CGACAGCGCGTGCCG -3'	*Bam*HI
UL14	5'-CTGAGAATTCGCCACC ATGGACCGAGATGCCGCC-3'	*Eco*RI
	5'-CTGAGGATCCTCA TTCGCCATCGGGATAGT-3'	*Bam*HI
UL16	5'-CTGAGAATTCGCCACC ATGGCGCAGCTGGGACCC-3'	*Eco*RI
	5'-CTGACTCGAGTCA TTCGGGATCGCTTGAGGAG-3'	*Xho*I
UL21	5'-CTGAGAATTCGCCACCATGGAGCTTAGCTACGCCAC-3'	*Eco*RI
	5'-CTGAGGATCCTCA CACAGACTGTCCGTGTTGG-3'	*Bam*HI
UL23	5'-CTGAGAATTCGCCACC ATGGCTTCGTACCCCTGCC-3'	*Eco*RI
	5'-CTGACTCGAGTCA GTTAGCCTCCCCCATC-3'	*Xho*I
UL37	5'-CTGAGAATTCGCCACC ATGGCAGACCGCGGTCTC-3'	*Eco*RI
	5'- GTATGGATCCGCTTATTGGTAACTAGTTAACGGC-3'	*Bam*HI
UL41	5'-CTGAGAATTCGCCACCATGGGTTTGTTCGGGATGATG-3'	*Eco*RI
	5'-CTGACTCGAGTCA CTCGTCCCAGAATTTGGCC-3'	*Xho*I
UL46	5'-CTGAGAATTCGCCACC ATGCAGCGCCGGACGCG-3'	*Eco*RI
	5'-CTGACTCGAGTCA CCGGCTCCGGCGTC-3'	*Xho*I
UL47	5'-CTGAGAATTCGCCACC ATGTCGGCTCGCGAACCC-3'	*Eco*RI
	5'-CTGACTCGAGTCA TGGGCGTGGCGGGCCTC-3'	*Xho*I
UL48	5'-CTGAGAATTCGCCACC ATGGACCTCTTGGTCGACG-3'	*Eco*RI
	5'-CTGACTCGAGTCA CCCACCGTACTCGTCAATTC-3'	*Xho*I
UL48 ΔAD	5'-CTGAGAATTCGCCACC ATGGACCTCTTGGTCGACG-3'	*Eco*RI
	5'-CTGACTCGAGTCA CGACAGTCTGCGCGTGTG-3'	*Xho*I
UL49	5'-CTGAGAATTCGCCACC ATGACCTCTCGCCGCTCC-3'	*Eco*RI
	5'-CTGAGGATCCTCA CTCGACGGGCCGTCT-3'	*Bam*HI
UL50	5'-CTGAGAATTCGCCACC ATGAGTCAGTGGGGGATCCG-3'	*Eco*RI
	5'-CTGAGCGGCCGCTCA ATACCGGTAGAACCAAAACC-3'	*Not*I
UL51	5'-CTGAGAATTCGCCACC ATGGCTTCTCTTCTCGGGG-3'	*Eco*RI
	5'-CTGAGGATCCTCA TTGACCCAAAACACACGGAG-3'	*Bam*HI
UL55	5'-CTGAGAATTCGCCACC ATGACAGCGACCCCCCTC-3'	*Eco*RI
	5'-CTGACTCGAGTCA CGCCTTAATTTTAATCTTGA-3'	*Xho*I
US2	5'-CTGAGAATTCGCCACC ATGGGCGTTGTTGTCGTCAA-3'	*Eco*RI
	5'-CTGACTCGAGTCA AAGGGTGGTAACCGGATAG-3'	*Xho*I
US3	5'-CTGAGAATTCGCCACC ATGGCCTGTCGTAAGTTTTGT-3'	*Eco*RI
	5'-CTGAGCGGCCGCTCA TTTCTGTTGAAACAGCGG-3'	*Not*I
US10	5'-CTGAGAATTCGCCACC ATGATCAAGCGGCGGGGC-3'	*Eco*RI
	5'-CTGACTCGAGTCA GCACAGGGGTGGGGTTAG-3'	*Xho*I
US11	5'-CTGAGAATTCGCCACC ATGAGCCAGACCCAACCCC-3'	*Eco*RI
	5'-CTGAGCGGCCGCTCA TACAGACCCGCGAGCCGT-3'	*Not*I

Table 6.7 Primers for generation of mutant viruses.

Name	Sequence	Purpose
SB003	5'-GCGGCCATTAATACAGGGAAAGGAAATACACG-3'	ΔgM/ΔUL43
SB004	5'-GCGGCCATTAATAGCCTTCTGGACTCGCTTC-3'	
SB005	5'-GCGGCCACGCGTCAATAAAAGGCATTAGTCCCG-3'	
SB009	5'-CAGGGGCACGTAGTGGGGCTGGAGGGTCAGAG-3'	
COL398	5'-TTCTTTTTTGGGGGGTAGCGGACATCCGATAACCCGC GTCTATCGCCACCATGGTGAGCAAGGGCGAGGAG-3'	ΔUL47
COL399	5'-GCGTTGAGCCCGCTGTTGGCGAGCAGCCGGCGCGCT GCGGTGTCGCCCAGTCACTATTACTTGTACAGCTCGTCCA TGCC-3'	

Table 6.8 Primers for ESCRT protein gene (domain) constructs cloning.

Name	Sequence	Restriction enzyme
CIN85-SH3(1-331)	5'-CTGAGAATTCGCCACCATGGTGGAGGCCATAGTGGA-3'	*Eco*RI
	5'-CTGACTCGAGTCATTCAAAGTCCGGTGGAAGTA-3'	*Xho*I
CIN85-PR (332-600)	5'-CTGAGAATTCGCCACCAAGGAAGGGAATAGACCCAA-3'	*Eco*RI
	5'-CTGACTCGAGTCACTCCATCTTTGGTTTTCCTT-3'	*Xho*I
CIN85-CC (594-665)	5'-CTGAGAATTCGCCACCGAAGGAAAACCAAAGATGGA-3'	*Eco*RI
	5'-CTGACTCGAG TCA TCATTTTGATTGTAGAGCTT-3'	*Xho*I
CC2D1B	5'-CTGAGAATTCGCCACCATGATGCCAGGGCCAAGACC-3'	*Eco*RI
	5'-CTGACTCGAG TCA TCACAAGCCCCTGGGCTCCAG-3'	*Xho*I

6.1.9 siRNA

Table 6.9 Sequences of siRNA oligonucleotides.

Name	Sequence
CHMP4A	CCCUGGAGUUUCAGCGUGATT
CHMP4B	CGAUAAAGUUGAUGAGUUATT
CHMP4C	CACUCAGAUUGAUGGCACATT
siCIN85-1	CAAGGUCAAUUGAAGUAGA
siCIN85-2	GGAGUGGACGCGUCAAAGA
siCIN85-3	CUAUCCAAGUCAAGUUUAA
siCIN85-4	ACGAGAGAUUAAACAGUUA
ALIX	GAAGGAUGCUUUCGAUAAAUU
CHMP6 SMARTpool	UCACCCAGAUCGAAAUGAAUU GGACAAGGCCAUCCUGCAAUU CGCAAUCACUCAGGAACAAUU GAGUACCAGCGGCAAAUAGUU
CC2D1A (1A02)	CCAAGGGACUGGAGCCUAU
CC2D1A (1A04)	GGACGGAUGAGGACGACUU
CC2D1B (1B01)	GAUCAACUCUUCAAACUAA
CC2D1B (1B03)	GAGCAAAGGCAUCAAGUUU
HD-PTP	A gift from P. Luzio.

siRNA related reagents were purchased from Qiagen and Dharmacon, Thermo Fisher Scientific. The siRNA oligonucleotides are dissolved in 1 × siRNA buffer with final concentration of 100 μM and aliquots are stored at -20 °C.

6.1.10 Buffers and media solutions

Table 6.10 Electrophoresis buffers and gels.

Name	Composition
TAE (1X)	40 mM Tris acetate, 1 mM EDTA pH7.8.
TBE (1X)	89 mM Tris base, 89 mM borate, 2.6 mM EDTA pH8.0.
DNA loading (10X)	50% glycerol, 100 mM EDTA (pH 8.0), 1% SDS, 0.25% bromophenol blue.
SDS-PAGE running buffer (1X)	25 mM Tris base, 200 mM glycine, 0.1% SDS.
SDS-PAGE transfer buffer (1X)	25 mM Tris base, 200 mM glycine, 10% methanol.
SDS-PAGE loading buffer (5X)	250 mM Tris-HCl pH6.8, 10% SDS, 50% glycerol, 0.05% bromophenol blue, 1.39% b-mercaptoethanol.
Acrylamide stock	30% (w/v) acrylamide/methylene bisacrylamide solution (ProtoGel).
5% stacking gel	0.67 ml stock acrylamide solution, 0.5 ml 1.0 M Tris-HCl (pH6.8), 40 μl 10% SDS, 40 μl 10% APS, 4 μl TEMED.
8/10/12% resolving gel	2.7/3.3/4.0 ml stock acrylamide solution, 2.5 ml 1.5 M Tris-HCl (pH8.8), 100 μl 10% SDS, 100 μl 10% ammonium persulfate (APS), up to 10 ml with dH_2O, 4 μl TEMED (N,N,N',N'-tetramethylethylenediamine).

Table 6.11 IF, FACS and TEM buffers.

Name	Composition
IF fix	3% formaldehyde in PBS.
IF perm/quench solution	50 mM NH_4CL, 0.2% saponin in PBS.
IF blocking PGAS	0.2% gelatin, 0.02% saponin, 0.02% NaN_3 in PBS.
IF gE/gI Fc receptor blocking	0.1 mg/ml human IgG (Sigma) in PGAS.
FACS blocking	3% BSA in PBS.
TEM saline	0.9% sodium chloride.
TEM wash	0.1 M HEPES.
TEM fix	2% glutaraldehyde, 0.1 M HEPES, pH7.4.

Table 6.12 Yeast two-hybrid solutions.

Name	Composition
LiAc working solution	0.1 M LiAc, pH7.5, in TE.
TE (10X)	100 mM Tris base, 10 mM EDTA, pH7.5.
PEG working solution	40% PEG 3350, 0.1 M LiAc, pH7.5, in TE.
Z buffer (5X)	0.3 M Na_2HPO_4, 0.14 M NaH_2PO_4, 0.05 M KCl, 0.01 $MgSO_4$, pH7.0.
Working buffer (10ml)	2ml of 5X Z buffer, 28 μl β-mercaptoethanol, 8ul 10% SDS and 8 ml H_2O.
Adenine hemisulfate (1000X)	100 mg/ml in H_2O.
CPRG solution	14 mg/ml in H_2O (store at -20 °C in dark).

Table 6.13 Buffers for high molecular weight DNA preparation.

Name	Composition
Lysis buffer	1 ml of 1M Tris pH7.5
	10 ml of 0.1M EDTA
	89 ml of H_2O
Lysis mixture	20 ml of lysis buffer
	1.2ml of 10% SDS
	Add proteinase K with final concentration of 50 μg/ml

Table 6.14 Buffers for GST pull-down and Co-IP.

Name	Composition
Lysis buffer	50 mM Tris-HCl, pH 7.4, 150 mM NaCl, 5 mM EDTA, 5% glycerol, 1% Triton ×-100.
Wash buffer	50 mM Tris-HCl, pH 7.4, 150mM NaCl, 5 mM EDTA, 5% glycerol, and 0.1% Triton ×-100.

Table 6.15 Miscellaneous.

Name	Composition
LB, 2TY, SOC, CMC	Prepared by technical staff at the Department of Pathology, University of Cambridge.
PEI	1mg/ml, pH 7.0, linear 25 kDa polyethylenimine from Polysciences.
YPD broth and agar	Purchased from Clontech and prepared according to the instructions. Contains 1x adenine hemisulfate.
SD agar	Purchased from Clontech and prepared according to the instructions. Yeast synthetic dropout medium supplement without Leucine and Tryptophan was added.
DMEM, GMEM, RPMI	Purchased from Sigma and supplemented with 100 U/ml penicillin, 100 mg/ml streptomycin, 2 mM L-glutamine from Gibco BRL, and 10% (vol/vol) fetal calf serum.
CCMB	11.8 g of $CaCl_2$, 4.0 g of $MnCl_2$, 2.0 g of $MgCl_2$, 0.7 g of KCl and 100 ml of glycerol dissolved in water with final volume of 1 litre.
mRIPA	50 mM Tris, pH 7.9, 150 mM NaCl, 1% NP-40, 1% sodium deoxycholate.
Acid wash	40 mM citric acid, 135 mM NaCl, 10 mM KCl, pH3.0.

6.1.11 General biochemical reagents and consumables

General biochemical reagents were supplied by the following companies: Amersham Bioscience, BDH Chemicals, Bethesda Research Laboratories (BRL), Roche, Fisher Scientific, Clontech, and Sigma-Aldrich. Materials for cell culture and plasticware were obtained from BD Biosciences, Sterilin Ltd, Corning, Gibco, Greiner Bio-One, Sigma Chemical, and Techno Plastic Products (TPP). Molecular biology reagents and enzymes were obtained from Roche, Clontech, Invitrogen, New England Biolabs, and Promega.

For chemiluminescence detection, medical X-ray film was supplied by Fuji Film. Immunological reagents were supplied by Abcam, Amersham Biosciences, Santa Cruz Biotechnology, Millipore, Abnova, BD Biosciences, AbD Serotec and Invitrogen.

6.2 Methods

6.2.1 Virus construction using homologous recombination

6.2.1.1 ΔgM and gMR

The gM deletion (ΔgM) and revertant (gMR) viruses were created through homologous recombination and the cloning details for construction are described as follows (carried out by Dr C. Crump and S. Bell). The plasmid pc73.1 contains the BamHI (21653)-BglII (25153) region of the HSV-1 genome that covers the UL10 ORF (23204-24625; numbering relates to strain 17 sequence available online: Refseq: NC_001806). The plasmid pc78.1 is pc73.1 with an SV40 promoter driven *lacZ* gene inserted into an NruI site (24343) near the 3' end of UL10 (MacLean *et al.*, 1991). Plasmid pc78.1 was digested with PpuMI and religated to generate pc78.1ΔPpuMI, in which the majority of the UL10 ORF (from 23765-24592) and the entire *lacZ* cassette were removed. A CMV promoter driven *lacZ* gene was excised from pMW10 with HindIII, ligated into pEGFP-C3 (Clontech) and screened for clones containing the *lacZ* cassette in the reverse orientation to the GFP ORF to generate pEGFPC3-LacZrev. The *lacZ* cassette was excised from pEGFPC3-LacZrev with SmaI + BsrGI and ligated into pc78.1ΔPpuMI cut with MscI and BsrGI to create pc78.1ΔMscI-BsrGI-LacZ. This deletes bases 23604-24599 and replaces this region of the UL10 ORF (corresponding to amino acids Ala134–Val466 of gM) with the selectable marker *lacZ*. Vero cells were transfected with pc78.1ΔMscI-BsrGI-LacZ together with high molecular weight DNA prepared from SC16 infected cells by calcium phosphate precipitation as previously described (Balan *et al.*, 1994). Resulting plaques were analysed for β-galactosidase activity by staining with X-gal (5-bromo-4-chloro-3-indolyl-β-D-galactopyranoside) and limiting dilution was used to isolate single blue plaques. As a more isogenic control for comparison, a revertant virus was made by transfecting Vero cells with pc73.1 together with high molecular weight DNA prepared from ΔgM infected cells. Resulting plaques were analysed for β-galactosidase activity by staining with X-gal and single white plaques were isolated.

6.2.1.2 ΔgM/ΔUL43 and gMR/ΔUL43

The design and construction of ΔgM/ΔUL43 and gMR/ΔUL43 were carried out by Dr C. Crump and S. Bell as follows. For ΔgM/ΔUL43, the HSV-1 genomic sequence at the 3' end of UL43 (96062-97138) was amplified by PCR using primers SB005 and SB009 (Table 6.6) and strain 17 genomic DNA as template. This introduced a 5' MluI site (encode in primer SB005) and included the DraIII site at position 97129. This 3' flanking region was then sub-cloned into the MluI/DraIII sites of pEGFPC2 (at the 3' end of the EGFP expression cassette poly-A signal) to generate pEGFPC2-3'flank. The HSV-1 genomic sequence (93269-94732) was amplified by PCR using primers SB003 and SB004 (Table 6.6) and strain 17 genomic DNA as template. This introduced 5' and 3' AseI sites (encoded in the primers). This 5' flanking region was then sub-cloned into the AseI site of pEGFPC2-3' flank (at the 5' end of the EGFP expression cassette promoter) and screened for correct orientation by restriction digest. The resulting plasmid (pEGFPC2-ΔUL43flanks) was cotransfected with high molecular weight DNA prepared from HSV-1ΔgM infected cells. Resulting plaques were screened for GFP fluorescence and single GFP/β-galactosidase positive plaques were isolated. gMR/ΔUL43 virus was prepared by co-transfecting pc73.1 with high molecular weight DNA from ΔgM/ΔUL43 infected cells. Resulting plaques were screened for GFP fluorescence positive (indicating remains ΔUL43) while for β-galactosidase activity negative (indicating gM revertant).

6.2.1.3 Wild type SC16

To generate an equivalently treated wild type SC16 strain, BHK cell were transfected with high molecular weight DNA prepared from SC16 infected cells. The progeny viruses generated were harvested and stocks prepared in Vero cells.

6.2.2 Two-step Red-mediated recombination for markerless mutant virus construction

The method used was from B. K. Tischer *et al.* with modifications (Tischer *et al.*, 2010). Briefly, PCR primers (Table 6.7) were designed to contain 50 bp homology sequences to HSV-1 genomic DNA for recombination at the desired location followed by sequences annealing to pEP-tdTomato-in. The PCR products were harvested and digested by DpnI enzyme to remove any potential template plasmid contamination. 100 ng of the PCR product was electroporated into *E. Coli* GS1783 containing KOS BAC. GS1783 contains heat shock inducible red recombination enzymes, and arabinose-inducible I-SceI. The

bacteria were selected in both kanamycin (Kan) and chloramphenicol (Cam). BAC DNA was harvested from liquid culture of the positive colonies and subjected to restriction enzyme digestion to confirm recombination.

Positive colonies were inoculated into LB containing Cam for starter cultures and then a final concentration of 1% arabinose was added to induce I-SceI expression. Subsequently the Red recombinase was induced at 42 °C for 30 min. The bacteria were plated out onto agar plates containing Cam and 1% arabinose and incubated for 1-2 days. Cam resistant but Kan sensitive colonies were identified by replica plating and then cultured. BAC DNA was harvested and subjected to restriction enzyme digestion to confirm recombination. BAC DNA and pGS403 were co-transfected into Vero cells and incubated at 37 °C until visible plaques were formed to generate a pre-master virus stock. The virus was harvested and used to generate virus stocks.

6.2.3 Production of virus working stocks

BHK or Vero cells growing in either 850 cm^2 roller bottles or 175 cm^2 flasks were infected with HSV-1 at 0.05-0.1 PFU/cell. The cells were incubated at 37 °C for two to three days until most has rounded up and could be detached by shaking. Cell-associated virus was obtained by harvesting the cells at 2000 rpm for 10 min at 4 °C (Beckman GH-3.8). The cell pellet was resuspended in a small volume of culture supernatant (1-2 ml per 175 cm^2 flask, 4-6 ml per 850 cm^2 roller bottle). Resuspended cell pellets were treated by sonication in iced water at 39% amplitude for 20 s using a cup-horn sonicator (Jencons) in order to liberate the viruses. 250 µl aliquots were stored at -70°C and the titres were determined by plaque assay on Vero cells.

6.2.4 Production of sucrose cushion purified HSV-1

Cells growing in 75 cm^2 flasks were infected with HSV-1 working stock at 10 PFU/cell. Infected cells were incubated in 10 ml DMEM growth medium per 75 cm^2 flask for ~24 hours. The cell culture supernatant was harvested and the cell debris removed by centrifugation at 1800 rpm for 15 min at 4 °C (Beckman GH-3.8). 9 ml of cleared culture supernatant was carefully overlaid onto a 2 ml cushion consisting of 33% (w/v) sucrose dissolved in PBS. Virus particles were harvested by centrifugation at 35000 rpm for 90 min at 4 °C (Beckman TLA-100.3) and resuspended in 50 µl SDS-PAGE loading buffer.

6.2.5 Gradient purified HSV-1 virions

Cells growing in 175 cm^2 flasks were infected either with HSV-1 at 0.01 PFU/cell. The cell culture medium was harvested three days after infection, and cellular debris was removed by low-speed centrifugation at 2000 rpm for 20 min at 4 °C (Beckman GH-3.8). Virus particles were pelleted at 18000 rpm for 2 hr at 4 °C (Beckman R19 rotor). The supernatant virus pellets were resuspended in 2 ml of PBS containing 1% fetal calf serum and layered onto a 30 ml 5 to 15% Ficoll 400 (in PBS) continuous gradient. After centrifugation at 12000 rpm for 90 min at 4 °C (Beckman SW 32 Ti), the visible band approximately in the middle of the gradient was collected carefully. The virus containing solutions were diluted in sterile PBS and harvested by centrifugation at 20000 rpm for 2 hr at 4 °C (Beckman SW 32 Ti). Virus pellets were resuspended in sterile PBS. The titres were determined by plaque assay on Vero cells and 20 µl aliquots were stored at -70 °C.

6.2.6 HSV-1 plaque assay and plaque size analysis

Infectious titres of wild-type HSV-1 or mutant viruses were determined by plaque assay on Vero cell monolayers in six-well plates. Ten-fold serial dilutions of virus samples were prepared with supplemented DMEM media. 0.5 ml of the virus dilutions were added to each well and incubated at 37 °C for one hour. Then each well was overlaid with two ml of DMEM solution containing 0.6% carboxymethyl cellulose, 2% FCS and antibiotics. After incubation for two to three days at 37 °C the monolayers were fixed in 3.7% formaldehyde in PBS for 20 min and then stained with 0.1% toluidine blue solution to visualise plaques in the cell layer. Plaques were counted using a plate microscope and the infectious virus titre was calculated as plaque forming units per ml (PFU/ml). For plaque size analysis, the plaques were scanned at 600 dpi and the diameters were determined by Adobe Photoshop in pixels.

6.2.7 Virus growth analysis

For single-step virus growth curves, cells were infected at 10 PFU/cell at 37 ºC for one hour. Unabsorbed viruses were inactivated with acid wash (Table 6.14) for 1 min at room temperature. Cells were washed 3 times in PBS and then cultured in complete media. At various times post infection, samples were harvested by scraping cells into the medium and liberating infectious viruses by sonication and then freezing at -70 ºC followed by thawing at 37 ºC. Infectious virus titres were determined by plaque assay on Vero cells. In multi-

step growth curves, cells were infected at 0.01 PFU/cell and the samples were treated as described above.

6.2.8 Western blot analysis and signal quantification

Cell lysates or purified virus samples were separated by SDS-PAGE followed by electro-transfer to nitrocellulose membrane. The presence of various proteins was determined by labelling with the primary and secondary antibodies (Table 6.3-6.4). The LI-COR Odyssey V3.0 software was used to calculate the integrated intensity for quantification.

6.2.9 Immunofluorescence microscopy

Vero cells were seeded on glass cover slips at a density of 2×10^5 cells per well in six-well dishes one day before infection. Cells were infected at 3 PFU/cell and washed in PBS. Depending on the purpose of the experiment, the infected cells were fixed at different times post infection in 3% paraformaldehyde in PBS for 10 min and then permeabilised in IF perm/quench solution (Table 6.10). After incubation in fresh IF perm/quench solution for 10-15min, the samples were incubated with IF blocking PGAS (Table 6.10) for at least 5min. Primary antibodies were appropriately diluted in PGAS and incubated for 45-60 min and then washed with PGAS for three times before the incubation with secondary antibodies (Alexa Fluor 488, 568 or 633-conjugated secondary antibody, 1:2000, Molecular Probes) in PGAS in the dark for about 30min. After three washes with PGAS, three washes with PBS and twice in water, the excess liquid was removed from the cover slips. The cell side of the cover slips were mounted in ProLong Gold antifade reagent with DAPI (4, 6-diamidino-2-phenylindole; Invitrogen) on glass slides. The samples were stored in drawer overnight before imaging on an Olympus IX70 microscope with a 60x oil immersion lens and a Retiga 2000R ccd camera. Images were acquired with the Q capture Pro software and processed with ImageJ (available from: http://rsbweb.nih.gov/ij/) and Photoshop (Adobe).

6.2.10 Virus penetration assay

Monolayers of Vero were chilled at 4 ºC for one hour followed by incubation with 300 PFU of purified viruses in ice cold HEPES (0.02 mM) buffered medium for one hour. The virus containing medium was removed followed by two ice cold PBS washes and the plates were incubated at 37 ºC. At various time points unabsorbed virus was inactivated by acid wash for one minute at room temperature followed by two PBS washes. For the zero minute time point, the acid wash was performed immediately at the end of the 4 ºC virus-

binding step. Samples that were not acid washed served as controls for input virus levels. The cells were overlaid with CMC and incubated at 37 ºC before fixing and staining as described above. Plaque numbers were counted for each time point and rate of penetration was calculated as the percentage of plaques produced at different time points in relation to the controls.

6.2.11 FACS

Vero cells were infected at 10 PFU/cell, harvested at 6 hpi and incubated with anti-gH/L (LP11, 1:2) or anti-gD (LP2, 1:2) antibodies on ice for one hour. After two ice cold PBS washes, the cells were incubated with Alexa Fluor® 488-conjugated goat anti-mouse (1:2000) on ice for one hour. Cells were washed and resuspended in cold PBS and analysed using a BD FACSort™ Cell Sorter. Data from 10000 cells for each sample were collected and the fluorescent signals were analysed using Software Summit 4.3.

6.2.12 Antibody internalisation assay

Vero cells grown on glass cover slips were infected at 10 PFU/cell. At 6 hpi the cells were incubated with anti-gH/L (LP11, 1:2), anti-gH (52S, 1:2) or anti-gD (LP2, 1:2) for one hour at 37 ºC in a humidified chamber. Cells were then washed in PBS, fixed in 3% formaldehyde, incubated in perm/quench solution for 10 min and blocked in PGAS before labelling with Alexa Fluor® 488-conjugated goat anti-mouse (1:2000). The samples were embedded and processed as described in 2.2.9.

6.2.13 Cloning

6.2.13.1 General conditions

Insertion fragments and plasmid backbone preparation

PCR reactions (Phusion High-Fidelity PCR Kit, NEB), DNA extraction (QIAquick Gel Extraction Kit, Qiagen), restriction enzyme digestions (NEB/Roch/Invitrogen), plasmid backbone de-phosphorylation (Antarctic Phosphatase, NEB), blunting sticky end (T4 polymerase, NEB), ligation (T4 ligase, NEB), plasmid miniprep (Wizard Plus SV Minipreps DNA Purification System, Promega) and plasmid midiprep (Nucleobond AX Xtra Midi, Macherey-Nagel) were all performed according to the manufacturer's instructions. All the clones obtained from PCR were sequenced (DNA Sequencing Facility, Department of Biochemistry, University of Cambridge) for confirmation. Some general conditions are listed in Table 6.16-6.18.

Table 6.16 PCR condition.

Reagent	Volume
HF/GC Buffer 5 ×	10 µl
dNTP (10 mM)	1 µl
Forward primer (5 µM)	5 µl
Reverse primer (5 µM)	5 µl
Template (plasmid, ~200 ng/µl)	1 µl
DNA polymerase	0.5 µl
DMSO (for GC rich amplicons)	1.5 µl
Betaine (2 M)*	25 µl
H_2O	Top up to 50 µl

*Betaine was only added into the reactions with high non-specific products.

Table 6.17 PCR program.

Temperature	Time	
98 °C	30 s	
98 °C	10 s	25 cycles
58 °C	30 s	
72 °C	15-30 s per kb	
72 °C	10 min	
4 °C	-	End

Table 6.18 Ligation condition.

Reagent	Volume	Others
PCR product	7 µl	The ligation mixture was incubated at 10 °C for overnight or longer.
Plasmid backbone	1 µl	
10 × buffer	1 µl	
T4 ligase	1 µl	

Competent DH5α preparation

Single colony of *E.coli* strain DH5α was inoculated in 3-4 ml of antibiotic free 2YT for a starter culture and incubated with shaking at 37 °C overnight. The start culture was inoculated into fresh 2YT with 100-fold dilution for an initial culture and incubated with shaking at 37 °C for 3 h. The bacteria were harvested by centrifugation at 4000 rpm for 10 min and the pellet was resuspended in ice cold CCMB (Table 6.15, one fourth of the initial culture volume) followed by incubation on ice for 4 h and centrifugation at 4000 rpm for 10 min at 4 °C. The pellet was resuspended in ice cold CCMB (one twelfths of the initial culture volume) and aliquots were stored at -70 °C. To test the competence, 10 pg of pUC19 was transformed into 50 µl of the competent DH5α and the colonies formed on

selective agar were counted to calculate the competence as colonies per μg of plasmid. A good competence is around 10^7 colonies/ μg.

Transformation

Frozen competent DH5α were thawed on ice and 3-5 μl of the ligation mixture was mixed with 50 μl competent DH5α. After 30 min incubation on ice, the bacteria were heat shocked at 42 °C for 30 sec and chilled on ice. 300 μl of pre-warmed SOC media was added and the bacteria were incubated with shake at 37 °C for 1 h. The culture was then plated onto selective agar and incubated at 37 °C overnight to form visible colonies.

6.2.13.2 Tegument gene cloning for Y2H assays

The plasmids containing KOS EcoRI fragments were used as templates (Table 6.5). Primers for tegument gene cloning were designed by Dr C. Crump according to the online sequence of HSV-1 strain 17 (NC_001806) with appropriate enzyme sites (Table 6.6). Tegument gene fragments were obtained by PCR and DNA gel electrophoresis followed by gel extraction. The PCR products were subjected to restriction enzyme digestions, ligation with plasmid backbones and transformation into competent DH5α. Colonies formed under selective culture conditions were amplified for plasmid mini prep. The new constructs were confirmed by restriction enzyme digestions before sending for sequencing and the sequencing results are shown in the appendix.

6.2.13.3 ICP0 cDNA sub-cloning

The ICP0 constructs for Y2H was sub-cloned from plasmid pT7-111 (containing HSV-1 strain 17 ICP0 cDNA) into pGBKT7 via NcoI and BamHI sites. In order to sub-clone ICP0 cDNA from pGBKT7 into pHB18, pGBKT7-ICP0 was cut by enzyme NcoI before creating a blunt end by Klenow fragment for the 5' end of the ICP0 cDNA fragment (Table 6.19). The DNA was quick purified (QIAquick Gel Extraction Kit, Qiagen). As there is a SalI site near the 3' end of ICP0 in addition to a SalI site in the pGBKT7 multiple cloning site, the NcoI digested and blunted pGBKT7-ICP0 was partially digested by SalI (2 μg DNA per unit of enzyme, incubated at 37 °C for 10 min followed by inactivation at 65 °C for 20 min). The resulting ICP0 fragment was cut from DNA gel, purified and then ligated into pHB18 that had been cut with EcoRI enzyme, blunted the EcoRI sticky end and then cut with XhoI. Positive clones were sequenced to confirm the presence of an intact ICP0 cDNA (appendix).

Table 6.19 Conditions for blunt reaction.

Reagent	Volume	Others
NcoI digestion reaction (5 μg plasmid, NEB buffer 3)	100 μl	Incubation at room temperature for 25-50 min.
dNPT (10 mM)	0.4 μl	
Klenow fragment	10 μl	

6.2.13.4 Full length CC2D1B cloning

For the full length CC2D1B cloning, the primers were designed according to the online sequence (Gene ID: 200014) with appropriate enzyme sites (Table 6.8). Human total cDNA library (prepared by Dr C. Crump) were used as the template. As the RCP reactions often had high non-specific background, betaine (Table 6.16) was added to improve the specificity. The PCR products were processed as described above. Positive clones were confirmed by sequencing (appendix).

6.2.13.5 CIN85 domain cloning

Primers for CIN85 domain constructs were designed with appropriate enzyme sites according to the full length CIN85 sequence and the reported aa positions of different domains (Zhang *et al.*, 2009b) (Table 6.8). Plasmid containing full length CIN85 gene (pHB18-CIN85) was used as the template. The cloning was performed as described above and positive clones were confirmed by sequencing.

6.2.14 Yeast two-hybrid

6.2.14.1 Preparation of competent yeast cells

Yeast colonies were inoculated in YPD broth for starter cultures and incubated with shake at 30°C overnight. The start culture was inoculated into fresh YPD broth with 8-fold dilution and grown at 30 °C for ~3.5 h until OD_{600} nm (1 cm cuvette) reach between 0.5 and 0.7. The yeast cells were harvest the by centrifugation at 1800 rpm for 10 min at room temperature (Megafuge 1.0R) and washed in water. The yeast pellet was resuspended in LiAc working solution (Table 6.12) and incubated at room temperature for 1.5 h. The volume of LiAc working solution = 0.5 × OD_{600} × yeast culture volume (ml). Aliquots of competent yeast suspension were stored at -70 °C.

6.2.14.2 Yeast transformation

For one reaction, 3 μl of single stranded DNA (ssDNA) from salmon testes (D9156, Sigma) was boiled for 8min and chilled on ice for 5min. 30 μl of the competent yeast cell

solution was mixed with the denatured ssDNA and 1 μg each of prey and bait plasmids. 230 μl of PEG working solution was added (Table 6.12) and mixed by vortex. The mixture was incubated at 30 °C for 45 min followed by heat shock at 42 °C for 15 min. Yeast cells were plated directly on SD agar plates containing yeast synthetic drop-out medium supplement without Leucine and Tryptophan and incubate at 42 °C for 3 days to form visible colonies.

6.2.14.3 Measuring β-Gal activity in yeast colonies

Yeast colonies were scraped off SD agar plates and resuspended in 250 μl Working buffer (Table 6.12). 25 μl of chloroform and 25 μl of CPRG solution (Table 6.12) were added and mixed by vortex. After incubation at room temperature for 30 min, the solution was clarified by centrifugation at 13000 rpm for 30 sec (Bench top centrifuge). 100 μl of each supernatant was transferred into 96-well plates and OD_{550} (or OD_{540}) measured in a microplate spectrophotometer.

6.2.15 Preparation of cell lysates

Cell samples for protein analysis were harvested by scraping into PBS and centrifugation at 4000 rpm for 5 min at 4°C in a bench-top centrifuge. Cell pellets were resuspended in mRIPA (Table 6.15) supplemented with protease inhibitor cocktail (Roche) and incubated on ice for 20 min. Cell debris and nuclei were removed by centrifugation at 13000 rpm for 15 min at 4°C in a bench-top centrifuge. The supernatants were collected and mixed with SDS-PAGE loading buffer (Table 6.10) and denatured in a boiling water bath for 5 min before separating by SDS-PAGE.

6.2.16 GST pull-down assay

293T cells were seeded into six-well plates at 6×10^5 cells per well and incubated at 37 °C overnight. Combinations of GST and GFP plasmids (0.5 μg each) were co-transfected by TransIT-LT1 (Mirus) according to the manufacture instructions. Cells were examined under a fluorescent microscope at 24-48 h post infection to examine GFP singles and harvested at 48 h post transfection by scrapping into PBS followed by centrifugation at 5000 rpm for 5 min at 4 °C. Cells from one well were lysed in 1 ml of ice cold lysis buffer (Table 6.14) supplemented with protease inhibitor cocktail (complete mini-EDTA free, Roche) and incubated on a rotating wheel at 4°C for 20 min. Cell lysates were clarified by centrifugation at 13000 rpm for 15 min at 4°C. 50 μl of the supernatant was retained to test protein expression levels in Western blotting. The rest of the supernatant was

incubated with 25 µl of bead suspension [Glutathione-Sepharose beads (GE Healthcare) that had been washed three times in ice cold wash buffer (Table 6.14) and resuspended in wash buffer (50% v/v)] on a rotating wheel at 4 °C for 3 h or longer. Beads fractions were harvested by centrifugation and washed three times in ice cold wash buffer. After the final wash, proteins in the beads fractions were eluted by resuspending in 50-100 µl of SDS sample buffer and incubating in a 98 °C water bath for 5 min. Samples were separated by SDS-PAGE gels (10 µl per lane) and examined using anti-GFP and anti-GST antibodies by Western blotting.

6.2.17 Co-immunoprecipitation

To preparae the protein A-Sepharose for co-immunoprecipitation, 100 mg of protein A-Sepharose was suspended in 2-3 ml of 25 mM Tris pH7.6 at 4 °C overnight. The supernatant was removed and the beads were resuspended in 350 µl of 25 mM Tris pH7.6.

HeLa cells were seeded in T75 flasks and infected with HSV-1 at 5 PFU/cell in 2 ml of media per flask at 37 °C for 1 h. The virus inocula were removed followed by a brief wash in PBS. Cells were incubated in complete DMEM at 37 °C and harvested at 24 hpi by scrapping. Mock infected cells were used as controls. Cells lysates were prepared as described in 6.2.16 and 200 µl of lysate from ~1 × 10^6 cells were incubated with each antibody on rotating wheel at 4 °C for 5 h or longer followed by incubation with protein A-Sepharose beads at 4 °C for 3 h or longer. The beads were harvested by centrifugation and washed three times in ice cold wash buffer (Table 6.14). After the final wash, proteins in the bead fractions were eluted by resuspending in 40 µl of SDS-PAGE loading buffer (Table 6.10) and incubating at 98 °C 5 min. Samples were separated by SDS-PAGE gels and analysed in Western blotting.

6.2.18 Protein co-localisation assay

HeLa cells were seeded in 24-well plates on cover slips at a density of 2 × 10^4 cells per well and incubated overnight at 37 °C with 5% CO_2. The cells were co-transfected with plasmids expressing GFP and Cherry tagged proteins (0.2 µg each for one well) using TransIT-LT1 (Mirus) according to the manufacturer's instructions. At 24 h post transfection, the cells were washed in PBS and fixed in 3% paraformaldehyde for 10 min. After three washes with PBS and twice with water, the excess liquid was removed and the cover slips were mounted and imaged as described in section 6.2.9.

6.2.19 Nucleic acid isolation

DNA and RNA were routinely purified according to the manufacturer's instructions using the following products: 1) Wizard Plus SV Minipreps DNA Purification System (Promega) for DNA Mini prep. 2) Nucleobond AX Xtra Midi (Macherey-Nagel) for DNA Midi prep. BAC DNA mini/midi preparation was performed by phenol and chloroform extraction. Briefly, the bacteria were harvested from 10 ml overnight culture by centrifugation at 3000 rpm for 10 min (Megafuge 1.0R). The pellet was resuspended in 200 µl of buffer P1 (supplemented with RNase A), lysed in 300 µl of buffer P2 and neutralised in 300 µl of buffer P3 (the P1, P2 and P3 buffers are from Qiagen). Samples were gently inverted for mixing and incubated on ice for 10 min before clarified by centrifugation at 13000 rpm for 10 min at 4 °C (bench-top centrifuge). The supernatant was transferred into tubes containing equal volume of phenol and chloroform (300 µl) and inverted gently for mixing. After centrifugation at 13000 rpm for 10 min, 700 µl of the top aqueous phase was transferred into a new tube, 800 µl of isopropanol for DNA precipitation. After incubation on bench for at least 5 min, the DNA was harvested by centrifugation at 13000 rpm for 10 min and the pellet was washed in 70% ethanol. The DNA was dissolved in 40 µl of EB (Qiagen) after drying.

For high molecular weight DNA preparation, Vero cells were infected in T75 flasks at 1 PFU/cell. At 26 hpi 5 ml of lysis mixture (Table 6.13) was added to lyse cells and the samples were incubated overnight at 37 °C with 5% CO_2. The high molecular weight DNA was extracted by phenol and chloroform extraction as described above. The DNA was precipitated by ethanol (NaCl was added with a final concentration of 0.1 M to facilitate the precipitation), spooled out using a glass pipette, dried at room temperature and dissolved in EB buffer.

6.2.20 Generation of stable cell lines

293T cells were seeded into six-well plates at a density of 1×10^6 cells per well and incubated at 37 °C incubator overnight. Cells in each well were transfected with 3 µg of plasmids mixture (0.5 µg plasmid expressing VSV G, 1.5 µg plasmid expressing Gag Pol and 1 µg plasmid pCMS28-YFP-CC2D1A or pCMS28-YFP-CC2D1B, plasmids are from J. Marin-Serrano at KCL, Table 6.5). The mixture of the plasmids, 150 µl of serum free DMEM and 12 µl of PEI (Table 6.15) was incubated for 10-15 min before adding to the cells. The culture medium was changed 1 day post transfection and 1 ml/well fresh medium was added for incubation. HaCaT cells were seeded into six-well plates at 1×10^5

cells per well and incubated overnight. The 293T culture supernatant was collected at 48 h post transfection, filtered through a sterile filter (0.2 μm) and supplemented with polybrene (10 μg/ml) before adding to the polybrene pre-treated (10 μg/ml, ~6 h) HaCaT cells. After incubation at 37 °C for one hour, 2 ml/well fresh DMEM was added and the cells were incubated for 24 h before the medium was changed. The cells were maintained in 200 ng/ml puromycin for selecting positive transduced cells. Fluorescent signals are examined (signals could be observed in 3 days) and cell lysates were prepared for western blotting to confirm the overexpression of YFP tagged CC2D1A or CC2D1B proteins using anti-GFP.

6.2.21 Chemical fixation of culture cells for TEM

293T cells were harvested by scrapping off the culture dishes and pelleted by centrifugation in a bench-top centrifuge at 4000 rpm for 5 min. The cells were gently rinsed in TEM saline (Table 6.11, phosphate and calcium free) and resuspended in TEM fix (Table 6.11) for 2-4 h on ice. After fixation, the cells were rinsed five times in ice cold TEM wash (Table 6.11) followed by centrifugation in a bench-top centrifuge at 13000 rpm for 5 min and stored at 4 °C overnight. The cells were then processed and sectioned by Dr J. Skepper at the Multi-Imaging Centre, Department of Physiology Development and Neuroscience, University of Cambridge. Briefly, the cells were treated with 1% osmium ferricyanide at room temperature for 2 h and then rinsed five times in deionised water and treated with 2% uranyl acetate in 0.05M maleate buffer at pH 5.5 for 2 h at room temperature. They were again rinsed in deionised water and dehydrated in an ascending series of ethanol solutions from 70% to 100%. This was followed by treatment with 2 changes of dry acetonitrile and infiltration with Quetol epoxy resin.

6.2.22 siRNA treatment and HSV-1 infection

293T and HeLa cells were seeded in antibiotic-free DMEM medium at a density of 4×10^5 and 2×10^5 cells per well of a six-well plate, respectively. Two hours post seeding, or on the following day, cells were transfected with a maximum of 100 nM total siRNA in Opti-MEM I (Gibco) using DharmaFECT 1 (Dharmacon) according to the manufacturer's instructions. If a second siRNA was performed, cells were split at 48 h post the first transfection, followed by the second siRNA transfection at 2 h post seeding. At 24 h post the second siRNA transfection, the cells were split to 24-wells for infection or 6-wells for cell lysate preparation. Cells were infected with HSV-1 at 5-10 PFU/cell at 37 °C for 1 h. Acid wash was performed at room temperature for 1 min followed by three PBS washes and the cells were incubated in fresh media. The cell samples for lysate preparation were

harvested immediately after infection for Western blot analysis. Infected cell samples were harvested between 16 and 24 hours post infection, and cell-associated viruses were liberated by freeze-thawing and sonication for 20 s at 39% amplitude. Infectious titres were determined by plaque assay on Vero cells as described in Section 6.2.6.

7 Appendix

7.1 DNA sequences

7.1.1 HSV-1 KOS tegument gene sequences

UL4

ATGTCCAATCCACAGACGACCATCGCGTATAGCCTATGCCACGCCAGGGCCT
CGCTGACCAGCGCACTGCCCGACGCCGCGCAGGTGGTGCATGTTTTTGAGT
ACGGCACCCGCGCGATCATGGTACGGGGCCGGGAGCGCCAGGACCGCCTG
CCGCGCGGAGGCGTTGTTATCCAGCACACCCCCATTGGGCTGTTGGTGATT
ATCGACTGTCGCGCCGAATTTTGTGCCTACCGCTTTATAGGCCGGGACAGCA
ACCAGAAGCTCGAACGCGGGTGGGACGCCCATATGTACGCGTATCCGTTCG
ACTCCTGGGTCAGCTCCTCGCGCGGCGAAAGCGCCCGGAGCGCCACGGCCG
GCATTTTGACCGTGGTCTGGACCGCGGACACCATTTACATCACTGCAACCAT
TTACGGGTCGCCCCCAGAGGAGACGCCAGGCGCGGCACACGGGGTGGGCG
CCGCGCCTCCACCCCCGACAACCGCCTGCCCCGGGACGGCCGAGTTTCTCCA
GCCCACCGCGGACCTGCTGGTAGAGGTGCTGCGGGAGATTCAACTGAGCCC
CACCCTGGAATACGCAGACAAACTTTTGGGGTCCTAG

UL7

ATGGCCGCCGCGACGGCCGACGATGAGGGGTCGGCCGCCACCATCCTCAAG
CAGGCCATCGCCGGGGACCGCAGCCTGGTCGAGGCGGCCGAGGCGATTAG
CCAGCAGACGCTGCTCCGCCTGGCATGCGAGGTGCGCCAGGTCGGCGACCG
CCAGCCGCGGTTTACCGCCACCAGCATCGCGCGCGTCGACGTCGCGCCTGG
GTGCCGGTTGCGGTTCGTTCTGGACGGGAGTCCCGAGGACGCCTATGTGAC
GTCGGAGGATTACTTTAAGCGCTGCTGCGGCCAGTCCAGTTATCGCGGCTT
CGCGGTGGCGGTCCTGACGGCCAACGAGGACCACGTGCACAGCCTGGCCGT
GCCCCCCCTCGTTCTGCTGCACCGGTTCTCCCTGTTCAACCCCAGGGACCTCC
TGGACTTTGAGCTTGCCTGTCTGCTGATGTACCTGGAGAACTGCCCCCGAAG
CCACGCCACCCCGTCGACCTTTGCCAAGGTTCTGGCGTGGCTCGGGGTCGC
GGGTCGCCGCACGTCCCCATTCGAACGCGTTCGCTGCCTTTTCCTCCGCAGT
TGCCACTGGGTCCTAAACACACTCATGTTCATGGTGCACGTAAAACCGTTCG

ACGACGAGTTCGTCCTGCCCCACTGGTACATGGCCCGGTACCTGCTGGCCAA
CAACCCGCCCCCCCGTTCTCTCGGCCCTGTTCTGTGCCACCCCGACGAGCTCCT
CATTCCGGCTGCCGGGGCCGCCCCCCCGCTCCGACTGCGTGGCCTATAACCC
CGCCGGGATCATGGGGAGCTGCTGGGCGTCGGAGGAGGTGCGCGCGCCTC
TGGTCTATTGGTGGCTTTCGGAGACCCCAAAACGACAGACGTCGTCGCTGTT
TTATCAGTTTTGTTGA

UL11

ATGGGCCTCTCGTTCTCCGGGACCCGGCCCTGCTGCTGCCGAAACAACGTCC
TCATCACCGACGACGGGGAGGTCGTCTCGCTGACCGCCCACGACTTTGACGT
CGTGGATATCGAGTCCGAAGAGGAAGGTAATTTCTACGTGCCCCCGGATAT
GCGCGGGGTTACGCGGGCCCCGGGGAGACAGCGCCTGCGTTCGTCGGATC
CCCCCTCGCGCCACACTCACCGGCGAACCCCCGGAGGCGCCTGCCCCGCCAC
CCAGTTTCCACCCCCCATGTCCGATAGCGAATAA

UL13

ATGGATGAGTCCCGCAGACAGCGACCTGCTGGTCATGTGGCAGCTAACCTC
AGCCCCCAAGGTGCACGCCAACAGTCCTTCAAGGATTGGCTCGCATCCTACA
TACACTCCAACCCACACGGGGCCTCCGGGCGCCCCAGCGGCCCCTCTCTCCA
GGACGCCGCCGGCTCCCGCTCCTCCCACGGGTCCCGCCACCGATCCGGCCTC
CGCGAGCGGCTTCGCGCGGGACTATCCCGATGGCGAATGAGCCGCTCGTCT
CATCGCCGCGCGTCCCCCGAGACGCCCGGTACGGCGGCCAAACTGAACCGC
CCGCCCCTGCGCAGATCCCAGGCGGCGTTAACCGCACCCCCCTCGTCCCCCT
CGCACATCCTTACCCTCACGCGCATCCGCAAGCTATGCAGCCCCGTGTTCGCC
ATCAACCCCGCCCTACACTACACGACCCTCGAGATCCCCGGGGCCCGAAGCT
TCGGGGGGTCTGGGGGATACGGCGACGTCCAACTGATTCGCGAACATAAG
CTTGCCGTTAAGACCATAAAGGAAAAGGAGTGGTTTGCCGTTGAGCTCATC
GCGACCCTGTTGGTCGGGGAGTGCGCTCTACGCGCCGGCCGCACCCACAAC
ATCCGCGGCTTCATCGCGCCCCTCGGGTTCTCGCTGCAACAACGACAGATAG
TGTTCCCCGCGTACGACATGGACCTCGGTAAGTATATCGGCCAACTGGCGTC
CCTGCGCACAACAAACCCCTCGGTCTCGACGGCCCTCCACCAGTGCTTCACG
GAGCTGGCCCGCGCCGTTGTGTTTTTAAACACCACCTGCGGGATCAGCCACC
TGGATATCAAGTGCGCCAACATCCTCGTCATGCTGCGGTCGGACGCCGTCTC
GCTCCGGCGGGCCGTCCTCGCCGACTTTAGCCTCGTCACCCTCAACTCCAACT
CCACGATCGCCCGGGGGCAGTTTTGCCTCCAGGAGCCGGACCTCAAGTCCCC

CCGGATGTTTGGCATGCCCACCGCCCTAACCACAGCCAACTTTCACACCCTG
GTGGGTCACGGGTATAACCAGCCCCCGGAGCTGTTGGTGAAATACCTTAAC
AACGAACGGGCCGAATTTACCAACCACCGCCTGAAGCACGACGTCGGGTTA
GCGGTTGACCTGTACGCCCTTGGCCAGACGCTGCTGGAGTTGGTGGTTAGC
GTGTACGTCGCCCCGAGCCTGGGCGTACCCGTGACCCGGTTTCCCGGTTACC
AGTATTTCAACAACCAGCTGTCGCTGGACTTCGCCCTGGCCCTGCTCGCCTA
TCGCCGCGTGCTGCACCCAGCCCTGTTTGTCAACTCGGCCGAGACCAACACC
CACGGCCTGGCGTATGACGTCCCAGAGGGCATCCGGCGCCACCTCCGCAAT
CCCAAGATTCGGCGCGCGTTTACGGATCGGTGTATAAATTACCAGCACACAC
ACAAGGCGATACTGTCGTCGGTGGCGCTGCCTCCCGAGCTTAAGCCTCTCCT
GGTGCTGGTGTCCCGCCTGTGTCACACCAACCCGTGCGCGCGGCACGCGCT
GTCGTGA

UL14

ATGGACCGAGATGCCGCCCACGCGGCCCTGCGCCGACGCCTGGCCGAGACG
CACCTCCGAGCCGAGATTTACAAGGACCAGACCCTGCAGCTGCACCGGGAG
GGCGTCAGCACCCAAGATCCTCGGTTTGTTGGCGCCTTTATGGCTGCAAAG
GCGGCCCACTTGGAATTGGAGGCGCGGCTAAAGTCCCGCGCGCGCTTAGAG
ATGATGCGACAGCGCGCGACCTGTGTTAAAATTCGCGTGGAGGAGCAAGCG
GCGCGTCGTGACTTTCTAACCGCACACCGACGGTACCTCGATCCGGCGCTTG
GTGAGCGCCTGGACGCCGTGGACGATCGTCTTGCGGACCAGGAGGAGCAA
CTCGAGGAAGCAGCGACCAACGCTTCTCTGTGGGAAGACGGCGACCTGGCC
GAAGGATGGATGAGTCCCGCAGACAGCGACCTGCTGGTCATGTGGCAGCTA
ACCTCAGCCCCCAAGGTGCACGCCAACAGTCCTTCAAGGATTGGCTCGCATC
CTACATACACTCCAACCCACACGGGGCCTCCGGGCGCCCCAGCGGCCCCTCT
CTCCAGGACGCCGCCGGCTCCCGCTCCTCCCACGGGTCCCGCCACCGATCCG
GCCTCCGCGAGCGGCTTCGCGCGGGACTATCCCGATGGCGAATGA

UL16

ATGGCGCAGCTGGGACCCCGGCGGCCCCTGGCGCCGCCTGGTCCCCCGGG
GACCTTGCCCCGGCCGGATTCCCGGGCCGGAGCTCGCGGCACGCGCGACAG
AGTCGACGACCTGGGGACGGACGTCGACTCTATCGCGCGCATTGTCAACTC
CGTCTTTGTGTGGCGCGTCGTTCGGGCGGACGAGCGGCTCAAGATCTTTCG
GTGTCTAACGGTCCTCACCGAGCCTCTGTGTCAGGTGGCCCTTCCTAACCCA
GACCCCGGGCGCGCCCTCTTCTGCGAGATTTTTCTGTATCTGACGCGCCCCA

AGGCGCTGCGGTTGCCCCCGAACACCTTCTTTGCCCTCTTTTTCTTTAACCGC
GAGCGCCGCTACTGCGCGATCGTCCACCTCCGGAGCGTGACGCACCCCCTG
ACCCCGCTCCTGTGCACCCTCACGTTCGCCCGCATACGGGCGGCCACCCCCC
CGGAGGAAACCCCCGACCCAACCACCGAACAGCTCGCGGAGGAGCCAGTGG
TCGGCGAGCTGGATGGCGCGTATCTGGTCCCCGCGAAGACCCCCCCGGAGC
CGGGCGCGTGTTGCGCCTTGGGCCCGGGGGGCCTGGTGGCACCTCCCCAGC
GGCCAGATCTACTGCTGGGCCATGGACAGCGACCTGGGGTCGCTCTGTCCA
CCGGGAAGCAGGGCCCGCCATCTGGGATGGCTCCTGGCCAGGATCACCAAC
CACCCGGGGGGCTGCGAGTCCTGCGCCCCGCCGCCCCACATCGATTCCGCCA
ACGCACTGTGGCTCTCCTCCGTCGTAACGGAGTCCTGTCCCTGCGTCGCCCC
GTGTCTGTGGGCCAAGATGGCCCAGTGTACCCTGGCGGTCCAGGGGGATG
CTAGCCTGTGTCCGCTTCTCTTTGGCCATCCCGTGGATACGGTCACCCTGCT
GCAGGCCCCCCGCCGTCCTTGCATCACGGACCGTCTGCAAGAGGTCGTCGG
GGGACGGTGCGGCGCGGACAACATCCCCCCGACCAGCGCCGGGTGGCGCC
TGTGTGTCTTCTCTTCGTACATCAGTCGCCTATTTGCTACGAGTTGCCCCACA
GTTGCCCGGGCCGTTGCCCGGGCCTCCTCAAGCGATCCCGAATAA

UL21

ATGGAGCTTAGCTACGCCACCACCATGCACTACCGGGACGTTGTGTTTTACG
TCACAACGGACCGAAACCGGGCCTACTTTGTGTGCGGGGGGTGTGTTTATT
CCGTGGGGCGGCCGTGTGCCTCGCAGCCCGGGGAGATTGCCAAGTTTGGT
CTGGTCGTTCGAGGGACAGGCCCAGACGACCGCGTGGTCGCCAACTATGTA
CGAAGCGAGCTCCGACAACGCGGCCTGCAGGACGTGCGTCCCATTGGGGA
GGACGAGGTGTTTCTGGACAGCGTGTGTCTTCTAAACCCGAACGTGAGCTC
CGAGCTGGATGTGATTAACACGAACGACGTGGAAGTGCTGGACGAATGTCT
GGCCGAGTACTGCACCTCGCTGCGAACCAGCCCGGGTGTGCTAATATCCGG
GCTGCGCGTGCGGGCGCAGGACAGAATCATCGAGTTGTTTGAACACCCAAC
GATAGTCAACGTTTCCTCGCACTTTGTGTATACCCCGTCCCCATACGTGTTCG
CCCTGGCCCAGGCGCACCTCCCCCGGCTCCCGAGCTCGCTGGAGGCCCTGGT
GAGCGGCCTGTTTGACGGCATCCCCGCCCCACGCCAGCCACTTGACGCCCAC
AACCCGCGCACGGATGTGGTTATCACGGGCCGCCGCGCCCCACGACCCATC
GCCGGGTCGGGGGCGGGGTCGGGGGGCGCGGGCGCCAAGCGGGCCACCG
TCAGCGAGTTCGTGCAAGTCAAACACATTGACCGCGTGGGCCCCGCTGGCG
TTTCGCCGGCGCCTCCGCCAAACAACACCGACTCAAGTTCCCTGGTGCCCGG
GGCCCAGGATTCCGCCCCGCCCGGCCCCACGCTAAGGGAGCTGTGGTGGGT

GTTTATGCCGCAGACCGGGCGCTGGAGGAGCCCCGCGCCGACTCTGGCCT
CACCCGCGAGGAGGTACGTGCCGTACGTGGGTTCCGGGAGCAGGCGTGGA
AACTGTTTGGCTCCGCGGGGGCCCCGCGGGCGTTTATCGGGGCCGCGTTG
GGCCTGAGCCCCCTCCAAAAGCTAGCCGTTTACTACTATATCATCCACCGAG
AGAGGCGCCTGTCCCCCTTCCCCGCGCTAGTCCGGCTCGTAGGCCGGTACAC
ACAGCGCCACGGCCTGTACGTCCCTCGGCCCGACGACCCAGTCTTGGCCGAT
GCCATCAACGGGCTGTTTCGCGACGCGCTGGCGGCCGGAACCACAGCCGAG
CAGCTCCTCATGTTCGACCTTCTCCCCCCAAAGGACGTGCCGGTGGGAAGCG
ACGTGCAGGCCGACAGCACCGCTCTGCTGCGCTTTATAGAATCGCAACGTCT
CGCCGTCCCCGGGGGGGGTGATCTCCCCCGAGCACGTCGCGTACCTTGGTGC
GTTCCTGAGCGTGCTGTACGCTGGCCGCGGGCGCATGTCCGCAGCCACGCA
CACCGCGCGGCTGACAGGGGTGACCTCCCTGGTGCTAGCGGTGGGTGACG
TGGACCGTCTTTCCGCGTTTGACCGCGGAGCGGCGGGCGCGGCCAGCCGCA
CGCGGGCCGCCGGGTACCTGGATGTGCTTCTTACCGTTCGTCTCGCTCGCTC
CCAACACGGACAGTCTGTGTAA

UL23

ATGGCTTCGTACCCCTGCCATCAACACGCGTCTGCGTTCGACCAGGCTGCGC
GTTCTCGCGGCCATAGCAACCGACGTACGGCGTTGCGCCCTCGCCGGCAGC
AAGAAGCCACGGAAGTCCGCCTGGAGCAGAAAATGCCCACGCTACTGCGGG
TTTATATAGACGGTCCTCACGGGATGGGGAAAACCACCACCACGCAACTGCT
GGTGGCCCTGGGTTCGCGCGACGATATCGTCTACGTACCCGAGCCGATGAC
TTACTGGCAGGTGCTGGGGGCTTCCGAGACAATCGCGAACATCTACACCAC
ACAACACCGCCTCGACCAGGGTGAGATATCGGCCGGGGACGCGGCGGTGG
TAATGACAAGCGCCCAGATAACAATGGGCATGCCTTATGCCGTGACCGACGC
CGTTCTGGCTCCTCATATCGGGGGGGAGGCTGGGAGCTCACATGCCCCGCC
CCCGGCCCTCACCCTCATCTTCGACCGCCATCCCATCGCCGCCCTCCTGTGCT
ACCCGGCCGCGCGATACCTTATGGGCAGCATGACCCCCCAGGCCGTGCTGG
CGTTCGTGGCCCTCATCCCGCCGACCTTGCCCGGCACAAACATCGTGTTGGG
GGCCCTTCCGGAGGACAGACACATCGACCGCCTGGCCAAACGCCAGCGCCC
CGGCGAGCGGCTTGACCTGGCTATGTTGGCCGCGATTCGCCGCGTTTACGG
GCTGCTTGCCAATACGGTGCGGTATCTGCAGGGCGGCGGGTCGTGGCGGG
AGGATTGGGGACAGCTTTCGGGGACGGCCGTACCGCCCCAGGGTGCCGAG
CCCCAGAGCAACGCGGGCCCACGACCCCATATCGGGGACACGTTATTTACCC
TGTTTCGGGCCCCCGAGTTGCTGGCCCCCAACGGCGACCTGTATAACGTGTT

TGCCTGGGCCTTGGACGTCTTGGCCAAACGCCTCCGTCCCATGCACGTCTTT
ATCCTGGATTACGACCAATCGCCCGCCGGCTGCCGGGACGCCCTGCTGCAAC
TTACCTCCGGGATGGTCCAGACCCACGTCACCACCCCAGGCTCCATACCGAC
GATCTGCGACCTGGCGCGCACGTTTGCCCGGGAGATGGGGGAGGCTAACT
GA

UL36

ATGATCGCGGGCACCCCACCGCACTCCACGATGGAACGCGGGGGGGATCGC
GACATCGTGGTCACCGGTGCTCGGAACCAGTTCGCGCCCGACCTGGAGCCG
GGGGGGTCGGTATCGTGCATGCGCTCGTCGCTGTCCTTTCTCAGCCTCATAT
TTGATGTGGGCCCTCGCGACGTTCTGTCCGCGGAGGCCATCGAGGGATGTT
TGGTCGAGGGGGGCGAGTGGACGCGCGCGACTGCGGGCCCTGGGCCGCC
GCGCATGTGTTCGATCGTCGAGCTCCCCAACTTCCTCGAGTACCCAGGGGCG
CGCGGCGGACTGCGCTGTGTCTTCTCGCGCGTATACGGCGAGGTGGGCTTC
TTCGGGGAGCCCGCGGCAGGCCTGCTGGAGACACAATGCCCCGCACACACG
TTCTTCGCCGGCCCGTGGGCCCTGCGCCCCCTGTCGTACACGCTCCTAACCA
TTGGCCCCCTAGGGATGGGGCTGTTCAGGGACGGCGACACCGCATACCTTT
TTGACCCGCATGGCCTTCCGGAGGGCACCCCCGCGTTCATCGCCAAAGTGCG
GGCGGGGGGACATGTATCCATACCTGACGTATTACACCCGCGATCGCCCGGA
CGTACGGTGGGCGGGAGCCATGGTGTTTTTCGTGCCGTCGGGCCCGGAACC
CGCGGCTCCTGCGGACTTGACGGCCGCGGCTCTGCATCTTTACGGGGCCAG
CGAGACTTACATGCAGGACGAAgCGTTCAGCGAACGGCGCGTGGCCATCAC
GCACCCCCTGCGGGGCGAGATCGCGGGCCTGGGGGAGCCCTGCGTCGGCG
TGGGCCCCCGGGAGGGGGGAGGGGGGCCGGGGCCACACCCGCCCACAGC
CGCCCAGTCGCCGCCACCGACCCGGGCCCGTCGCGACGACAGGGCCTCCGA
GACATCCCGGGGGGACGGCCGGTCCGTCGGCAAAACCAGAGGCCAAGCGCCC
GAATCGGGCGCCCGACGATGTATGGGCGGTGGCCCTAAAGGGTACCCCACC
CACGGATCCCCCCTCCGCCGACCCACCCTCCGCGATCCCACCACCGCCTCCCT
CCGCCCCCAAGACCCCCGCCGCAGAGGCGGCCGAAGAAGATGACGACGACA
TGCGGGTCCTGGAGATGGGCGTCGTCCCGGTTGGTCGGCACCGGGCACGC
TACTCGGCCGGCCTTCCCAAGCGCCGCCGACCCACCTGGACTCCGCCTTCCA
GCGTCGAAGACCTGACTTCGGGGGAGAAAACGAAACGCTCGGCCCCCCCTG
CCAAAACCAAGAAGAAATCCACCCCCAAAGGCAAAACCCCCGTCGGGGCCGC
GGTCCCCGCCTCCGTTCCGGAGCCTGTCCTCGCCTCGGCACCCCCCGACCCG
GCCGGGCCGCCGGTCGCCGAGGCGGGCGAGGACGACGGGCCCATGGTTCC

GGCGTCCTCACAGGCCCTCGAGGCGCTGAAGACTCGCCGCTCACCCGAGCC
CCCGGGCGCAGACCTCGCCCAGCTGTTCGAGGCCCACCCAAACGTGGCCGC
CACGGCGGTTAAGTTCACCGCGTGCTCCGCCACCCTGGCCCGCGAGGTCGC
CGCGTGTTCGCGGCTCACCATCAGCGCCTTACGGTCGCCGTATCCGGCTTCT
CCGGGGCTGCTGGAGCTCTGTGTTATTTTTTTCTTTGAACGCGTCCTCGCCT
TTCTCATCGAGAACGGGGCCCGGACGCACACCCAGGCCGGGGTGGCCGGCC
CGGCCGCCGCCCTGCTGGAGTTTACCCTGAGCATGCTGCCCCGGAAAACGG
CCGTGGGGGACTTTCTGGCCTCCACGCGCCTGAGCCTGGCCGACGTGGCCG
CCCATCTGCCCCTCGTCCAGCACGTGCTGGACGAAAACTCTCTGATCGGTCG
CCTGGCGCTGGCGAAGCTGATCCTTGTGGCTAGGGATGTCATTCGGGAGAC
GGACGCCTTTTACGGGGAACTCGCGGACCTGGAGCTGCAGCTTCGCGCGGC
CCCGCCGGCCAATCTGTATACACGCCTCGGCGAGTGGCTTCTGGAGCGCTC
GCAGGCCCACCCGGACACCCTTTTTGCCCCCGCCACCCCGACGCACCCAGAA
CCGCTTCTGTATAGAGTCCAGGCTCTGGCCAAATTTGCCCGTGGCGAAGAG
ATTAGGGTGGAGGCGGAGGATCGCCAGATGCGCGAGGCCCTCGACGCCCT
CGCTCGCGGGGTCGACGCGGTCTCACAGCACGCCGGGCCCCTCGGCGTAAT
GCCCGCCCCGGCCGGGGCGGCCCCGCAGGGGGCTCCGCGCCCACCCCCCCT
GGGCCCCGAGGCCGTTCAGGTTCGGCTGGAGGAGGTGCGGACCCAGGCCC
GTCGGGCGATCGAGGGCGCGGTTAAGGAGTACTTTTACCGGGGGGCCGTA
TACAGCGCCAAGGCTCTACAGGCCAGCGACAACAACGACCGCCGGTTTCAC
GTGGCTTCGGCCGCCGTCGTGCCCGTGGTCCAGCTGCTCGAGTCCCTGCCT
GTCTTCGACCAGCACACGCGGGACATCGCGCAGCGCGCCGCCATTCCCGCCC
CGCCCCCGATCGCGACCAGCCCCACGGCCATCCTGTTGCGGGATCTGATCCA
GCGGGGCCAGACGCTGGACGCCCCCGAGGACCTGGCGGCCTGGCTCTCCGT
CCTGACGGACGCCGCCAACCAAGGGCTGATAGAACGCAAGCCGCTGGACGA
GCTGGCGCGCAGCATCCGCGACATTAACGACCAGCAGGCGCGCCGCAGCTC
GGGTCTGGCCGAGCTGCGGCGCTTCGACGCCCTAGATGCGGCCCTGGGCCA
GCAGCTGGACAGCGACGCGGCCTTTGTTCCTGCGCCCGGCGCGTCGCCCTA
CCCCGACGACGGCGGGCTGTCGCCAGAGGCCACGCGCATGGCCGAGGAAG
CGCTGCGGCAGGCGCGGGCCATGGATGCCGCCAAGCTGACGGCAGAGCTC
GCCCCCGATGCGCGTGCCCGTTTGCGGGAGCGCGCGCGCTCCCTGGAGGCA
ATGCTCGAGGGAGCGCGGGAGCGGGCGAAGGTGGCCCGCGACGCCCGGG
AGAAGTTCTTGCACAAACTCCAGGGGGTCCTGCGCCCCCTCCCTGACTTTGT
GGGGCTAAAGGCCTGTCCGGCCGTCCTGGCGACCCTGCGGGCCTCCCTGCC

GGCGGGCTGGTCGGACCTCCCCGAGGCCGTTCGGGGGGCGCCCCCTGAGG
TTACGGCGGCGCTGCGGGCGGACATGTGGGGGCTGCTGGGGCAGTACCGA
GATGCCCTGGAGCACCCGACTCCGGACACGGCGACGGCTCTGTCTGGCTTG
CATCCCAGCTTCGTGGTGGTGCTGAAGAACCTGTTCGCCGACGCCCCAGAG
ACTCCGTTTCTCTTGCAGTTCTTCGCCGATCACGCCCCGATCATAGCCCACGC
CGTCTCGAACGCCATCAACGCCGGCAGCGCCGCCGTCGCGACGGCAGACCC
CGCGTCGACGGTGGATGCGGCCGTGCGGGCGCACCGCGTCCTGGTCGACG
CGGTGACGGCCCTGGGCGCGGCCGCCAGCGACCCGGCCTCCCCCCTGGCCT
TCCTAGCGGCCATGGCCGACAGCGCCGCGGGATACGTCAAGGCGACTCGGT
TGGCCCTGGACGCGCGGGGGGCCATCGCCCAGCTCACGACCTTAGGGTCGG
CGGCAGCCGACCTTGTCGTCCAGGTGCGCCGGGCCGCCAACCAACCGGAGG
GAGAGCATGCCTCCCTGATCCAGGCCGCGACGCGCGCGACCACCGGCGCGC
GGGAAAGCCTCGCGGGCCACGAGGGCAGGTTCGGGGGCCTGTTGCACGCC
GAAGGGACGGCCGGGGACCACTCCCCCAGCGGGCGCGCCCTGCAGGAGCT
GGGAAAGGTCATCGGCGCCACGCGACGCCGCGCCGACGAACTTGAGGCCG
CCATCGCCGACCTGAGAGAGAAGATGGCGGCCCAGCGCGCCCGCAGTAGCC
ATGAGCGCTGGGCCGCCGACGTGGAGGCCGTGCTGGACCGCGTGGAAAGC
GGTGCCGAGTTTGACGTGGTCGAGCTCCGTCGCCTGCAGGCGCTGGCGGG
CACGCACGGCTACAACCCCCGGGACTTCCGAAAGCGGGCCGAACAGGCGCT
GGGAACCAACGCCAAGGCGGTGACCCTTGCCCTGGAGACGGCCCTTGCGTT
TAACCCATACACCCCCGAGAACCAGCGCCACCCCATGCTCCCCCCGCTCGCAG
CCATTCACCGCATCGACTGGAGCGCGGCCTTCGGGGCCGCGGCCGACACGT
ACGCCGACATGTTTCGGGTGGACACCGAGCCCCTGGCGCGGCTTCTGCGGC
TGGCGGGGGGGGCTGCTGGAGCGGGCCCAGGCGAACGACGGGTTTATCGAC
TACCACGAGGCCGTCCTACACCTGTCGGAAGACTTGGGGGGCGTGCCGGCC
CTGCGCCAGTACGTGCCGTTTTTTCAAAAGGGCTACGCCGAGTACGTGGAT
ATCCGCGATCGCCTGGACGCCCTCCGGGCCGACGCGCGGCGCGCGATCGGA
AGCGTGGCGCTGGACCTGGCCGCCGCCGCGGAGGAGATATCCGCGGTGCG
CAACGACCCGGCGGCGGCCGCCGAGCTTGTCCGGGCAGGGGTCACCCTGCC
CTGCCCGAGCGAGGACGCGCTGGTGGCGTGCGTGGCGGCGCTGGAGCGCG
TGGACCAGAGCCCCGTGAAGGACACGGCGTACGCCGACTACGTCGCATTCG
TGACCCGACAGGACCTGGCCGATACCAAGGACGCCGTGGTGCGCGCCAAAC
AGCAGCGCGCCGAAGCCACCGAGCGGGTCACGGCGGGGCTGCGGGAGGT
GCTGGCCGCGCGCGAGCGCCGGGCCCAGCTCGAGGCCGAGGGTCTGGCCA

ATCTGAAGACCCTGCTGAAGGTGGTCGCCGTCCCGGCGACCGTGGCCAAGA
CGCTGGACCAGGCGCGCTCGGCGGAGGAGATCGCGGATCAGGTCGAAATT
CTGTTGGACCAGACGGAGAAGGCGCGCGAGCTCGACGTGCAGGCGGTCGC
CTGGTTGGAACATGCCCAGCGTACCTTTGAGACGCACCCGCTAAACGCGGCC
AGCGGCGACGGCCCGGGCCTCCTGACGCGACAGGGCGCGCGCCTGCAGGC
GCTCTTCGACACCCGTCGCCGCGTCGAGGCCCTGCGGAGGTCTCTCGAGGA
GGCCGAGGCGGAGTGGGACGAGGTATGGGGTCGCTTCGGCCGCGTTCGCG
GGGGGGCCTGGAAATCGCCCGAGGGATTTCGCGCGGCATGCGAGCAGCTT
CGCGCCCTGCAGGACACCACCAACACTGTGTCGGGGCTGCGAGCCCAGCGG
GACTACGAGCGCCTTCCCGCCAAGTACCAGGGCGTCCTGGGCGCCAAGAGC
GCCGAGCGGGCCGGGGCCGTGGAGGAGCTCGGGGGGCGCGTGGCCCAAC
ACGCCGACCTGAGCGCCCGGCTGCGGGACGAGGTGGTGCCAAGGGTGGCC
TGGGAGATGAACTTTGACACCCTGGGGGGCCTGTTGGCGGAATTCGACGC
GGTGGCCGGGGACCTGGCCCCATGGGCGGTGGAGGAGTTCCGGGGCGCG
CGGGAGCTCATCCAACGCCGCATGGGCTTATATAGCGCGTACGCCAAGGCC
ACAGGCCAGACGGGCGCGGGCGCGGCGGCCGCGCCCGCGCCCCTGCTCGT
GGATCTTCGCGCCCTAGACGCCCGCGCCCGGGCGTCCGCCCCACCCGGCCAA
GAGGCCGACCCGCAGATGCTGCGCCGCCGGGGCGAGGCGTACCTGCGAGT
GAGCGGAGGCCCGGGGCCCCTGGTGCTGCGCGAGGCCACCAGTACGCTGG
ATCGGCCGTTCGCCCCCAGCTTTTTGGTCCCGGATGGAACGCCACTGCAGTA
CGCGCTCTGCTTCCCGGCCGTGACCGACAAGCTCGGCGCGCTGCTGATGTG
TCCCGAGGCGGCATGCATTCGCCCCCCGCTTCCGACGGACACCCTGGAGTCG
GCCTCGACCGTCACGGCCATGTACGTCATCACCGTCATCAACCGGCTTCAGC
TGGCCCTCAGCGACGCCCAGGCCGCCAACTTTCAGCTCTTCGGACGCTTTGT
GCGCCACCGCCAGGCGAGATGGGGGGCCTCGATGGATGCGGCGGCCGAGC
TCTACGTCGCCCTCGTCGCGACCACTCTCACGCGCGAGTTTGGGTGTCGCTG
GGCCCAGCTGGAATGGGGGGGTGACGCGGCGGCCCCGGGACCGCCGCTCG
GGCCCCACAGCTCCACTAGGCACCGCGTTTCCTTTAACGAGAACGACGTGCT
GGTGGCGCTGGTGGCCAGCTCCCCGGAACACATTTACACCTTTTGGCGCCT
GGATCTGGTCCGCCAACACGAGTACATGCATCTCACCCTCCCCCGTGCGTTT
CAGAACGCAGCAGATTCCATGCTATTCGTGCAGCGCCTGACCCCGCATCCAG
ACGCCCGCATCCGCGTGCTGCCAGTGTTTTCGACCGGAGGCCCTCCGACCCG
GGGCCTCATGTTCGGCACGCGGCTGGCAGACTGGCGCCGCGGCAAGTTGTC
CGAAACCGACCCCCTGGCGCCCTGGCGCTCGGTCCCCGAGCTGGGAACCGA

GCGCGGCGCCGCGCTGGGAAAGCTGAGTCCCGCCCAGGCGCTGGCGGCGG
TGAGCGTCCTCGGGCGCATGTGTCTCCCAAGCACCGCTCTGGCCGCTCTTTG
GACCTGCATGTTTCCGGACGACTACACAGAGTATGACAGTTTCGACGCCCTT
CTGACCGCGCGTCTGGAATCTGGGCAGACGCTGAGCCCCTCGGGGGGGCG
CGAGGCGTCACCCCCCGCTCCCCCCAACGCCCTCTACCGGCCCACGGGCCAG
CACGTCGCCGTGCCGGCCGCCGCCACCCACCGCACCCCCGCGGCGCGCGTTA
CGGCCATGGACCTGGTGCTGGCGGCAGTGCTCCTGGGCGCGCCCGTCGTCG
TGGCGCTCCGCAACACCACGGCCTTTTCCCGCGAGTCGGAGCTGGAGCTGT
GTCTCACGCTGTTTGACTCACGCGCTCGCGGGCCGGACGCCGCCTTGCGCG
ATGCCGTGTCGTCCGACATCGAGACGTGGGCCGTCCGCCTCCTGCACGCCG
ACCTGAACCCGATTGAAAACGCGTGTCTGGCGGCACAGCTCCCGCGCCTGTC
CGCGCTCATCGCCGAGCGGCCCCTCGCCCGGGGCCCGCCGTGTCTGGTGCT
CGTGGACATCTCCATGACCCCGGTCGCGGTGTTGTGGGAAAACCCGGACCC
CCCCGGCCCCCCCCGACGTGCGGTTTGTTGGCAGCGAGGCCACCGAGGAGCT
CCCGTTTGTGGCGGGCGGCGAGGACGTCCTCGCCGCCAGCGCCACCGACGA
GGACCCCTTCCTCGCGCGAGCTATCCTCGGGCGGCCGTTCGACGCCTCCCTC
CTGTCGGGGGAGCTATTCCCGGGGCATCCGGTGTACCAGCGCGCCCCCGAC
GACCAGAGCCCCTCGGTCCCGAACCCGACCCCCGGCCCGGCGGACCTTGTTG
GGACGGAGGGCTCGTTGGGGCCCGGAAGCCTGGCCCCCACGCTATTCACCG
ACGCCACCCCCGGCGAGCCCGTCCCCCCTCGCATGTGGGCATGGATTCACGG
CCTGGAGGAGCTCGCGTCTGACGACTCCGGCGGCCCCGCGCCCCTCCTTGCC
CCGGACCCCCTTTCGCCCACCGCCGATCAGTCCGTCCCCACGTCCCAGTGTGC
ACCGCGGCCCCCTGGGCCGGCAGTCACGGCTCGCGAAGCACGACCGGGCGT
CCCGGCCGAAAGCACGCGGCCGGCGCCCGTGGGCCCCCGCGACGACTTCCG
GCGCTTGCCGTCCCCCCAAAGTTCCCCGGCGCCCCCCGATGCCACCGCCCCC
CGCCCCCCCGCCTCCTCCCGCGCTTCTGCCGCTTCTTCGTCCGGGTCGCGCGC
GCGCCGACACCGCCGGGCACGCTCCCTGGCGCGCGCCACCCAGGCTTCCGC
GACCACCCAGGGTTGGCGGCCGCCTGCCCTCCCCGACACGGTCGCCCCGGT
TACCGATTTCGCGCGCCCCCCGGCCCCTCCCAAACCCCCAGAGCCAGCGCTCC
ACGCTTTGGTGTCTGGTGTGCCCCTCCCGCTCGGTCCCCAGTTCGCCGGCCA
GGCTTCTCCCGCTCTCCCTATCGATCCCGTTCCGCCCCCGGTCGCAACCGGCA
CGGTTTTGCCCGGGGGCGAAAACCGCCGCCCCCCGCTAACCTCGGGTCCCG
CGCCAACCCCCCCCCAGGGTTCCCGTAGGCGGGCCGCAGCGGCGCCTTACGC
GCCCCGCTGTCGCGTCGCTGTCCGAATCGCGGGAATCCCTCCCTTCACCCTG

GGACCCCGCCGACCCCACGGCCCCTGTTTTAGGCCGCAACCCGGCCGAGCC
GACCTCATCCTCTCCCGCAGGTCCCTCTCCCCCGCCTCCCGCGGTCCAACCCG
TCACCCCGCCCCCGACGTCAGGCCCGCCCCCCACATACTTGACGCTGGAGGG
CGGTGTTACGCCCGGAGGCCCGGTTTCCCGCCGCCCCACTACACGGCAGCC
GGTGGCCACGCCCACCACATCTGCGCGCCCCCGGGGGCATTTGACCGTCAA
CCGCCTGTCCGCGCCCCAGCCCCAACCCCAGCCCCAACCCCAGCCCCAACCCC
AGCCCCAACCCCAGCCCCAACCCCAGCCCCAACCCCAGCCCCAACCCCAGCCC
CAACCCCAGCCCCAACCCCAGCCCCAACCCCAGCCCCAACCCCAGCCCCAACC
CCAGCCCCAACCCCAACCCCAGCCCCAACCCCAACCCCAGCCCCAACCCCAAC
CCCAGCCCCAACCCCAACCCCAACCCCAGCCCCAGCCCCAGCCCCAACCCCAG
CCCCAACCCCAGCCCCAACCCCAGCCCCAACCCCAGCCCCAGCCCCAGCCCCA
GCCCCAACCCCAGCCCCAACCCCAACCCCAGCCCCAGCCCCAGCCCCAACCCC
AGCCCCAGCCCCAGCCCCAGCCCCAACCCCAGCCCCAACCCCAACCCCAGCCC
CAACCCCAACCCCAGCCCCAACCCCAGCCCCAGCCCCAGCCCCAACCCCAACC
CCAGCCCCAACCCCAACCCCAACCCCAGCCCCAGCCCCAACCCCAGCCCCAAC
CCCAGCCCCAGCCCCAACCCCAGCCCCAGCCCCAGCCCCAGCCCCAGCCCCAA
CCCCAGCCCCAAAACGGGCATGTAGCACCCGGGGAGTATCCGGCGGTTCGG
TTCCGGGCACCGCAAAACCGCCCATCCGTCCCGGCTTCCGCGTCGTCCACAA
ATCCACGCACGGGCAGCTCCTTGTCTGGGGTGTCTTCGTGGGCATCCTCCCT
CGCGCTACACATTGACGCTACCCCCCCGCCCGTGTCGCTGCTTCAGACCCTGT
ATGTCTCTGACGACGAAGACTCCGACACCACCTCGTTGTTCCTCTCGGATTCC
GAGGCCGAGGCGCTCGACCCACTCCCTCGGGAACCACACTCCCCCATAACCA
ACGAACCATTCAGTGCGTTATCCGCCGATGACTCCCAAGAGGTGACGCGCTT
ACAATTCGGCCCCCCGCCCGTATCGGCAAACGCAGTTCTGTCGCGACGCTAC
GTGCAACGCACCGGTCGTAGCGCCCTGGCGGTGCTGATCCGCGCCTGTTAC
CGCCTACAACAGCAGTTACAGCGGACCCGCCGGGCGCTGCTTCATCACAGC
GACGCCGTGCTGACCAGCCTACATCACGTGCGCATGTTACTGGGCTAG

UL37

ATGGCAGACCGCGGTCTCCCGTCCGAGGCCCCCGTCGTCACGACCTCACCCG
CCGGTCCGCCCTCGGACGGACCTATGCAGCGCCTATTGGCGAGCCTAGCCG
GCCTTCGCCAACCGCCAACCCCCACGGCCGAGACGGCAAACGGGGCGGACG
ACCCGGCGTTTCTGGCCACGGCCAAGCTGCGCGCCGCCATGGCGGCGTTTC
TGTTGTCGGGAACGGCCATCGCCCCGGCAGACGCGCGGGCATGCTGGCGG
CCGCTGCTGGAACACCTGTGCGCGCTCCACCGGGCCCACGGGCTTCCGGAG

ACGGCGCTCTTGGCCGAGAACCTCCCCGGGTTGCTCGTACACCGCTTGGTG
GTGGCTCTCCCCGAGGCCCCCGACCAGGCCTTCCGGGAGATGGAGGTCATC
AAGGACACCATCCTCGCGGTCACCGGCTCCGACACGTCCCATGCGCTGGAGT
CCGCCGGCCTGCGCACCGCGGCGGCCCTGGGGCCGGTCCGCGTCCGCCAGT
GCGCCGTGGAGTGGATAGACCGCTGGCAAACCGTCACCAAGAGCTGCTTGG
CCATGAGCCCGCGGACCTCCATCGAGGCCCTTGGGGAGACGTCGCTCAAGC
TGGCGCCGGTCCCGTTGGGGCAGCCCAGCGCGAACCTTACCACCCCGGCGT
ACAGCCTGCTCTTCCCCGCCCCGTTCGTGCAAGAGGGCCTCCGGTTCTTGGC
CCTGGTGAGTAATCGGGTGACGCTGTTCTCGGCGCACCTCCAGCGCATAGA
CGACGCGACCCTCACTCCCCTCACACGGGCCCTCTTTACGTTGGCCCTGGTG
GACGAGTACCTGACGACCCCCGAGCGGGGGGCTGTGGTCCCGCCGCCCCTG
TTGGCGCAGTTTCAGCACACCGTGCGGGAGATCGACCCGGCCATAATGATT
CCGCCACTGGAGGCCAACAAGATGGTTCGCAGCCGCGAGGAGGTGCGCGT
GTCGACGGCCCTCAGCCGCGTCAGCCCGCGCTCGGCCTGTGCGCCCCCGGG
GACGCTAATGGCGCGCGTGCGGACGGACGTGGCCGTGTTTGATCCCGACGT
GCCGTTCCTGAGTTCGTCGGCACTGGCAGTCTTCCAGCCTGCCGTCTCCAGC
CTGCTGCAGCTCGGGGAGCAGCCCTCCGCCGGCGCCCAGCAGCGGCTGCTG
GCTCTGCTGCAGCAGACGTGGACGTTGATCCAGAATACCAATTCGCCCTCCG
TGGTGATCAACACCCTGATCGACGCTGGGTTCACGCCCTCGCACTGCACGCA
CTACCTTTCGGCCCTGGAGGGGTTTCTGGCGGCGGGCGTCCCCGCGCGGAC
GCCCGCCGGCCACGGACTCGGCGAAGTCCAGCAGCTCTTTGGGTGCATTGC
CCTCGCGGGGTCGAACGTGTTTGGTCTGGCGCGGGAATACGGGTACTATGC
CAACTACGTAAAAACTTTCAGGCGGGTCCAGGGCGCCAGCGAGCACACGCA
CGGGCGGCTCTGTGAGGCGGTCGGCCTGTCGGGGGGCGTTCTGAGCCAGA
CGCTGGCGCGTATCATGGGGCCGGCCGTGCCGACGGAACATCTGGCGAGC
CTGCGGCGGGCGCTCGTGGGGGAGTTTGAGACGGCCGAGCGCCGCTTTAG
TTCCGGTCAACCCAGCCTTCTCCGCGAGACGGCGCTCATCTGGATCGACGTG
TATGGTCAGACCCACTGGGACATCACCCCCACCACCCCGGCCACGCCGCTGT
CCGCGCTTCTCCCCGTCGGGCAGCCCAGCCATGCCCCCTCTGTCCACCTGGC
CGCGGCGACCCAGATCCGCTTCCCCGCCCTCGAGGGCATTCACCCCAACGTC
CTCGCCGACCCGGGCTTCGTCCCCTACGTTCTGGCCCTGGTGGTTGGGGAC
GCGCTGAGGGCCACGTGTAGCGCGGCCTACCTTCCCCGCCCGGTCGAGTTC
GCCCTGCGTGTGTTGGCCTGGGCCCGGGACTTTGGGCTGGGCTATCTCCCC
ACGGTCGAGGGCCATCGCACCAAACTGGGCGCGCTGATCACTCTCCTCGAAC

CGGCCGCCCGGGGCGGCCTCGGCCCCACTATGCAGATGGCCGACAACATAG
AGCAGCTGCTCCGGGAGCTGTACGTGATCTCCAGGGGTGCCGTCGAGCAGC
TGCGGCCCCTGGTCCAACTGCAGCCCCCCCCGCCCCCCGAGGTGGGCACCAG
CCTCCTGTTGATTAGCATGTACGCCCTGGCTGCCCGGGGGGTGCTGCAGGA
CCTCGCCGAGCGCGCCGACCCCCTGATTCGCCAACTGGAGGACGCCATCGT
GCTGCTGCGGCTGCACATGCGCACGCTCTCCGCCTTTTTCGAGTGTCGGTTC
GAGAGCGACGGGCGCCGCCTGTATGCGGTGGTCGGGGACACGCCCGACCG
CCTGGGGCCCTGGCCCCCCGAGGCCATGGGGGACGCGGTGAGTCAGTACT
GCAGCATGTATCACGACGCCAAGCGCGCGCTGGTCGCGTCCCTCGCGAGCC
TGCGTTCCGTCATCACCGAAACCACGGCGCACCTGGGGGTGTGCGACGAGC
TGGCGGCCCAGGTGTCGCACGAGGACAACGTGCTGGCCGTGGTCCGGCGC
GAAATTCACGGGTTTCTGTCCGTCGTGTCCGGCATTCACGCCCGGGCGTCGA
AGCTGCTGTCGGGAGACCAGGTCCCCGGGTTTTGTTTCATGGGTCAGTTTCT
AGCGCGCTGGCGGCGTCTGTCGGCCTGCTATCAAGCCGCGCGCGCGGCCGC
GGGACCCGAGCCCGTGGCCGAGTTTGTCCAGGAACTCCACGACACGTGGAA
GGGCCTGCAGACGGAGCGCGCCGTGGTCGTGGCGCCCTTGGTCAGCTCGG
CCGACCAGCGCGCCGCGGCCATCCGAGAGGTAATGGCGCATGCGCCCGAG
GACGCCCCCCCGCAAAGCCCCGCGGCCGACCGCGTCGTGCTTACGAGCCGT
CGCGACCTAGGGGCCTGGGGGGGACTACAGCCTCGGCCCCCTGGGCCAGAC
GACCGCGGTTCCGGACTCCGTGGATCTGTCTCGCCAGGGGTTGGCCGTTAC
GCTGAGTATGGATTGGTTACTGATGAACGAGCTCCTGCGGGTCACCGACGG
CGTGTTTCGCGCTTCCGCGTTTCGTCCGTTAGCCGGACCGGAGGCTCCCAGG
GACCTGGAGGTCCGCGACGCCGGAAACAGTCTCCCCGCGCCTACGCCCATG
GACGCACAGAAGCCGGAGGCCTATGGGCACGGCCCACGCCAGGTGGACCG
CGAGGAGGCGCCTCATTCCAACACCCCCGTCGAGGACGACGAGATGATCCC
GGAGGACACCGTCGCGCCACCCACGGACTTGCCGTTAACTAGTTACCAATAA

UL41

ATGGGTTTGTTCGGGATGATGAAGTTTGCCCACACACACCATCTGGTCAAGC
GCCAGGGCCTTGGGGCCCCGGCCGGGTACTTCACCCCCATCGCCGTGGACC
TGTGGAACGTCATGTACACGTTGGTGGTCAAATATCAGCGCCGATACCCCAG
TTACGACCGCGAGGCCATTACGCTACACTGCCTCTGTCGCTTATTAAAGGTG
TTTACCCAAAAGTCCCTTTTCCCCATCTTCGTTACCGATCGCGGGGTCAATTG
TATGGAGCCGGTTGTGTTTGGAGCCAAGGCCATCCTGGCCCGCACGACGGC
CCAATGCCGGACGGACGAGGAGGCCAGTGACGTGGACGCCTCTCCACCGCC

TTCCCCCATCACCGACTCCAGACCCAGCTCTGCCTTTTCCAACATGCGCCGGC
GCGGCACCTCTCTGGCCTCGGGGACCCGGGGGACGGCCGGGTCCGGAGCC
GCGCTGCCGTCCGCCGCGCCCTCGAAGCCGGCCCTGCGTCTGGCGCATCTG
TTCTGTATTCGCGTTCTCCGGGCCCTGGGGTACGCCTACATTAACTCGGGTC
AGCTGGAGGCGGACGATGCCTGCGCCAACCTCTATCACACCAACACGGTCG
CGTACGTGTACACCACAGACACTGACCTCCTGTTGATGGGCTGTGATATTGT
GTTGGATATTAGCGCCTGCTACATTCCCACGATCAACTGTCGCGATATACTA
AAGTACTTTAAGATGAGCTACCCCCAGTTCCTGGCCCTCTTTGTCCGCTGCCA
CACCGACCTCCATCCCAATAACACCTACGCCTCCGTGGAGGATGTGCTGCGC
GAATGTCACTGGACCCCCCCGAGTCGCTCTCAGACCCGGCGGGCCATCCGCC
GGGAACACACCAGCTCGCGCTCCACGGAAACCAGGCCCCCTTTGCCGCCGG
CCGCCGGCGGCACCGAGATGCGCGTCTCGTGGACCGAAATTCTAACCCAAC
AGATCGCCGGCGGATACGAAGACGACGAGGACCTCCCCCTGGATCCCCGGG
ACGTTACCGGGGGCCACCCCGGCCCCAGGTCGTCCTCCTCGGAGATACTCAC
CCCGCCCGAGCTCGTCCAGGTCCCGAACGCGCAGCTGCTGGAAGAGCACCG
CAGTTATGTGGCCAGCCGGCGACGCCACGTCATCCACGACGCCCCAGAGTCC
CTGGACTGGCTCCCCGATCCCATGACCATCACCGAGCTGGTGGAACACCGCT
ACATTAAGTACGTCATATCGCTTATCGGCCCCAAGGAGCGGGGGCCGTGGA
CTCTTCTGAAACGCCTGCCTATCTACCAGGACATCCGCGACGAAAACCTGGC
GCGATCTATTGTGACCCGGCATATCACGGCCCCTGATATCGCCGACAGGTTT
CTGGAGCAGCTGCGGACCCAGGCCCCCCCACCCGCGTTCTACAAGGACGTCC
TGGCCAAATTCTGGGACGAGTAG

UL46

ATGCAGCGCCGGACGCGCGGCGCGAGCTCCCTGCGGCTGGCGCGGTGCCT
GACGCCTGCCAACCTGATCCGCGGCGACAACGCGGGCGTTCCCGAGCGGCG
CATCTTCGGCGGGTGTCTGCTCCCCACCCCGGAGGGGCTCCTTAGCGCGGC
CGTGGGCGCCTTGCGGCAGCGCTCCGACGACGCGCAGCCGGCGTTTCTGAC
CTGCACCGATCGCAGCGTCCGGTTGGCCGCGCGGCAACACAACACGGTTCC
CGAGAGTTTGATCGTGGACGGGCTCGCCAGCGACCCGCACTACGAGTACAT
CCGGCACTACGCTTCGGCCGCCACCCAGGCGCTGGGCGAGGTGGAGCTGCC
CGGCGGCCAGTTGAGCCGCGCCATCCTCACGCAGTACTGGAAGTACCTGCA
GACGGTGGTGCCCAGCGGCCTGGACGTCCCCGAGGACCCCGTGGGCGACT
GCGACCCCAGCCTTCACGTGCTGCTGCGGCCCACCCTGGCGCCAAAGCTGCT
GGCGCGCACCCCGTTCAAGAGCGGGGCCGCGGCGGCCAAGTACGCCGCCA

CCGTGGCCGGCCTGCGCGACGCCCTCCATCGGATTCAGCAGTACATGTTCTT
TATGCGCCCGGCGGACCCAAGCCGCCCCAGCACCGACACCGCACTGCGGCTC
AACGAGCTCCTGGCCTACGTCTCCGTGCTGTACCGGTGGGCGTCCTGGATG
CTGTGGACGACGGACAAGCACGTATGTCACCGGCTGAGTCCCTCCAATCGCC
GGTTCCTCCCGCTCGGCGGCAGCCCGGAGGCGCCCGCGGAAACGTTCGCGC
GCCATCTGGACCGGGGTCCCAGCGGCACGACCGGCTCCATGCAGTGCATGG
CGCTCAGGGCGGCGGTCAGCGACGTCCTGGGCCACCTGACGTGCCTAGCCA
ACCTGTGGCAGACCGGCAAGCGGAGCGGCGGTACGTACGGGACCGTGGAT
ACCGTGGTATCCACGGTGGAGGTTCTGTCGATCGTCCATCACCACGCCCAGT
ATATCATCAACGCGACCCTCACCGGGTACGGCGTCTGGGCCACCGACAGCCT
GAACAACGAGTATCTGCGGGCCGCGGTGGACAGCCAGGAGCGTTTCTGTCG
GACCACCGCCCCCCTGTTCCCCACGATGACCGCCCCCAGCTGGGCCCGGATG
GAGTTGAGCATCAAGGCTTGGTTCGGGGCCGCCCTGGCCGCGGATCTGCTC
CGCAGCGGGGCGCCGTCGCTCCACTACGAGTCCATCCTGCGGCTCGTGGCG
TCTCGCCGGACGACGTGGTCCGCGGGGCCTCCCCCGGACGACATGGCCCGC
GGCCCGGGGGGGGCATCGCGCGGGGGGTGGGACCTGTCGGGAAAAGATTC
AGCGGGCGCGGCGCGACAACGAGCCCCCGCCCCTCCCCCGACCTCGCCTACA
CTCGACCCCCGCGCCGTCCACCCGGCGGTTCCGGAGGCGCCGTGCGGACGG
CGCGGGGCCCCCGCTTCCGGATGCGGACGACCCGGTCGCCGAGCCCCCCGC
TGCGGCCGCACAGCCGGCCACGTATTACACGCACATGGGGGAGGTGCCCCC
GCGCCTCCCGGCCCGTAACGTCGCGGGACCCGACAGGCGACCGCCGGCGGC
GACGTGCCCCCTTCTTGTCCGGCGCGCGTCTCTGGGGAGCCTCGATCGGCC
ACGGGTGTGGGGACCCGCCCCGGAGGGAGAACCCGACCAGATGGAAGCCA
CGTATCTGACGGCCGACGACGACGACGACGACGCCCGCCGCAAAGCCACCC
ACGCCGCCTCGGCCCGCGAACGGCACGCCCCCTACGAGGACGACGAGTCAA
TATACGAGACCGTGAGCGAGGACGGGGGGCGTGTCTACGAGGAAATACCA
TGGATGCGGGTCTACGAAAACGTCTGCGTGAACACGGCGAATGCAGCGCCG
GCCTCCCCGTACATTGAGGCGGAAAATCCCCTGTACGACTGGGGGGGATCC
GCCCTATTTTCCCCCCCGGGCCGCACCGGACCCCCGCCCCCGCCGTTGAGCC
CCTCGCCCGTCCTCGCCCGCCATCGAGCCAACGCCCTGACCAACGACGGCCC
GACCAACGTCGCCGCCCTGAGCGCCCTCCTGACCAAGCTTAAACGCGAAGGA
CGCCGGAGCCGGTGA

UL47

ATGTCGGCTCGCGAACCCGCGGGGCGCAGGAGGCGCGCATCCACCCGCCCC
CGCGCCTCGCCCGTGGCGGACGAGCCAGCGGGCGATGGGGTGGGGTTCAT
GGGGTACCTGCGTGCGGTGTTCCGCGGGGATGACGACAGCGAGCTAGAGG
CTCTGGAGGAGATGGCGGGCGACGAGCCGCCCGTGCGCCGTCGACGGGAA
GGCCCGCGAGCCCGACGACGGCGCGCGTCGGAAGCCCCGCCCTCATCCCAT
CGCCGAGCGTCCCGGCAGCGCCCCGGGCCCGATGCGGCCCGTAGCCAGTCG
GTGCGCGGTCGCCTGGACGATGATGATGAGGTTCCCCGCGGTCCTCCGCAG
GCCCGGCAGGGGGGATACCTGGGTCCCGTCGACGCGCGGGCTATTTTGGG
GCGGGTCGGCGGTTCGCGGGTGGCGCCGTCGCCGCTGTTCCTAGAGGAAC
TGCAGTACGAGGAGGACGACTACCCGGAAGACGTCGGGCCGGAGGACGGC
GGCGGGGCCCGTTCCCCGCCCAAGGTGGAGGTTCTGGAGGGACGCGTGCC
GGGCCCGGAGCTCCGGGCGGCATTCCCGTTGGATCGACTGGCCCCTCAGGT
TGCCGTGTGGGACGAGTCCGTGCGCTCCGCCCTAGCCCTGGGGCATCCGGC
CGGGTTTTACCCGTGTCCGGATAGCGCGTTCGGGTTATCGCGCGTGGGGGT
CATGCACTTCGCCTCCCCCGACAACCCCGCGGTGTTTTTCCGCCAAACCCTGC
AGCAGGGCGAGGCGTTGGCCTGGTATATCACGGGCGATGGGATTCTTGAC
CTGACGGATCGTCGAACAAAAACCAGCCCCGCCCAGGCGATGAGCTTTTTG
GCGGATGCCGTCGTGCGGCTGGCCATCAACGGGTGGGTGTGCGGGACGCG
CCTTCACGCAGAGGCGCGCGGGTCGGACCTGGACGACAGGGCTGCCGAGC
TGAGGCGGCAGTTCGCGAGCCTCACGGCGTTGCGTCCCGTCGGGGCCGCG
GCCGTGCCGTTACTGAGCGCGGGGGGGTTAGTGTCCCCCCAATCCGGCCCC
GACGCCGCGGTGTTTCGCAGCTCGCTGGGGTCCCTGCTGTACTGGCCCGGG
GTGCGCGCGCTGCTGGACCGCGACTGTCGCGTGGCCGCCCGCTATGCCGGC
CGCATGACGTACCTGGCCACCGGGGCCCTGCTCGCCCGCTTCAATCCCGACG
CCGTCCGGTGCGTTTTGACGCGGGAGGCCGCCTTCCTGGGGCGCGTGCTGG
ATGTGTTGGCGGTGATGGCGGAACAGACGGTCCAGTGGCTCTCGGTGGTC
GTGGGGGCGCGCCTGCACCCGCACGTGCACCACCCCGCCTTTGCGGACGTG
GCGCGGGAGGAGCTGTTTCGCGCCCTGCCCCTGGGAAGCCCCGCGGTCGT
GGGGGCCGAGCACGAGGCGCTGGGCGACACCGCAGCGCGCCGGCTGCTCG
CCAACAGCGGGCTCAACGCCGTGCTGGGCGCTGCGGTGTACGCGCTGCACA
CGGCCCTGGCGACAGTGACCTTAAAGTACGCCCGGGCGTGCGGGGACGCG
CACCGGCGCCGGGACGACGCTGCGACCACGCGCGCCATTCTGGCCGCCGGG
CTCGTCCTGCAGCGGCTGCTGGGCTTTGCCGACACCGTGGTGGCGTGCGTG
ACACTGGCCGCGTTTGACGGGGGATTCACGGCCCCCGAGGTGGGCACGTAC

ACCCCCCTGCGCTACGCGTGTGTCCTCCGAGCGACCCAGCCCCTGTACGCGC
GCACCACCCCCGCCAAGTTCTGGGCGGACGTCCGCGCGGCCGCGGAGCACG
TGGATCTGCGCCCCGCCTCCTCCGCGCCCCGGGCCCCCGTGTCCGGGACGG
CAGACCCCGCCTTTCTGCTCAAGGACCTGGAGCCCTTCCCCCCCGCCCCCGTA
AGCGGCGGGTCCGTGTTGGGCCCGCGGGTCCGCGTGGTGGACATCATGTC
CCAGTTTAGGAAACTGCTGATGGGAGACGAGGGGGCCGCCGCCCTGCGGG
CGCACGTGTCGGGGAGGCGCGCGACCGGGCTGGGAGGCCCGCCACGCCCA
TAA

UL48

ATGGACCTCTTGGTCGACGAGCTGTTTGCCGACATGGACGCGGACGGCGCT
TCGCCACCACCCCCCCGCCCGGCCGGGGGTCCCAAAAACACCCCGGCGGCCC
CTCCGCTGTACGCAACGGGGCGCCTGAGCCAGGCCCAGCTCATGCCCTCCCC
GCCCATGCCCGTCCCCCCCGCCGCCCTCTTTAACCGTCTCCTCGACGACTTGG
GCTTTAGCGCGGGCCCCGCGCTATGTACCATGCTCGATACCTGGAACGAGG
ATTTGTTTTCGGCGTTACCGACCAACGCCGACCTGTACCGGGAGTGTAAATT
CCTATCAACGCTGCCCAGCGATGTGGTGGAATGGGGGGACGCGTACGTCCC
CGAACGCGCCCAAATCGACATTCGCGCCCACGGCGACGTGGCCTTCCCGACG
CTTCCGGCCACCCGCGACGGCCTCGGGCTCTACTACGAAGCGCTCTCTCGTT
TCTTCCACGCCGAGCTACGGGCGCGGGAGGAGAGCTATCGAACCGTGTTGG
CCAACTTCTGCTCGGCCCTGTACCGGTACCTGCGCGCCAGCGTCCGGCAGCT
GCACCGCCAGGCGCACATGCGCGGACGCGATCGCGACCTGGGAGAAATGCT
GCGCGCCACGATCGCGGACAGGTACTACCGAGAGACCGCTCGTCTGGCGCG
TGTTCTGTTTTTGCATTTGTATCTATTTTTGACCCGCGAGATCCTATGGGCCG
CGTACGCCGAGCAGATGATGCGGCCCGACCTGTTTGACTGCCTCTGTTGCG
ACCTGGAGAGCTGGCGTCAGTTGGCGGGTCTGTTCCAGCCCTTCATGTTCG
TCAACGGAGCGCTCACCGTCCGGGGAGTGCCAATCGAGGCCCGCCGGCTGC
GGGAGCTAAACCACATTCGCGAGCACCTTAACCTCCCGCTGGTGCGCAGCGC
GGCTACGGAGGAGCCAGGGGCGCCGTTGACGACCCCTCCCACCCTGCATGG
CAACCAGGCCCGCGCCTCTGGGTACTTTATGGTGTTGATTCGGGCGAAGTT
GGACTCGTATTCCAGCTTCACGACCTCGCCCTCCGAGGCGGTCATGCGGGAA
CACGCGTACAGCCGCGCGCGTACGAAAAACAATTACGGGTCTACCATCGAG
GGCCTGCTCGATCTCCCGGACGACGACGCCCCCGAAGAGGCGGGGCTGGC
GGCTCCGCGCCTGTCCTTTCTCCCCGCGGGACACACGCGCAGACTGTCGACG
GCCCCCCCGACCGATGTCAGCCTGGGGGACGAGCTCCACTTAGACGGCGAG

GACGTGGCGATGGCGCATGCCGACGCGCTAGACGATTTCGATCTGGACATG
TTGGGGGGACGGGGATTCCCCGGGTCCGGGATTTACCCCCCACGACTCCGCC
CCCTACGGCGCTCTGGATATGGCCGACTTCGAGTTTGAGCAGATGTTTACCG
ATGCCCTTGGAATTGACGAGTACGGTGGGTAG

UL49

ATGACCTCTCGCCGCTCCGTGAAGTCGGGTCCGCGGGAGGTTCCGCGCGAT
GAGTACGAGGATCTGTACTACACCCCGTCTTCATGTATGGCGAGTCCCGATA
GTCCGCCTGACACCTCCCGCCGTGGCGCCCTACAGACACGCGCGCGCCCAAG
GGGCGAGGTCCGTTTCGTCCAGTACGACGAGTCGGATTATGCCCTCTACGG
GGGCTCGTCATCCGAAGACGACGAACACCCGGAGGTCCCCCGGACGCGGCG
TCCCGTTTCCGGGGCGGTTTTGTCCGCCCCGGGGCCTGCGCGGGCGCCTCC
GCCGCCCGCTGGGTCCGGAGGGGCCGGACGCACACCCACCACCGCCCCCCG
GGCCCCCCCGAACCCAGCGGGTGGCGACTAAGGCCCCCGCGGCCCCGGCGGC
GGAGACCACCCGCGGCAGGAAATCGGCCCAGCCAGAATCCGCCGCACTCCC
AGACGCCCCCGCGTCGACGGCGCCAACCCGATCCAAGACACCCGCGCAGGG
GCTGGCCAGAAAGCTGCACTTTAGCACCGCCCCCCCAAACCCCGACGCGCCA
TGGACCCCCCGGGTGGCCGGCTTTAACAAGCGCGTCTTCTGCGCCGCGGTT
GGGCGCCTGGCGGCCATGCATGCCCGGATGGCGGCGGTCCAGCTCTGGGA
CATGTCGCGTCCGCGCACAGACGAAGACCTCAACGAACTCCTTGGCATCACC
ACCATCCGCGTGACGGTCTGCGAGGGCAAAAACCTGATTCAGCGCGCCAAC
GAGTTGGTGAATCCAGACGTGGTGCAGGACGTCGACGCGGCCACGGCGAC
TCGAGGGCGTTCTGCGGCGTCGCGCCCCACCGAGCGACCTCGAGCCCCAGC
CCGCTCCGCTTCTCGCCCCAGACGGCCCGTCGAGTGA

UL50

ATGAGTCAGTGGGGATCCGGGGCGATCCTTGTCCAGCCGGACAGCTTGGGT
CGGGGGTACGATGGCGACTGGCACACGGCCGTCGCTACTCGCGGGGGCGG
AGTCGTGCAACTGAACCTGGTCAACAGGCGCGCGGTGGCTTTTATGCCGAA
GGTCAGCGGGGACTCCGGATGGGCCGTCGGGCGCGTCTCTCTGGACCTGC
GAATGGCTATGCCGGCTGACTTTTGTGCGATTATTCACGCCCCCGCGCTATC
CAGCCCAGGGCACCACGTAATACTGGGTCTTATCGACTCGGGGTACCGCGG
AACCGTTATGGCCGTGGTCGTAGCGCCTAAAAGGACGCGGGAATTTGCCCC
CGGGACCCTGCGGGTCGACGTGACGTTCCTGGACATCCTGGCGACCCCCCC
GGCCCTCACCGAGCCGATTTCCCTGCGGCAGTTCCCGCAACTGGCGCCCCCC

CCTCCAACCGGGGCCGGGATACGCGCAGATCCTTGGTTGGAGGGGGCGCTC
GGGGACCCAAGCGTGACTCCTGCCCTACCGGCGCGACGCCGAGGGCGGTCC
CTCGTCTATGCCGGCGAGCTGACGCCGGTTCAGACGGAACACGGGGACGGC
GTACGAGAAGCCATCGCCTTCCTTCCAAAACGCGAGGAGGATGCCGGTTTC
GACATTGTCGTCCGTCGCCCGGTCACCGTCCCGGCAAACGGCACCACGGTCG
TGCAGCCATCCCTCCGCATGCTCCACGCGGACGCCGGGCCCGCGGCCTGCTA
TGTGCTGGGGCGGTCGTCGCTCAACGCCCGCGGCCTCCTGGTCGTTCCTAC
GCGCTGGCTCCCCGGGCACGTATGTGCGTTTGTTGTTTACAACCTTACGGG
GGTTCCTGTGACCCTCGAGGCCGGCGCCAAGGTCGCCCAGCTCCTGGTTGC
GGGGGCGGACGCTCTTCCTTGGATCCCCCCGGACAACTTTCACGGGACCAA
AGCGCTTCGAAACTACCCCAGGGGTGTTCCGGACTCAACCGCCGAACCCAG
GAACCCGCCGCTCCTGGTGTTTACGAACGAGTTTGACGCGGAGGCCCCCCC
GAGCGAGCGCGGGACCGGGGGTTTTGGTTCTACCGGTATTTAG

UL51

ATGGCTTCTCTTCTCGGGGCTATATGTGGCTGGGGAGCGCGCCCCGAGGAA
CAATATGAGATGATCCGCGCGGCCGTTCCGCCCTCGGAGGCGGAGCCGCGG
CTGCAGGAGGCCCTGGTGGTCGTTAACGCGCTACTTCCCGCCCCCATCACGC
TCGATGACGCCCTGGGGTCCCTGGACGACACCCGACGCCTCGTGAAGGCCC
GCGCCTTGGCCCGCACGTACCACGCCTGCATGGTGAACCTAGAACGACTGG
CGCGCCACCACCCCGGGCTCGAGGCCCCCACGATCGACGGGGCCGTGGCGG
CCCATCAGGACAAGATGCGGCGCCTGGCGGACACGTGTATGGCCACCATCC
TGCAGATGTACATGTCCGTGGGGGCGGCTGACAAGTCCGCGGATGTGCTCG
TCTCCCAGGCTATTCGGAGCATGGCCGAGAGCGACGTGGTCATGGAGGATG
TGGCCATCGCCGAACGGGCCCTTGGCCTCTCCGCCTTCGGGGTTGCCGGGG
GAACCCGCTCGGGGGGGGCTTGGGGTGACCGAGGCGCCCTCCTTGGGGCAC
CCCCACACGCCGCCCCCGGAGGTTACGCTGGCGCCTGCCGCCCGAAACGGC
GACGCCCTCCCGGACCCCAAACCGGAATCGTGTCCCCGCGTGTCCGTTCCCA
GACCTACAGCCTCCCCAACCGCACCTCGCCCTGGCCCATCTCGAGCAGCTCC
GTGTGTTTTGGGTCAATAA

UL55

ATGACAGCGACCCCCCTCACCAACCTGTTCTTACGGGCCCCGGACATAACCC
ACGTGGCCCCCCCTTACTGCCTCAACGCCACCTGGCAGGCCGAAACGGCCAT
GCACACCAGCAAAACGGACTCCGCTTGCGTGGCCGTGCGGAGTTACCTGGT

CCGCGCCTCCTGTGAGACCAGCGGCACAATCCACTGCTTTTTCTTTGCGGTA
TACAAGGACACCCACCATACCCCTCCGCTGATTACCGAGCTCCGCAACTTTGC
GGACCTGGTTAACCACCCGCCGGTCCTACGCGAACTGGAGGATAAGCGCGG
GGTGCGGCTGCGGTGTGCGCGGCCGTTTAGCGTCGGGACGATTAAGGACG
TCTCTGGGTCCGGCGCGTCCTCGGCGGGAGAGTACACGATAAACGGGATCG
TGTACCACTGCCACTGTCGGTATCCGTTCTCAAAAACATGCTGGATGGGGGC
CTCCGCGGCCCTACAGCACCTGCGCTCCATCAGCTCCAGCGGCATGGCCGCC
CGCGCGGCAGAGCATCGACGCGTCAAGATTAAAATTAAGGCGTGA

US2

ATGGGCGTTGTTGTCGTCAACGTAATGACCCTCCTTGACCAGAACAACGCCC
TGCCCCGGACTTCCGTCGACGCAAGCCCGGCCCTGTGGAGCTTCCTGCTTAG
GCAGTGCCGCATTTTGGCATCAGAACCCCTGGGTACCCCGGTCGTCGTTCGC
CCGGCCAACCTTCAACGGTTGGCCGAGCCGCTGATGGACTTACCCAAACCCA
CCCGCCCGATCGTGCGCACTAGGTCCTGTCGCTGCCCCCCAAACATCACCAC
GGGCCTGTTTGCGGAGGACAGCCCCTTGGAGAGCACCGAGGTCGTGGACG
CCGTGGCGTGCTTCCGACTGTTGCACCGAGACCAACCCAGCCCCCCTCGCCT
CTACCACTTGTGGGTGGTAGGCGCGGCGGATCTGTGTGTGCCGTTTCTCGA
ATACGCCCAAAAAATCCGGCTCGGGGTAAGATTTATCGCCATCAAGACCCCA
GACGCGTGGGTGGGAGAACCGTGGGCCGTGCCGACTCGGTTTTTGCCCGA
GTGGACCGTGGCGTGGACCCCGTTCCCCGCGGCACCCAACCACCCCCTGGA
GACCCTGCTCAGCCGGTACGAATACCAGTACGGCGTGGTCCTGCCCGGGAC
CAACGGACGGGAGCGCGATTGTATGCGCTGGCTGCGGTCCCTGATTGCTCT
GTACAAACCCCACCCAGCTACCTCCCACCCCCTTACGACGTCCCATTCGGTGC
GGCGTCCGTGTTGTGCGTGTATGGGTATGCCCGAGATTTTAGACGAGCAAC
CCACATCACCGGGCCGTGGTCCGCAAGAAACGGACCCTCTGATCGCCGTTCG
CGGCGAACGGCCCAGACTTCCTCACATCTGCTATCCGGTTACCACCCTTTAG

US3

ATGGCCTGTCGTAAGTTTTGTCGCGTTTACGGGGGACAGGGCAGGAGGAA
GGAGGAGGCCGTCCCGCCGGAGACAAAGCCGTCCCGGGTGTTTCCTCATGG
CCCCTTTTATACCCCAGCCGAGGACGCGTGCCTGGACTCCCCGCCCCCGGAG
ACCCCCAAACCTTCCCACACCACACCACCCGGCGATGCCGAGCGCCTGTGTC
ATCTGCAGGAGATCCTGGCCCAGATGTACGGAAACCAGGACTACCCCATAG
AGGACGACCCCAGCGCGGATGCCGCGGACGATGTCGACGAGGACGCCCCG

GACGACGTGGCCTATCCGGAGGAATACGCAGAGGAGCTTTTTCTGCCCGGG
GACGCGACCGGTCCCCTTATCGGGGCCAACGACCACATCCCTCCCCCGCGTG
GCGCATCTCCCCCCCGGTATACGACGACGCAGCCGGGATGAGATTGGGGCCA
CGGGATTTACCGCAGAAGAGCTGGACGCCATGGACAGGCAGGCGGCTCGA
GCCATCAGCCGCGGCGGCAAGCCCCCCTCGACCATGGCCAAGCTGGTGACT
GGCATGGGCTTTACGATCCACGGAGCGCTCACCCCAGGATCGGAGGGGTGT
GTCTTTGACAGCAGCCACCCAGATTACCCCCAACGGGTAATCGTGAAGGCG
GGGTGGTACACGAGCACGAGCCACGAGGCGCGACTGCTGAGGCGACTGGA
CCACCCGGCGATCCTGCCCCTCCTGGACCTGCATGTCGTCTCCGGGGTCACG
TGTCTGGTCCTCCCCAAGTACCAGGCCGACCTGTATACCTATCTGAGTAGGC
GCCTGAACCCACTGGGACGCCCGCAGATCGCAGCGGTCTCCCGGCAGCTCC
TAAGCGCCGTTGACTACATTCACCGCCAGGGCATTATCCACCGCGACATTAA
GACCGAAAATATTTTTATTAACACCCCCGAGGACATTTGCCTGGGGGACTTT
GGTGCCGCGTGCTTCGTGCAGGGTTCCCGATCAAGCCCCTTCCCCTACGGAA
TCGCCGGAACCATCGACACCAACGCCCCCGAGGTCCTGGCCGGGGATCCGT
ATACCACGACCGTCGACATTTGGAGCGCCGGTCTGGTGATCTTCGAGACTGC
CGTCCACAACGCGTCCTTGTTCTCGGCCCCCCGCGGCCCCAAAAGGGGCCCG
TGCGACAGTCAGATCACCCGCATCATCCGACAGGCCCAGGTCCACGTTGACG
AGTTTTCCCCGCATCCAGAATCGCGCCTCACCTCGCGCTACCGCTCCCGCGC
GGCCGGGAACAATCGCCCGCCTTACACCCGACCGGCCTGGACCCGCTACTAC
AAGATGGACATAGACGTCGAATATCTGGTTTGCAAAGCCCTCACCTTCGACG
GCGCGCTTCGCCCCAGCGCCGCAGAGCTGCTTTGTTTGCCGCTGTTTCAACA
GAAATGA

US10

ATGATCAAGCGGCGGGGCAATGTGGAGATTCGGGTCTACTACGAGTCGGT
GCGGACACTACGATCTCGAAGCCATCTGAAGCCGTCCGACCGCCAACAATCC
CCAGGACACCGCGTGTTCCCCGGGAGCCCCGGGTTCCGCGACCACCCCGAG
AACCTAGGGAACCCAGAGTACCGCGAGCTCCCAGAGACCCCAGGGTACCGC
GTGACCCCAGGGATCCACGACAACCCCGGTCTCCCAGGGAGCCCCGGACCC
CACGCACCCCCCGCGAACCACGTACGGCTCGCGGGTCTGTATAGCCCGGGC
AAGTATGCCCCCCTGGCGAGCCCAGACCCCTTCTCCCCACAAGATGGAGCAT
ACGCTCGGGCCCGCGTCGGGATCCACACCGCGGTTCGCGTCCCGCCCACCG
GAAGCCCAACCCACACGCACTTGCGGCAAGACCCGGGCGATGAGCCAACCT
CGGATGACTCAGGGCTCTACCCTCTGGACGCCCGGGCGCTTGCGCACCTGG

TGATGTTGCCCGCGGACCACCGGGCCTTCTTTCGAACCGTGGTCGAGGTGT
CTCGCATGTGCGCTGCAAACGTGCGCGATCCCCCGCCCCCGGCTACAGGGG
CCATGTTGGGCCGCCACGCGCGGCTGGTCCACACCCAGTGGCTCCGGGCCA
ACCAAGAGACGTCGCCCCTGTGGCCCTGGCGGACGGCGGCCATTAACTTTA
TCACCACCATGGCCCCCCGCGTCCAAACCCACCGACACATGCACGACCTGTT
GATGGCCTGTGCTTTCTGGTGCTGTCTGACACACGCATCGACGTGTTCGTAC
GCGGGGCTGTACTCGACCCACTGCCTGCATCTGTTTGGTGCGTTTGGGTGT
GGGGACCCGGCCCTAACCCCACCCCTGTGCTAG

US11

ATGAGCCAGACCCAACCCCCGGCCCCAGTTGGGCCGGGCGACCCAGATGTT
TACTTAAAAGGCGTGCCGTCCGCCGGCATGCACCCCAGAGGTGTTCACGCAC
CTCGAGGACACCCGCGCATGATCTCCGGACCCCCGCAACGGGGTGATAATG
ATCAAGCGGCGGGGCAATGTGGAGATTCGGGTCTACTACGAGTCGGTGCG
GACACTACGATCTCGAAGCCATCTGAAGCCGTCCGACCGCCAACAATCCCCA
GGACACCGCGTGTTCCCCGGGAGCCCCGGGTTCCGCGACCACCCCGAGAAC
CTAGGGAACCCAGAGTACCGCGAGCTCCCAGAGACCCCAGGGTACCGCGTG
ACCCCAGGGATCCACGACAACCCCGGTCTCCCAGGGAGCCCCGGACCCCACG
CACCCCCCGCGAACCACGTACGGCTCGCGGGTCTGTATAG

Strain 17 ICP0 sequence from pGBKT7-ICP0 with 5' NcoI site and 3' BamHI site underlined

CCATGGAGCCCCGCCCCGGAGCGAGTACCCGCCGGCCTGAGGGCCGCCCCC
AGCGCGAGCCCGCCCCGGATGTCTGGGTGTTTCCCTGCGACCGAGACCTGC
CGGACAGCAGCGACTCTGAGGCGGAGACCGAAGTGGGGGGGGCGGGGGGA
CGCCGACCACCATGACGACGACTCCGCCTCCGAGGCGGACAGCACGGACAC
GGAACTGTTCGAGACGGGGCTGCTGGGGCCGCAGGGCGTGGATGGGGGG
GCGGTCTCGGGGGGGGAGCCCCCCCCGCGAGGAAGACCCCGGCAGTTGCGG
GGGCGCCCCCCCTCGAGAGGACGGGGGGAGCGACGAGGGCGACGTGTGC
GCCGTGTGCACGGATGAGATCGCGCCCCACCTGCGCTGCGACACCTTCCCGT
GCATGCACCGCTTCTGCATCCCGTGCATGAAAACCTGGATGCAATTGCGCAA
CACCTGCCCGCTGTGCAACGCCAAGCTGGTGTACCTGATAGTGGGCGTGAC
GCCCAGCGGGTCGTTCAGCACCATCCCGATCGTGAACGACCCCCAGACCCGC
ATGGAGGCCGAGGAGGCCGTCAGGGCGGGCACGGCCGTGGACTTTATCTG
GACGGGCAATCAGCGGTTCGCCCCGCGGTACCTGACCCTGGGGGGGCACAC

GGTGAGGGCCCTGTCGCCCACCCACCCGGAGCCCACCACGGACGAGGATGA
CGACGACCTGGACGACGCAGACTACGTACCGCCCGCCCCCCGCCGGACGCC
CCGCGCCCCCCCACGCAGAGGCGCCGCCGCGCCCCCCGTGACGGGCGGGGC
GTCTCACGCAGCCCCCCAGCCGGCCGCGGCTCGGACAGCGCCCCCCTCGGC
GCCCATCGGGCCACACGGCAGCAGTAACACCAACACCACCACCAACAGCAGC
GGCGGCGGCGGCTCCCGCCAGTCGCGAGCCGCGGCGCCGCGGGGGGCGTC
TGGCCCCTCCGGGGGGGGTTGGGGTTGGGGTTGGGGTTGTTGAAGCGGAG
GCGGGGCGGCCGAGGGGCCGGACGGGCCCCCTTGTCAACAGACCCGCCCC
CCTTGCAAACAACAGAGACCCCATAGTGATCAGCGACTCCCCCCCGGCCTCT
CCCCACAGGCCCCCCGCGGCGCCCATGCCAGGCTCCGCCCCCCGCCCCGGGC
CCCCCGCGTCCGCGGCCGCGTCGGGACCCGCGCGCCCCCGCGCGGCCGTGG
CCCCGTGCGTGCGAGCGCCGCCTCCGGGGCCCGGCCCCCGCGCCCCGGCCC
CCGGGGCGGAGCCGGCCGCCCGCCCCGCGGACGCGCGCCGTGTGCCCCAG
TCGCACTCGTCCCTGGCTCAGGCCGCGAACCAAGAACAGAGTCTGTGCCGG
GCGCGTGCGACGGTGGCGCGCGGCTCGGGGGGGCCGGGCGTGGAGGGTG
GGCACGGGCCCTCCCGCGGCGCCGCCCCCTCCGGCGCCGCCCCGCTCCCCTC
CGCCGCCTCTGTCGAGCAGGAGGCGGCGGTGCGTCCGAGGAAGAGGCGCG
GGTCGGGCCAGGAAAACCCCTCCCCCCAGTCCACGCGTCCCCCCCTCGCGCC
GGCAGGGGCCAAGAGGGCGGCGACGCACCCCCCCTCCGACTCAGGGCCGG
GGGGGCGCGGCCAGGGTGGGCCCGGGACCCCCCTGACGTCCTCGGCGGCC
TCCGCCTCTTCCTCCTCTGCCTCTTCCTCCTCGGCCCCGACCCCCGCGGGGGC
CGCCTCTTCCGCCGCCGGGGCCGCGTCCTCCTCCGCTTCCGCCTCCTCGGGC
GGGGCCGTCGGTGCCCTGGGAGGGAGACAAGAGGAAACCTCCCTCGGCCC
CCGCGCTGCTTCTGGGCCGCGGGGGCCGAGGAAGTGTGCCCGGAAGACGC
GCCACGCGGAGACTTCCGGGGCCGTCCCCGCGGGCGGCCTCACGCGCTACC
TGCCCATCTCGGGGGTCTCTAGCGTGGTCGCCCTGTCGCCTTACGTGAACAA
GACTATCACGGGGGACTGCCTGCCCATCCTGGACATGGAGACGGGGAACAT
CGGGGCGTACGTGGTCCTGGTGGACCAGACGGGAAACATGGCGACCCGGC
TGCGGGCCGCGGTCCCCGGCTGGAGCCGCCGCACCCTGCTCCCCGAGACCG
CGGGTAACCACGTGATGCCCCCCGAGTACCCGACGGCCCCCGCGTCGGAGT
GGAACAGCCTCTGGATGACCCCCGTGGGGAACATGCTGTTCGACCAGGGCA
CCCTAGTGGGCGCCCTGGACTTCCGCAGCCTGCGGTCTCGGCACCCGTGGT
CCGGGGAGCAGGGGGCGTCGACCCGGGACGAGGGAAAACAATAAGGGAC
GCCCCCCGTGTTTGTGGGGAGGGGGGGGTCGGGCGCTGGGTGGTCTCTGG

CCGCGCCCACTACACCAGCCAATCCGTGTCGGGGAGGGGAAAAGTGAAAGA
CACGGGCACCACACACCAGCGGGTCTTTTGTGTTGGCCCTAATAAAAAAAAA
CTCAGGGGATTTTTGCTGTCTGTTGGGAAATAAAGGTTTACTTTTGTATCTT
TTCCCTGTCTGTGTTGGATGTATCGCGGGGATGCGTGGGAGTGGGGGTGC
GTGGGAGTGGGGGTGCGTGGGAGTGGGGGTGCGTGGGAGTGGGGGTGC
GTGGGAGTGGGGGTGCGTGGGAGTGGGGGTGCGTGGGAGTGGGGGTGC
GTGGGAGTGGGGGTGCGTGGGAGTGGGGGTGCCATGTTGGGCAGGCTCT
GGTGTTAGCTTCGGGGGATCC

7.1.2 CC2D1B sequence

CC2D1B sequence from pHB18-CC2D1B full length cloned by PCR using human cDNA library as library with the missing 18 bp underlined compared to the CC2D1B full length ORF (2577bp, Gene ID: 200014). This 18 bp deletion was confirmed by independent sequencing of plasmid pcDNA3-CC2D1B-flag (kindly provided by P. Albert at University of Ottawa).

ATGATGCCAGGGCCAAGACCTCGGAAGGGCCCTCAGGCCAGAGGCCAAGG
GGTGGCCGCTGCCAAGCAGATGGGGCTCTTTATGGAGTTTGGCCCTGAGGA
CATGCTGCTGGGCATGGATGAGGCTGAAGATGATGAGGACCTGGAGGCTG
AGCTGCTGGCTCTCACAGGGGAAGCACAAACCACAGGCAAGAAGCCAGCAC
CCAAGGGGCAGGCCCCCCTGCCCATGGCCCACATCGAGAAGTTGGCGGCAG
ACTGTATGCGGGATGTGGAGGAGGAGGAGGAGGAGGAAGGGCTGGAGGA
AGATGCAGAGCTGCTGACGGAGCTGCAGGAGGTCTTAGGTGTGGACGAGG
AGACTGAGCCCCTGGATGGTGATGAGGTAGCTGACCCAGGCGGCTCTGAG
GAGGAGAACGGCCTAGAAGACACTGAACCTCCAGTGCAGACAGCCGTCCTG
ACAGCTTCAGCCCCAGCAGCTCAGGCCGGAGCATCTCAGGGGCTACACGCTT
TGCTGGAGGAACGGATTCACAACTACCGAGAGGCTGCGGCCAGTGCCAAGG
AGGCAGGCGAAGCAGCCAAAGCCAGGCGCTGCGAGCGCGGCCTGAAGACC
TTGGAGTCGCAGCTAGCCTCTGTGAGGAGAGGCAGAAAGATCAATGAGGA
TGAGATCCCACCTCCAGTGGCCTTAGGAAAGCGGCCCCTGGCCCCCCAGGA
ACCAGCCAACAGGAGCCCTGAGACAGACCCTCCAGCTCCCCCTGCCTTGGAG
TCAGACAACCCCTCCCAACCTGAGACCAGCCTCCCTGGCATTTCTGCCCAGCC
CGTTTCAGACTTAGACCCAGACCCGCGGGCCCTGCTGTCATCCCGACAGAGA
GAGTACAAAGTGGCTGCCCTCAGTGCCAAGCGGGCTGGAGAGCTAGACCGT
GCCCGAGAGCTCATGAGGATTGGGAAGAGATTCGGTGCTGTCCTGGAGGC

CCTGGAGAAGGGGCAGCCCGTGGATCTGAGTGCCATGCCCCCGGCACCTGA
GGATCTGAAGCCCCAGCAGGCTTCTCAGGCTCCCACAGCACCCTCAGTCATT
CCCCCAGCCGTGGAGCGAGTGCAGCCAGTGATGGCCCCTGACGTCCCAGCA
ACCCCAGTGGCCCCTACAGAGTCACAGACAGTGCTGGATGCCCTGCAGCAG
AGGCTGAACAAGTACCGCGAGGCGGGCATCCAGGCCCGGAGTGGTGGGGA
CGAGCGCAAGGCTCGGATGCATGAGCGCATTGCCAAGCAATATCAAGATGC
TATTCGAGCACACCGAGCAGGACGGAAAGTCAACTTTGCTGAATTGCCTGTT
CCTCCAGGATTTCCCCCCATCCCTGGCCTGGAGTCCACTATGGGTGTTGAGG
AGGACGCAGTGGCAGCGACATTGGCAGCTGCAGAGAAACTGGCCTCTGCAG
AGGATTCAGCCCCGGCTGATAAAGACGAGGACGAGCCTCCTGGGCACCTGC
AGGGTGAGCCCCCAGCACAGGCCCCAGTGGCCAAGAAACCTGCACGGCCCA
CAGTCCCTTCATCCCAGCGCCTGCCTGAGCCCAGGGCCTCAAGTTCTAAGGA
GTCACCGAGTCCATCTGTGCGGGAGCAGCTGGCACTGCTGGAGGCACGGAA
ACTGCAGTATCAGCGGGCAGCCCTGCAGGCCAAGCGCAGCCAGGACCTGGA
GCAGGCCAAAGCCTATCTGCGGGTAGCCAAATGGCTTGAGGCTCAGATCAT
CCAGGCCCGATCTGGCAGACCTGTTGATCTGTCCAAGGTGCCTTCGCCCTTG
ACGGATGAGGAGGGTGACTTCATCCTCATCCACCATGAGGACCTGCGACTCT
CCCAGAAGGCGGAGGAGGTGTATGCCCAGCTGCAAAAAATGCTTCTGGAGC
AACAAGAGAAGTGCCTGCTGTTCTCCAAGCAGTTCATGCACCAGGGCAACGT
GGCTGAGACCACCCGATTTGAGAAGCTTGCTCAGGACCGCAAGAAACAGCT
GGAGATCCTGCAGCTGGCCCAGGCTCAGGGCCTCGACCCTCCCACCCACCAC
TTTGAGTTGAAGACATTCCAGACTGTGAGGATCTTCTCAGAACTCAACAGCA
CAGAAATGCATCTGATCATTGTCCGGGGAATGAACCTCCCAGCCCCTCCAGG
GGTGACTCCCGATGACCTGGATGCTTTTGTGCGGTTTGAGTTTCACTACCCT
AACTCGGACCAGGCTCAAAAAAGCAAAACAGCTGTGGTGAAGAACACAAAC
TCTCCAGAATTTGATCAACTCTTCAAACTAAACATCAACCGAAACCACCGGGG
CTTCAAGAGGGTGATCCAGAGCAAAGGCATCAAGTTTGAGATCTTCCACAAA
GGGTCCTTCTTCAGAAGCGACAAGCTGGTTGGCACAGCACACCTGAAACTG
GAGCGGCTGGAGAATGAGTGTGAGATCAGAGAAATTGTGGAGGTCCTGGA
TGGAAGGAAGCCCACCGGGGGGAAGCTGGAGGTGAAGGTGAGGCTGCGG
GAGCCTCTGAGTGGCCAGGATGTGCAGATGGTCACTGAGAACTGGCTGGTT
CTGGAGCCCAGGGGCTTGTGA

7.2 Tubulin quantification of Figure 4.10

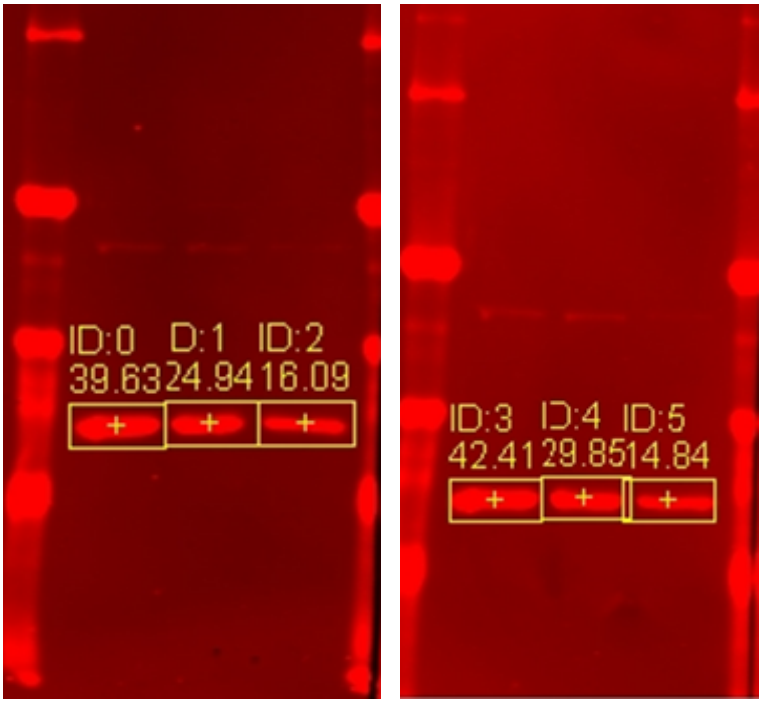

Bibliography

Abaitua, F. & O'Hare, P. (2008). Identification of a highly conserved, functional nuclear localization signal within the N-terminal region of herpes simplex virus type 1 VP1-2 tegument protein. *J Virol* **82**, 5234-5244.

Adams, R., Cunningham, C., Davison, M. D., MacLean, C. A. & Davison, A. J. (1998). Characterization of the protein encoded by gene UL49A of herpes simplex virus type 1. *J Gen Virol* **79 (Pt 4)**, 813-823.

Agromayor, M., Carlton, J. G., Phelan, J. P., Matthews, D. R., Carlin, L. M., Ameer-Beg, S., Bowers, K. & Martin-Serrano, J. (2009). Essential role of hIST1 in cytokinesis. *Mol Biol Cell* **20**, 1374-1387.

Alconada, A., Bauer, U., Sodeik, B. & Hoflack, B. (1999). Intracellular traffic of herpes simplex virus glycoprotein gE: characterization of the sorting signals required for its trans-Golgi network localization. *J Virol* **73**, 377-387.

Allen, T. D., Cronshaw, J. M., Bagley, S., Kiseleva, E. & Goldberg, M. W. (2000). The nuclear pore complex: mediator of translocation between nucleus and cytoplasm. *J Cell Sci* **113 (Pt 10)**, 1651-1659.

Ariumi, Y., Kuroki, M., Maki, M., Ikeda, M., Dansako, H., Wakita, T. & Kato, N. (2011). The ESCRT system is required for hepatitis C virus production. *PLoS One* **6**, e14517.

Atanasiu, D., Saw, W. T., Cohen, G. H. & Eisenberg, R. J. (2010). Cascade of events governing cell-cell fusion induced by herpes simplex virus glycoproteins gD, gH/gL, and gB. *J Virol* **84**, 12292-12299.

Audhya, A., McLeod, I. X., Yates, J. R. & Oegema, K. (2007). MVB-12, a fourth subunit of metazoan ESCRT-I, functions in receptor downregulation. *PLoS One* **2**, e956.

Avitabile, E., Lombardi, G., Gianni, T., Capri, M. & Campadelli-Fiume, G. (2004). Coexpression of UL20p and gK inhibits cell-cell fusion mediated by herpes simplex virus glycoproteins gD, gH-gL, and wild-type gB or an endocytosis-defective gB mutant and downmodulates their cell surface expression. *J Virol* **78**, 8015-8025.

Babst, M., Katzmann, D. J., Snyder, W. B., Wendland, B. & Emr, S. D. (2002). Endosome-associated complex, ESCRT-II, recruits transport machinery for protein sorting at the multivesicular body. *Dev Cell* **3**, 283-289.

Babst, M., Sato, T. K., Banta, L. M. & Emr, S. D. (1997). Endosomal transport function in yeast requires a novel AAA-type ATPase, Vps4p. *EMBO J* **16**, 1820-1831.

Babst, M., Wendland, B., Estepa, E. J. & Emr, S. D. (1998). The Vps4p AAA ATPase regulates membrane association of a Vps protein complex required for normal endosome function. *EMBO J* **17**, 2982-2993.

Bache, K. G., Stuffers, S., Malerod, L., Slagsvold, T., Raiborg, C., Lechardeur, D., Walchli, S., Lukacs, G. L., Brech, A. & Stenmark, H. (2006). The ESCRT-III subunit hVps24 is required for degradation but not silencing of the epidermal growth factor receptor. *Mol Biol Cell* **17**, 2513-2523.

Backovic, M., DuBois, R. M., Cockburn, J. J., Sharff, A. J., Vaney, M. C., Granzow, H., Klupp, B. G., Bricogne, G., Mettenleiter, T. C. & Rey, F. A. (2010). Structure of a core fragment of glycoprotein H from pseudorabies virus in complex with antibody. *Proc Natl Acad Sci U S A* **107**, 22635-22640.

Baines, J. D., Hsieh, C. E., Wills, E., Mannella, C. & Marko, M. (2007a). Electron tomography of nascent herpes simplex virus virions. *J Virol* **81**, 2726-2735.

Baines, J. D. & Roizman, B. (1991). The open reading frames UL3, UL4, UL10, and UL16 are dispensable for the replication of herpes simplex virus 1 in cell culture. *J Virol* **65**, 938-944.

Baines, J. D. & Roizman, B. (1993). The UL10 gene of herpes simplex virus 1 encodes a novel viral glycoprotein, gM, which is present in the virion and in the plasma membrane of infected cells. *J Virol* **67**, 1441-1452.

Baines, J. D., Wills, E., Jacob, R. J., Pennington, J. & Roizman, B. (2007b). Glycoprotein M of herpes simplex virus 1 is incorporated into virions during budding at the inner nuclear membrane. *J Virol* **81**, 800-812.

Baird, N. L., Yeh, P. C., Courtney, R. J. & Wills, J. W. (2008). Sequences in the UL11 tegument protein of herpes simplex virus that control association with detergent-resistant membranes. *Virology* **374**, 315-321.

Bajorek, M., Schubert, H. L., McCullough, J., Langelier, C., Eckert, D. M., Stubblefield, W. M., Uter, N. T., Myszka, D. G., Hill, C. P. & Sundquist, W. I. (2009). Structural basis for ESCRT-III protein autoinhibition. *Nat Struct Mol Biol* **16**, 754-762.

Balan, P., Davis-Poynter, N., Bell, S., Atkinson, H., Browne, H. & Minson, T. (1994). An analysis of the in vitro and in vivo phenotypes of mutants of herpes simplex virus type 1 lacking glycoproteins gG, gE, gI or the putative gJ. *J Gen Virol* **75 (Pt 6)**, 1245-1258.

Baradaran, K., Dabrowski, C. E. & Schaffer, P. A. (1994). Transcriptional analysis of the region of the herpes simplex virus type 1 genome containing the UL8, UL9, and UL10 genes and identification of a novel delayed-early gene product, OBPC. *J Virol* **68**, 4251-4261.

Barelli, H. & Antonny, B. (2009). Cell biology: Detached membrane bending. *Nature* **458**, 159-160.

Barker, D. E. & Roizman, B. (1990). Identification of three genes nonessential for growth in cell culture near the right terminus of the unique sequences of long component of herpes simplex virus 1. *Virology* **177**, 684-691.

Barnett, B. C., Dolan, A., Telford, E. A., Davison, A. J. & McGeoch, D. J. (1992). A novel herpes simplex virus gene (UL49A) encodes a putative membrane protein with counterparts in other herpesviruses. *J Gen Virol* **73 (Pt 8)**, 2167-2171.

Batterson, W., Furlong, D. & Roizman, B. (1983). Molecular genetics of herpes simplex virus. VIII. further characterization of a temperature-sensitive mutant defective in release of viral DNA and in other stages of the viral reproductive cycle. *J Virol* **45**, 397-407.

Beitia Ortiz de Zarate, I., Cantero-Aguilar, L., Longo, M., Berlioz-Torrent, C. & Rozenberg, F. (2007). Contribution of endocytic motifs in the cytoplasmic tail of herpes simplex virus type 1 glycoprotein B to virus replication and cell-cell fusion. *J Virol* **81**, 13889-13903.

Bilodeau, P. S., Urbanowski, J. L., Winistorfer, S. C. & Piper, R. C. (2002). The Vps27p Hse1p complex binds ubiquitin and mediates endosomal protein sorting. *Nat Cell Biol* **4**, 534-539.

Bishop, N. & Woodman, P. (2001). TSG101/mammalian VPS23 and mammalian VPS28 interact directly and are recruited to VPS4-induced endosomes. *J Biol Chem* **276**, 11735-11742.

Bonifacino, J. S. & Rojas, R. (2006). Retrograde transport from endosomes to the trans-Golgi network. *Nat Rev Mol Cell Biol* **7**, 568-579.

Boukamp, P., Petrussevska, R. T., Breitkreutz, D., Hornung, J., Markham, A. & Fusenig, N. E. (1988). Normal keratinization in a spontaneously immortalized aneuploid human keratinocyte cell line. *J Cell Biol* **106**, 761-771.

Boutell, C., Canning, M., Orr, A. & Everett, R. D. (2005). Reciprocal activities between herpes simplex virus type 1 regulatory protein ICP0, a ubiquitin E3 ligase, and ubiquitin-specific protease USP7. *J Virol* **79**, 12342-12354.

Bowers, K., Piper, S. C., Edeling, M. A., Gray, S. R., Owen, D. J., Lehner, P. J. & Luzio, J. P. (2006). Degradation of endocytosed epidermal growth factor and virally ubiquitinated major histocompatibility complex class I is independent of mammalian ESCRTII. *J Biol Chem* **281**, 5094-5105.

Brack, A. R., Dijkstra, J. M., Granzow, H., Klupp, B. G. & Mettenleiter, T. C. (1999). Inhibition of virion maturation by simultaneous deletion of glycoproteins E, I, and M of pseudorabies virus. *J Virol* **73**, 5364-5372.

Brown, D. G., Visse, R., Sandhu, G., Davies, A., Rizkallah, P. J., Melitz, C., Summers, W. C. & Sanderson, M. R. (1995). Crystal structures of the thymidine kinase from herpes simplex virus type-1 in complex with deoxythymidine and ganciclovir. *Nat Struct Biol* **2**, 876-881.

Brown, S. M., Harland, J., MacLean, A. R., Podlech, J. & Clements, J. B. (1994). Cell type and cell state determine differential in vitro growth of non-neurovirulent ICP34.5-negative herpes simplex virus types 1 and 2. *J Gen Virol* **75 (Pt 9)**, 2367-2377.

Browne, H., Bell, S. & Minson, T. (2004). Analysis of the requirement for glycoprotein m in herpes simplex virus type 1 morphogenesis. *J Virol* **78**, 1039-1041.

Browne, H., Bell, S., Minson, T. & Wilson, D. W. (1996). An endoplasmic reticulum-retained herpes simplex virus glycoprotein H is absent from secreted virions: evidence for reenvelopment during egress. *J Virol* **70**, 4311-4316.

Bruce, E. A., Medcalf, L., Crump, C. M., Noton, S. L., Stuart, A. D., Wise, H. M., Elton, D., Bowers, K. & Digard, P. (2009). Budding of filamentous and non-filamentous influenza A virus occurs via a VPS4 and VPS28-independent pathway. *Virology* **390**, 268-278.

Caballe, A. & Martin-Serrano, J. (2011). ESCRT Machinery and Cytokinesis: the Road to Daughter Cell Separation. *Traffic* **12**, 1318-1326.

Cairns, T. M., Shaner, M. S., Zuo, Y., Ponce-de-Leon, M., Baribaud, I., Eisenberg, R. J., Cohen, G. H. & Whitbeck, J. C. (2006). Epitope mapping of herpes simplex virus type 2 gH/gL defines distinct antigenic sites, including some associated with biological function. *J Virol* **80**, 2596-2608.

Calistri, A., Sette, P., Salata, C., Cancellotti, E., Forghieri, C., Comin, A., Gottlinger, H., Campadelli-Fiume, G., Palu, G. & Parolin, C. (2007). Intracellular trafficking and maturation of herpes simplex virus type 1 gB and virus egress require functional biogenesis of multivesicular bodies. *J Virol* **81**, 11468-11478.

Campbell, M. E., Palfreyman, J. W. & Preston, C. M. (1984). Identification of herpes simplex virus DNA sequences which encode a trans-acting polypeptide responsible for stimulation of immediate early transcription. *J Mol Biol* **180**, 1-19.

Cano-Monreal, G. L., Wylie, K. M., Cao, F., Tavis, J. E. & Morrison, L. A. (2009). Herpes simplex virus 2 UL13 protein kinase disrupts nuclear lamins. *Virology* **392**, 137-147.

Carlton, J. G., Agromayor, M. & Martin-Serrano, J. (2008). Differential requirements for Alix and ESCRT-III in cytokinesis and HIV-1 release. *Proc Natl Acad Sci U S A* **105**, 10541-10546.

Carlton, J. G. & Martin-Serrano, J. (2007). Parallels between cytokinesis and retroviral budding: a role for the ESCRT machinery. *Science* **316**, 1908-1912.

Carter, K. L., Ward, P. L. & Roizman, B. (1996). Characterization of the products of the U(L)43 gene of herpes simplex virus 1: potential implications for regulation of gene expression by antisense transcription. *J Virol* **70**, 7663-7668.

Chang, J. T., Schmid, M. F., Rixon, F. J. & Chiu, W. (2007). Electron cryotomography reveals the portal in the herpesvirus capsid. *J Virol* **81**, 2065-2068.

Chowdary, T. K., Cairns, T. M., Atanasiu, D., Cohen, G. H., Eisenberg, R. J. & Heldwein, E. E. (2010a). Crystal structure of the conserved herpesvirus fusion regulator complex gH-gL. *Nature structural & molecular biology* **17**, 882-888.

Chowdary, T. K., Cairns, T. M., Atanasiu, D., Cohen, G. H., Eisenberg, R. J. & Heldwein, E. E. (2010b). Crystal structure of the conserved herpesvirus fusion regulator complex gH-gL. *Nat Struct Mol Biol* **17**, 882-888.

Coller, K. E. & Lee, J. I. (2007). The capsid and tegument of the alphaherpesviruses are linked by an interaction between the UL25 and VP1/2 proteins. *Journal of virology* **81**, 11790.

Coller, K. E., Lee, J. I., Ueda, A. & Smith, G. A. (2007). The capsid and tegument of the alphaherpesviruses are linked by an interaction between the UL25 and VP1/2 proteins. *J Virol* **81**, 11790-11797.

Connolly, S. A., Jackson, J. O., Jardetzky, T. S. & Longnecker, R. (2011). Fusing structure and function: a structural view of the herpesvirus entry machinery. *Nat Rev Microbiol* **9**, 369-381.

Connolly, S. A., Landsburg, D. J., Carfi, A., Whitbeck, J. C., Zuo, Y., Wiley, D. C., Cohen, G. H. & Eisenberg, R. J. (2005). Potential nectin-1 binding site on herpes simplex virus glycoprotein d. *J Virol* **79**, 1282-1295.

Coonrod, E. M. & Stevens, T. H. (2010). The yeast vps class E mutants: the beginning of the molecular genetic analysis of multivesicular body biogenesis. *Mol Biol Cell* **21**, 4057-4060.

Crump, C. M., Bruun, B., Bell, S., Pomeranz, L. E., Minson, T. & Browne, H. M. (2004). Alphaherpesvirus glycoprotein M causes the relocalization of plasma membrane proteins. *J Gen Virol* **85**, 3517-3527.

Crump, C. M., Yates, C. & Minson, T. (2007). Herpes simplex virus type 1 cytoplasmic envelopment requires functional Vps4. *J Virol* **81**, 7380-7387.

Davison, A. J., Eberle, R., Ehlers, B., Hayward, G. S., McGeoch, D. J., Minson, A. C., Pellett, P. E., Roizman, B., Studdert, M. J. & Thiry, E. (2009). The order Herpesvirales. *Arch Virol* **154**, 171-177.

De Domenico, I., Ward, D. M., Langelier, C., Vaughn, M. B., Nemeth, E., Sundquist, W. I., Ganz, T., Musci, G. & Kaplan, J. (2007). The molecular mechanism of hepcidin-mediated ferroportin down-regulation. *Mol Biol Cell* **18**, 2569-2578.

Deane, C. M., Salwinski, L., Xenarios, I. & Eisenberg, D. (2002). Protein interactions: two methods for assessment of the reliability of high throughput observations. *Mol Cell Proteomics* **1**, 349-356.

Desai, P. J. (2000). A null mutation in the UL36 gene of herpes simplex virus type 1 results in accumulation of unenveloped DNA-filled capsids in the cytoplasm of infected cells. *J Virol* **74**, 11608-11618.

Desai, P. J., Schaffer, P. A. & Minson, A. C. (1988). Excretion of non-infectious virus particles lacking glycoprotein H by a temperature-sensitive mutant of herpes simplex virus type 1: evidence that gH is essential for virion infectivity. *J Gen Virol* **69 (Pt 6)**, 1147-1156.

Diefenbach, R. J., Miranda-Saksena, M., Douglas, M. W. & Cunningham, A. L. (2008). Transport and egress of herpes simplex virus in neurons. *Rev Med Virol* **18**, 35-51.

Dijkstra, J. M., Visser, N., Mettenleiter, T. C. & Klupp, B. G. (1996). Identification and characterization of pseudorabies virus glycoprotein gM as a nonessential virion component. *J Virol* **70**, 5684-5688.

Dodding, M. P. & Way, M. (2011). Coupling viruses to dynein and kinesin-1. *EMBO J* **30**, 3527-3539.

Donnelly, M. & Elliott, G. (2001). Nuclear localization and shuttling of herpes simplex virus tegument protein VP13/14. *J Virol* **75**, 2566-2574.

Donnelly, M., Verhagen, J. & Elliott, G. (2007). RNA binding by the herpes simplex virus type 1 nucleocytoplasmic shuttling protein UL47 is mediated by an N-terminal arginine-rich domain that also functions as its nuclear localization signal. *J Virol* **81**, 2283-2296.

Doyotte, A., Mironov, A., McKenzie, E. & Woodman, P. (2008). The Bro1-related protein HD-PTP/PTPN23 is required for endosomal cargo sorting and multivesicular body morphogenesis. *Proc Natl Acad Sci U S A* **105**, 6308-6313.

Duyk, G., Longiaru, M., Cobrinik, D., Kowal, R., deHaseth, P., Skalka, A. M. & Leis, J. (1985). Circles with two tandem long terminal repeats are specifically cleaved by pol gene-associated endonuclease from avian sarcoma and leukosis viruses: nucleotide sequences required for site-specific cleavage. *J Virol* **56**, 589-599.

Elia, N., Sougrat, R., Spurlin, T. A., Hurley, J. H. & Lippincott-Schwartz, J. (2011). Dynamics of endosomal sorting complex required for transport (ESCRT) machinery during cytokinesis and its role in abscission. *Proc Natl Acad Sci U S A* **108**, 4846-4851.

Elliott, G., Mouzakitis, G. & O'Hare, P. (1995). VP16 interacts via its activation domain with VP22, a tegument protein of herpes simplex virus, and is relocated to a novel macromolecular assembly in coexpressing cells. *J Virol* **69**, 7932-7941.

Enquist, L. W., Husak, P. J., Banfield, B. W. & Smith, G. A. (1998). Infection and spread of alphaherpesviruses in the nervous system. *Adv Virus Res* **51**, 237-347.

Everett, R. D. (2000a). ICP0 induces the accumulation of colocalizing conjugated ubiquitin. *J Virol* **74**, 9994-10005.

Everett, R. D. (2000b). ICP0, a regulator of herpes simplex virus during lytic and latent infection. *Bioessays* **22**, 761-770.

Fan, Z., Grantham, M. L., Smith, M. S., Anderson, E. S., Cardelli, J. A. & Muggeridge, M. I. (2002). Truncation of herpes simplex virus type 2 glycoprotein B increases its cell surface expression and activity in cell-cell fusion, but these properties are unrelated. *J Virol* **76**, 9271-9283.

Farnsworth, A., Wisner, T. W., Webb, M., Roller, R., Cohen, G., Eisenberg, R. & Johnson, D. C. (2007). Herpes simplex virus glycoproteins gB and gH function in fusion between the virion envelope and the outer nuclear membrane. *Proc Natl Acad Sci U S A* **104**, 10187-10192.

Favoreel, H. W. (2006). The why's of Y-based motifs in alphaherpesvirus envelope proteins. *Virus Res* **117**, 202-208.

Field, M. C. & Dacks, J. B. (2009). First and last ancestors: reconstructing evolution of the endomembrane system with ESCRTs, vesicle coat proteins, and nuclear pore complexes. *Curr Opin Cell Biol* **21**, 4-13.

Fisher, R. D., Chung, H. Y., Zhai, Q., Robinson, H., Sundquist, W. I. & Hill, C. P. (2007). Structural and biochemical studies of ALIX/AIP1 and its role in retrovirus budding. *Cell* **128**, 841-852.

Fossum, E., Friedel, C. C., Rajagopala, S. V., Titz, B., Baiker, A., Schmidt, T., Kraus, T., Stellberger, T., Rutenberg, C., Suthram, S., Bandyopadhyay, S., Rose, D., von Brunn, A., Uhlmann, M., Zeretzke, C., Dong, Y. A., Boulet, H., Koegl, M., Bailer, S. M., Koszinowski, U., Ideker, T., Uetz, P., Zimmer,

R. & Haas, J. (2009). Evolutionarily conserved herpesviral protein interaction networks. *PLoS Pathog* **5**, e1000570.

Foster, T. P., Melancon, J. M. & Kousoulas, K. G. (2001a). An alpha-helical domain within the carboxyl terminus of herpes simplex virus type 1 (HSV-1) glycoprotein B (gB) is associated with cell fusion and resistance to heparin inhibition of cell fusion. *Virology* **287**, 18-29.

Foster, T. P., Melancon, J. M., Olivier, T. L. & Kousoulas, K. G. (2004). Herpes simplex virus type 1 glycoprotein K and the UL20 protein are interdependent for intracellular trafficking and trans-Golgi network localization. *J Virol* **78**, 13262-13277.

Foster, T. P., Rybachuk, G. V. & Kousoulas, K. G. (2001b). Glycoprotein K specified by herpes simplex virus type 1 is expressed on virions as a Golgi complex-dependent glycosylated species and functions in virion entry. *J Virol* **75**, 12431-12438.

Fuchs, W., Granzow, H., Klupp, B. G., Kopp, M. & Mettenleiter, T. C. (2002). The UL48 tegument protein of pseudorabies virus is critical for intracytoplasmic assembly of infectious virions. *J Virol* **76**, 6729-6742.

Fuchs, W. & Mettenleiter, T. C. (1999). DNA sequence of the UL6 to UL20 genes of infectious laryngotracheitis virus and characterization of the UL10 gene product as a nonglycosylated and nonessential virion protein. *J Gen Virol* **80 (Pt 8)**, 2173-2182.

Gaidos, G., Soni, S., Oswald, D. J., Toselli, P. A. & Kirsch, K. H. (2007). Structure and function analysis of the CMS/CIN85 protein family identifies actin-bundling properties and heterotypic-complex formation. *J Cell Sci* **120**, 2366-2377.

Gallagher, C. M. & Knoblich, J. A. (2006). The conserved c2 domain protein lethal (2) giant discs regulates protein trafficking in Drosophila. *Dev Cell* **11**, 641-653.

Garber, D. A., Beverley, S. M. & Coen, D. M. (1993). Demonstration of circularization of herpes simplex virus DNA following infection using pulsed field gel electrophoresis. *Virology* **197**, 459-462.

Ghiasi, H., Nesburn, A. B., Cai, S. & Wechsler, S. L. (1998). The US5 open reading frame of herpes simplex virus type 1 does encode a glycoprotein (gJ). *Intervirology* **41**, 91-97.

Giard, D. J., Aaronson, S. A., Todaro, G. J., Arnstein, P., Kersey, J. H., Dosik, H. & Parks, W. P. (1973). In vitro cultivation of human tumors: establishment of cell lines derived from a series of solid tumors. *J Natl Cancer Inst* **51**, 1417-1423.

Gierasch, W. W., Zimmerman, D. L., Ward, S. L., Vanheyningen, T. K., Romine, J. D. & Leib, D. A. (2006). Construction and characterization of bacterial artificial chromosomes containing HSV-1 strains 17 and KOS. *J Virol Methods* **135**, 197-206.

Gilden, D. H., Mahalingam, R., Cohrs, R. J. & Tyler, K. L. (2007). Herpesvirus infections of the nervous system. *Nat Clin Pract Neurol* **3**, 82-94.

Goldin, A. L., Sandri-Goldin, R. M., Levine, M. & Glorioso, J. C. (1981). Cloning of herpes simplex virus type 1 sequences representing the whole genome. *J Virol* **38**, 50-58.

Goshima, F., Watanabe, D., Suzuki, H., Takakuwa, H., Yamada, H. & Nishiyama, Y. (2001). The US2 gene product of herpes simplex virus type 2 interacts with cytokeratin 18. *Arch Virol* **146**, 2201-2209.

Gottlinger, H. G., Dorfman, T., Sodroski, J. G. & Haseltine, W. A. (1991). Effect of mutations affecting the p6 gag protein on human immunodeficiency virus particle release. *Proc Natl Acad Sci U S A* **88**, 3195-3199.

Gross, S. T., Harley, C. A. & Wilson, D. W. (2003). The cytoplasmic tail of Herpes simplex virus glycoprotein H binds to the tegument protein VP16 in vitro and in vivo. *Virology* **317**, 1-12.

Grunewald, K., Desai, P., Winkler, D. C., Heymann, J. B., Belnap, D. M., Baumeister, W. & Steven, A. C. (2003). Three-dimensional structure of herpes simplex virus from cryo-electron tomography. *Science* **302**, 1396-1398.

Hadjighassem, M. R., Austin, M. C., Szewczyk, B., Daigle, M., Stockmeier, C. A. & Albert, P. R. (2009). Human Freud-2/CC2D1B: a novel repressor of postsynaptic serotonin-1A receptor expression. *Biol Psychiatry* **66**, 214-222.

Hadjighassem, M. R., Galaraga, K. & Albert, P. R. (2011). Freud-2/CC2D1B mediates dual repression of the serotonin-1A receptor gene. *Eur J Neurosci* **33**, 214-223.

Hafezi, W., Bernard, E., Cook, R. & Elliott, G. (2005). Herpes simplex virus tegument protein VP22 contains an internal VP16 interaction domain and a C-terminal domain that are both required for VP22 assembly into the virus particle. *J Virol* **79**, 13082-13093.

Haigler, H. T., McKanna, J. A. & Cohen, S. (1979). Direct visualization of the binding and internalization of a ferritin conjugate of epidermal growth factor in human carcinoma cells A-431. *J Cell Biol* **81**, 382-395.

Hanson, P. I., Roth, R., Lin, Y. & Heuser, J. E. (2008). Plasma membrane deformation by circular arrays of ESCRT-III protein filaments. *J Cell Biol* **180**, 389-402.

Harper, A. L., Meckes, D. G., Jr., Marsh, J. A., Ward, M. D., Yeh, P. C., Baird, N. L., Wilson, C. B., Semmes, O. J. & Wills, J. W. (2010). Interaction domains of the UL16 and UL21 tegument proteins of herpes simplex virus. *J Virol* **84**, 2963-2971.

Heldwein, E. E. & Krummenacher, C. (2008). Entry of herpesviruses into mammalian cells. *Cell Mol Life Sci* **65**, 1653-1668.

Heldwein, E. E., Lou, H., Bender, F. C., Cohen, G. H., Eisenberg, R. J. & Harrison, S. C. (2006). Crystal structure of glycoprotein B from herpes simplex virus 1. *Science* **313**, 217-220.

Henne, W. M., Buchkovich, N. J. & Emr, S. D. (2011). The ESCRT pathway. *Dev Cell* **21**, 77-91.

Hewitt, E. W., Duncan, L., Mufti, D., Baker, J., Stevenson, P. G. & Lehner, P. J. (2002). Ubiquitylation of MHC class I by the K3 viral protein signals internalization and TSG101-dependent degradation. *EMBO J* **21**, 2418-2429.

Hicke, L. & Dunn, R. (2003). Regulation of membrane protein transport by ubiquitin and ubiquitin-binding proteins. *Annu Rev Cell Dev Biol* **19**, 141-172.

Hidalgo, I. J., Raub, T. J. & Borchardt, R. T. (1989). Characterization of the human colon carcinoma cell line (Caco-2) as a model system for intestinal epithelial permeability. *Gastroenterology* **96**, 736-749.

Hill, T. J., Field, H. J. & Blyth, W. A. (1975). Acute and recurrent infection with herpes simplex virus in the mouse: a model for studying latency and recurrent disease. *J Gen Virol* **28**, 341-353.

Hobom, U., Brune, W., Messerle, M., Hahn, G. & Koszinowski, U. H. (2000). Fast screening procedures for random transposon libraries of cloned herpesvirus genomes: mutational analysis of human cytomegalovirus envelope glycoprotein genes. *J Virol* **74**, 7720-7729.

Hurley, J. H. & Emr, S. D. (2006). The ESCRT complexes: structure and mechanism of a membrane-trafficking network. *Annu Rev Biophys Biomol Struct* **35**, 277-298.

Igarashi, K., Fawl, R., Roller, R. J. & Roizman, B. (1993). Construction and properties of a recombinant herpes simplex virus 1 lacking both S-component origins of DNA synthesis. *J Virol* **67**, 2123-2132.

Im, Y. J. & Hurley, J. H. (2008). Integrated structural model and membrane targeting mechanism of the human ESCRT-II complex. *Dev Cell* **14**, 902-913.

Jacob, R. J., Morse, L. S. & Roizman, B. (1979). Anatomy of herpes simplex virus DNA. XII. Accumulation of head-to-tail concatemers in nuclei of infected cells and their role in the generation of the four isomeric arrangements of viral DNA. *J Virol* **29**, 448-457.

Jaekel, R. & Klein, T. (2006). The Drosophila Notch inhibitor and tumor suppressor gene lethal (2) giant discs encodes a conserved regulator of endosomal trafficking. *Dev Cell* **11**, 655-669.

Johnson, D. C. & Baines, J. D. (2011). Herpesviruses remodel host membranes for virus egress. *Nat Rev Microbiol* **9**, 382-394.

Jons, A., Dijkstra, J. M. & Mettenleiter, T. C. (1998). Glycoproteins M and N of pseudorabies virus form a disulfide-linked complex. *J Virol* **72**, 550-557.

Jons, A. & Mettenleiter, T. C. (1996). Identification and characterization of pseudorabies virus dUTPase. *J Virol* **70**, 1242-1245.

Jovasevic, V., Liang, L. & Roizman, B. (2008). Proteolytic cleavage of VP1-2 is required for release of herpes simplex virus 1 DNA into the nucleus. *J Virol* **82**, 3311-3319.

Kamen, D. E., Gross, S. T., Girvin, M. E. & Wilson, D. W. (2005). Structural basis for the physiological temperature dependence of the association of VP16 with the cytoplasmic tail of herpes simplex virus glycoprotein H. *J Virol* **79**, 6134-6141.

Kato, A., Arii, J., Shiratori, I., Akashi, H., Arase, H. & Kawaguchi, Y. (2009). Herpes simplex virus 1 protein kinase Us3 phosphorylates viral envelope glycoprotein B and regulates its expression on the cell surface. *J Virol* **83**, 250-261.

Kato, A., Yamamoto, M., Ohno, T., Kodaira, H., Nishiyama, Y. & Kawaguchi, Y. (2005). Identification of proteins phosphorylated directly by the Us3 protein kinase encoded by herpes simplex virus 1. *J Virol* **79**, 9325-9331.

Kato, A., Yamamoto, M., Ohno, T., Tanaka, M., Sata, T., Nishiyama, Y. & Kawaguchi, Y. (2006). Herpes simplex virus 1-encoded protein kinase UL13 phosphorylates viral Us3 protein kinase and regulates nuclear localization of viral envelopment factors UL34 and UL31. *J Virol* **80**, 1476-1486.

Katzmann, D. J., Babst, M. & Emr, S. D. (2001). Ubiquitin-dependent sorting into the multivesicular body pathway requires the function of a conserved endosomal protein sorting complex, ESCRT-I. *Cell* **106**, 145-155.

Kelly, B. J., Fraefel, C., Cunningham, A. L. & Diefenbach, R. J. (2009). Functional roles of the tegument proteins of herpes simplex virus type 1. *Virus Res* **145**, 173-186.

Klupp, B., Altenschmidt, J., Granzow, H., Fuchs, W. & Mettenleiter, T. C. (2008). Glycoproteins required for entry are not necessary for egress of pseudorabies virus. *J Virol* **82**, 6299-6309.

Klupp, B. G., Altenschmidt, J., Granzow, H., Fuchs, W. & Mettenleiter, T. C. (2005). Identification and characterization of the pseudorabies virus UL43 protein. *Virology* **334**, 224-233.

Klupp, B. G., Baumeister, J., Dietz, P., Granzow, H. & Mettenleiter, T. C. (1998). Pseudorabies virus glycoprotein gK is a virion structural component involved in virus release but is not required for entry. *J Virol* **72**, 1949-1958.

Klupp, B. G., Nixdorf, R. & Mettenleiter, T. C. (2000). Pseudorabies virus glycoprotein M inhibits membrane fusion. *J Virol* **74**, 6760-6768.

Ko, D. H., Cunningham, A. L. & Diefenbach, R. J. (2010). The major determinant for addition of tegument protein pUL48 (VP16) to capsids in herpes simplex virus type 1 is the presence of the major tegument protein pUL36 (VP1/2). *J Virol* **84**, 1397-1405.

Konig, P., Giesow, K. & Keil, G. M. (2002). Glycoprotein M of bovine herpesvirus 1 (BHV-1) is nonessential for replication in cell culture and is involved in inhibition of bovine respiratory syncytial virus F protein induced syncytium formation in recombinant BHV-1 infected cells. *Vet Microbiol* **86**, 37-49.

Kopp, M., Granzow, H., Fuchs, W., Klupp, B. & Mettenleiter, T. C. (2004). Simultaneous deletion of pseudorabies virus tegument protein UL11 and glycoprotein M severely impairs secondary envelopment. *J Virol* **78**, 3024-3034.

Kostelansky, M. S., Schluter, C., Tam, Y. Y., Lee, S., Ghirlando, R., Beach, B., Conibear, E. & Hurley, J. H. (2007). Molecular architecture and functional model of the complete yeast ESCRT-I heterotetramer. *Cell* **129**, 485-498.

Koyano, S., Mar, E. C., Stamey, F. R. & Inoue, N. (2003). Glycoproteins M and N of human herpesvirus 8 form a complex and inhibit cell fusion. *J Gen Virol* **84**, 1485-1491.

Krautwald, M., Fuchs, W., Klupp, B. G. & Mettenleiter, T. C. (2009). Translocation of incoming pseudorabies virus capsids to the cell nucleus is delayed in the absence of tegument protein pUL37. *J Virol* **83**, 3389-3396.

Krummenacher, C., Nicola, A. V., Whitbeck, J. C., Lou, H., Hou, W., Lambris, J. D., Geraghty, R. J., Spear, P. G., Cohen, G. H. & Eisenberg, R. J. (1998). Herpes simplex virus glycoprotein D can bind to poliovirus receptor-related protein 1 or herpesvirus entry mediator, two structurally unrelated mediators of virus entry. *J Virol* **72**, 7064-7074.

La Boissière, S., Hughes, T. & O'Hare, P. (1999). HCF-dependent nuclear import of VP16. *The EMBO journal* **18**, 480-489.

Lake, C. M., Molesworth, S. J. & Hutt-Fletcher, L. M. (1998). The Epstein-Barr virus (EBV) gN homolog BLRF1 encodes a 15-kilodalton glycoprotein that cannot be authentically processed unless it is coexpressed with the EBV gM homolog BBRF3. *J Virol* **72**, 5559-5564.

Langelier, C., von Schwedler, U. K., Fisher, R. D., De Domenico, I., White, P. L., Hill, C. P., Kaplan, J., Ward, D. & Sundquist, W. I. (2006). Human ESCRT-II complex and its role in human immunodeficiency virus type 1 release. *J Virol* **80**, 9465-9480.

Lata, S., Schoehn, G., Jain, A., Pires, R., Piehler, J., Gottlinger, H. G. & Weissenhorn, W. (2008). Helical structures of ESCRT-III are disassembled by VPS4. *Science* **321**, 1354-1357.

Lata, S., Schoehn, G., Solomons, J., Pires, R., Gottlinger, H. G. & Weissenhorn, W. (2009). Structure and function of ESCRT-III. *Biochem Soc Trans* **37**, 156-160.

Lee, J. A., Beigneux, A., Ahmad, S. T., Young, S. G. & Gao, F. B. (2007). ESCRT-III dysfunction causes autophagosome accumulation and neurodegeneration. *Curr Biol* **17**, 1561-1567.

Lee, J. H., Vittone, V., Diefenbach, E., Cunningham, A. L. & Diefenbach, R. J. (2008). Identification of structural protein-protein interactions of herpes simplex virus type 1. *Virology* **378**, 347-354.

Leege, T., Fuchs, W., Granzow, H., Kopp, M., Klupp, B. G. & Mettenleiter, T. C. (2009). Effects of simultaneous deletion of pUL11 and glycoprotein M on virion maturation of herpes simplex virus type 1. *J Virol* **83**, 896-907.

Leopardi, R., Van Sant, C. & Roizman, B. (1997). The herpes simplex virus 1 protein kinase US3 is required for protection from apoptosis induced by the virus. *Proc Natl Acad Sci U S A* **94**, 7891-7896.

Lipinska, A. D., Koppers-Lalic, D., Rychlowski, M., Admiraal, P., Rijsewijk, F. A., Bienkowska-Szewczyk, K. & Wiertz, E. J. (2006). Bovine herpesvirus 1 UL49.5 protein inhibits the transporter associated with antigen processing despite complex formation with glycoprotein M. *J Virol* **80**, 5822-5832.

Loomis, J. S., Courtney, R. J. & Wills, J. W. (2003). Binding partners for the UL11 tegument protein of herpes simplex virus type 1. *J Virol* **77**, 11417-11424.

Loret, S., Guay, G. & Lippe, R. (2008). Comprehensive characterization of extracellular herpes simplex virus type 1 virions. *J Virol* **82**, 8605-8618.

Lycke, E., Kristensson, K., Svennerholm, B., Vahlne, A. & Ziegler, R. (1984). Uptake and transport of herpes simplex virus in neurites of rat dorsal root ganglia cells in culture. *J Gen Virol* **65 (Pt 1)**, 55-64.

Lyman, M. G. & Enquist, L. W. (2009). Herpesvirus interactions with the host cytoskeleton. *J Virol* **83**, 2058-2066.

Mach, M., Kropff, B., Dal Monte, P. & Britt, W. (2000). Complex formation by human cytomegalovirus glycoproteins M (gpUL100) and N (gpUL73). *J Virol* **74**, 11881-11892.

MacLean, C. A., Efstathiou, S., Elliott, M. L., Jamieson, F. E. & McGeoch, D. J. (1991). Investigation of herpes simplex virus type 1 genes encoding multiply inserted membrane proteins. *J Gen Virol* **72 (Pt 4)**, 897-906.

MacLean, C. A., Robertson, L. M. & Jamieson, F. E. (1993). Characterization of the UL10 gene product of herpes simplex virus type 1 and investigation of its role in vivo. *J Gen Virol* **74 (Pt 6)**, 975-983.

Maringer, K. & Elliott, G. (2010). Recruitment of herpes simplex virus type 1 immediate-early protein ICP0 to the virus particle. *J Virol* **84**, 4682-4696.

Martin-Serrano, J. & Neil, S. J. (2011). Host factors involved in retroviral budding and release. *Nat Rev Microbiol* **9**, 519-531.

Martin-Serrano, J., Yarovoy, A., Perez-Caballero, D. & Bieniasz, P. D. (2003a). Divergent retroviral late-budding domains recruit vacuolar protein sorting factors by using alternative adaptor proteins. *Proc Natl Acad Sci U S A* **100**, 12414-12419.

Martin-Serrano, J., Zang, T. & Bieniasz, P. D. (2001). HIV-1 and Ebola virus encode small peptide motifs that recruit Tsg101 to sites of particle assembly to facilitate egress. *Nat Med* **7**, 1313-1319.

Martin-Serrano, J., Zang, T. & Bieniasz, P. D. (2003b). Role of ESCRT-I in retroviral budding. *J Virol* **77**, 4794-4804.

Masters, J. R. (2002). HeLa cells 50 years on: the good, the bad and the ugly. *Nat Rev Cancer* **2**, 315-319.

Matsuura, H., Kirschner, A. N., Longnecker, R. & Jardetzky, T. S. (2010). Crystal structure of the Epstein-Barr virus (EBV) glycoprotein H/glycoprotein L (gH/gL) complex. *Proc Natl Acad Sci U S A* **107**, 22641-22646.

May, J. S., Colaco, S. & Stevenson, P. G. (2005). Glycoprotein M is an essential lytic replication protein of the murine gammaherpesvirus 68. *J Virol* **79**, 3459-3467.

McCullough, J., Fisher, R. D., Whitby, F. G., Sundquist, W. I. & Hill, C. P. (2008). ALIX-CHMP4 interactions in the human ESCRT pathway. *Proc Natl Acad Sci U S A* **105**, 7687-7691.

McGeoch, D. J., Rixon, F. J. & Davison, A. J. (2006). Topics in herpesvirus genomics and evolution. *Virus Res* **117**, 90-104.

McNab, A. R., Desai, P., Person, S., Roof, L. L., Thomsen, D. R., Newcomb, W. W., Brown, J. C. & Homa, F. L. (1998). The product of the herpes simplex virus

type 1 UL25 gene is required for encapsidation but not for cleavage of replicated viral DNA. *J Virol* **72**, 1060-1070.

Meckes, D. G., Jr. & Wills, J. W. (2007). Dynamic interactions of the UL16 tegument protein with the capsid of herpes simplex virus. *J Virol* **81**, 13028-13036.

Mettenleiter, T. C. (2002). Herpesvirus assembly and egress. *J Virol* **76**, 1537-1547.

Mettenleiter, T. C. (2004). Budding events in herpesvirus morphogenesis. *Virus Res* **106**, 167-180.

Mettenleiter, T. C. (2006). Intriguing interplay between viral proteins during herpesvirus assembly or: the herpesvirus assembly puzzle. *Vet Microbiol* **113**, 163-169.

Mettenleiter, T. C., Klupp, B. G. & Granzow, H. (2006). Herpesvirus assembly: a tale of two membranes. *Curr Opin Microbiol* **9**, 423-429.

Mettenleiter, T. C., Klupp, B. G. & Granzow, H. (2009). Herpesvirus assembly: an update. *Virus Res* **143**, 222-234.

Michael, K., Klupp, B. G., Karger, A. & Mettenleiter, T. C. (2007). Efficient incorporation of tegument proteins pUL46, pUL49, and pUS3 into pseudorabies virus particles depends on the presence of pUL21. *J Virol* **81**, 1048-1051.

Mijatov, B., Cunningham, A. L. & Diefenbach, R. J. (2007). Residues F593 and E596 of HSV-1 tegument protein pUL36 (VP1/2) mediate binding of tegument protein pUL37. *Virology* **368**, 26-31.

Montgomery, R. I., Warner, M. S., Lum, B. J. & Spear, P. G. (1996). Herpes simplex virus-1 entry into cells mediated by a novel member of the TNF/NGF receptor family. *Cell* **87**, 427-436.

Morita, E., Sandrin, V., Alam, S. L., Eckert, D. M., Gygi, S. P. & Sundquist, W. I. (2007a). Identification of human MVB12 proteins as ESCRT-I subunits that function in HIV budding. *Cell Host Microbe* **2**, 41-53.

Morita, E., Sandrin, V., Chung, H. Y., Morham, S. G., Gygi, S. P., Rodesch, C. K. & Sundquist, W. I. (2007b). Human ESCRT and ALIX proteins interact with proteins of the midbody and function in cytokinesis. *EMBO J* **26**, 4215-4227.

Morita, E., Sandrin, V., McCullough, J., Katsuyama, A., Baci Hamilton, I. & Sundquist, W. I. (2011). ESCRT-III protein requirements for HIV-1 budding. *Cell Host Microbe* **9**, 235-242.

Morita, E. & Sundquist, W. I. (2004). Retrovirus budding. *Annu Rev Cell Dev Biol* **20**, 395-425.

Mouzakitis, G., McLauchlan, J., Barreca, C., Kueltzo, L. & O'Hare, P. (2005). Characterization of VP22 in herpes simplex virus-infected cells. *J Virol* **79**, 12185-12198.

Naldinho-Souto, R., Browne, H. & Minson, T. (2006). Herpes simplex virus tegument protein VP16 is a component of primary enveloped virions. *J Virol* **80**, 2582-2584.

Nam, J. M., Onodera, Y., Mazaki, Y., Miyoshi, H., Hashimoto, S. & Sabe, H. (2007). CIN85, a Cbl-interacting protein, is a component of AMAP1-mediated breast cancer invasion machinery. *EMBO J* **26**, 647-656.

Neil, S. J., Zang, T. & Bieniasz, P. D. (2008). Tetherin inhibits retrovirus release and is antagonized by HIV-1 Vpu. *Nature* **451**, 425-430.

Newcomb, W. W., Homa, F. L., Thomsen, D. R., Booy, F. P., Trus, B. L., Steven, A. C., Spencer, J. V. & Brown, J. C. (1996). Assembly of the herpes simplex virus capsid: characterization of intermediates observed during cell-free capsid formation. *J Mol Biol* **263**, 432-446.

Newcomb, W. W., Homa, F. L., Thomsen, D. R., Trus, B. L., Cheng, N., Steven, A., Booy, F. & Brown, J. C. (1999). Assembly of the herpes simplex virus procapsid from purified components and identification of small complexes containing the major capsid and scaffolding proteins. *J Virol* **73**, 4239-4250.

Newcomb, W. W., Trus, B. L., Booy, F. P., Steven, A. C., Wall, J. S. & Brown, J. C. (1993). Structure of the herpes simplex virus capsid. Molecular composition of the pentons and the triplexes. *J Mol Biol* **232**, 499-511.

Nickerson, D. P., Russell, M. R. & Odorizzi, G. (2007). A concentric circle model of multivesicular body cargo sorting. *EMBO Rep* **8**, 644-650.

Nozawa, N., Kawaguchi, Y., Tanaka, M., Kato, A., Kimura, H. & Nishiyama, Y. (2005). Herpes simplex virus type 1 UL51 protein is involved in maturation and egress of virus particles. *J Virol* **79**, 6947-6956.

Oestreich, A. J., Davies, B. A., Payne, J. A. & Katzmann, D. J. (2007). Mvb12 is a novel member of ESCRT-I involved in cargo selection by the multivesicular body pathway. *Mol Biol Cell* **18**, 646-657.

Oien, N. L., Thomsen, D. R., Wathen, M. W., Newcomb, W. W., Brown, J. C. & Homa, F. L. (1997). Assembly of herpes simplex virus capsids using the human cytomegalovirus scaffold protein: critical role of the C terminus. *J Virol* **71**, 1281-1291.

Ojala, P. M., Sodeik, B., Ebersold, M. W., Kutay, U. & Helenius, A. (2000). Herpes simplex virus type 1 entry into host cells: reconstitution of capsid binding and uncoating at the nuclear pore complex in vitro. *Mol Cell Biol* **20**, 4922-4931.

Osterrieder, N., Neubauer, A., Brandmuller, C., Braun, B., Kaaden, O. R. & Baines, J. D. (1996). The equine herpesvirus 1 glycoprotein gp21/22a, the herpes simplex virus type 1 gM homolog, is involved in virus penetration and cell-to-cell spread of virions. *J Virol* **70**, 4110-4115.

Ou, X. M., Lemonde, S., Jafar-Nejad, H., Bown, C. D., Goto, A., Rogaeva, A. & Albert, P. R. (2003). Freud-1: A neuronal calcium-regulated repressor of the 5-HT1A receptor gene. *J Neurosci* **23**, 7415-7425.

Padula, M. E., Sydnor, M. L. & Wilson, D. W. (2009). Isolation and preliminary characterization of herpes simplex virus 1 primary enveloped virions from the perinuclear space. *J Virol* **83**, 4757-4765.

Parent, L. J., Bennett, R. P., Craven, R. C., Nelle, T. D., Krishna, N. K., Bowzard, J. B., Wilson, C. B., Puffer, B. A., Montelaro, R. C. & Wills, J. W. (1995). Positionally independent and exchangeable late budding functions of the Rous sarcoma virus and human immunodeficiency virus Gag proteins. *J Virol* **69**, 5455-5460.

Pasdeloup, D., Beilstein, F., Roberts, A. P., McElwee, M., McNab, D. & Rixon, F. J. Inner tegument protein pUL37 of herpes simplex virus type 1 is involved in directing capsids to the trans-Golgi network for envelopment. *J Gen Virol* **91**, 2145-2151.

Pasdeloup, D., Blondel, D., Isidro, A. L. & Rixon, F. J. (2009). Herpesvirus capsid association with the nuclear pore complex and viral DNA release involve the nucleoporin CAN/Nup214 and the capsid protein pUL25. *J Virol* **83**, 6610-6623.

Pawliczek, T. & Crump, C. M. (2009). Herpes simplex virus type 1 production requires a functional ESCRT-III complex but is independent of TSG101 and ALIX expression. *J Virol* **83**, 11254-11264.

Peck, J. W., Bowden, E. T. & Burbelo, P. D. (2004). Structure and function of human Vps20 and Snf7 proteins. *Biochem J* **377**, 693-700.

Pellett, P. E. & Roizman, B. (2007). The family Herpesviridae: a brief introduction. *Fields virology, 5th ed Lippincott Williams & Wilkins, Philadelphia, PA*, 2479-2499.

Pincetic, A., Medina, G., Carter, C. & Leis, J. (2008). Avian sarcoma virus and human immunodeficiency virus, type 1 use different subsets of ESCRT proteins to facilitate the budding process. *J Biol Chem* **283**, 29822-29830.

Piper, R. C. & Katzmann, D. J. (2007). Biogenesis and function of multivesicular bodies. *Annu Rev Cell Dev Biol* **23**, 519-547.

Polvino-Bodnar, M., Orberg, P. K. & Schaffer, P. A. (1987). Herpes simplex virus type 1 oriL is not required for virus replication or for the establishment and reactivation of latent infection in mice. *J Virol* **61**, 3528-3535.

Popov, S., Popova, E., Inoue, M. & Gottlinger, H. G. (2009). Divergent Bro1 domains share the capacity to bind human immunodeficiency virus type 1 nucleocapsid and to enhance virus-like particle production. *J Virol* **83**, 7185-7193.

Pornillos, O., Alam, S. L., Davis, D. R. & Sundquist, W. I. (2002). Structure of the Tsg101 UEV domain in complex with the PTAP motif of the HIV-1 p6 protein. *Nat Struct Biol* **9**, 812-817.

Powers, L., Wilkinson, K. S. & Ryan, P. (1994). Characterization of the prv43 gene of pseudorabies virus and demonstration that it is not required for virus growth in cell culture. *Virology* **199**, 81-88.

Quinlan, M. P., Chen, L. B. & Knipe, D. M. (1984). The intranuclear location of a herpes simplex virus DNA-binding protein is determined by the status of viral DNA replication. *Cell* **36**, 857-868.

Raiborg, C. & Stenmark, H. (2009). The ESCRT machinery in endosomal sorting of ubiquitylated membrane proteins. *Nature* **458**, 445-452.

Rauch, S. & Martin-Serrano, J. (2011). Multiple interactions between the ESCRT machinery and arrestin-related proteins: implications for PPXY-dependent budding. *J Virol* **85**, 3546-3556.

Ren, X., Kloer, D. P., Kim, Y. C., Ghirlando, R., Saidi, L. F., Hummer, G. & Hurley, J. H. (2009). Hybrid structural model of the complete human ESCRT-0 complex. *Structure* **17**, 406-416.

Renvoise, B., Parker, R. L., Yang, D., Bakowska, J. C., Hurley, J. H. & Blackstone, C. (2010). SPG20 protein spartin is recruited to midbodies by ESCRT-III protein Ist1 and participates in cytokinesis. *Mol Biol Cell* **21**, 3293-3303.

Reske, A., Pollara, G., Krummenacher, C., Chain, B. M. & Katz, D. R. (2007). Understanding HSV-1 entry glycoproteins. *Rev Med Virol* **17**, 205-215.

Rey, F. A. (2006). Molecular gymnastics at the herpesvirus surface. *EMBO Rep* **7**, 1000-1005.

Reynolds, A. E., Wills, E. G., Roller, R. J., Ryckman, B. J. & Baines, J. D. (2002). Ultrastructural localization of the herpes simplex virus type 1 UL31, UL34, and US3 proteins suggests specific roles in primary envelopment and egress of nucleocapsids. *J Virol* **76**, 8939-8952.

Rixon, F. J. (2008). A good catch: packaging the virus genome. *Cell Host & Microbe* **3**, 120-122.

Roberts, A. P., Abaitua, F., O'Hare, P., McNab, D., Rixon, F. J. & Pasdeloup, D. (2009). Differing roles of inner tegument proteins pUL36 and pUL37 during entry of herpes simplex virus type 1. *J Virol* **83**, 105-116.

Roizman, B. & Sears, A. E. (2001). Herpes simplex viruses and their replication. *Fields virology* **2**, 2399-2459.

Roizman, B. & Whitley, R. J. (2001). The nine ages of herpes simplex virus. *Herpes* **8**, 23-27.

Roller, R. J. & Roizman, B. (1990). The herpes simplex virus Us11 open reading frame encodes a sequence-specific RNA-binding protein. *J Virol* **64**, 3463-3470.

Rossman, J. S., Jing, X., Leser, G. P. & Lamb, R. A. (2010). Influenza virus M2 protein mediates ESCRT-independent membrane scission. *Cell* **142**, 902-913.

Rout, M. P., Aitchison, J. D., Suprapto, A., Hjertaas, K., Zhao, Y. & Chait, B. T. (2000). The yeast nuclear pore complex: composition, architecture, and transport mechanism. *J Cell Biol* **148**, 635-651.

Rudolph, J., Seyboldt, C., Granzow, H. & Osterrieder, N. (2002). The gene 10 (UL49.5) product of equine herpesvirus 1 is necessary and sufficient for functional processing of glycoprotein M. *J Virol* **76**, 2952-2963.

Rusten, T. E., Vaccari, T., Lindmo, K., Rodahl, L. M., Nezis, I. P., Sem-Jacobsen, C., Wendler, F., Vincent, J. P., Brech, A., Bilder, D. & Stenmark, H. (2007). ESCRTs and Fab1 regulate distinct steps of autophagy. *Curr Biol* **17**, 1817-1825.

Saffran, H. A., Read, G. S. & Smiley, J. R. (2010). Evidence for translational regulation by the herpes simplex virus virion host shutoff protein. *J Virol* **84**, 6041-6049.

Saksena, S., Wahlman, J., Teis, D., Johnson, A. E. & Emr, S. D. (2009). Functional reconstitution of ESCRT-III assembly and disassembly. *Cell* **136**, 97-109.

Salmon, B., Cunningham, C., Davison, A. J., Harris, W. J. & Baines, J. D. (1998). The herpes simplex virus type 1 U(L)17 gene encodes virion tegument proteins that are required for cleavage and packaging of viral DNA. *J Virol* **72**, 3779-3788.

Samson, R. Y. & Bell, S. D. (2009). Ancient ESCRTs and the evolution of binary fission. *Trends Microbiol* **17**, 507-513.

Scheuring, S., Rohricht, R. A., Schoning-Burkhardt, B., Beyer, A., Muller, S., Abts, H. F. & Kohrer, K. (2001). Mammalian cells express two VPS4 proteins both of which are involved in intracellular protein trafficking. *J Mol Biol* **312**, 469-480.

Schleiss, M. R. (2009). Persistent and recurring viral infections: the human herpesviruses. *Curr Probl Pediatr Adolesc Health Care* **39**, 7-23.

Schlieker, C., Korbel, G. A., Kattenhorn, L. M. & Ploegh, H. L. (2005). A deubiquitinating activity is conserved in the large tegument protein of the herpesviridae. *J Virol* **79**, 15582-15585.

Schmidt, M. H., Hoeller, D., Yu, J., Furnari, F. B., Cavenee, W. K., Dikic, I. & Bogler, O. (2004). Alix/AIP1 antagonizes epidermal growth factor receptor downregulation by the Cbl-SETA/CIN85 complex. *Mol Cell Biol* **24**, 8981-8993.

Schuh, M. (2011). An actin-dependent mechanism for long-range vesicle transport. *Nat Cell Biol.*

Seaman, M. N. (2008). Endosome protein sorting: motifs and machinery. *Cell Mol Life Sci* **65**, 2842-2858.

Sette, P., Jadwin, J. A., Dussupt, V., Bello, N. F. & Bouamr, F. (2010). The ESCRT-associated protein Alix recruits the ubiquitin ligase Nedd4-1 to facilitate HIV-1 release through the LYPXnL L domain motif. *J Virol* **84**, 8181-8192.

Seyboldt, C., Granzow, H. & Osterrieder, N. (2000). Equine herpesvirus 1 (EHV-1) glycoprotein M: effect of deletions of transmembrane domains. *Virology* **278**, 477-489.

Shanda, S. K. & Wilson, D. W. (2008). UL36p is required for efficient transport of membrane-associated herpes simplex virus type 1 along microtubules. *J Virol* **82**, 7388-7394.

Showalter, S. D., Zweig, M. & Hampar, B. (1981). Monoclonal antibodies to herpes simplex virus type 1 proteins, including the immediate-early protein ICP 4. *Infect Immun* **34**, 684-692.

Shukla, D., Liu, J., Blaiklock, P., Shworak, N. W., Bai, X., Esko, J. D., Cohen, G. H., Eisenberg, R. J., Rosenberg, R. D. & Spear, P. G. (1999). A novel role for 3-O-sulfated heparan sulfate in herpes simplex virus 1 entry. *Cell* **99**, 13-22.

Skepper, J. N., Whiteley, A., Browne, H. & Minson, A. (2001). Herpes simplex virus nucleocapsids mature to progeny virions by an envelopment --> deenvelopment --> reenvelopment pathway. *J Virol* **75**, 5697-5702.

Smibert, C. A., Popova, B., Xiao, P., Capone, J. P. & Smiley, J. R. (1994). Herpes simplex virus VP16 forms a complex with the virion host shutoff protein vhs. *J Virol* **68**, 2339-2346.

Smiley, J. R. (2004). Herpes simplex virus virion host shutoff protein: immune evasion mediated by a viral RNase? *J Virol* **78**, 1063-1068.

Smith, C. A., Bates, P., Rivera-Gonzalez, R., Gu, B. & DeLuca, N. A. (1993). ICP4, the major transcriptional regulatory protein of herpes simplex virus type 1, forms a tripartite complex with TATA-binding protein and TFIIB. *J Virol* **67**, 4676-4687.

Smith, K. O. (1964). Relationship between the Envelope and the Infectivity of Herpes Simplex Virus. *Proc Soc Exp Biol Med* **115**, 814-816.

Sodeik, B. (2000). Mechanisms of viral transport in the cytoplasm. *Trends in microbiology* **8**, 465-472.

Sodeik, B., Ebersold, M. W. & Helenius, A. (1997). Microtubule-mediated transport of incoming herpes simplex virus 1 capsids to the nucleus. *The Journal of cell biology* **136**, 1007.

Soubeyran, P., Kowanetz, K., Szymkiewicz, I., Langdon, W. Y. & Dikic, I. (2002). Cbl-CIN85-endophilin complex mediates ligand-induced downregulation of EGF receptors. *Nature* **416**, 183-187.

Spitzer, C., Schellmann, S., Sabovljevic, A., Shahriari, M., Keshavaiah, C., Bechtold, N., Herzog, M., Muller, S., Hanisch, F. G. & Hulskamp, M. (2006). The Arabidopsis elch mutant reveals functions of an ESCRT component in cytokinesis. *Development* **133**, 4679-4689.

Stackpole, C. W. (1969). Herpes-type virus of the frog renal adenocarcinoma. I. Virus development in tumor transplants maintained at low temperature. *J Virol* **4**, 75-93.

Stern, S. & Herr, W. (1991). The herpes simplex virus trans-activator VP16 recognizes the Oct-1 homeo domain: evidence for a homeo domain recognition subdomain. *Genes & development* **5**, 2555.

Stern, S., Tanaka, M. & Herr, W. (1989). The Oct-1 homoeodomain directs formation of a multiprotein-DNA complex with the HSV transactivator VP16. *Nature* **341**, 624-630.

Strack, B., Calistri, A., Craig, S., Popova, E. & Gottlinger, H. G. (2003). AIP1/ALIX is a binding partner for HIV-1 p6 and EIAV p9 functioning in virus budding. *Cell* **114**, 689-699.

Strang, B. L. & Stow, N. D. (2005). Circularization of the herpes simplex virus type 1 genome upon lytic infection. *J Virol* **79**, 12487-12494.

Stuchell-Brereton, M. D., Skalicky, J. J., Kieffer, C., Karren, M. A., Ghaffarian, S. & Sundquist, W. I. (2007). ESCRT-III recognition by VPS4 ATPases. *Nature* **449**, 740-744.

Stylianou, J., Maringer, K., Cook, R., Bernard, E. & Elliott, G. (2009). Virion incorporation of the herpes simplex virus type 1 tegument protein VP22 occurs via glycoprotein E-specific recruitment to the late secretory pathway. *J Virol* **83**, 5204-5218.

Takakuwa, H., Goshima, F., Koshizuka, T., Murata, T., Daikoku, T. & Nishiyama, Y. (2001). Herpes simplex virus encodes a virion-associated protein which promotes long cellular processes in over-expressing cells. *Genes Cells* **6**, 955-966.

Take, H., Watanabe, S., Takeda, K., Yu, Z. X., Iwata, N. & Kajigaya, S. (2000). Cloning and characterization of a novel adaptor protein, CIN85, that interacts with c-Cbl. *Biochem Biophys Res Commun* **268**, 321-328.

Tanaka, M., Sata, T. & Kawaguchi, Y. (2008). The product of the Herpes simplex virus 1 UL7 gene interacts with a mitochondrial protein, adenine nucleotide translocator 2. *Virol J* **5**, 125.

Taylor, T. J., Brockman, M. A., McNamee, E. E. & Knipe, D. M. (2002). Herpes simplex virus. *Front Biosci* **7**, d752-764.

Teis, D., Saksena, S. & Emr, S. D. (2008). Ordered assembly of the ESCRT-III complex on endosomes is required to sequester cargo during MVB formation. *Dev Cell* **15**, 578-589.

Teo, H., Perisic, O., Gonzalez, B. & Williams, R. L. (2004). ESCRT-II, an endosome-associated complex required for protein sorting: crystal structure and interactions with ESCRT-III and membranes. *Dev Cell* **7**, 559-569.

Tischer, B. K., Schumacher, D., Messerle, M., Wagner, M. & Osterrieder, N. (2002). The products of the UL10 (gM) and the UL49.5 genes of Marek's disease virus serotype 1 are essential for virus growth in cultured cells. *J Gen Virol* **83**, 997-1003.

Tischer, B. K., Smith, G. A. & Osterrieder, N. (2010). En passant mutagenesis: a two step markerless red recombination system. *Methods Mol Biol* **634**, 421-430.

Tischer, B. K., von Einem, J., Kaufer, B. & Osterrieder, N. (2006). Two-step red-mediated recombination for versatile high-efficiency markerless DNA manipulation in Escherichia coli. *Biotechniques* **40**, 191-197.

Tiwari, V., Clement, C., Duncan, M. B., Chen, J., Liu, J. & Shukla, D. (2004). A role for 3-O-sulfated heparan sulfate in cell fusion induced by herpes simplex virus type 1. *J Gen Virol* **85**, 805-809.

Toomre, D., Keller, P., White, J., Olivo, J. C. & Simons, K. (1999). Dual-color visualization of trans-Golgi network to plasma membrane traffic along microtubules in living cells. *J Cell Sci* **112 (Pt 1)**, 21-33.

Toyooka, S., Ouchida, M., Jitsumori, Y., Tsukuda, K., Sakai, A., Nakamura, A., Shimizu, N. & Shimizu, K. (2000). HD-PTP: A novel protein tyrosine phosphatase gene on human chromosome 3p21.3. *Biochem Biophys Res Commun* **278**, 671-678.

Tsang, H. T., Connell, J. W., Brown, S. E., Thompson, A., Reid, E. & Sanderson, C. M. (2006). A systematic analysis of human CHMP protein interactions: additional MIT domain-containing proteins bind to multiple components of the human ESCRT III complex. *Genomics* **88**, 333-346.

Turcotte, S., Letellier, J. & Lippe, R. (2005). Herpes simplex virus type 1 capsids transit by the trans-Golgi network, where viral glycoproteins accumulate independently of capsid egress. *J Virol* **79**, 8847-8860.

Turner, A., Bruun, B., Minson, T. & Browne, H. (1998). Glycoproteins gB, gD, and gHgL of herpes simplex virus type 1 are necessary and sufficient to mediate membrane fusion in a Cos cell transfection system. *J Virol* **72**, 873-875.

Usami, Y., Popov, S. & Gottlinger, H. G. (2007). Potent rescue of human immunodeficiency virus type 1 late domain mutants by ALIX/AIP1 depends on its CHMP4 binding site. *J Virol* **81**, 6614-6622.

Vajjhala, P. R., Catchpoole, E., Nguyen, C. H., Kistler, C. & Munn, A. L. (2007). Vps4 regulates a subset of protein interactions at the multivesicular endosome. *FEBS J* **274**, 1894-1907.

van Genderen, I. L., Brandimarti, R., Torrisi, M. R., Campadelli, G. & van Meer, G. (1994). The phospholipid composition of extracellular herpes simplex virions differs from that of host cell nuclei. *Virology* **200**, 831-836.

Verhagen, J., Donnelly, M. & Elliott, G. (2006a). Characterization of a novel transferable CRM-1-independent nuclear export signal in a herpesvirus tegument protein that shuttles between the nucleus and cytoplasm. *J Virol* **80**, 10021-10035.

Verhagen, J., Hutchinson, I. & Elliott, G. (2006b). Nucleocytoplasmic shuttling of bovine herpesvirus 1 UL47 protein in infected cells. *J Virol* **80**, 1059-1063.

Verweij, M. C., Lipinska, A. D., Koppers-Lalic, D., Quinten, E., Funke, J., van Leeuwen, H. C., Bienkowska-Szewczyk, K., Koch, J., Ressing, M. E. & Wiertz, E. J. (2011). Structural and functional analysis of the TAP-inhibiting UL49.5 proteins of varicelloviruses. *Mol Immunol* **48**, 2038-2051.

Vittone, V., Diefenbach, E., Triffett, D., Douglas, M. W., Cunningham, A. L. & Diefenbach, R. J. (2005). Determination of interactions between tegument proteins of herpes simplex virus type 1. *J Virol* **79**, 9566-9571.

Wagner, M. J. & Smiley, J. R. (2009). Herpes simplex virus requires VP11/12 to induce phosphorylation of the activation loop tyrosine (Y394) of the Src family kinase Lck in T lymphocytes. *J Virol* **83**, 12452-12461.

Wagner, M. J. & Smiley, J. R. (2011). Herpes simplex virus requires VP11/12 to activate Src family kinase-phosphoinositide 3-kinase-Akt signaling. *J Virol* **85**, 2803-2812.

Weinheimer, S. P., Boyd, B. A., Durham, S. K., Resnick, J. L. & O'Boyle, D. R., 2nd (1992). Deletion of the VP16 open reading frame of herpes simplex virus type 1. *J Virol* **66**, 258-269.

Weir, J. P. (1998). Genomic organization and evolution of the human herpesviruses. *Virus Genes* **16**, 85-93.

Weiss, E. R. & Gottlinger, H. (2011). The role of cellular factors in promoting HIV budding. *J Mol Biol* **410**, 525-533.

Whiteley, A., Bruun, B., Minson, T. & Browne, H. (1999). Effects of targeting herpes simplex virus type 1 gD to the endoplasmic reticulum and trans-Golgi network. *J Virol* **73**, 9515-9520.

Williams, P., Verhagen, J. & Elliott, G. (2008). Characterization of a CRM1-dependent nuclear export signal in the C terminus of herpes simplex virus type 1 tegument protein UL47. *J Virol* **82**, 10946-10952.

Wisner, T. W., Wright, C. C., Kato, A., Kawaguchi, Y., Mou, F., Baines, J. D., Roller, R. J. & Johnson, D. C. (2009). Herpesvirus gB-induced fusion between the virion envelope and outer nuclear membrane during virus egress is regulated by the viral US3 kinase. *J Virol* **83**, 3115-3126.

Wolfstein, A., Nagel, C. H., Radtke, K., Dohner, K., Allan, V. J. & Sodeik, B. (2006). The inner tegument promotes herpes simplex virus capsid motility along microtubules in vitro. *Traffic* **7**, 227-237.

Wollert, T. & Hurley, J. H. (2010). Molecular mechanism of multivesicular body biogenesis by ESCRT complexes. *Nature* **464**, 864-869.

Wollert, T., Wunder, C., Lippincott-Schwartz, J. & Hurley, J. H. (2009). Membrane scission by the ESCRT-III complex. *Nature* **458**, 172-177.

Wu, S. X., Zhu, X. P. & Letchworth, G. J. (1998). Bovine herpesvirus 1 glycoprotein M forms a disulfide-linked heterodimer with the U(L)49.5 protein. *J Virol* **72**, 3029-3036.

Yamada, H., Daikoku, T., Yamashita, Y., Jiang, Y. M., Tsurumi, T. & Nishiyama, Y. (1997). The product of the US10 gene of herpes simplex virus type 1 is a capsid/tegument-associated phosphoprotein which copurifies with the nuclear matrix. *J Gen Virol* **78 (Pt 11)**, 2923-2931.

Yamada, H., Jiang, Y. M., Oshima, S., Wada, K., Goshima, F., Daikoku, T. & Nishiyama, Y. (1998). Characterization of the UL4 gene product of herpes simplex virus type 2. *Arch Virol* **143**, 1199-1207.

Yamagishi, Y., Sadaoka, T., Yoshii, H., Somboonthum, P., Imazawa, T., Nagaike, K., Ozono, K., Yamanishi, K. & Mori, Y. (2008). Varicella-zoster virus glycoprotein M homolog is glycosylated, is expressed on the viral envelope, and functions in virus cell-to-cell spread. *J Virol* **82**, 795-804.

Yamauchi, Y., Kiriyama, K., Kubota, N., Kimura, H., Usukura, J. & Nishiyama, Y. (2008). The UL14 tegument protein of herpes simplex virus type 1 is required for efficient nuclear transport of the alpha transinducing factor VP16 and viral capsids. *J Virol* **82**, 1094-1106.

Yang, D. & Hurley, J. H. (2010). Structural role of the Vps4-Vta1 interface in ESCRT-III recycling. *Structure* **18**, 976-984.

Yeh, P. C., Han, J., Chadha, P., Meckes, D. G., Jr., Ward, M. D., Semmes, O. J. & Wills, J. W. (2011). Direct and specific binding of the UL16 tegument protein of herpes simplex virus to the cytoplasmic tail of glycoprotein E. *J Virol* **85**, 9425-9436.

Yorikawa, C., Shibata, H., Waguri, S., Hatta, K., Horii, M., Katoh, K., Kobayashi, T., Uchiyama, Y. & Maki, M. (2005). Human CHMP6, a myristoylated ESCRT-III protein, interacts directly with an ESCRT-II component EAP20 and regulates endosomal cargo sorting. *Biochem J* **387**, 17-26.

Zhang, J., Nagel, C. H., Sodeik, B. & Lippe, R. (2009a). Early, active, and specific localization of herpes simplex virus type 1 gM to nuclear membranes. *J Virol* **83**, 12984-12997.

Zhang, J., Zheng, X., Yang, X. & Liao, K. (2009b). CIN85 associates with endosomal membrane and binds phosphatidic acid. *Cell Res* **19**, 733-746.

Zhang, Y. & McKnight, J. L. (1993). Herpes simplex virus type 1 UL46 and UL47 deletion mutants lack VP11 and VP12 or VP13 and VP14, respectively, and exhibit altered viral thymidine kinase expression. *J Virol* **67**, 1482-1492.

Zhu, Q. & Courtney, R. J. (1994). Chemical cross-linking of virion envelope and tegument proteins of herpes simplex virus type 1. *Virology* **204**, 590-599.

Ziegler, C., Just, F. T., Lischewski, A., Elbers, K. & Neubauer, A. (2005). A glycoprotein M-deleted equid herpesvirus 4 is severely impaired in virus egress and cell-to-cell spread. *J Gen Virol* **86**, 11-21.